Synthèse, caractérisation et criblage biologique de nouveaux dérivés ferrocéniques des flavonoïdes : chalcones, aurones, flavones et flavonols

Jean-Philippe Monserrat

Ecole Doctorale de Chimie Moléculaire Paris-Centre (ED406)
Spécialité : Chimie Bioorganométallique

Thèse de doctorat
de l'université Pierre et Marie Curie (Paris VI)

Présentée par Jean-Philippe Monserrat
Pour obtenir le grade de docteur de l'université Paris VI

Synthèse, caractérisation et criblage biologique de nouveaux dérivés ferrocéniques des flavonoïdes : chalcones, aurones, flavones et flavonols

---

Soutenue le 23 Septembre 2011,
devant le jury composé de

Pr.	Giovanni Poli, Professeur à l'UPMC	Examinateur
Dr.	John Spencer, Reader à l'université de Greenwich, UK	Rapporteur
Dr.	Christian Hartinger, Assistant Professor à l'université de Vienne, Autriche	Rapporteur
Pr.	Gérard Jaouen, Professeur à Chimie ParisTech	Directeur de thèse
Dr.	Anne Vessières, Directrice de Recherche à Chimie ParisTech	Invitée
Dr.	Elizabeth Hillard, Chargée de Recherche à Chimie ParisTech	Invitée

Préparée à l'École nationale supérieure de chimie de Paris

The most exciting phrase to hear in science, the one that heralds new discoveries, is not “Eureka!” (I found it!) but “That's funny ...”

Isaac Asimov

Acknowledgments

I owe my deepest gratitude to Elizabeth Hillard for being a great boss. Her ideas and tremendous support had a major influence on this thesis. I learned a lot from her in science as well as how to become a scientist. She also spent a lot of time correcting my manuscript, and giving me advice.

It was an honor for me to work under Gérard Jaouen's supervision. His wide knowledge and his availability made me feel secure anytime.

I would like to thank Anne Vessières for having welcomed me in her laboratory, and for all the enriching discussions we have had, concerning my thesis and everything else.

I would like to express my deep gratitude to Giovanni Poli, John Spencer and Christian Hartinger for having accepted to be members of my jury. Thank you for sharing your expertise and evaluating my work.

A special thanks to Keshri Tiwari, who has worked with me at the bench for two years. Keshri's experience made me learn a lot about organic synthesis, as well as about Indian culture.

This thesis would not have been possible without our collaborators: Marie-Noëlle Rager and Sophie Walmé for NMR spectroscopy, Céline Fosse and Claudine Fleurant for mass spectrometry, Michel Huché for docking experiments, Nouri Neamati for HIV tests, Guy Chabot for antiproliferative and antiangiogenic tests and finally Claude Jolivalt and Carine Ganem-Elbaz for anti-bacterial tests. My greatest thanks to them all.

I am indebted to my many of my colleagues for their everyday help. I especially remember Didier Hamels, my elder and friend, who showed me the true face of the PhD, Michèle Salmain and Nathalie Durand who helped me with the UV/visible spectroscopy, Siden Top and Pascal Pigeon for having shared their extended experience and for having always been available when I needed them, and Marie-Aude Richard, who helped me with my lab duties

while I was at home writing this thesis. Of course, I also thank all the members of the lab that I haven't cited.

I would also like to thank all the internship students that have worked under my direction, for having helped me on this project, and all my students at the university, who taught me a lot. I hope to have been a good teacher, because as Ernest Boyer says, "A poor surgeon hurts 1 person at a time. A poor teacher hurts 130".

Finally, I want to thank my whole family, and especially my companion Maria Proetto and my sister Delphine Monserrat, who assisted me a lot during the writing of this dissertation.

Résumé

Introduction

Les flavonoïdes sont d'origine essentiellement végétale et forment l'une des familles les plus étendues d'antioxydants.[1] Leur histoire commence à l'ère primaire, au moment de la colonisation des continents par les êtres vivants. Leur origine semble être la conséquence d'un dévoiement d'activité cellulaire : les gênes codant certaines enzymes responsables de la biosynthèse des flavonoïdes ont une séquence proche de ceux codant des enzymes du métabolisme primaire.[2]

Les flavonoïdes sont des molécules de faible poids moléculaire, dont la structure comporte deux cycles phényles reliés par un pont comportant trois atomes de carbones. Différentes sous-classes de flavonoïdes existent et ont une nomenclature propre ; les plus importantes d'entre-elles sont présentées en Figure 1.

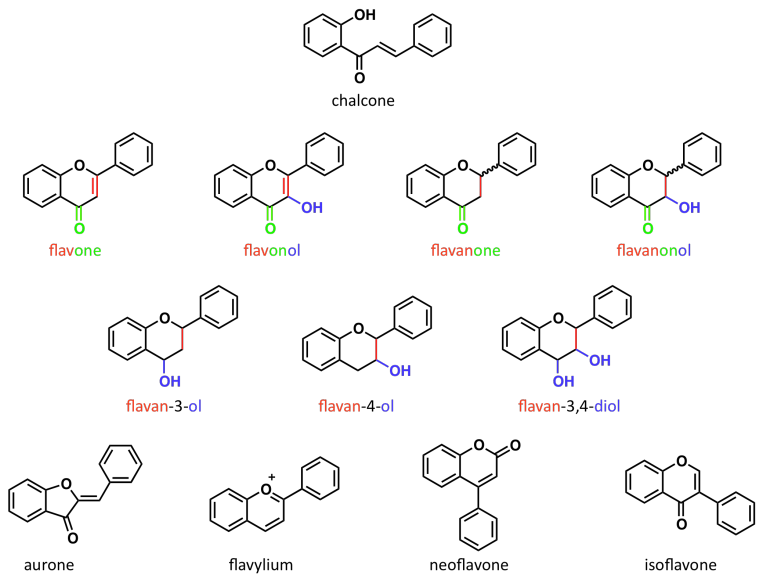

Figure 1. Principales sous-classes de flavonoïdes

Les flavonoïdes ont des rôles très divers au sein des organismes végétaux. Ils sont par exemple utilisés comme colorants : la couleur des fleurs est la conséquence de la présence

de molécules dérivées de l'ion flavylium, présenté en Figure 1.[1] Ils peuvent également avoir une fonction de protection contre les rayons UV : les mutants incapables d'effectuer la biosynthèse des flavonoïdes sont généralement très sensibles au rayonnement solaire.[3] D'un point de vue métabolique, les flavonoïdes sont impliqués dans le transport d'auxines qui sont des phytohormones nécessaires au développement des plantes : les mutants déficients ont des malformations.[4] Ces molécules ont également un rôle très important dans la reproduction.[5]

Chez les animaux, les flavonoïdes ont avant tout un effet de protection de l'organisme, ce qui leur a valu d'être considérés comme « alicament ».[6] En effet, ils préviennent l'apparition de certaines maladies, principalement le cancer et les maladies cardiovasculaires. Les effets des flavonoïdes sur ces dernières sont illustrés par le concept de « paradoxe français » qui part d'une simple observation : de par leur alimentation, les français consomment en général des graisses saturées, mais ne sont pour autant pas affectés par les maladies cardiovasculaires autant qu'ils le devraient.[7] Ce phénomène semble être la conséquence de la présence de flavonoïdes dans le vin, ces derniers ayant un effet protecteur sur l'organisme.[8]

Les flavonoïdes sont des antioxydants et à ce titre ils interagissent avec les radicaux libres.[9] Leur structure phénolique leur permet de subir des oxydations au contact de ces derniers. Leur combinaison avec une autre entité réactive sur le plan redox semblait donc une voie intéressante à explorer.

Notre choix s'est porté sur le ferrocène dont la structure est présentée en Figure 2. Il est composé de deux ions cyclopentadiényles et d'un atome de fer. Le ferrocène est un complexe organométallique isolé dans les années 1950,[10] dont la stabilité et la facilité de manipulation en ont fait l'initiateur de la chimie organométallique moderne.

Figure 2. Structure du ferrocène

D'un point de vue pharmaceutique, le ferrocène a prouvé ses qualités de groupement de choix : son insertion dans le squelette organique de différentes molécules bioactives s'est traduite par une augmentation de l'activité et/ou un élargissement du spectre thérapeutique, ainsi que par un contournement du phénomène de résistance aux médicaments.

Un exemple de ce phénomène est illustré par la ferroquine,[11] dérivé ferrocénique de la chloroquine ; ces deux molécules sont présentées en Figure 3. La chloroquine est un antipaludique découvert dans les années 1930 qui connaît beaucoup de problèmes de souches résistantes. La ferroquine est au contraire active sur plusieurs de ces souches,[12] ce qui en fait l'antipaludique numéro un de Sanofi-Aventis. La ferroquine est en phase II de tests cliniques.

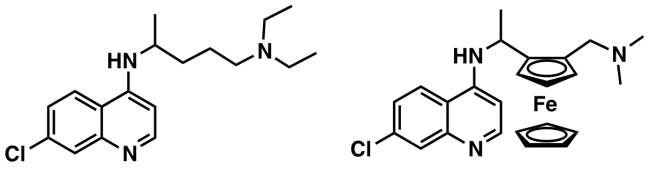

Figure 3. Structures de la chloroquine et de la ferroquine

Un autre exemple de molécule ferrocénique biologiquement active est le ferrocifène, dérivé ferrocénique du tamoxifène. Les métabolites actifs de ces deux molécules sont présentés en Figure 4. Le tamoxifène est un antagoniste de certains récepteurs à œstrogènes situés dans le sein, et à ce titre il enraye la prolifération du cancer du sein hormono-dépendant ; la prolifération de celui-ci est rythmée par la détection d'œstrogènes par ces récepteurs. Le spectre thérapeutique du tamoxifène est donc limité, à l'inverse de celui de son analogue ferrocénique qui est actif sur tout type de cancer du sein.[13] La source de l'activité de ces dérivés ferrocéniques semble être les propriétés redox du ferrocène, qui permettent une oxydation intramoléculaire produisant ainsi un métabolite toxique.[14]

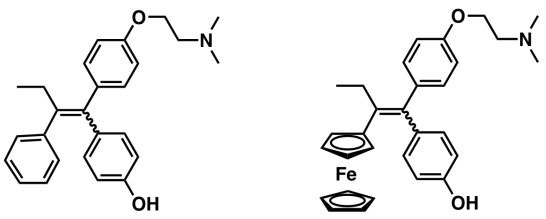

Figure 4. Structures de l'hydroxytamoxifène et de l'hydroxyferrocifène

Ainsi, la combinaison du ferrocène et des flavonoïdes semble être une voie prometteuse pour l'obtention de molécules bioactives. Les chalcones ferrocéniques sont connues depuis les années 1950,[15,16] bien que leurs activités biologiques n'aient été explorées que récemment.[17] Cependant, aucune des autres sous-classes de flavonoïdes n'avait été précédemment décrites ; l'objectif de ce travail a donc été de synthétiser plusieurs de ces sous-classes, ainsi que d'en explorer leurs propriétés, tant sur le plan chimique que biologique.

Résultats et discussion

Synthèse

Les chalcones étant les précurseurs chimiques et biochimiques des autres sous-classes de flavonoïdes, elles constituent le point de départ de notre étude. Par une simple condensation aldolique entre une acétophénone et l'aldéhyde du ferrocène, une série de 10 chalcones ferrocéniques, nommée série **1**, a été obtenue, et est présentée en Figure 5.

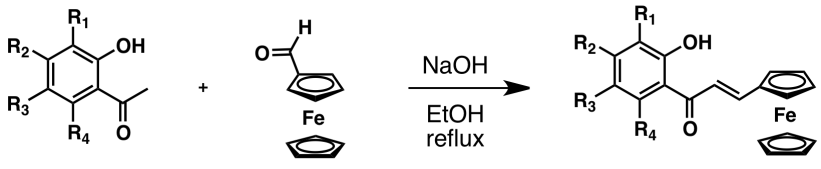

1a: R_1=R_2=R_3=R_4=H (81%)
1b: R_3=Cl (82%)
1c: R_3=Br (79%)
1d: R_1= R_3=Cl (82%)
1e: R_1=R_3=Br (76%)
1f: R_1=R_3=F (80%)
1g: R_2=OMe (80%)
1h: R_3=OMe (85%)
1i: R_4=OMe (81%)
1j: R_2=R_4=OMe (78%)

Figure 5. Synthèse de la série **1**

Leurs adduits qui possèdent une entité BF_2 présentent un intérêt particulier vis-à-vis du SIDA. Ces molécules, présentées en Figure 6, ont donc été synthétisées et représentent la série **2**.

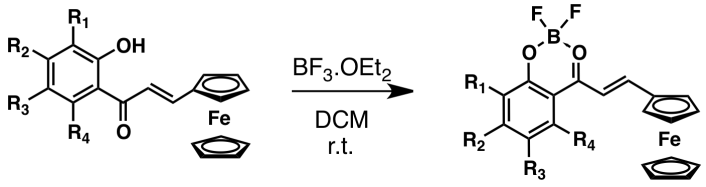

2a: R_1=R_2=R_3=R_4=H (80%)
2b: R_3=Cl (85%)
2c: R_3=Br (98%)
2d: R_1=R_3=Cl (84%)
2e: R_1=R_3=Br (67%)
2f: R_1=R_3=F (75%)
2g: R_2=OMe (84%)
2h: R_3=OMe (86%)
2i: R_4=OMe (82%)
2j: R_2=R_4=OMe (74%)

Figure 6. Synthèse de la série **2**

Dans l'optique d'accéder aux autres sous-classes de flavonoïdes, nous avons ensuite cherché à cycliser ces chalcones. La première série obtenue dans ces conditions a été la série des aurones ferrocéniques, nommée série **3**, qui résulte d'une cyclisation oxydante des chalcones. La synthèse de cette série est présentée en Figure 7. Nous avons aussi développé une procédure à partir de sels d'argent qui est ineffective sur les chalcones organiques.

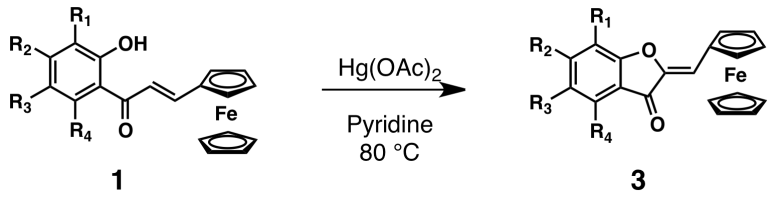

1 **3**

5a: R_1=R_2=R_3=R_4=H (75%)
5b: R_3=Cl (65%)
5c: R_3=Br (71%)
5d: R_1=R_3=Cl (64%)
5e: R_1=R_3=Br (60%)
5f: R_1=R_3=F (66%)
5g: R_2=OMe (75%)
5h: R_3=OMe (85%)
5i: R_4=OMe (66%)
5j: R_2=R_4=OMe (68%)

Figure 7. Synthèse de la série **3**

Au contraire des aurones organiques, les aurones férrocéniques soumises à une base forte se réarrangent en dérivés ynones. Trois représentants de cette famille ont été synthétisés, et sont présentés sous le nom de série **4** en Figure 8.

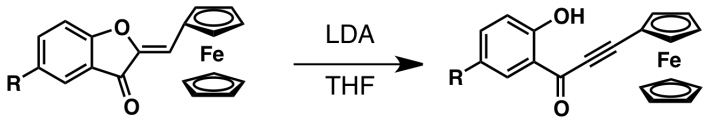

4a: R=H (78%)
4c: R=Br (65%)
4h: R=OMe (73%)

Figure 8. Synthèse de la série **4**

Ces dérivés, quand ils sont soumis à une base de type alcoolate, se cyclisent en flavones uniquement, série **5**. Cette sélectivité est également propre aux dérivés ferrocéniques : en série organique, un mélange flavone-aurone est obtenu,[18] et l'utilisation d'un catalyseur permet l'obtention exclusive de l'aurone.[19] Ceci étant, ce moyen de synthétiser les flavones n'est pas le plus efficace, et le traitement direct des aurones avec un alcoolate, ou encore leur isomérisation assistée par des sels de cyanure, présentée en Figure 9, est plus avantageuse.

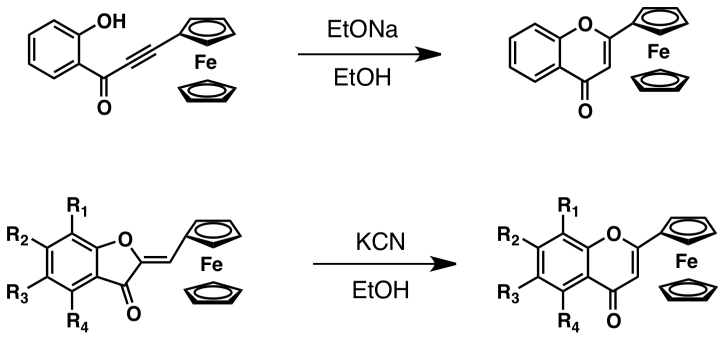

5a: R_1=R_2=R_3=R_4=H (88%)
5b: R_3=Cl (72%)
5c: R_3=Br (75%)
5d: R_1=R_3=Cl (60%)
5e: R_1=R_3=Br (55%)
5f: R_1=R_3=F (60%)
5g: R_2=OMe (70%)
5h: R_3=OMe (78%)
5i: R_4=OMe (68%)
5j: R_2=R_4=OMe (67%)

Figure 9. Synthèse de la série **5**

Enfin, certains flavonols ferrocéniques, série **7**, ont également été obtenus et ce à partir de la série **5**. Ce protocole ne constitue pas le protocole de choix dans la littérature, cependant les réactifs utilisés pour la synthèse de flavonols à partir de chalcones se sont révélés

incompatibles avec la présence du ferrocène. La synthèse de la série **7** est présentée en Figure 10.

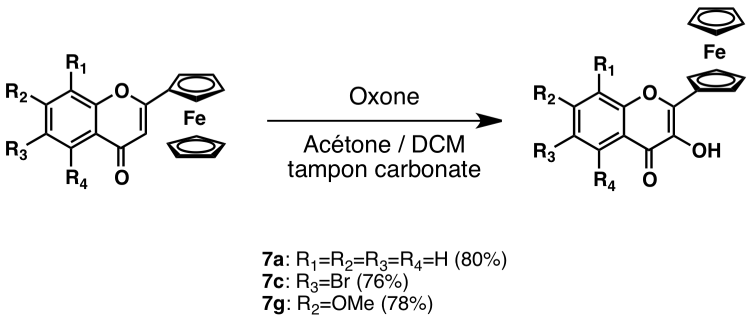

Figure 10. Synthèse de la série **7**

Aspect analytique des composés

Les composés appartenant aux différentes séries ont été décrits par les techniques usuelles, telles que la RMN, la spectrométrie de masse, les spectroscopies UV/visible et infrarouge, et enfin la cyclovoltamétrie. Plusieurs structures cristallographiques obtenues par diffraction des rayons X sont présentées dans ce travail. Leurs représentations réalisées avec le logiciel Mercury sont présentées en Figure 11.

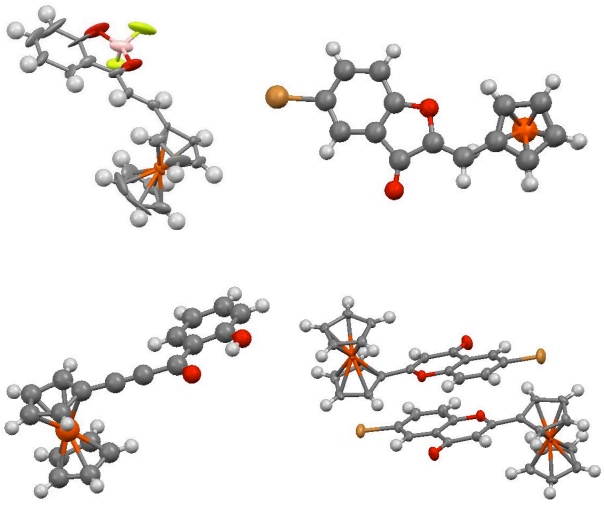

Figure 11. Représentation des structures RX de **2a** (en haut à gauche), **3c** (en haut à droite), **4a** (en bas à gauche) et **5c** (en bas à droite) réalisées avec le logiciel Mercury

Propriétés biologiques des composés

Les effets biologiques de ces molécules sur plusieurs cibles ont été évalués. Les molécules ont notamment été soumises au test MTT avec des cellules de mélanome de souris, lignée B16, afin d'évaluer leur potentiel antiprolifératif. Elles ont également été soumises à des expériences d'arrondissement de cellules endothéliales de type EA·hy 926, la présence duquel est indicatrice d'effets antiangiogéniques. Les molécules ont également été évaluées comme inhibiteurs de la protéine HIV intégrase, centrale dans le cycle de vie du SIDA. Enfin, leurs effets antibactériens ont été évalués sur une souche d'*Escherichia coli* et sur trois souches de *Staphylococcus aureus*. Pour chaque famille, seuls les résultats marquants sont présentés dans ce résumé.

La série **1** n'a pas présenté d'intérêt biologique majeur, mais plutôt un intérêt synthétique. Au contraire, les composés de la série **2** se sont remarquablement bien illustrés pour leurs qualités d'inhibiteurs d'HIV intégrase. Cette enzyme tire son nom de sa fonction qui est d'intégrer le génome pro-viral dans le génome hôte. Ce phénomène se décompose en deux processus : 3'P, qui prépare le génome pro viral, et ST, qui l'insère. L'activité des séries **1** et **2** à cet égard est présentée en Table **1**.

Table 1. IC_{50} (μM) de **1a**-**j** et **2a**-**j** pour l'inhibition de HIV intégrase

Composé	R	3' P	ST	IS
1a	H	>20	>20	--
2a		10.7 ± 4.25	6.0 ± 2	0.6
1b		n.d.	n.d.	--
2b	5-Cl	5.6 ±4.13	6.0 ± 4.36	1.1
1c		>20	>20	--
2c	5-Br	4.6 ± 0.53	5.7 ± 4.73	1.2
1d		n.d.	n.d.	--
2d	3,5-diCl	7.8± 2.93	0.7 ± 0.14	0.1
1e		>20	>20	--
2e	3,5-diBr	4.3 ±2.52	3.6 ± 3.84	0.8
1f		12	6.2	--
2f	3,5-diF	5.0 ± 2.83	2.0 ±0.2	0.4
1g		>20	>20	--
2g	4-OMe	4.7 ± 1.53	2.6 ± 1.15	0.5
1h		14	10.3	--
2h	5-OMe	8.7 ± 1.53	7.3 ± 4.6	0.8
1i		>20	>20	--
2i	6-OMe	16.3 ± 7.52	9.3 ± 2.31	0.6
1j		>33	11.6	--
2j	4,6-diOMe	10.5 ± 5.6	7.6 ± 5.56	0.7

Les aurones ferrocéniques, série **3**, se sont quant à elles illustrées pour leurs propriétés antibactériennes, comme le montre la table 2 qui présente les CMI (concentrations minimales inhibitrices) pour différentes souches bactériennes. Les résultats sur *S. aureus* se trouvant entre 5 et 10 µM sont très intéressants. D'une manière générale, les composés sont plus actifs sur la souche MsrA, qui est une souche résistante surexprimant une pompe d'efflux, tout comme la souche 1199B. Le meilleur résultat est obtenu pour le composé **3j**, avec une CMI de 5 µM sur la souche MsrA.

Table 2. Détermination des CMI des composés les plus actifs de la série **3** (µM)

	E. coli ATCC25922	*S. aureus* ATCC25923	*S. aureus* 1199B	*S. aureus* MsrA
3a	100	100/25	25	12.5
3g	44/22	11	11	5.5
3h	88	22	44	22
3i	44	11	11	11
3j	40/20	10	10	5

Les flavones ferrocéniques, série **5**, se sont quant à elles démarquées en raison de leur caractère prometteur contre le cancer. Leurs résultats d'activité sont présentés avec ceux de la série **6**, équivalent organique de la série **5**. Les premiers tests ayant été menés concernent les effets antiprolifératifs des séries **5** et **6** sur des cellules de mélanome (B16) chez la souris. Les résultats sont présentés en Figure 12. Bien que plus actives que leurs analogues organiques, les molécules de la série **5** ont des effets antiprolifératifs très faibles.

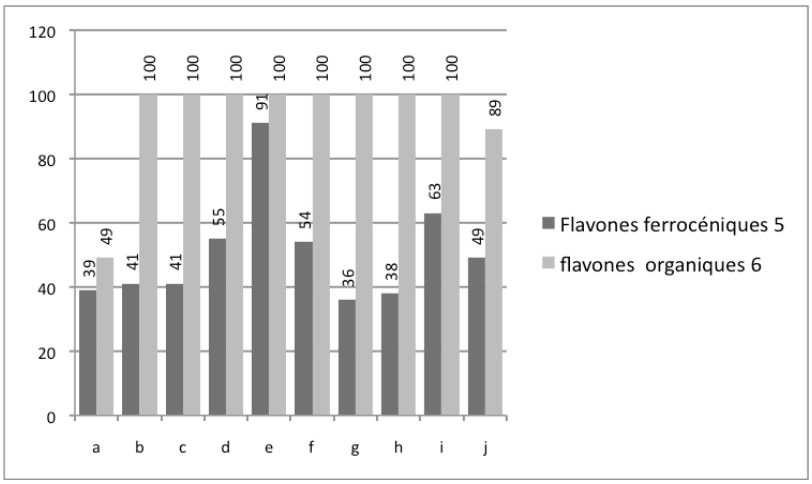

Figure 12. Valeurs d'IC_{50} (µM) des composés **5a-j** et **6a-j** sur des cellules B16 de mélanome chez la souris

Les effets antiangiogéniques de ces molécules ont également été évalués, par arrondissement de cellules endothéliales. Les résultats des séries **5** et **6** sont présentés en Figure 13.

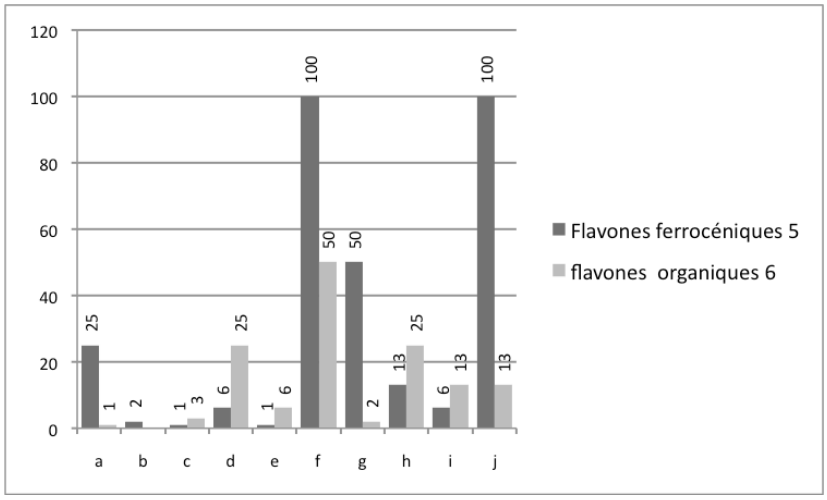

Figure 12. Concentration minimum (μM) pour l'arrondissement de cellules EA·hy 926 par **5a-j** and **6a-j**

La première observation est que les valeurs obtenues sont basses, ce qui est la preuve d'une grande activité. De plus, aucun parallèle ne peut être établi entre la série **5** et la série **6**, ce qui suggère que la présence du ferrocène induit un mode d'action différent pour ces molécules. Enfin, un intérêt particulier doit être porté à la molécule **5e** qui possède une concentration minimale d'arrondissement très basse, ainsi qu'une très faible cytotoxicité sur les cellules B16 : cette molécule semble donc être un agent purement antiangiogénique.

Conclusion

Les flavonoïdes forment une des familles d'antioxydants les plus étendues. Ils présentent une incroyable diversité de propriétés biologiques, aussi bien sur les organismes végétaux qu'animaux. Du fait de leur caractère antioxydant, ils protègent les mammifères contre toute sorte d'agressions et de maladies, comme par exemple le cancer.

La combinaison de molécules bioactives avec une entité ferrocénique est connue en chimie médicinale pour augmenter aussi bien leur activité que leur spectre thérapeutique. C'est cette stratégie qui nous a conduit à la synthèse des premiers dérivés flavones, aurones et flavonols ferrocéniques, à partir des chalcones. Ce travail présente la conception, la synthèse et la caractérisation chimique et biologique de tels composés.

De mêmes que pour les dérivés organiques, les effets biologiques des flavonoïdes ferrocéniques sont très variés, et certaines molécules sortent du lot pour chacun des maux testés ; ces dérivés sont présentés en Figure 13. Le dérivé **2d** possède d'intéressantes propriétés en tant qu'inhibiteur de l'enzyme HIV-intégrase. Le dérivé **3j** est un agent antibactérien prometteur, efficace contre la souche résistante *S. aureus* MsrA. Enfin, le dérivé **5e** possède d'intéressantes caractéristiques antiangiogéniques.

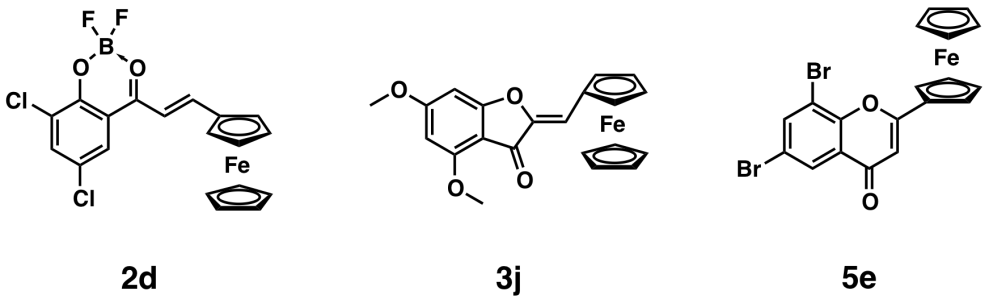

2d **3j** **5e**

Figure 13. Composés possédant les activités biologiques les plus intéressantes.

Ce travail montre que la combinaison du ferrocène avec un squelette flavonoïde donne accès à d'intéressantes molécules bioactives. De plus, la chimie développée pour la synthèse de ces composés est originale et présente de nouvelles réactivités et sélectivités.

Références

1 : Williams, C. A.; Grayer, R. J. “Anthocyanins and other flavonoids” *Nat. Prod. Rep*. **2004** 21(4), 539-573

2 : Rausher, M. D. *The science of flavonoids* **2006** chap.7; New York: Springer, 2006

3 : Lois, R.; Buchanan, B. B. “Severe sensitivity to ultraviolet radiation in an Arabidopsis mutant deficient in flavonoid accumulation” *Planta* **1994** 194, 504-509

4 : Buer, C. S.; Djordjevic M. A. “Architectural phenotypes in the transparent testa mutants of *Arabidopsis thaliana*” *J. Exp. Bot.* **2009** 60, 751-763

5 : Napoli, C. A.; Fahy, D.; Wang, H. Y.; Taylor, L. P. “*White anther*: A petunia mutant that abolishes pollen flavonol accumulation, induces male sterility, and is complemented by a chalcone synthase transgene” *Plant Physiol*. **1999** 120, 615-622

6 : DeFelice, S. L. *Scrip Mag.* **1992** « Nutraceuticals: Opportunities in an Emerging Market »

7 : Ferrières, J. “The French paradox: lessons for other countries” *Heart* **2004** 90, 107-111

8 : Corder, R.; Mullen, W.; Khan, N. Q.; Marks, S. C.; Wood, E. G.; Carrier, M. J.; Crozier A. “Oenology: Red wine procyanidins and vascular health” *Nature* **2006** 444, 566

9 : Pietta, P.-G. “Flavonoids as Antioxidants” *J. Nat. Prod.* **2000** 63, 1035-1042

10 : Kealy, T. J.; Pauson, P. L. “A New Type of Organo-Iron Compound” *Nature* **1951** 168,1039-1040

11 : Biot, C.; Glorian, G.; Maciejewski, L.A.; Brocard, J.S. “Synthesis and antimalarial activity *in vitro* and *in vivo* of a new ferrocene-chloroquine analogue” *J. Med. Chem.* **1997** 40, 3715–3718

12 : Delhaes, L.; Abessolo, H.; Biot, C.; Berry, L.; Delcourt, P.; Maciejewski, L.A.; Brocard, J. S.; Camus, D.; Dive, D. “*In vitro* and *in vivo* antimalarial activity of ferrochloroquine, a ferrocenyl analogue of chloroquine against chloroquine-resistant malaria parasites” *Parasitol. Res.* **2001** 87(3), 239-244

13 : Top, S.; Vessieres, A.; Leclercq, G.; Quivy, J.; Tang, J.; Vaissermann, J.; Huché, M.; Jaouen, G. “Synthesis, Biochemical Properties and Molecular Modelling Studies of Organometallic Specific Estrogen Receptor Modulators (SERMs), the Ferrocifens and Hydroxyferrocifens: Evidence for an Antiproliferative Effect of Hydroxyferrocifens on both Hormone-Dependent and Hormone-Independent Breast Cancer Cell Lines” *Chem. Eur. J.* **2003** 9, 5223–5236

14 : Hillard, E. A.; Vessières, A.; Thouin, L.; Jaouen, G.; Amatore, C. “Ferrocene-mediated proton-coupled electron transfer in a series of ferrocifen-type breast cancer drug candidates” *Angew. Chem. Int. Ed.* **2006** 45, 285 –290

15 : Hauser C. R.; Lindsay, J. K. “Certain Acylations of Ferrocene and Some Condensations Involving the α-Hydrogen of Acetylferrocene” *J. Org. Chem.* **1957** 22(5), 482-485

16 : Hauser C. R.; Lindsay, J. K. “Some Typical Aldehyde Addition and Condensation Reactions of Formylferrocene” *J. Org. Chem.* **1957** 22(8), 906–908

17 : Wu, X.; Wilairat, P.; Go, M. L. “Antimalarial Activity of Ferrocenyl Chalcones” *Bioorg. Med. Chem. Lett.* **2002** 12, 2299–2302

18 : Garcia, H.; Iborra, S.; Primo, J.; Miranda, M. A. “6-Endo-Dig vs. 5-Exo-Dig ring closure in o-hydroxyaryl phenylethynyl ketones. A new approach to the synthesis of flavones and aurones.” *J. Org. Chem.* **1986** 51(23), 4432-4436

19 : Harkat, H.; Blanc, A.; Weibel, J.-M.; Pale, P. “Versatile and Expeditious Synthesis of Aurones via Au(I)-Catalyzed Cyclization.” *J. Org. Chem.* **2008** 73(4), 1620-1623

Table of contents

Chapter 1

Flavonoids and ferrocene-containing molecules as bioactive agents

A. Flavonoids

"Flavonoids may have existed in nature for over 1 billion years and thus have interacted with evolving organisms over the eons. ... The very long association of plant flavonoids with various animal species and other organisms throughout evolution may account for the extraordinary range of biochemical and pharmacological activities of these chemicals in mammalian and other biological systems". T.C. Theoharides [1]

Indeed, with over 9000 natural known derivatives, flavonoids are omnipresent in the plant kingdom, where they are produced, as well as in animal kingdom, where they are taken in *via* the diet.[2] Being synthesized since the appearance of the very first plants on Earth, these secondary metabolites are crucial at all stages of the plant and animal life cycle, and subsequently interact with many biological entities. The beneficial effects of flavonoids on human health are also well-known, and have become a very popular field of study. Typing "flavonoid" in Scifinder results in more than 88 000 answers, including more than 40 000 since 2005. Companies selling parapharmaceutical products often use "flavonoids" in their

advertising, as this term has become synonymous with health. For example, Figure 1.1 presents a nutritional supplement of the brand “Flavin 7”.

Figure 1.1. Advertising for the brand “Flavin7”

1. Flavonoids: definition and nomenclature

Flavonoids are low molecular weight molecules, with a structure consisting of two phenyl rings, ring A and ring B, linked by a three carbon atom bridge. This class of molecules is divided into several subgroups, depending on the functions present in the structure. The main subgroups are presented in figure 1.2.

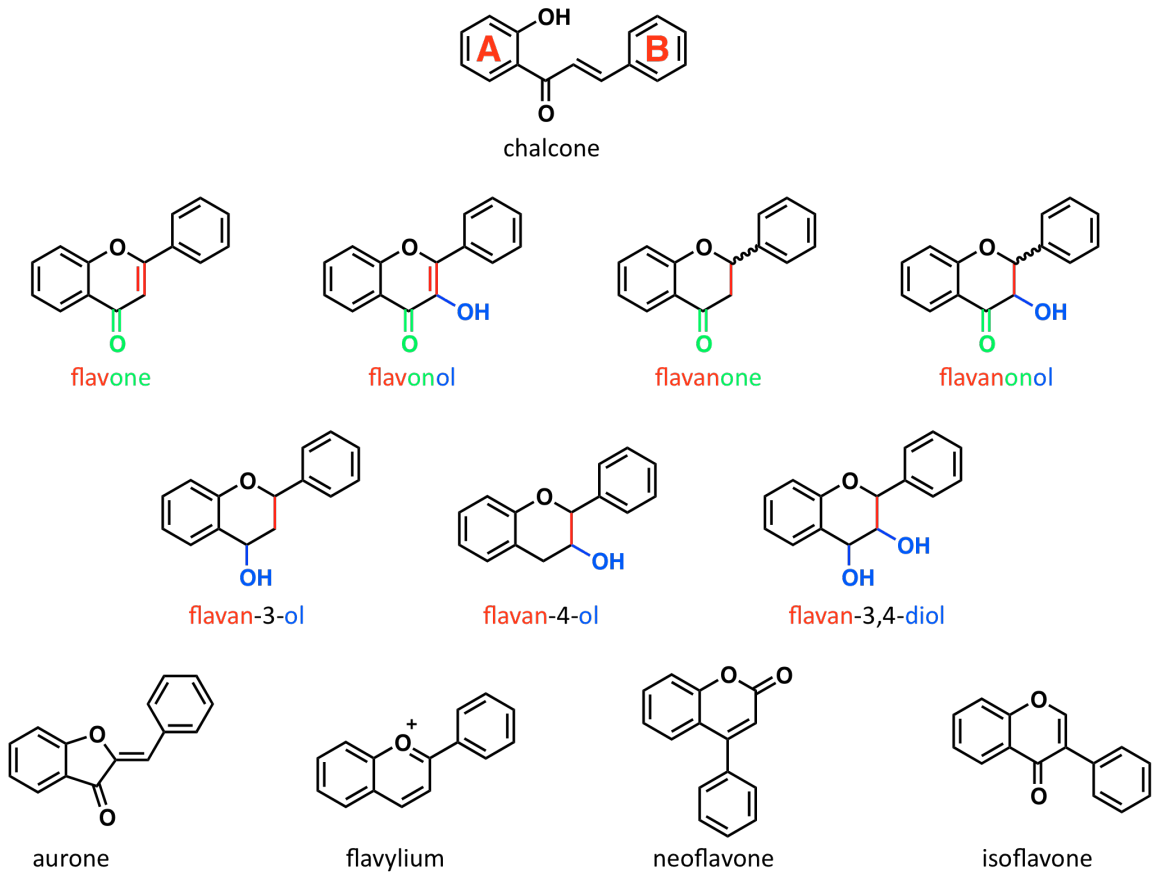

Figure 1.2: Principal subclasses of flavonoids.

Chalcones are the chemical and biochemical precursors of all the other subclasses of flavonoids. The prefix “flav” derives from the Latin “flavus”, meaning “yellow”, and corresponds to the three carbon atom chain in the form of an unsaturated 6-membered ring (in red). By contrast, the prefix “flavan” corresponds to the same ring, but in its saturated form. The suffix “on” or “one” refers to the presence of a ketone function (in green). Similarly, the suffix “ol” corresponds to the presence of a hydroxy group on the heterocycle. Aurones are flavone isomers, possessing a benzofuranone instead of a benzopyranone motif. Anthocyanidins, flavylium ion derivatives, correspond to the aromatized form of the three carbon chain. Finally, neoflavone and isoflavone are isomers of flavone, possessing the B-ring and/or the ketone function in different positions of the three carbon atom chain.

2. Flavonoids in the plant kingdom

2.1. Biosynthesis

Flavonoids are only biosynthesized by plants. They are secondary metabolites, meaning that they are not essential for short-term plant survival. Indeed, several studies in the literature compare mutants that do not produce certain flavonoids with the wild-type organism. Although weakened by the lack of flavonoids, the mutants are able to survive.[3]

In fact, it even seems that flavonoids appeared by "mistake",[4] during the era when the earliest forms of plants, the bryophytes*, emerged from the sea and started to colonize the land. Bryophytes possess the first three enzymes of the flavonoid biosynthetic pathway: chalcone synthase (CHS) chalcone-flavanone isomerase (CHI) and flavanone 3-hydroxylase (F3H), and thus can biosynthesize chalcones, flavanones and flavanonols. Similarities between the genetic sequence coding for these enzymes and the sequence coding for enzymes of primary metabolism strongly suggest that their appearance is due to a mutation of the original genetic sequence of another enzyme. For example, the CHS genetic sequence exhibits strong similarities with genes coding for polyketide synthases in bacteria,[5] and their function is in fact very similar.

As with any evolutionary phenomenon, the production of such molecules led to favorable effects on early plants. The initial advantages given by flavonoids remain unclear and two schools of thought exist on this subject. One suggests that plants used flavonoids for their UV absorption properties,[6] so that they acted as a protective sunscreen. This hypothesis is supported by several facts: flavonoids appeared with the very first organisms present on earth, even the simplest flavonoids absorb UV light, and mutants that do not produce flavonoids are very sensitive to UV light.[7,8] The other hypothesis suggests that flavonoids first regulated plant hormones.[9] For example, their contribution to auxin transport has been shown in angiosperms (more specific examples are detailed in section 2.2.b).[10, 11]

The flavonoid pathway is a branch of the phenylpropanoid pathway, which uses phenylalanine as a primary substrate. Through evolution, plants have created many other enzymes, even lost some, and the flavonoid pathway has become quite intricate.[3] This

* The term "bryophyte" is still employed for current plants, like mosses for example.

complexity can be seen even in a highly simplified representation of flavonoid synthesis in *Arabidopsis*, a small flowering plant often used as a model in biology (Figure 1.3).

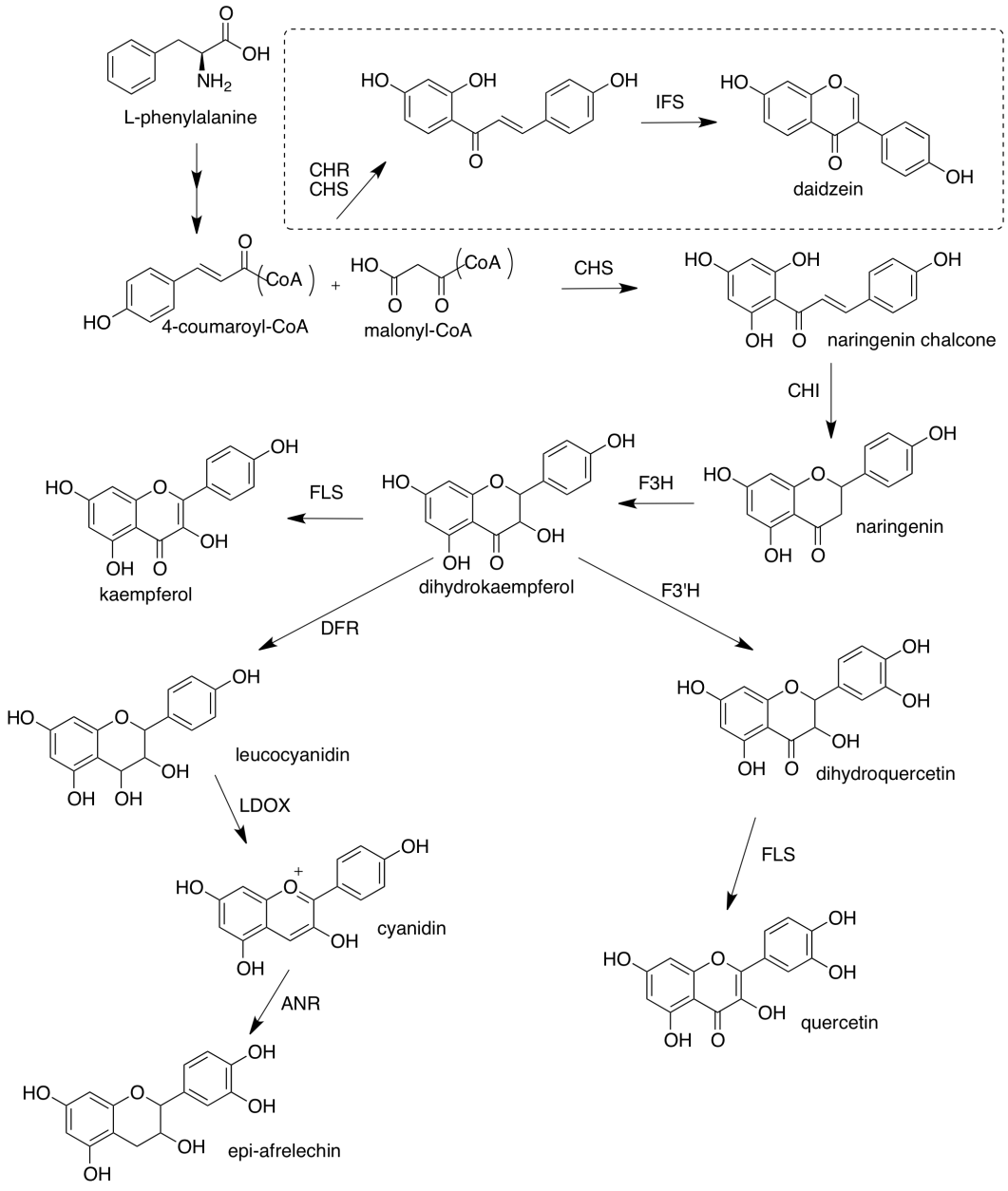

Figure 1.3: The flavonoid pathway in *Arabidopsis*.

The first step of the flavonoid pathway involves chalcone synthase (CHS). In *Arabidopsis*, the second step involves chalcone-flavanone isomerase (CHI), whose role is to cyclize the chalcone to form a bicyclic system. In the presented pathway, the molecule obtained

following the scheme is naringenin. The third step of this pathway involves the action of flavanone-3-hydroxylase (F3H), thus resulting in the production of a flavanonol, in this case dihydrokaempferol. This combination of these three enzymes constitutes the foundation of flavonoid biosynthesis.

From the flavanonols, many different structural modifications are possible, some of which are detailed in Figure 1.3. The presence of dihydroflavonol 4-reductase (DFR) results in the production of a flavan-3,4-diol, in this case leucocyanidin. The action of leucoanthocyanidin dioxygenase (LDOX), gives the cyanidin salt, which can then be reduced by anthocyanidin reductase (ANR) thus producing epi-afrelechin, which belongs to the flavan-4-ol subclass.

Another branch of the flavonoid pathway, starting from dihydrokaempferol, results in the synthesis of quercetin, which is without any doubt the most well-known flavonoid derivative. The action of flavonoid 3'-hydroxylase (F3'H) in grafting a hydroxyl group on the B-ring of dihydrokaempferol results in the production of dihydroquercetin, which is then oxidized into the flavonol quercetin by flavone synthase (FLS).

Although well investigated through the analysis of several mutants, the *Arabidopsis* flavonoid pathway is quite limited; for example, *Arabidopsis* doesn't produce isoflavone, which is however present in legumes. Indeed, the presence of chalcone reductase (CHR), whose action is inverted compared to F3'H, together with isoflavone synthase (IFS) allow some plants to biosynthezise isoflavones, such as daidzein.

The least extended subclass of flavonoids is without any doubt the aurone subclass. Their name comes from "aurum", gold in Latin, due to their bright yellow color. In 2001, Nakamaya isolated the enzyme responsible for their biosynthesis, aureusidin synthase, from *Antirrhinum majus*.[12]

The schematic biosynthetic pathway presented previously explains the formation of most of the flavonoid skeletons, and also shows the addition of hydroxyl groups in different positions of the molecules. However, natural flavonoids often present methoxy groups instead of hydroxyl groups, or exhibit a complex glycosylation pattern.[13] These substitutions are responsible for the very broad structural and functional diversity of these molecules. Indeed, these modifications often result in the ultimate bioactive properties of flavonoids,

modulating their color and enhancing their reactivity and solubility. Moreover, the enzymes being very species-specific, structural modifications permit the regulation of the biosynthetic pathway itself.

The two main classes of enzymes implicated in these last modifications are flavonoid methyltransferases and flavonoid glycotransferases. These enzymes are very regiospecific. As an example, the action of a flavonoid O-methyltransferase (OMT) isolated from *Mesembryanthemum crystallinium* is presented in Figure 1.4.[14]

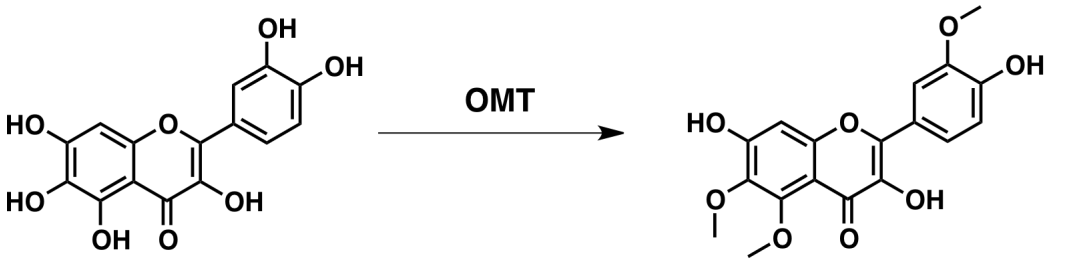

6-hydroxy quercetin

3,7,4'- trimethyl 6-hydroxy quercetin

Figure 1.4: Action of OMT on 6-hydroxy quercetin

The solubility of flavonoids is crucial in their transport and storage in biological media. Therefore, glycosylation is a key step at the last stage of their biosynthesis. An example of glycosylation sequence is shown in Figure 1.5. In this Figure, rhamnosylisoorientin, a poly-glycosylated form of luteolin, is obtained *via* the action of two flavonoid glycotransferases, glucosyl transferase (GT) and rhamnosyl transferase (RT).[15] Glycosylation is at the heart of some controversy concerning the beneficial effects of flavonoids in the human diet. Because flavonoids can also be glycosylated in animals, they are rapidly excreted in urine and are not available to cells.

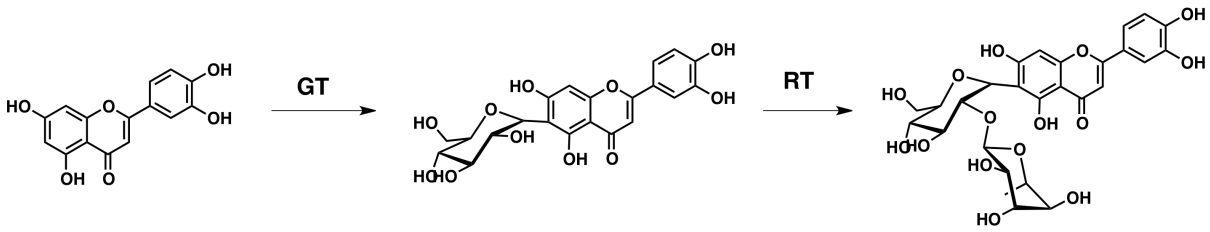

Figure 1.5: Successive glycosylations of luteolin

2.2. Role of flavonoids in plants

The huge diversity in structure, through both the different subclasses and the different substitutions, generates a similar diversity in the roles of flavonoids. Flavonoids are present in all parts of the plant, and at all stages of the plants life cycle. That said, while many of their activities have been experimentally measured, the precise mechanisms of action often remain elusive.

2.2.a. Nucleus level

Several biological entities are known to be molecular targets of flavonoids. The influence of flavonoids on plants starts inside the nucleus of the cell itself, by affecting primary biological functions, such as genetic transcription.[16] Many reports of flavonoids found inside the nucleus of plant cells can be found in the literature, and they mainly concern flavonol and flavanol derivatives.[17-22] More precisely, Feucht and coworkers have shown that catechins (flavan-3-ol derivatives) have the ability to bind with histone,[22] suggesting their involvement in genetic transcription. He has also reported the presence of flavonoids in the nucleus of a number of plants.[21, 22]

In addition, naringenin chalcone and apigenin (Figure 1.6) may influence flavonoid biosynthesis by regulating the transcription of flavonoid biosynthesis enzymes.[23, 24] Finally, Winkel and coworkers have shown the presence of CHS and CHI in both the cytoplasm and the nucleus of *Arabidopsis thaliana.*[20]

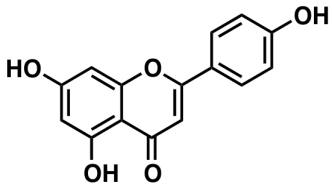

Figure 1.6: Structure of apigenin

2.2.b. Enzyme activity and hormonal function

One of the most remarkable influences of flavonoids in plants is their impact on the plant's architecture, principally due to their effects on auxin transport.[25] Auxin is a growth phytohormone that is absolutely necessary for plant development. Buer and coworkers studied wild-type *Arabidopsis thaliana* and its mutant form,[26] where the flavonoid biosynthetic pathway had been genetically modified. He demonstrated that the architecture of the plant is dependant on flavonoid biosynthesis, and that different mutations affecting this pathway produce different phenotypes. From root growth to the number of flowers, the consequences of these mutations implicate, for example, the stature of the plant and seed density. Supplementation with flavonoids restored the wild-type characteristics, showing the unambiguous source of these variations.[3]

The distribution of auxin throughout the plant begins in the roots, from which it is then transported to the other parts of the plant. Inside the cells, auxin can only be transported *via* anionic efflux carriers. Flavonoids are known to be able to compete with other efflux inhibitors (like NPA), thus suggesting their ability to control auxin efflux.[27] Bernasconi has shown that genistein (Figure 1.7) could modulate the phosphorylation state of proteins associated with auxin efflux, through inhibition of kinases.[28] The observation that flavonoids, and especially flavonols, can interact and modulate PID (a protein kinase needed for proper organ formation) has been well documented.[11]

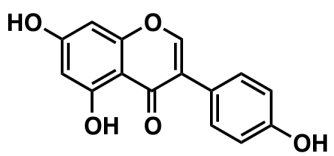

Figure 1.7: Structure of genistein

2.2.c. Role in reproduction

Flavonoids play a major role in the reproduction of a number of plant species. They accumulate in most flowers and pollen, and flavonoid-deficient mutants are generally sterile males, like in the case of petunia.[29, 30] In other plants, such as *Arabidopsis,* such mutants are fertile, but exhibit a reduced seed set.[31] Kaempferol intake promotes pollen germination in these mutants, showing the flavonoid-dependant character of this process.

More externally, certain flavonoids, especially anthocyanidins and flavonols, also contribute to reproduction by influencing the appearance of the plant. The anthocyanidins are strongly colored, and are present in most flower petals. Natural pollinators, such as bees or birds, will often prefer a colored flower, thus enhancing the reproduction yield of the concerned plant.[32, 33] In addition, UV-fluorescent flavonols act as nectar guide for bees and other insects.[34]

2.2.d. Extraorganism level

The effects on reproduction are not the only example of flavonoid-mediated interactions with other organisms. Certain symbioses between plants and fungi need flavonoids to operate. For example, *Arbuscular mycorrhizae*, a fungus found in plant roots, causes an accumulation of quercetin and rhamnetin (Figure 1.8) in clover roots, while this phenomenon doesn't occur in non-symbiotic clover.[35] This suggests that flavonoids may play a role in the infection of the clover by the fungi. Similarly, under low phosphate conditions, melons produce certain flavonoids that increase mycorrhizal colonization, and subsequently enhance phosphate uptake.[36]

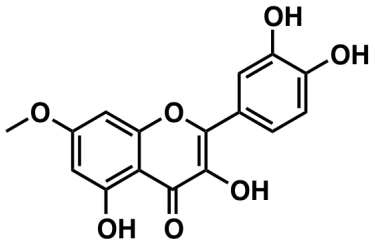

Figure 1.8: Structure of rhamnetin

Flavonoids are also able to protect plants from infectious fungi, such as in the case of taxifolin (Figure 1.9), a flavonol known to be an antifungal agent in pine.[37, 38, 39]

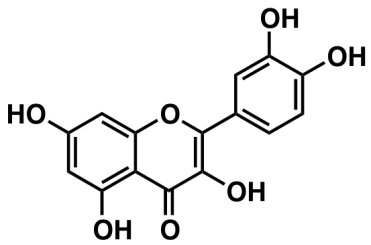

Figure 1.9: Structure of taxifolin

Plant-microbe interactions are very similar to plant-fungi interactions. The flavonoid can either act as an antimicrobial agent in the case of pathogens,[40] or favor symbiosis. A good example of such symbiosis is nodulation. This phenomenon occurs when legumes (pea or clover for example), in association with *Rhizobia* bacteria, form nitrogen-fixing nodules to enhance the legumes' nitrogen intake. For nodulation to occur, the legume must possess flavonoids that are perceived by the bacteria as a signal to activate the transcription of the *nod* gene, and subsequently form a nodule. This recognition is flavonoid-specific: naringenin induces nodulation by *Rhizobium leguminosarum* in pea, while quercetin inhibits nodulation.[41]

Flavonoids are very versatile molecules, and the plant kingdom uses them for many purposes, exploiting their structural properties as well as their photochemical properties. One of the main impacts of flavonoids is their interactions with proteins, such as with kinases for example.[11, 28] Another important property is the antioxidant character of these molecules, which protect organisms against ROS.[25] In this regard, some parallels between the plant and animal kingdom can be found.

3. Flavonoids in the animal kingdom

Although flavonoids are only produced by plants, they have a variety of activities in all types of organisms. In this section, we will be more specifically interested in their role in

mammals. As mentioned previously, parallels can be established between the animal and the plant world, especially concerning flavonoid-protein interactions and their antioxidant behavior. The present section will detail these two aspects more specifically, using selected examples.

3.1. Flavonoids and proteins

3.1.a. Flavonoids and cell membranes

Cell membranes present many proteins on their surface, some of them regulating what enters or leaves the cell. Similar to PIN proteins, the channels implicated in auxin transport, permeability glycoproteins (PGPs) are efflux proteins in mammals. Efflux proteins are often responsible for drug multiresistance in tumor cells. To circumvent this phenomenon is a great medical challenge. Flavonols and isoflavones such as quercetin, kaempferol or daizein, are known to alter the function of PGPs. For example, they have been shown to sensitize colon epidermal carcinoma KB-V1 cells to chemotherapeutic agents, such as paclitaxel or vinblastine, without having any impact on equivalent PGP-lacking KB3.1 cell lines.[42] In this case, we can observe that the addition of a non-cytotoxic sensitizing agent to an existing therapy can extend its therapeutic spectrum, and provide a solution to the multiresistance problem.

Glucose transporters, (GLUTs) are a family of membrane-spanning proteins that are responsible for insulin-mediated glucose uptake in cells. Flavonoids, such as quercetin, myricetin and catechin-gallate (Figure 1.10) are known to inhibit glucose uptake mediated by GLUT4, a predominant member of this family of transporters in isolated rat adipocytes.[43] Morover, genistein, quercetin, myricetin, rhamnetin and isorhamnetin (Figure 1.10) inhibit GLUT1-mediated glucose transport through a direct interaction with this protein.[44]

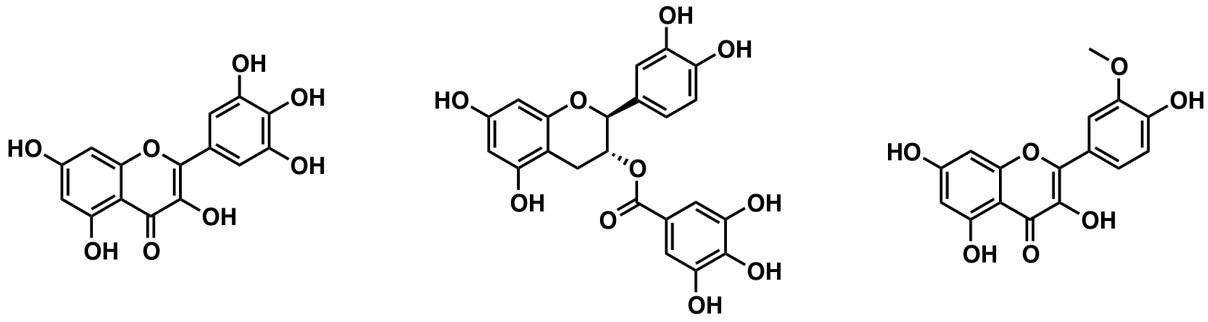

Figure 1.10: Structures of myricetin and catechin gallate and isorhamnetin

In addition to the regulation of membrane proteins, flavonoids are also able to directly influence the nature of the lipid bilayer of the membrane, by modifying its fluidity.[45]

3.1.b. HIV proteins

A remarkable example of flavonoid-enzyme interactions pertaining to a very crucial subject for current medicine is their interactions with HIV proteins. HIV treatment strategies are mostly oriented towards the inhibition of the three main enzymes of the HIV life cycle: reverse transcriptase (RT), integrase (IN) and protease (PR). Current treatments for HIV usually contain a combination of RT and PR inhibitors.

HIV belongs to the retrovirus family, meaning that its original genetic material is RNA. The role of RT is to produce DNA from RNA, in order to transfer its genes into the host cells. Kitamura has shown that the flavone baicalin (Figure 1.11) inhibits the replication of the HIV virus, probably due to the demonstrated affinity of this molecule for RT.[46] Other examples of inhibition of non-HIV RT by flavonoids are widely described in the literature.[47]

Once the proviral DNA is produced, it is inserted into the host DNA *via* the enzyme IN. Fesen has shown that quercetin is able to inhibit IN,[48] and has performed a structure-activity relationship study on the subject.[49] Inhibition of IN will be more widely detailed in a further section.

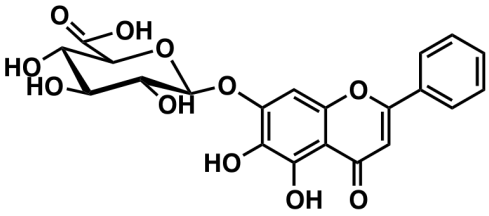

Figure 1.11: Structure of baicalin

Once the viral genes are implanted in the host cell genome, the cell produces polyproteins. Another crucial step of the HIV replication is the transformation of the newly created polyproteins in mature proteins, which confers to the virions their infectious properties. This step corresponds to the PR action. Therefore, the inhibition of this protein would leave the virions non infectious, and would block HIV proliferation. Several flavonols, such as fisetin, morin (Figure 1.12), quercetin and myricetin have been shown to inhibit PR.[50]

fisetin morin

Figure 1.12: Structures of fisetin and morin

3.1.c. Flavonoid-kinase interactions

As a consequence of their structural similarities with adenosine triphosphate (ATP), flavonoids, and especially flavones, flavonols[13] and aurones[51] possess good affinity with ATP-binding proteins, such as protein kinases. These enzymes catalyze the phosphorylation of proteins from ATP, and are therefore crucial for cell signaling. Their functions are extremely varied, for example they are implicated in cell growth, cell proliferation and apoptosis.[13] Protein kinase inhibitors are therefore excellent candidates to treat diseases

caused by cell growth dysregulation, such as cancer or polycystic kidney disease, for which the protein kinase inhibitor PLX5568 is currently under clinical trials.

There are many examples of flavonoid kinase inhibition. Protein kinase C (PKC), a family of mammalian kinases, control the function of other proteins *via* phosphorylation; their impact is extremely broad, affecting for example tumor promotion, secretory processes, and T lymphocyte function.[52] Similarly, phosphoinositide 3-kinases (PI 3-kinases) are a family of enzymes that specifically catalyze the phosphorylation of inositol lipids, and play a crucial role in cell signaling and in regulating cellular functions, including proliferation, apoptosis and cytoskeleton organization among others.[53, 54] Flavonoids have been shown to inhibit PKC *in vitro*,[55] while Middleton and coworkers have shown that fisetin and luteolin blocks the ATP binding site on the catalytic unit of PKC.[56]

Myosin light chain kinase (MLCK), which plays a crucial role in the proliferation and the migration of human breast cancer cells,[57] has been extracted from bovine aorta and exposed to different flavonoids. Kaempferol was shown to be a specific inhibitor.[58] Protein tyrosine kinase (PTK), which is implicated in many different biological functions, such as cell growth, gene expression and cell mobility,[59] is inhibited by genistein;[60] rabbit muscle phosphorylase kinase is inhibited by quercetin and fisetin, while the flavanone hesperetin (Figure 1.13) stimulates this enzyme.[61]

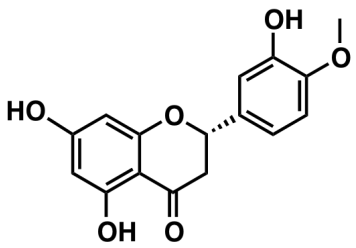

Figure 1.13: Structure of hesperetin

Some protein kinases are also involved in the generation of cancer cells, such as members of the mitogen-activated protein kinase (MAPK) family. When activated by external stimuli, such as stress or UV-irradiation, they play a critical role in transmitting signals to tumor

promoters. Evidence strongly suggest that the activation of MAPKs by such promoters plays a functional role in malignant transformation.[62] Different flavonoids, such as epigallocatechin (Figure 1.14), inhibit the activation of MAPKs.[63]

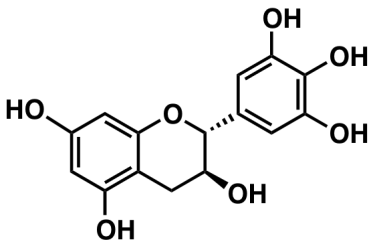

Figure 1.14: structure of epigallocatechin

3.1.d. Flavonoids and the immune system

The immune system is a highly complex machine, constituted of many different types of cells that are essential to good health. The cells of the immune system can either interact directly with other cells (cell-cell interactions), or *via* signaling compounds, such as hormones or cytokines. Flavonoids can interact at different levels of this system, especially by interacting with protein kinases involved in inflammatory processes, as presented below.

T lymphocytes belong to the family of white blood cells. Their action is broad, including for example T-cell-mediated immunity. Their growth is thought to be induced by protein tyrosine kinases (PTKs), such as p56.[64] Atluru and coworkers have shown that genistein inhibits T cell proliferation without any toxic effect.[65] PTKs are known to be generally sensitive to flavonoids. However, their action is not universal, since flavonoids do not have the same impact depending on their substitutions or on the cellular source of PTKs. For example, genistein is inactive against purified bovine thymocyte PTK (p40).[66]

Natural killer cells (NKC) are a type of cytotoxic lymphocyte that play a major role against tumors. When activated, they release proteins such as perforine and granzyme causing apoptosis of the target cell. In this case, again, the influence of flavonoids can be observed. Flavone acetic acid (Figure 1.15), also called FAA, is a synthetic flavonoid that reached phase

II clinical trials as anti-cancer agent. FAA exhibits antitumor activity against renal tumors in mice, and enhances NKC activity *in vivo*. [67,68]

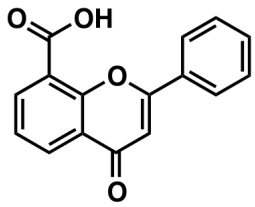

Figure 1.15: Structure of flavone acetic acid (FAA)

Mast cells are found in many types of tissues, and are known for their implication in allergic responses.[69] They are considered to be part of the immune system, since they are very similar to basophil granulocytes, which belong to the white blood cell family. Mast cells possess granules containing histamine, which is secreted when the cell is activated, thus producing characteristic symptoms of the allergic reaction. It has been shown that the flavone baicalein inhibits mast cell proliferation, and that genistein as well as quercetin, kaempferol and myricetin inhibits the histamine release of the same mast cells.[70, 71] Involvement of PTKs in mast cell histamine release has been documented.[72]

3.1.e. Flavonoids and other proteins related to cancer

One of the most common characteristics among cancer cells is their inability to undergo apoptosis, or programmed cell death. Some anticancer drugs induce apoptosis in cancer cells. For example, the naturally occurring flavone tangeritin (Figure 1.16) induces apoptosis in HL-60 leukemia cells.[73] The induction of apoptosis by quercetin has also been well documented; this has been shown to proceed via heat shock proteins in several cell lines.[74] Genistein also induces apoptosis in HL-60 and M07e leukemia cells.[75]

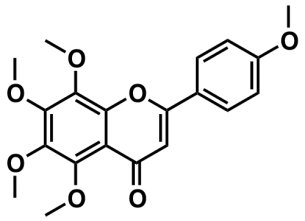

Figure 1.16: Structure of tangeritin

Aromatase is an enzyme responsible for the conversion of androgens into estrogens, by aromatizing a part of the steroid skeleton. Aromatase inhibitors are often used in the treatment of hormono-dependent cancers, such as breast cancer for example, where proliferation is enhanced by the presence of estrogens. There are several reports of aromatase inhibition by naturally occurring flavonoids, such as the flavones chrysin and apigenin (Figure 1.17).[76] A structure-activity relationship study of synthetic flavonoids was performed on the inhibition of the aromatization of androstenedione. Flavone and flavanones exhibited the best results, with IC_{50} values in the low micromolar range.[77] Kaempferol has also been shown to inhibit aromatase activity in a human preadipocytes.[78]

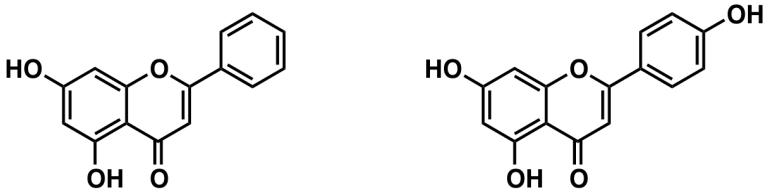

chrysin apigenin

Figure 1.17: Structures of chrysin and apigenin

Decreasing tumor size is not generally the main goal of anti-cancer therapy. Solid tumors can usually be surgically removed, and local treatments such as radiotherapy applied. The main difficulty of cancer therapy is the development of metastasis. Since all solid tumors need nutrients to survive, a vascular system is required which comes about *via* angiogenesis. Genistein has been shown to inhibit endothelial cell proliferation stimulated

by bFGF (fibroblast growth factor: a glycoprotein essential for angiogenesis) *in vitro*, and also to inhibit angiogenesis *in vivo*.[79] bFGF is a well known growth factor; its function is to produce a plasminogen activator called urokinase-type plasminogen activator, which ultimately induces the production of plasmin protein from its proenzyme plasminogen. Plasmin subsequently starts the neovascularization process. Genistein has been shown to reduce the production of plasminogen activator, suggesting that it interacts with bFGF.[79] Other flavonoids such as fisetin, apigenin, and luteolin also inhibit the proliferation of normal and tumor cells, in addition to inhibiting *in vitro* angiogenesis.[80]

Other proteins are implicated in the metastasis process, such as extracellular matrix proteins, which are related to cell adhesion and migration. Laminins belong to this class of proteins, and catechin has been shown to bind laminins. The treatment of a laminin-coated surface with catechin abrogates their effects on different cell types.[81] In addition, it has been reported that the invasion of an embryonic chick heart fragment by MO4 murine fibrosarcoma cells is inhibited by tangeretin in vitro; this inhibition is reversible by simply removing the tangeretin from the culture medium.[81] Related studies show that genistein inhibits the invasion of BALB/c mammary carcinoma on a basement membrane-like material without affecting the cellular growth.[82]

Tubulin is a family of globular proteins responsible for the formation of microtubules, which are constitutive elements of the cytoskeleton. Tubulin is a target for several anti-cancer drugs, such as paclitaxel.[83] Direct interactions between quercetin and tubulin have been shown, resulting in the inhibition of microtubule polymerization and causing depolymerization of microtubules made from purified tubulin *in vitro*. A conformational change of tubulin due to binding with quercetin has been shown, suggesting that quercetin inhibits cancer cell proliferation at least in part by perturbing microtubule function.[84]

3.2. Flavonoids as antioxidants

Another extensive area of flavonoid activity concerns the inhibition of enzymes involved in the production of reactive oxygen species (ROS). Indeed, part of the beneficial effects of the flavonoids found in our diet is due to their antioxidant properties that protect the

metabolism against ROS. For this reason, flavonoids are considered to be “nutraceuticals” and are receiving much attention for their positive effects on health.

DeFelice coined the term “nutraceutical” in 1979 and defined a nutraceutical as “food or parts of food that provides medical or health benefits, including the prevention and treatment of disease”.[85] Flavonoids currently represent the major active nutraceutical ingredients in food plants.[62] A good illustration of the nutraceutical concept is the French paradox:[86] French people, while consuming a diet high in saturated fat, are relatively protected against cardiovascular diseases. This is thought to be the consequence of the antioxidant procyanidin flavonoids present in red wine.[87]

Reactive oxygen species include free radicals, such as superoxide ($O_2^{\cdot-}$) and hydroxyl radical ($HO^{\cdot}$) but also non-radical species, like hydrogen peroxide (H_2O_2). They are constantly produced in the body, by a variety of different enzymatic or non-enzymatic pathways. For example, mitochondria are a source of cellular ROS,[88] which are generated during the oxidative phosphorylation process. As with any energy-associated process, side events can occur, and when electrons escape the mitochondrial electron transport chain, their reaction with molecular oxygen results in the production of superoxide.[89, 90] This is the case for approximately 2% of the oxygen used by mitochondria.[91] The superoxide ions can then be converted into hydrogen peroxide and other ROS. ROS can also have an enzymatic origin, such as NADPH oxidases. ROS seem to affect cell proliferation and apoptosis of prostate cancer cells.[92, 93]Due to their reactive properties, ROS represent the main source of DNA damage.[94] This damage can cause malfunction of the respiratory chain and further amplify the generation of ROS, and therefore promote mutations and genetic instability. ROS have very deep implication in a number of diseases, especially cancer.

In general, cancer cells produce more superoxide ions than normal cells, so they are under higher oxidative stress than normal cells. This difference creates a specific vulnerability. Criteria differentiating cancer cells and normal cells are very precious, since the selectivity of anti-cancer agents is currently one of the biggest challenges in anti-cancer therapy.[95] There are several ways for flavonoids to modulate ROS production and ROS levels inside the cells.

3.2.a. Enzymatic approach

Much like pH, the redox status of the cell is buffered, primarily by the GSSG (glutathione disulfide)/GSH (glutathione) ratio. GSH is most present in the cells is its reduced form. When GSH reacts with an oxidant, it is oxidized to GSSG. The concentration of GSH in a normal cell is about 1 mmol, and the cell's "redox potential" rises when the level of GSSG increases. A rapid decrease in GSH is associated with cell death for both normal and cancer cells.[96] GSSG can be reduced back to GSH by the enzyme glutathione reductase (GSR or GR) and the coenzyme nicotinamide adenine dinucleotide phosphate (NADPH).[97] Therefore, inhibiting GSR undermines the cellular redox buffer.

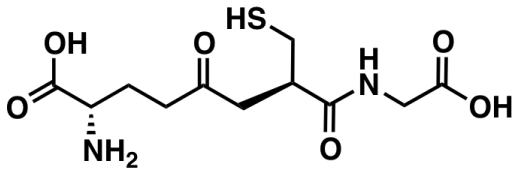

Figure 1.18. Structure of GSH

Paradoxally, quercetin and other flavonoids have been shown to inhibit GSR, and an extensive structure-activity relationship study involving the main class of flavonoids has been conducted.[98] However, these inhibition properties appear only at relatively high concentrations (> 25 μM). At lower concentrations, around 10 μM, quercetin significantly increases the GSH level of murine L1210 leukemia cells, while galangin (Figure 1.19) has no effect.[99] Later, it was shown that quercetin is able to increase the activity of the rate-limiting synthesizing enzyme of the GSH metabolism, glutamate cysteine ligase (GCL).[100]

Green tea is a well-known nutraceutical, and it is very rich in flavonoids, especially in catechins and flavonols. When the tea has been allowed to ferment for a longer period of time, black tea is obtained. The fermentation has a very important effect on the tea's flavonoid derivatives, which are chemically modified to more complex structures, the teaflavins (Figure 1.19). These teaflavins inhibit another ROS-producing enzyme called xanthine oxidase (XO).

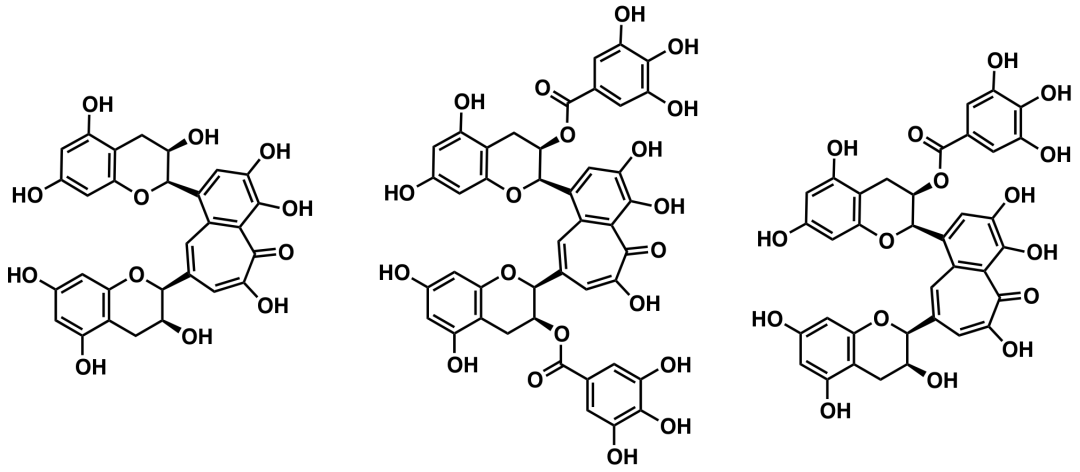

teaflavin teaflavin-3,3'-digallate teaflavin-3-gallate

Figure 1.19: Structures of some teaflavins

XO's function is to oxidize hypoxanthine into xanthine and then xanthine into uric acid from oxygen, thus releasing hydrogen peroxide (Figure 1.20). Teaflavins reduce the production of superoxide in HL-60 cells, and therefore reduce their oxidative stress.[101]

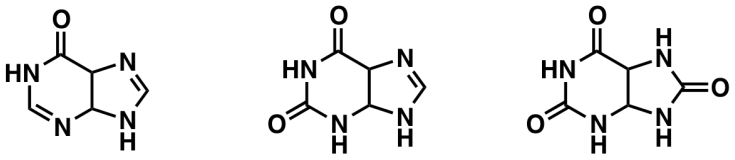

hypoxanthine xanthine uric acid

Figure 1.20. Structures of hypoxanthine, xanthine and uric acid

Since superoxide is naturally produced, and because of its high toxicity, cells possess pathways for its removal: superoxide dismutases (SODs). SODs are a family of metalloenzymes whose role is to induce the dismutation of superoxide ions into less toxic species, hydrogen peroxide and dioxygen. Therefore, they are essential components of the biological antioxidant system, as well as a target for redox chemotherapeutics.[102]

In green tea, polyphenols account for up to 30% of the dry weight, and most of them are flavonoids. An up-regulation of the SOD activity caused by green tea has been observed in rats. When fed with green tea (up to 2.5% of their diet), during extended periods of time (63 weeks), the rats exhibited no lesions in the liver, and they showed a decrease of weight of about 10-18%, together with a decrease of triglycerides and total cholesterol of about 25-30%, clearly showing a hypolipidemic effect. In addition, the increase of SOD activity was superior to 100%. This could help explain the observed chemopreventive effects of green tea.[103]

By affecting the enzymes that constitute the cellular antioxidant machinery, flavonoids have an indirect impact on ROS. The flavonoid-enzyme interaction is not the only source of the preventative effects of these molecules. For example, their polyphenolic skeleton confers them radical scavenging properties.

3.2.b. Radical scavenging

Radical scavenging is a crucial issue for the protection of the body. The deactivation of highly aggressive species, like hydroxyl radical, is not the only aim. Scavenging the less aggressive superoxide ion is also important, since $O_2^{\cdot-}$ can produce hydroxyl radicals *via* the Fenton and Haber-Weiss reactions.[104]

Due to their polyphenolic structures, flavonoids possess several sites that are sensitive to oxidation by ROS.[105] Moreover, the radical created by the oxidation of a flavonoid skeleton can be delocalized all over the pi-system, therefore giving rise to a stabilized aroxyl radical. An example of this is presented in Figure 1.21, using 3',4'-dihydroxyflavone as an example. The fate of the radical species can follow two different paths. The ideal case is when a second monoelectronic oxidation of the aroxyl radical occurs due to its reaction with another radical, thus scavenging another equivalent of undesirable free radical. However, in the presence of free metals in high concentration, the aroxyl radical can interact with dioxygen to release superoxide. In this case not only has the ROS problem not been solved, but quinones are created. This event is thought to be responsible for the observed

prooxidant behavior of flavonoids.[105] The problem of metals reacting with ROS and their deactivation by chelation is the subject of the following section.

Radical scavenging properties have been reported for most flavonoids, and many structure-activity relationship studies have been conducted. For example, in 2006, Asres and coworkers identified some crucial fragments inducing high radical scavenging properties: the ease of the phenol deprotonation and the ease of the termination step.[106] It should be specified that some flavonoids, such as morin, do not scavenge either superoxide or hydroxyl ions, but still exhibit antioxidant properties.[107] This shows that radical scavenging properties are not always essential in the antioxidant activity of a compound.

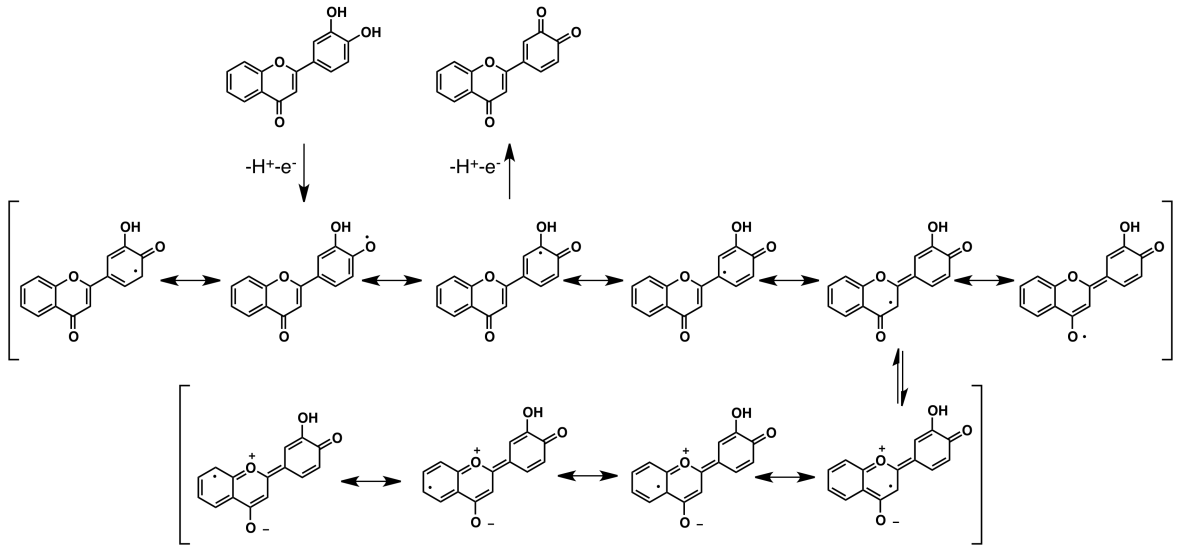

Figure 1.21. Monoelectronic oxidation of the 3',4'-dihydroxyflavone, delocalization of the radical over the skeleton, and termination resulting in a quinone structure

The importance of the flavonoid radical scavenging properties toward hydroxyl radicals has not convinced the entire scientific community, although it generally is recognized. In 1997, Wu and coworkers published a study on five well-known flavonoids: baicalin, hesperidin, naringin, quercetin and rutin, in order to determine the origin of their antioxidant properties. The authors concluded that the scavenging properties towards hydroxyl radicals are very limited, and that antioxidant properties of flavonoids are mainly due to their iron chelation properties.[108]

3.2.c. Metal chelation

Free iron is known to have harmful effects, especially through Fenton chemistry:

$$Fe_3^{+} + O_2^{\bullet -} \longrightarrow Fe_2^{+} + O_2$$

$$Fe^{2+} + H_2O_2 \longrightarrow Fe^{3+} + HO^{-} + HO$$

$$O_2^{\bullet -} + H_2O_2 \longrightarrow HO^{-} + HO^{\bullet} + O_2$$

In order to avoid these effects, iron is "protected" in vivo, that is to say sequestered *via* complexation with transferrin, ferritin or heme proteins.[109] However, iron can transiently be found in forms where it is free enough to interact with ROS in the labile iron pool (LIP), whose deregulation is harmful.[110]

Treatment of GSH-lacking erythrocytes with different oxidizing agents, such as phenylhydrazine or acrolein, results in the production of free iron. This phenomenon and its subsequent production of ROS provide a good platform for studying the relationship between antioxidant effects and metal chelation. As a consequence of this oxidative stress, different harmful phenomena are observed, for example lipid peroxidation.[110] The addition of quercetin decreases these negative effects, probably by the chelation of iron. At concentrations comparable to those used in the *in vitro* experiment, quercetin has been shown to chelate iron in buffer solution. When added to the free iron releasing erythrocyte, it decreases lipid peroxidation, and eliminates it completely when two equivalents of quercetin are added. Depending on the flavonoid, the stoichiometry of the chelation can vary, as shown in Figure 1.22. Quercetin, kaempferol, myricetin and morin chelate iron with a stochiometry of 2:1, baicalein with a stochiometry 1:1 and 3-hydroxyflavone 3:1. These proportions may vary with pH.[111]

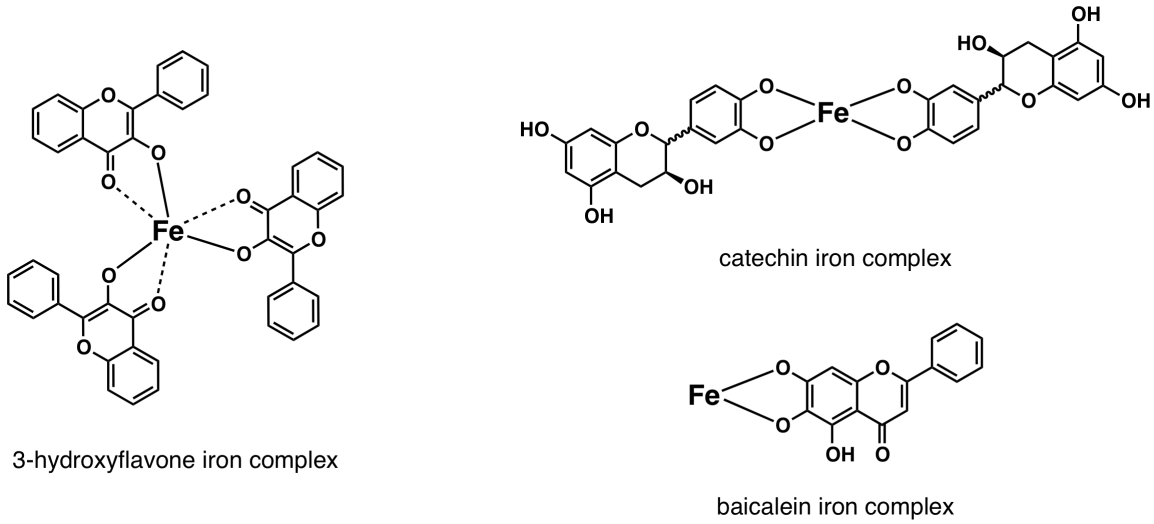

Figure 1.22. Iron-chelation modes for 3-hydroxyflavone, catechin and baicalein

As nutraceuticals, flavonoids protect the cell from damaging ROS, either by preventing their formation or by destroying them when already formed. In this regard, the preventive effect of flavonoids is obvious. However, from a therapeutic point of view, the antioxidant effect does not represent the only approach to redox-active drugs design. It is known that, as a consequence of their intrinsic high oxidative stress, the biological antioxidant system of cancer cells is often saturated. Therefore, since an exaggerated level of ROS inside a cell results in its death, a prooxidant approach for redox-active chemotherapeutics has therefore been investigated.[112] In addition, Boots and coworkers highlighted the singular behavior of the flavonoid quercetin that she called the “quercetin paradox”. She has shown that as a consequence of its protective reaction with hydrogen peroxide, quercetin forms toxic electrophilic quinoid metabolites. Therefore, it can be hypothesized that beneficial effects of the quercetin can be partially attributed to the death induced in undesirable cells.[113]

Following the same concept, Jaouen and coworkers have developed a ferrocenyl derivative of the anti-cancer metabolite hydroxytamoxifen, called hydroxyferrocifen (Figure 1.23), which is thought to behave similarly.[114] Its behavior will be detailed in a following section.

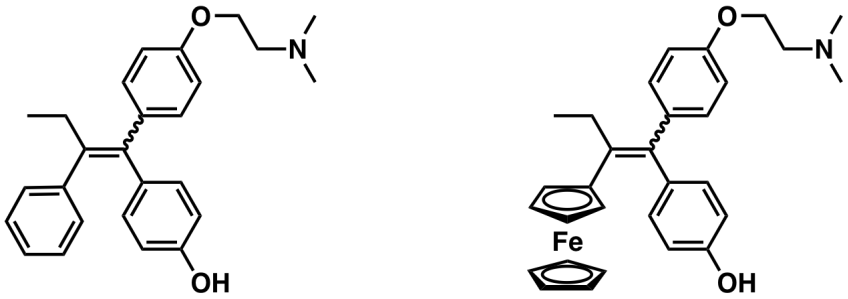

hydroxytamoxifen hydroxy-ferrocifen

Figure 1.23. Structures of hydroxytamoxifen and hydroxyferrocifen

B. Ferrocene

1. Generalities

In 1951, Kealy first reported a new compound made of an iron atom together with two cyclopentadienyl moieties. The first property that was recognized was its high stability, which was in contrast with other attempts to make similar compounds.[115] The correct structure was proposed the following year by Wilkinson and Fisher,[116, 117] and the name "ferrocene" was invented by Woodward the same year,[118] for its resemblance with benzene.

The discovery of ferrocene marked the birth of modern organometallic chemistry. Nowadays, an incredible diversity of organometallic complexes exists, and they are used for all imaginable purposes. Ferrocene, however, still remains a special case. Its external surface resembling an aromatic core, it can easily be functionalized, using for example Friedel-Craft or lithiation reactions. Moreover, it is stable in physiological conditions, in non-oxidizing environments, and it is lipophilic and compact. Ferrocene is non-toxic: No deaths were observed for dogs daily fed with 300 $mg.kg^{-1}$ of ferrocene for 6 months, although an iron overload was observed.[119] In this regard, a ferrocene compound has been used to treat iron deficiency in the clinic, thanks to its lipophilicity.[120] In addition, ferrocene possesses a stable and reversible Fe^{II}/Fe^{III} couple, which adds to its characteristics a redox behavior. All these

parameters make it a suitable isostere for pharmaceutical uses; those where it replaces an existing group in a biomolecule, particularly a phenyl ring, will be studied in this section.

2. Ferrocene in medicinal chemistry

Ferrocene-containing bioactive molecules possess activities against all kind of diseases, and these activities take advantage of different properties of the ferrocene moiety. An overview of this subject will be presented below. One of the major uses of ferrocene-containing molecules as bio-active agentd concerns the field of oncology. Many other uses of ferrocene in medicinal chemistry have been investigated, but they will not be detailed here. This section is not meant to be exhaustive, but rather aims to give an overview of ferrocene relating to topics that we interested ourselves in during this study. Comprehensive reviews exist on the subject.[121, 122]

2.1. Anti-cancer properties

Although ferrocene itself doesn't possess anti-cancer properties, its oxidized form, ferricenium, has been shown to be anti-proliferative against Ehrlich ascite tumors in 1984.[123,124] Later on, Neuse proposed that ferrocenyl compounds could be oxidized *in vivo*, so that both ferricenium- and ferrocene-containing compounds could exhibit cytotoxic properties.[125] This concept was most fully demonstrated by Jaouen and coworkers' discovery of the hydroxyferrocifens. [126, 127]

2.1.a. Hydroxyferrocifens

Hormone-dependent breast cancer cells over express the estrogen receptor (ER) on the cell surface, and breast cancer cell proliferation is linked to the interaction of the ER with its agonist estradiol. Such hormone-dependent cases represent approximately two thirds of the diagnoses, and subsequent treatment involves ER antagonists, such as tamoxifen, which is metabolized *in vivo* to the active agent hydroxytamoxifen. [128, 129] However, drug resistance

is an important phenomenon with such selective estrogen receptor modulators (SERMs), and treatment with tamoxifen is only efficient for one-third of all breast cancer patients over the long term. Moreover, tamoxifen exhibits side effects, such as the increased risk of uterine cancer. So while the treatment options available for hormone-dependent breast cancers are still better than those for hormone-independent cancers, progress still needs to be made on both fronts.

The "hydroxyferrocifens" were designed to be bi-functional drugs, exhibiting both anti-estrogenic and cytotoxic (or cytostatic) properties. On one hand, because of the resemblance of ferrocene with a phenyl ring, it was hoped that the affinity with the ER and therefore the antiestrogenic effect could be maintained. On the other hand, additional cytotoxic effects induced by the ferrocene moiety were desired. On MCF-7, a hormone-dependent breast cancer cell line, the antiproliferative behavior of hydroxyferrocifen (*n* = 3) is greater than that of hydroxytamoxifen. The addition of estradiol shows an incomplete reversal of the phenomenon, indicating the contribution of a partial cytotoxic effect.[130] Moreover, on MDA-MB-231, a hormone-independent cancer cell line, hydroxyferrocifen (with n=3) had an IC_{50} value of 0.5 µM, while OH-Tam was completely inactive. From this observation, it is clear that the hydroxyferrocifens exhibit cytotoxic effects that involve the ferrocene moiety. A family of compounds has been synthesized on the hydroxyferrocifen model, by replacing the amino chain by different substituents.

The mode of action of these compounds seems to be the consequence of an intracellular redox activation of the ferrocene moiety, causing an intramolecular electron transfer and a subsequent oxidation of the hydroxyferrocifen derivatives into a quinone methide form, as shown in Figure 1.24.[114] As in the case of quercetin oxidation, this electrophilic product is cytotoxic. [131]

Moreover, hydroxyferrocifen derivatives show selectivity toward cancer cells. Bernard and coworkers have shown a selective cytotoxic effect of these compounds for several melanoma cell lines *vs.* melanocytes.[132] Similarly, Benoit and coworkers have shown that the compound where R = OH displays cytotoxic effects on 9L glioma cells, with an IC_{50} of 0.6 µM. The same compound was not active on normal brain cells at concentrations inferior to 10 µM.[133] The selectivity of this molecule for cancer cells can be explained by its selective

activation in high oxidative stress condition, which is known to be the case for most of the cancer cells.[112]

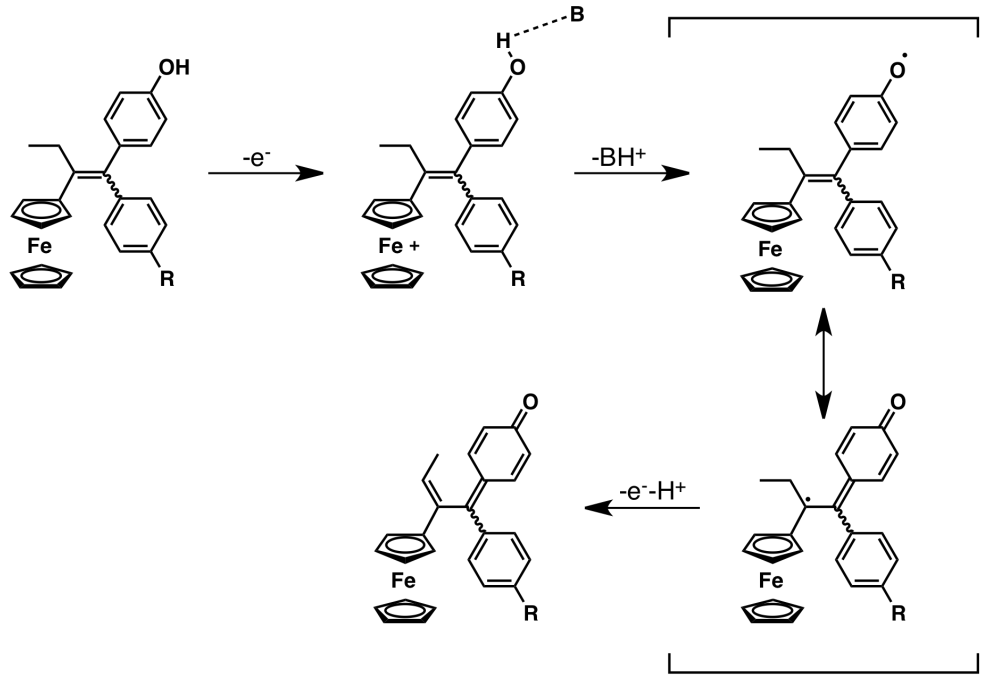

Figure 1.24. Oxidation of hydroxyferrocifens

2.1.b. Raloxifens

Another original candidate for the treatment of hormone-dependent breast cancer was raloxifen,[134] shown in Figure 1.25. Raloxifen acts similarly to tamoxifen, but is somewhat less active; the main advantage of this molecule is its ability to maintain bone density, unlike tamoxifen.[135, 136] Ferrocenyl derivatives of raloxifen (Figure 1.25) have been synthesized and evaluated against several cancer cell lines, such as ovarian (2008, C13*, RH4), cervical (A431), lung (A549), colon (HCT-15) and breast (MCF-7, MCF-7 ADR), exhibiting IC_{50} values in the low micromolar range.[137]

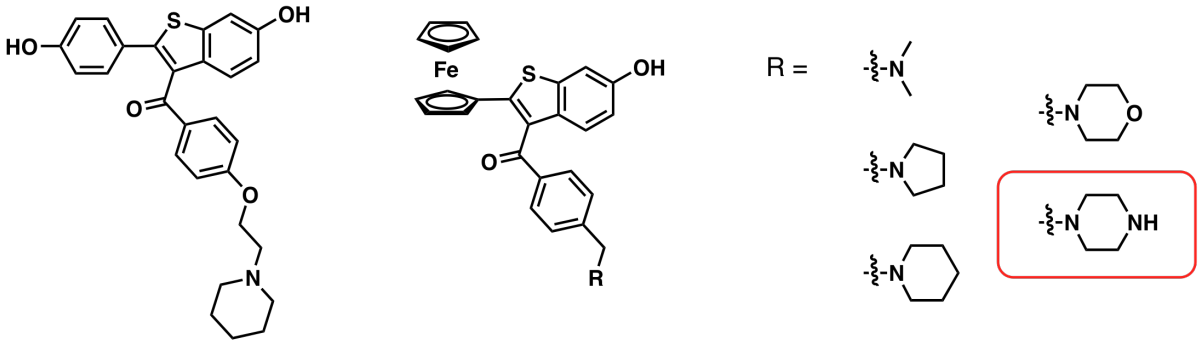

Figure 1.25. Structure of raloxifen and ferrocenyl raloxifens

The piperazinyl derivatives (framed in Figure 1.25) exhibit the best results, and its ability to activate caspase-3 in ovarian cells suggests a mode of action *via* induction of apoptosis.

2.1.c. Anti-androgens

Like breast cancer, prostate cancer can be hormone-dependent. In this case, androgen receptors are activated by dihydrotestoterone (DHT), the active metabolite of testosterone, and therefore induce proliferation. Hormone-dependent forms of prostate cancer represent the majority of the cases, at least at the initial development of the tumour.[138] Thus, anti-androgens such as flutamide, niflutamide and bicalutamide have been designed (Figure 1.26). However, resistance phenomena have subsequently appeared, similar to what has been observed for breast cancer.

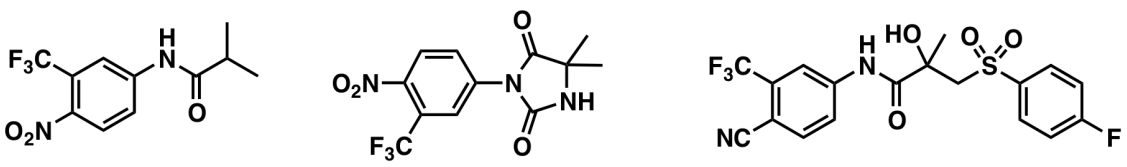

flutamide nilutamide bicalutamide

Figure 1.26. Structures of nilutamide, flutamide and bicalutamide

Following the example of the hydroxyferrocefins, but here grafting the ferrocene moiety onto the skeleton of a known molecule, several nilutamide derivatives have been synthesized (Figure 1.27) and biologically evaluated on hormone-independent prostate cancer cells (PC-3). PC-3 cells were exposed to 10 µM of each compound.

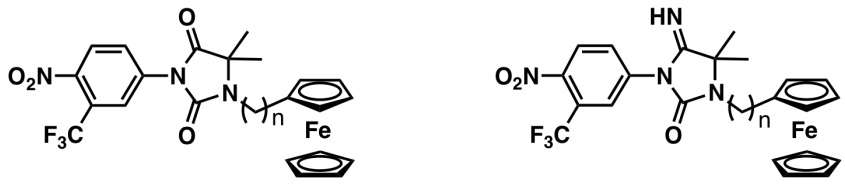

n = 1,2 n = 1,2

A **B**

Figure 1.27. Ferrocenyl nilutamide derivatives

In these experiments, bicalutamide showed a weak anti-proliferative effect (15%), compounds **A** in Figure 1.27 exhibited a better anti-proliferative effect (37–34%), and compounds B showed almost no anti-proliferative effect (less than 10%).

The ferrocene derivatives of testosterone shown in Figure 1.28 have also been synthesized and tested against prostate cancer cells. On PC-3 hormone-independent cells, these compounds exhibited an antiproliferative effect with IC_{50} values ranging from 4.7 to 12.2 µM. Compound A in figure 1.28, with an IC_{50} value of 4.7, is one of the most active organometallic complexes of an androgen or anti-androgen.[139]

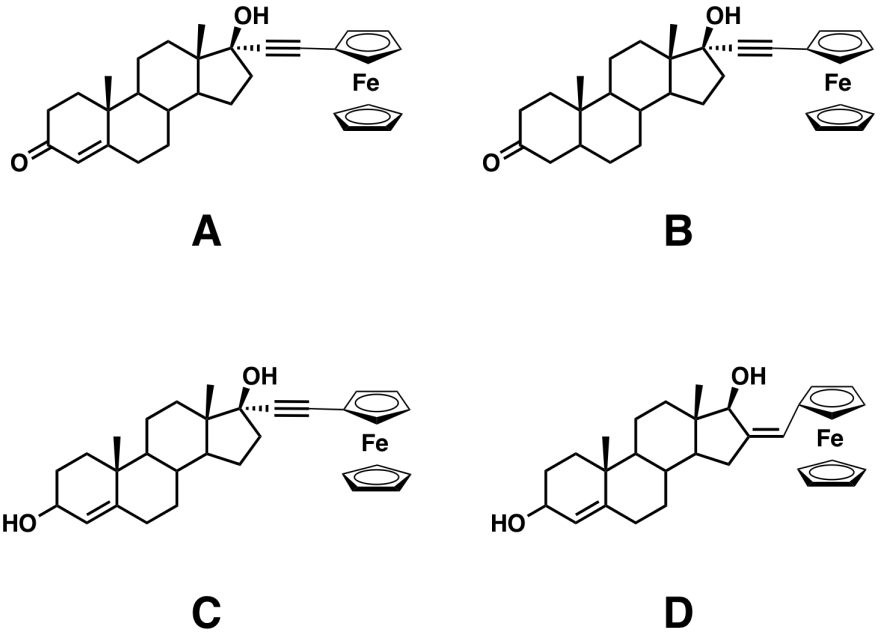

Figure 1.28. Structures of some testosterone ferrocene derivatives

For both breast and prostate cancer, the presence of ferrocene in the structure of existing receptor-modulating molecules resulted in an additional cytotoxic component. This characteristic is particularly useful in extending the therapeutic spectrum of drugs, and to avoid problems of drug resistance.

2.1.d. Ferrocenyl curcuminoids

Curcumin (Figure 1.29) is a natural compound, found in important quantities in the rhizome *Curcuma longa*. It is present in turmeric, where it is a yellow pigment. Its biological activities have long been recognized, especially in Asian traditional medicine. Different properties such as antioxidant, chemopreventive and antitumor activities on several cancer types have been reported for this compound.[140]

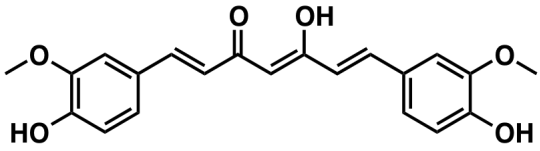

Figure 1.29. Structure of curcumin

Recently, ferrocenyl curcuminoids have been synthesized, and some of their biological properties have been evaluated, such as cytotoxicity on B16 melanoma cells, and antiangiogenic effects such as inhibition of tubulin polymerization and rounding-up of endothelial cells. In general, the ferrocenyl moiety improved the curcuminoids' biological effects, the spacer between the curcuminoid skeleton and the ferrocenyl moiety playing a central role.

For example, curcuminoids possessing a methylene linker (Figure 1.30A) exhibit the best cytotoxic effects on murine B16 cells, with IC_{50} between 2.2 and 7.1 µM, whereas a propenone linker (Figure 1.30B) results in the best tubulin polymerization inhibition and the lowest concentrations for the rounding up of endothelial cells.[141] In this case, the ferrocene moiety's behavior is more complex, and two different biological effects are induced; its mode of connection to the curcumin's skeleton modulates the nature of the curcuminoids' biological properties.

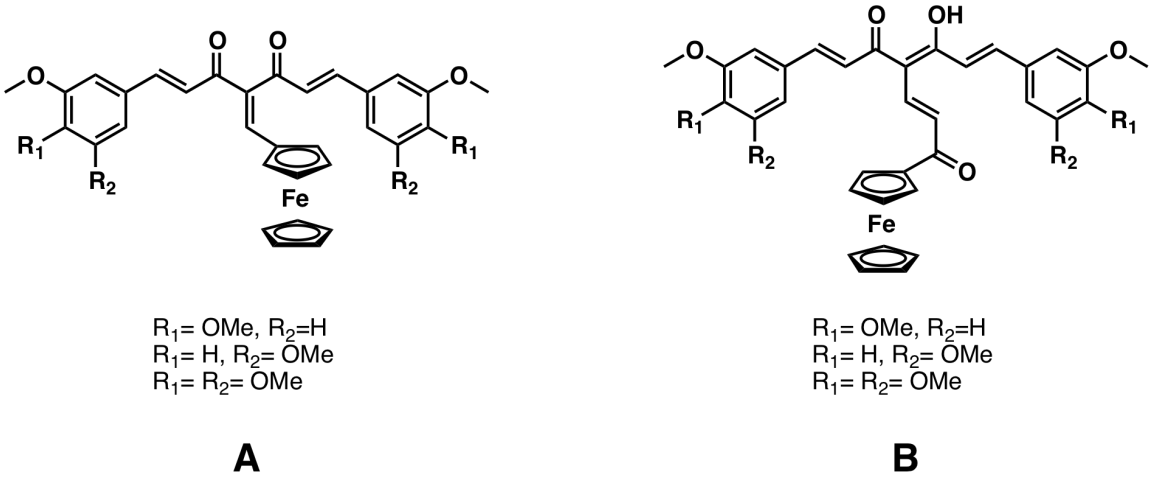

Figure 1.30. Structures of some ferrocenyl curcuminoids

2.1.e. JAHAs

From a purely steric point of view, ferrocene and phenyl possess a major difference, namely, ferrocene is three-dimensional. In some cases, such as using ferrocene-containing compounds as enzyme inhibitors, this characteristic is crucial. An illustration of this concept is the design of ferrocene derivatives of suberoyl anilide hydroxamic acid (SAHA), shown in Figure 1.31.

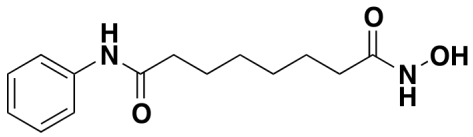

Figure 1.31. Structure of SAHA

In cell nuclei, DNA is packaged into the nucleosome, which is a segment of DNA wound around a histone protein core. For genetic transcription to occur, the DNA has to be released by histone for the transcription enzyme to reach the DNA strand. The winding dynamics are ruled by acetylation-deacetylation process. Histone acetyl transferase (HAT) enzymes induce unwinding of the DNA strain, while histone desacetylases (HDAC) induce the winding, thus allowing genetic transcription. In cancer, some of the transcription processes are silenced, particularly those resulting in the production of pro-apoptotic and growth arrest proteins.

Inhibiting HDAC could thus restore these functions, and therefore represent a promising approach for the design of new anti-cancer agents. SAHA is a HDAC inhibitor, which is currently in clinical trials for the treatment of cutaneous T-cell lymphoma.

Very recently, Spencer and coworkers designed ferrocenyl derivatives of SAHA (Figure 1.32), and tested them against MCF-7 breast cancer cells. Docking experiments on the compound figure 1.32.A show a good fitting of the ferrocenyl moiety with the cavity of HDAC8, this part of the cavity being known to be malleable, and therefore adaptable to different ligands. Compounds 1.32.A and B display an IC_{50} concentration in the low micromolar range for the inhibition of HDAC8, as well as SAHA. The compound 1.32.C, on the other hand, presented

an IC_{50} value of 2 nm. The IC_{50} values of these compounds for MCF-7 cell proliferation were in the low micromolar range.[142]

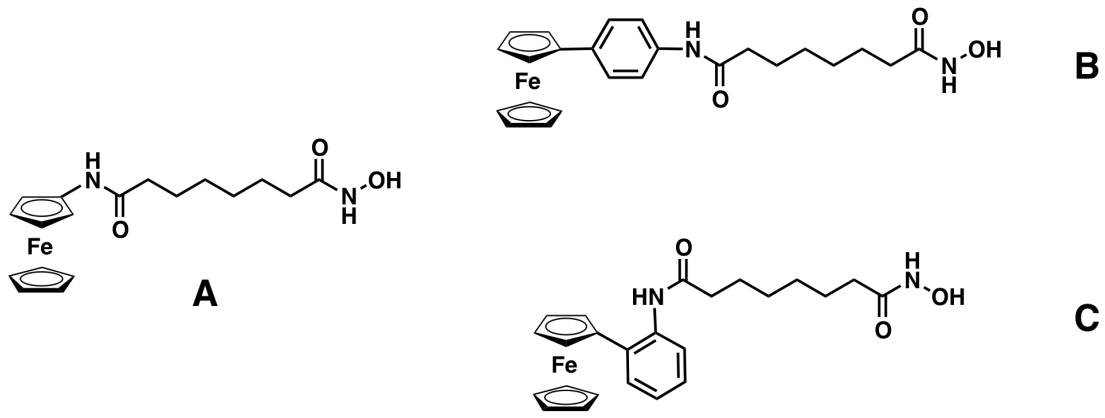

Figure 1.32. Ferrocenyl derivatives of SAHA

2.1.f. Kinase inhibition

Receptor tyrosine kinase (RTK) is a family of proteins known for their implication in cancer development, particularly the transformation process associated with human cancers.[143] The oxindole motif is found in several anticancer agents, and has been shown to be an interesting core for PTK inhibition.[144]

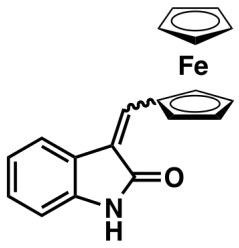

Figure 1.33. Structure of the ferrocene oxindole derivatives (Z and E isomers)

Spencer and coworkers have developed ferrocene 1,3-dihydro-2H-indol-2-one (oxindole) derivatives, shown in Figure 1.33. Ferrocene oxindoles selectively inhibited the vascular endothelial growth factor receptor VEGFR-2, a PTK receptor whose activation influences endothelial cell mitogenesis and cell migration. Ferrocene oxindoles exhibited an IC_{50} value

against VEGFR-2 of 200 nM, and also displayed antiproliferative properties against B16 melanoma in mice and Vero (African Green Monkey Kidney Epithelia), with an IC_{50} value of 0.7-1.2 μM.[145]

2.2. Anti-HIV properties

Topoisomerases are enzymes that control the topological structure of DNA, by cutting one (topoisomerase I) or both (topoisomerase II) DNA strands. They play a central role in cellular division and transcription. The inhibition of topoisomerases is an important target in anticancer drug discovers, as well as in anti-HIV therapy. Indeed, it has also been shown that topoisomerase II activity is required for HIV-1 replication.[146]

Thiomorpholide amido methyl ferrocene and azalactone ferrocene (Figure 1.34) are selective topoisomerase II inhibitors, and display IC_{50} values for the inhibition of catalytic activity of 50 and 100 μM, respectively.[147] Kondapi and coworkers further studied the impact of azalactone ferrocene and thiomorpholide amido methyl ferrocene on cell proliferation and also on various events of HIV-1 replication cycle. The two topoisomerase II inhibitors showed significant anti-HIV activity on the nanomolar scale against an Indian isolate of HIV-193IN101 in the Sup-T1 cell line, together with inhibition of the proviral DNA synthesis as well as the formation of pre-integration complexes.[146]

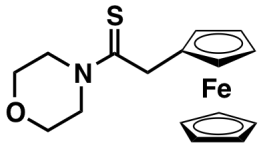

thiomorpholine amido methyl ferrocene

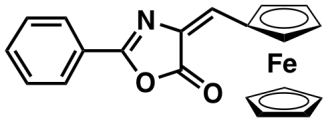

azalactone ferrocene

Figure 1.34. Structures of thiomorpholide amido methyl ferrocene and azalactone ferrocene

2.3. Anti-bacterial properties

Some known β-lactam antibiotics have also been modified by insertion of a ferrocene moiety in their structure. For example, penicillin and cephalosporin ferrocene derivatives were created in the 1970s (Figure 1.35).[148]

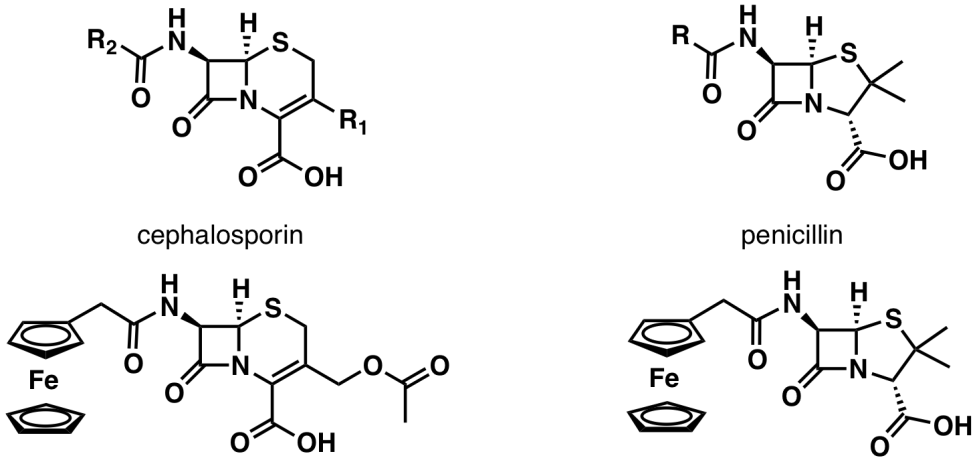

Figure 1.35. Structures of penicillin, cephalosporin, and the corresponding ferrocene derivatives

Not only have the ferrocene derivatives of these families of antibiotics been shown to maintain their biological properties for many different bacteria lines, but they also exhibit activity for penicillinase producing strains. Penicillinase is a subfamily of enzyme belonging to the β-lactamase family, which are responsible for resistance of bacteria against β-lactam antibiotics. The ferrocene derivatives of penicillin and cephalosporin contravert this drug resistance by acting as β-lactamase inhibitors.[149]

2.4. Anti-parasitic properties

Malaria is an infectious disease caused by parasites of the genus *Plasmodium*, which is transmitted by the mosquito, and primarily affects populations living in tropical climate zones. Among the four species of *Plasmodium* invading humans, the most deadly is

Plasmodium falciparum. Malaria causes millions of deaths every year; therefore its treatment is of great importance.

2.4.a. Ferroquine

One of the leading treatments of malaria is a molecule called chloroquine (Figure 1.36). However, its intensive use has led to the appearance of chloroquine-resistant strains of *Plasmodium*. The concept of introducing a ferrocene moiety in order to avoid resistance problems is perfectly illustrated with the synthesis of ferroquine (Figure 1.36) by Brocard and coworkers.[150]

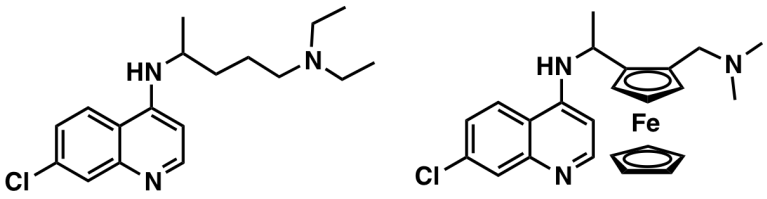

Figure 1.36. Structures of chloroquine and ferroquine

In vitro, ferroquine displays similar results to chloroquine for chloroquine-sensitive strains, but is also very active against chloroquine-resistant strains of *P. falciparum*. *In vivo*, ferroquine is as efficient as chloroquine on a short-term period in *P. berghei N.* and *P. NS.* However, ferroquine prevents all recrudescence phenomena over a long-term period, while recrudescence is always observed in case of chloroquine.[150] A later study has shown an *in vivo* improvement for ferroquine *vs* chloroquine in *P. vinckei* and in *P. falciparum*.[151] Ferroquine is currently in phase II clinical trials.

2.4.b. Ferrocenyl chalcones

Another study on ferrocene-based anti-malarial agents focused on ferrocenyl chalcone derivatives. Two compounds, shown in Figure 1.37, were identified as lead compounds

when tested against a chloroquine-resistant strain of *Plasmodium falciparum*, with moderate IC_{50} values of 4-5 µM.[152]

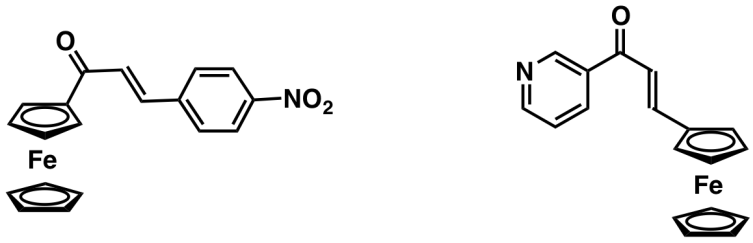

Figure 1.37. Structures of the leads ferrocenyl chalcones

The authors specifically studied the influence of the ferrocenyl moiety on the anti-malarial activity of these chalcone-based compounds. Radical scavenging properties of the ferrocenyl chalcones and the formation of hydroxyl radical adducts was demonstrated. Moreover, a parallel between the anti-malarial activity and oxidation properties of the ferrocene moiety was established: Surprisingly, the most active compounds were the ones where the ferrocene was more resistant to oxidation. Therefore, a purely structural role of ferrocene seems unlikely.[153]

Ferrocene chalcones were first synthesized in the 1950s.[154, 155] It is interesting to note that it was only fifty years later that scientists became interested in their biological properties. Indeed, as we have seen, there exist many examples of ferrocene-containing molecules with interesting biological activity. Often, as the case of the hydroxyferrocifens or the ferrocenyl chalcones, the ferrocene group plays a role *via* its redox behavior. Flavonoids, which are the most extended family of natural antioxidants, and interact with all kinds of biological targets, also display biologically-relevant redox behavior. Therefore, from a bioorganometallic perspective, the extension of ferrocenyl chalcones to the other classes of the flavonoid family seems very promising for the elaboration of new bioactive molecules.

References

1: Middleton, E. Jr.; Kandaswami, C.; Theoharides, T. C. "The Effects of Plant Flavonoids on Mammalian Cells: Implications for Inflammation, Heart Disease, and Cancer" *Pharmacol. Rev.* **2000** 52, 673-751

2: Williams, C. A.; Grayer, R. J. "Anthocyanins and other flavonoids" *Nat. Prod. Rep*. **2004** 21(4), 539-573

3: Buer, C. S.; Imin, N.; Djordjevic, M. A. "Flavonoids: New Roles for Old Molecules" *J. of Integr. Plant Biol.* **2010** 52(1), 98-111

4: Rausher, M. D. *The science of flavonoids* **2006** chap.7; New York: Springer, 2006

5: Verwoert, I. I. G. S.; Verbree, E. C.; Van der Linden, K. H.; Nijkamp, H. J. J.; Stuitje, A. R. "Cloning, nucleotide sequence and expression of the Escherichi coli fabD gene, encoding malonyl coenzyme A-acyl carrier protein transacylase" *J. Bact* **1992** 174, 2851-2857

6: Shirley, B. W. "Flavonoids biosynthesis "new" function for an "old" pathway" *Trends Plant. Sci.* **1996** 1, 377-382

7: Li, J.; Ou-Lee, T. M.; Raba, R.; Amundson, R. G.; Last, R. L. "*Arabidopsis* flavonoid mutants are hypersensitive to UV-B radiation" *Plant Cell* **1993** 5, 171-179

8: Lois, R.; Buchanan, B. B. "Severe sensitivity to ultraviolet radiation in an Arabidopsis mutant deficient in flavonoid accumulation" *Planta* **1994** 194, 504-509

9: Stafford, H. A. "Flavonoid evolution: an enzymatic approach" *Plant Physiol.* **1991** 96, 680-685

10: Brown, D. E.; Rashotte, A. M.; Murphy, A. S.; Normanly, J.; Tague, B. W.; Peer, W. A.; Taiz, L.; Muday, G. K. "Flavonoids act as negative regulatorys of auxin transport *in vivo* in *Arabidopsis*" *Plant Physiol.* **2001** 126, 524-535

11: Peer, W. A.; Bandyopadhyay, A.; Blakeslee, J. JU.; Makam, S. N.; Chen, R. J.; Masson, P. H.; Murphy, A. S. "Variation in expression and protein localization of the PIN family of auxin efflux facilitator proteins in flavonoid mutants with altered auxin transport in *Arabidopsis thaliana*" *Plant Cell* **2004** 16, 1898-1911

12: Nakamaya, T.; Yonekura-Sakakibara, K.; Sato, T.; Kikuchi, S.; Fukui, Y.; Fukuchi-Mizutani, M.; Ueda, T.; Nakao, M.; Tanaka, Y.; Kusumi, T.; Nishino, T. "Aureusidin synthase: a polyphenol oxidase homolog responsible for flower coloration" *Science* **2000** 290, 1163-1166

13: Winkel, B. S. J. *The science of flavonoids* **2006** chap.3; New York: Springer, 2006

14: Vogt, T. "Regiospeci¢city and kinetic properties of a plant natural product O-methyltransferase are determined by its N-terminal domain" *FEBS Lett*. **2004** 561 159-162

15: Vermerris, W. et al. *Phenolic compound biochemistry* **2008** chap 6, 220-221; New York: springer 2008

16: Peer, W. A.; Murphy, A. S. *The science of flavonoids* **2006** chap.9; New York: Springer, 2006

17: Grandmaison, J.; Ibrahim, R. "Evidence for nuclear protein binding of flavonol sulfate esters in *Flaveria chloraefolia*" *J. Plant Physiol.* **1996** 147, 653-660

18: Peer, W. A.; Brown, D. E.; Tague, B. W.; Muday, G. K.; Taiz, L.; Murphy, A. S. "Flavonoid accumulation patterns of transparent testa mutants of *Arabidopsis*" *Plant Physiol*. **2001** 126, 536-548

19: Buer, C. S.; Muday, G. K. "The transparent testa4 mutation prevents flavonoid synthesis and alters auxin transport and the response of *Arabidopsis* roots to gravity and light" *Plant Cell* **2004** 16, 1191-1205

20: Saslowsky, D. E.; Warek, U.; Winkel, B. S. J. "Nuclear localization of flavonoid enzymes in *Arabidopsis*" *J. Biol. Chem.* **2005** 280(25), 23735–23740

21: Feucht, W.; Dithmar, H.; Polster, J. "Nuclei of tea flowers as targets for flavanols" *Plant Biol.* **2004** 6, 696-701

22: Feucht, W.; Treutter, D.; Polster, J. "Flavanol binding of nuclei from tree species" *Plant Cell Rep.* **2004** 22, 430-436

23: Pelletier, M. K.; Burbulis, I. E.; Winkel-Shirley, B. "Disruption of specific flavonoid genes enhances the accumulation of flavonoid enzymes and end-products in *Arabidopsis* seedlings" *Plant Mol. Biol.* **1999** 40, 45-54

24: Quattrocchio, F.; Baudry, A.; Lepiniec, L.; Grotewold, E. *The science of flavonoids* **2006** chap.4; New York: Springer, 2006

25: taylor, L. P.; Grotewold, E. "Flavonoids as developmental regulators" *Curr. Opin. Plant Biol.* **2005** 8, 317-323

26: Buer, C. S.; Djordjevic M. A. "Architectural phenotypes in the transparent testa mutants of *Arabidopsis thaliana*" *J. Exp. Bot.* **2009** 60, 751-763

27: Jacobs, M.; Rubery, P. H. "Naturally-occurring auxin transport regulators" *Science* **1988** 241, 346-349

28: Bernasconi, P. "Effect of synthetic and natural protein tyrosine kinase inhibitors on auxin efflux in zucchini (*Cucurbita pepo*) hypocotyls" *Physiol. Plant* **1996** 96, 205-210

29: Napoli, C. A.; Fahy, D.; Wang, H. Y.; Taylor, L. P. "*White anther*: A petunia mutant that abolishes pollen flavonol accumulation, induces male sterility, and is complemented by a chalcone synthase transgene" *Plant Physiol*. **1999** 120, 615-622

30: Robbins, T. P.; Harbord, R. M.; Sonneveld, T.; Clarke, K. "The molecular genetics of self-incompatibility in *Petunia* hybrida" *Ann. Bot.* **2000** 85, 105-112

31: Burbulis, I. E.; Iacobucci, M.; Shirley, B. W. "A null mutation in the first enzyme of flavonoid biosynthesis does not affect male fertility in *Arabidopsis*" *Plant Cell* **1996** 8, 1013-1025

32: Clegg M. T.; Durbin, M. L. "Flower color variation: A model for the experimental study of evolution" *PNAS* **2000** 97, 7016-7023

33: Jones, K. N.; Reithel, J. S. "Pollinator-mediated selection on a flower color polymorphism in experimental populations of *Antirrhinum* (Scrophulariaceae)" *Am. J. Bot.* **2001** 88, 447-454

34: Thompson, W. R.; Meinwald, J.; Aneshansley, D.; Eisner, T. "Flavonols: pigments responsible for ultraviolet absorption in nectar guide of flower" *Science* **1972** 177, 528-530

35: Ponce, M. A.; Scervino, J. M.; Erra-Balsells, R.; Ocampo, J. A.; Godeas, A. M. "Flavonoids from shoots and roots of *Trifolium repens* (white clover) grown in presence or absence of the arbuscular mycorrhizal fungus *Glomus intraradices*" *Phytochem.* **2004** 65, 1925-1930

36: Akiyama, K.; Matsuoka, H.; Hayashi, H. “Isolation and identification of a phosphate deficiency- induced C-glycosylflavonoid that stimulates arbuscular *mycorrhiza* formation in melon roots” *MPMI* **2002** 15, 334-340

37: Bonello, P.; Blodgett, J. “*Pinus nigra-Sphaeropsis sapinea* as a model pathosystem to investigate local and systemic effects of fungal infection of pines” *Physiol. Mol. Plant Path.* **2003** 63, 249-261

38: Kong, C. H.; Xu, X. H.; Zhou, B.; Hu, F.; Zhang, C. X.; Zhang, M. X. “Two compounds from allelopathic rice accession and their inhibitory activity on weeds and fungal pathogens” *Phytochem.* **2004** 65, 1123-1128

39: Parvez, M. M.; Tomita-Yokotani, K.; Fujii, Y.; Konishi, T.; Iwahina, T. “Effects of quercetin and its seven derivatives on the growth of *Arabidopsis thaliana* and *Neurospora crassa*” *Biol. System Ecol.* **2004** 32, 631-635

40: Teutter, D. “Significance of flavonoids in plant resistance and enhancement of their biosynthesis” *Plant Biol.* **2005** 7, 581-591

41: Novak, K.; Chovanec, P.; Skrdleta, V.; Kropacova, M.; Lisa, L.; Nemcova, M. “Effect of exogenous flavonoids on nodulation of pea (*Pisum sativum L.*)” *J. Exp. Bot.* **2002** 53, 1735-1745

42: Limtrakul, P.; Khantamat, O.; Pintha, K. « Inhibition of P-glycoprotein function and expression by kaempferol and quercetin » *J. Chemother.* **2005** 17, 86-95

43: Strobel , P.; Allard, C.; Perez-Acle, T.; Calderon, R.; Aldunate, R.; Leighton, F. “Myricetin, quercetin and catechin-gallate inhibit glucose uptake in isolated rat adipocytes” *Biochem. J.* **2005** 386, 471-478

44: Vera, J.-C.; Reyes, A. M.; Velásquez, F. V.; Rivas, C. I.; Zhang, R. H.; Strobel, P.; Slebe, J.-C.; Núñez-Alarcón, J.; Golde, D. W. “Direct Inhibition of the Hexose Transporter GLUT1 by Tyrosine Kinase Inhibitors” *Biochemistry* **2001** 40, 777-790

45: Arora, A.; Byrem, T. M.; Nair, M. G.; Strasburg, G. M. “Modulation of Liposomal Membrane Fluidity by Flavonoids and Isoflavonoids” *Arch. Biochem. Biophys*. **2000** 373, 102–109

46: Kitamura, K.; Mitsuo Honda, M.; Yoshizaki, H.; Yamamoto, S.; Nakane, H.; Fukushima, M.; Ono, K.; Tokunaga, T. "Baicalin, an inhibitor of HIV-1 production in vitro" *Antiviral Res.* **1998** 37, 131–140

47: Spedding, G.; Ratty, A.; Middleton, E. "Inhibition of reverse transcriptases by flavonoids" *Antiviral Res.* **1989** 12, 99-110

48: Fesen, M. R.; Kohn, K. W.; Leteurtre, F.; Pommier, Y. "Inhibitors of human immunodeficiency virus integrase". *Proc. Natl. Acad. Sci. USA* **1993** 90, 2399–2403

49: Fesen, M. R.; Pommier, Y.; Leteurtre, F.; Hiroguchi, S. Yung, J.; Kohn, K. W. "Inhibition of HIV-1 integrase by flavones, caffeic acid phenethyl ester (CAPE) and related compounds" *Biochem. Pharmacol.* **1994** 48, 595–608

50: Brinkworth, R. I.; Stoermer, M. J.; Fairlie, D. P. "Flavones are inhibitors of HIV-1 proteinase" *Biochem Biophys Res Commun* **1992** 2, 631–637

51: Boumendjel, A. "Aurones: A Subclass of Flavones with Promising Biological Potential" *Curr. Med. Chem.* **2003** 10(1), 1-10

52: Nishizuka Y. "The molecular heterogeneity of protein kinase C and its impli- cations for cellular regulation"*Nature* **1988** 334, 661-665

53: Toker, A.; Cantley, L. C.; "Signaling through the lipid products of phosphoinositide-3-OH kinase" *Nature* **1997** 387, 673–676

54: Vanhaesebroeck, B.; Leevers S. J.; Panayotou, G.; Waterfield, M. D. "Phosphoinositide 3-kinases: a conserved family of signal transducers" *Trends. Biochem. Sci.* **1997** 22, 267–272

55: Gamet-Payrastre, L.; Manenti, S.; Gratacap, M.-P.; Tulliez, J.; Chap, H.; Payrastre, B." Flavonoids and the inhibition of PKC and PI 3-kinase" *Gen. Pharmacol.* **1999** 32, 279–286

56: Ferriola, P.C.; Cody, V.; Middleton, E. "Protein kinase C inhibition by plant flavonoids, kinetic mechanism and structure-activity relationships" *Biochem Pharmac* **1989** 38, 1617–1624

57: Zhou, X.; Liu, Y.; You, J.; Zhang, H.; Zhang, X.; Ye, L. "Myosin light-chain kinase contributes to the proliferation and migration of breast cancer cells through cross-talk with activated ERK1/2" *Cancer Lett.* **2008** 270(2), 312-327

58: Rogers, J. C.; Williams, D. L. “Kaempferol inhibits myosin light chain kinase” *Biochem. Biophys. Res. Commun.* **1989** 164, 419–425

59: Huang, C.-K. “Protein kinases in neutrophils: A review” *Membr. Biochem.* **1989** 8, 61– 79.

60: Akiyama, T. J.; Ishida, J.; Nakagawa, S.; Ogawara, H.; Watanabe, S.; Itoh, N.; Shibuya, M.; Fukami, Y. ”Genistein, a specific inhibitor of tyrosine-specific protein kinases” *Biol. Chem.* **1987** 262, 5592–5595.

61: Kyriakidis, S. N.; Sotiroudis, T. G.; Evangelopoulos, A. E. “Interaction of flavonoids with rabbit muscle phosphorylase kinase” *Biochim Biophys Acta* **1986** 871, 121– 129

62: Lin, J.-K.; Weng, M.-S. *The science of flavonoids* **2006** chap.8; New York: Springer, 2006

63: Dong, Z.; Ma, W.; Huang, C.; Yang, C. S. “Inhibition of tumor promoter-induced activator protein 1 activation and cell transformation by tea polyphenols, (-)-epigallocatechin gallate, and theaflavins” *Cancer Res* **1997** 57, 4414-4419

64: Rudd, C. E. “CD4, CD8 and the TCR-CD3 complex: A novel class of protein- tyrosine kinase receptor” *Immunol Today* **1990** 11, 400–406

65: Atluru, S.; Atluru, D. “Evidence that genistein, a protein-tyrosine kinase inhibitor, inhibits CD 28 monoclonal-antibody-stimulated human T cell proliferation” *Transplantation* **1991** 51, 448–450.

66: Geahlen, R. L.; Koonchanok, N. M; McLaughlin, J. L. “Inhibition of protein-tyrosine kinase activity by flavonoids and related compounds” *J. Nat. Prod.* **1989** 52, 982–986

67: Hornung, R. L.; Back, T. C.; Zaharko, D. S.; Urba, W. J.; Longo, D. L.; Wiltrout, R. H. “Augmentation of natural killer activity, induction of IFN and development of tumor immunity during the successful treatment of established murine renal cancer using flavone acetic acid and JL-2” *J. Immunol.* **1988** 141, 3671–3679

68: Hornung, R. L.; Young, H. A.; Urba, W. J.; Wiltrout, R. H. “Immunomodulation of natural killer cell activity by flavone acetic acid: Occurrence via induction of interferon alpha/beta” *J. Natl. Cancer Inst.* **1988** 80, 1226–1231

69: Prussin, C.; Metcalfe, D. D. “IgE, mast cells, basophils, and eosinophils” *J. Allergy Clin. Immunol.* **2003** 111(2), 486-494

70: Nagai, S.; Kitani, S.; Hirai, K.; Takaishi, T.; Nakajima, K.; Kihara, H.; Nonomura, Y.; Ito, K.; Morita, Y. "Pharmacological study of stem-cell-factor-induced mast cell histamine release with kinase inhibitors" *Biochem. Biophys. Res. Commun*. **1995** 208, 576 – 581

71: Grossman, N. "Inhibitory effects of phloretin on histamine release from isolated rat mast cells" *Agents Actions* **1988** 25, 284–290

72: Benhamou, M.; Gutkind, J. S.; Robbins, K. C.; Siraganian, R. P. "Tyrosine phosphorylation coupled to IgE receptor-mediated signal transduction and histamine release" *Proc Natl Acad Sci USA* **1990** 87, 5327–5330

73: Hirano, T.; Abe, K.; Gotoh, M.; Oka, K. "Citrus flavone tangeretin inhibits leukaemic HL-60 cell growth partially through induction of apoptosis with less cytotoxicity on normal lymphocytes" *Br. J. Cancer* **1995** 72, 1380–1388

74: Wei, Y. O.; Zhao, X.; Kariya, Y.; Fukata, H.; Teshigawara, K.; Uchida, A. "Induction of apoptosis by quercetin: Involvement of heat shock protein" *Cancer Res.* **1994** 4, 4952–4957

75: Bergamaschi, G.; Rosti, V.; Danova, M.; Ponchio, L.; Lucotti, C.; Cazzola, M. "Inhibitors of tyrosine phosphorylation induce apoptosis in human leukemic cell lines" *Leukemia* **1993** 7, 2012–2018

76: Kellis, J. T.; Vickery, L. E. "Inhibition of human estrogen synthetase (aromatase) by flavones" *Science* **1984** 225, 1032–1034

77: Ibrahim, A. R.; Abul-Hajj, Y. J. "Aromatase inhibition by flavonoids" *J. Steroid Biochem. Mol. Biol.* **1990** 37, 257-260

78: Wang, C.; Mäkelä, T.; Hase, T.; Adlercreutz, H.; Kurzer, M. S. "Lignans and Isoflavonoids Inhibit Aromatase Enzyme in Human Preadipocytes" *J. Steroid Biochem. Mol. Biol.* **1994** 50, 205–212

79: Fotsis, T.; Pepper, M.; Adlercreutz, H.; Fleischmann, G.; Hase, T.; Montesano, R.; Schweigerer, L. "Genistein, a dietary-derived inhibitor of in vitro angiogenesis" *Proc. Natl. Acad. Sci. USA* **1993** 90, 2690–2694

80: Fotsis, T.; Pepper, M. S.; Aktas, E.; Breit, S.; Rasku, S.; Adlercreutz, H.; Wahala, K.; Montesano, R.; Schweigerer, L. "Flavonoids, dietary-derived inhibitors of cell proliferation and in vitro angiogenesis" *Cancer Res.* **1997** 57, 2916–2921

81: Bracke, M. E.; Castronovo, V.; Van Cauwenberge, R. M. L.; Coopman, P.; Vakaet, L.; Strojny, P.; Foidart, J.-M.; Mareel, M. M. "The anti-invasive flavonoid (+)-catechin binds to laminin and abrogates the effect of laminin on cell morphology and adhesion" *Exp. Cell Res.* **1987** 173, 193–205

82: Scholar, E.M.; Toews, M.L. "Inhibition of invasion of murine mammary carcinoma cells by the tyrosine kinase inhibitor genistein" *Cancer Lett.* **1994** 87, 159 –162

83: Belotti, D.; Vergani, V.; Drudis, T.; Borsotti, P.; Pitelli, M. R.; Viale, G.; Giavazzi, R.; Taraboletti, G. "The microtubule-affecting drug paclitaxel has antiangiogenic activity" *Clin. Cancer Res.* **1996** 2, 1843-1849

84: Gupta, K.; Panda, D. "Perturbation of Microtubule Polymerization by Quercetin through Tubulin Binding: A Novel Mechanism of Its Antiproliferative Activity" *Biochemistry* **2002** 41(43), 13029–13038

85: DeFelice, S. L. *Scrip Mag.* **1992** « Nutraceuticals: Opportunities in an Emerging Market »

86: Ferrières, J. "The French paradox: lessons for other countries" *Heart* **2004** 90, 107-111

87: Corder, R.; Mullen, W.; Khan, N. Q.; Marks, S. C.; Wood, E. G.; Carrier, M. J.; Crozier A. "Oenology: Red wine procyanidins and vascular health" *Nature* **2006** 444, 566

88: Richter, C.; Gogvadze, V.; Laffranchi, R.; Schlapbach, R.; Schweizer, M.; Suter, M.; Walter, P.; Yaffee, M. "Oxidants in mitochondria: from physiology to diseases" *Biochim. Biophys. Acta* **1995** 1271, 67–74

89: Saybasili, H.; Yuksel, M.; Haklar, G.; Yalcin, A.S. "Effect of mitochondrial electron transport chain inhibitors on superoxide radical generation in rat hippocampal and striatal slices" *Antioxid. Redox Signal.* **2001** 3, 1099–1104

90: Staniek, K.; Gille, L.; Kozlov, A.V.; Nohl, H. "Mitochondrial superoxide radical formation is controlled by electron bifurcation to the high and low potential pathways" *Free Radic. Res.* **2002** 36, 381–387

91: Boveris, A.; Chance, B. "The mitochondrial generation of hydrogen peroxide: general properties and effect of hyperbaric oxygen" *Biochem. J.* 1973 134, 707–716

92: Vignais, P.V. "The superoxide-generating NADPH oxidase: structural aspects and activation mechanism" *Cell Mol. Life Sci.* **2002** 59, 1428–1459

93: Brar, S.S.; Corbin, Z.; Kennedy, T.P. "NOX5 NAD(P)H oxidase regulates growth and apoptosis in DU 145 prostate cancer cells" *Am. J. Physiol. Cell Physiol.* **2003** 285, C353–C369

94: Dipple, A. "DNA adducts of chemical carcinogens" *Carcinogenesis* **1995** 16, 437–441

95: Hileman, E. O.; Liu, J.; Albitar, M.; Keating, M.J.; Huang, P. "Intrinsic oxidative stress in cancer cells: a biochemical basis for therapeutic selectivity" *Cancer Chemother. Pharmacol.* **2004** 53, 209–219

96: Nicole, A.; Santiard-Baron, D.; Ceballos-Picot, I. "Direct evidence for glutathione as mediator of apoptosis in neuronal cells" *Biomedicine and Pharmacotherapy* **1998** 52, 349-355

97: Pai, E. F.; Schulz, G. E. "The catalytic mechanism of glutathione reductase as derived from x-ray diffraction analyses of reaction intermediates" *J. Biol. Chem.* **1983** 258(3), 1752-1757

98: Elliott, A. J.; Schreiber, S. A.; Thomas, C.; Pardi M.R.S. "Inhibition of glutathione reductase by flavonoids. A structure-activity study" *Biochem. Pharmacol.* **1992** 44, 1603-1608

99: Cipak, L.; Berczeliova, E.; Paulikova, H. "Effects of flavonoids on glutathione and glutathione-related enzymes in cisplatin-treated L1210 leukemia cells" *Neoplasma* **2003** 50, 443-446

100: Lavoie, S.; Chen, Y.; Dalton, T. P.; Gysin, R.; Cuénod, M.; Steullet, P.; Do, K. Q. "Curcumin, quercetin, and tBHQ modulate glutathione levels in astrocytes and neurons: importance of the glutamate cysteine ligase modifier subunit" *Journal of neurochemistry* **2009** 108(6), 1410-1422

101: Lin, J.-K.; Chen, P.-C.; Ho, C.-T.; Lin-Shiau S.-Y. "Inhibition of Xanthine Oxidase and Suppression of Intracellular Reactive Oxygen Species in HL-60 Cells by Theaflavin-3,3′-digallate, (-)-Epigallocatechin-3-gallate, and Propyl Gallate" *J. Agric. Food Chem.* **2000** 48(7), 2736–2743

102: Wondrak, G. T. "Redox-Directed Cancer Therapeutics: Molecular Mechanisms and Opportunities" *Antioxidants & Redox Signaling* **2009** 11(12), 3013-3069

103: Lin, Y.-L.; Chen, P.-C.; Lin, Y.-P.; Lau, Y.-W.; Juan, I-M.; Lin, J.-K. "Hypolipidemic Effect of

Green Tea Leaves through Induction of Antioxidant and Phase II Enzymes Including Superoxide Dismutase, Catalase, and Glutathione S-Transferase in Rats" *J. Agric. Food Chem.* **1998** 46(5), 1893−1899

104: Koppenol, W. H. "The Haber-Weiss cycle—70 years later" *Redox Rep.* **2001** 6(4), 229-234

105: Pietta, P.-G. "Flavonoids as Antioxidants" *J. Nat. Prod.* **2000** 63, 1035-1042

106: Seyoum, A.; Asres, K.; El-Fiky, F. K. "Structure–radical scavenging activity relationships of flavonoids" *Phytochemistry* **2006** 67, 2058–2070

107: Hanasaki, Y. Ogawa, S.; Fukui, S. "The correlation between active oxygens scavenging and antioxidative effects of flavonoids" *Free Rad. Biol. & Med.* **1994** 16(6), 845-850

108: Deng, W.; Fang, X.; Wu, J. "Flavonoids function as antioxidants: by scavenging reactive oxygen species or by chelating iron?" *Radiat. Phys. Chem.* **1997** 50(3), 271-276

109: Ferrali, M.; Signorini, C., Caciotti, B.; Sugherini, L.; Ciccoli, L.; Giachetti, D.; Comproti, M. "Protection against oxidative damage of erythrocyte membrane by the flavonoid quercetin and its relation to iron chelating activity" *FEBS Lett.* **1997** 416, 123-129

110: Kruszewski, M. "Labile iron pool: the main determinant of cellular response to oxidative stress" *Mutat. Res. Fundam. Mol. Mech. Mugag.* **2003** 531, 81-92

111: Mladěnka, P.; Macáková, K.; Filipský, T.; Zatloukalová, L.; Jahodár, L.; Bovicelli, P. Proietti Silvestri, I.; Hrdina, R.; Saso, L.; "*In vitro* analysis of iron chelating activity of flavonoids" *J. of Inorg. Biochem.* **2011** 105, 693–701

112: Pelicano, H.; Carney, D.; Huang, P. "ROS stress in cancer cells and therapeutic implications" *Drug Resist. Updates* **2004** 7, 97–110

113: Boots, A.W.; Lib, H.; Schinsb, R. P.F.; Duffinb, R.; Heemskerkc, J. W.M.; Bast, A.; Haenen, G. R.M.M. "The quercetin paradox" *Toxicol. Appl. Pharm.* **2007** 222, 89–96

114: Hillard, E. A.; Vessières, A.; Thouin, L.; Jaouen, G.; Amatore, C. "Ferrocene-mediated

proton-coupled electron transfer in a series of ferrocifen-type breast cancer drug candidates" *Angew. Chem. Int. Ed.* **2006** 45, 285 –290

115: Kealy, T. J.; Pauson, P. L. "A New Type of Organo-Iron Compound" *Nature* **1951**

168,1039-1040

116: Wilkinson, G.; Rosenblum, M.; Whiting, M. C.; Woodward, R. B. "The structure of iron bis-cyclopentadienyl" *J. Am. Chem. Soc.* **1952** 74, 2125-2126

117: Fischer, E. O.; Pfab, W. "Cyclopentadien-metallkomplexe, ein neuer typ metallorganischer verbidungen" *Z. Naturforsh.* **1952** 7b, 377-379

118: Woodward, R. B.; Rosenblum, M.; Whiting, M. C. "A new aromatic system" *J. Am. Chem. Soc.* **1952** 74, 3458-3459

119: Yeary R. A. "Chronic toxicity of dicyclopentadienyliron (ferrocene) in dogs" *Toxicol. Appl. Pharmacol.* **1969** 15, 666–676

120: Nesmeyanov, A. N.; Bogomolova, L.G.; Viltchevskaya, V.; Palitsyne, N.; Andrianova, I.; Belozerova, O. "Ferrocerone" **1971** *US Patent* 119356

121: van Staveren, D. R.; Metzler-Nolte, N. "Bioorganometallic Chemistry of Ferrocene" *Chem. Rev.* **2004** 104(12), 5931–5986

122: Fouda, M. F. R.; Abd-Elzaher, M. M.; Abdelsamaia, R. A.; Labib, A. A. "On the medicinal chemistry of ferrocene" *Appl. Organomet. Chem.* **2007** 21, 613–625

123: Köpf-Maier, P.; Köpf, H.; Neuse, E. W. "Ferrocenium Salts- The First Antineoplastic Iron Compounds" *Angew. Chem. Int. Ed. Engl.* **1984** 23, 456–457

124: Köpf-Maier, P.; Köpf, H.; Neuse, E. W. "Ferricenium complexes: A new type of water-soluble antitumor agent" *J. Cancer Res. Clin. Oncol.* **1984** 108, 336–340

125: Neuse, E. W.; Kanzawa, F. " Evaluation of the activity of some water-soluble ferrocene and ferricinium compounds against carcinoma of the lung by the human tumor clonogenic assay" *Appl. Organomet. Chem.* **1990** 4, 19–26

126: Top, S.; Tang, J.; Vessieres, A.; Carrez, D.; Provot, C.; Jaouen, G. "Ferrocenyl hydroxytamoxifen: a prototype for a new range of oestradiol receptor site-directed cytotoxics" *Chem. Commun.* **1996** 8, 955–956

127: Top, S.; Dauer, B.; Vaisserman, J.; Jaouen, G. "Facile route to ferrocifen, 1-[4-(2-dimethylaminoethoxy)]-1-(phenyl-2-ferrocenyl-but-1-ene), first organometallic analogue of tamoxifen, by the McMurry reaction" .*J. Organomet. Chem.* **1997** 541, 355–361

128: Jordan, V. C. “The role of tamoxifen in the treatment and prevention of breast cancer” *Curr. Probl. Cancer* **1992** 16, 129–176

129: Jordan, V. C. “Antiestrogens and selective estrogen receptor modulators as multifunctional medicines. 1. Receptor interactions” *J. Med. Chem.* **2003** 46, 883–908

130: Top, S.; Vessieres, A.; Leclercq, G.; Quivy, J.; Tang, J.; Vaissermann, J.; Huché, M.; Jaouen, G. “Synthesis, Biochemical Properties and Molecular Modelling Studies of Organometallic Specific Estrogen Receptor Modulators (SERMs), the Ferrocifens and Hydroxyferrocifens: Evidence for an Antiproliferative Effect of Hydroxyferrocifens on both Hormone-Dependent and Hormone-Independent Breast Cancer Cell Lines” *Chem. Eur. J.* **2003** 9, 5223–5236

131: Hamels, D.; Dansette, P.; Hillard, E. A.; Top, S.; Vessières, A.; Herson, P.; Jaouen, G.; Mansuy, D. “Ferrocenyl quinone methides as new strong antiproliferative agents: formation by metabolic and chemical oxidation of ferrocenyl phenols” *Angew. Chem. Int. Ed. Engl.* **2009** 48, 9124–9126

132: Michard, Q.; Jaouen, G.; Vessieres, A.; Bernard, B.A. “Evaluation of cytotoxic properties of organometallic ferrocifens on melanocytes, primary and metastatic melanoma cell lines” *J. Inorg. Chem.* **2008** 102, 1980–1985

133: Allard, E.; Passirani, C.; Garcion, E.; Pigeon, P.; Vessières, A.; Jaouen, G.; Benoit, J. P. “Lipid nanocapsules loaded with an organometallic tamoxifen derivative as a novel drug-carrier system for experimental malignant gliomas” *J. Control. Release* **2008** 130, 146–153

134: Clemens, J. A.; Bennett, D.R.; Black, L. J.; Jones, C. D. “Effects of a new antiestrogen, keoxifene (LY156758), on growth of carcinogen-induced mammary tumors and on LH and prolactin levels” *Life Sci.* **1983** 32, 2869–2875

135: Jordan, V. C. “Alternate antiestrogens and approaches to the prevention of breast cancer” *J. Cell Biochem. Suppl.* **1995** 22, 51–57

136: Willhite, S. L.; Goebel, S. R.; Scoggin, J. A. “Raloxifene provides an alternative for osteoporosis prevention” *Ann. Pharmacother.* **1998** 32, 834–837

137: Ferreira, A. P.; da Silva, J. L. F.; Duarte, M. T.; da Piedade, M. F. M.; Robalo, M. P.; Harjivan, S. G.; Marzano, C.; Gandin, V.; Marques, M. M. “Synthesis and characterization of

new organometallicbenzo[b]thiophene derivatives with potential antitumor properties" *Organometallics* **2009** 28, 5412–5423

138: Newling D. W. "Anti-androgens in the treatment of prostate cancer" *Br. J. Urol.* **1996** 77, 776–784

139: Hillard, E. A.; Vessières, A.; Jaouen, G. *Medicinal Organometallic Chemistry,* "Ferrocene Functionalized Endocrine Modulators as Anticancer Agents" *Topics in Organometallic Chemistry* (Springer-Verlag Berlin Heidelberg) **2010** 32, 81-117

140: Maheshwari, R. K.; Singh, A. K.; Gaddipati, J.; Srimal, R. C. "Multiple biological activities of curcumin: A short review" *Life Sci.* **2006** 78(18), 2081-2087

141: Arezki, A.; Chabot, G. G.; Quentin, L.; Scherman, D.; Jaouen, G.; Brulé E. "Synthesis and biological evaluation of novel ferrocenyl curcuminoid derivatives" *Med. Chem. Commun.* **2011** 2, 190-195

142: Spencer, J.; Amin, J.; Wang, M.; Packham, G.; Syed Alwi, S. S.; Tizzard, G. J.; Coles, S. J.; Paranal, R. M.; Bradner, J. E.; Heightman, T. D. "Synthesis and Biological Evaluation of JAHAs: Ferrocene-Based Histone Deacetylase Inhibitors" *Med. Chem. Lett.* **2011** 2, 358–362

143: Plowman, G. D.; Ullrich, A.; Shawver, L. K. "Identification of receptors and signaling molecules that play crucial roles in proliferative, endocrine and immune disease processes will provide exciting opportunities for targeted drug discovery" *DN&P* **1994** 7(6), 334-339

144: Sun, L.; Tran, N.; Tang, F.; App, H.; Hirth, P.; McMahon, G.; Tang, C. "Synthesis and Biological Evaluations of 3-Substituted Indolin-2-ones: A Novel Class of Tyrosine Kinase Inhibitors That Exhibit Selectivity toward Particular Receptor Tyrosine Kinases" *J. Med. Chem.* **1998** 41, 2588-2603

145: Spencer, J.; Mendham, A.P.; Kotha, A.K.; Richardson, S.C.W.; Hillard, E. A.; Jaouen, G.; Male, L.; Hursthouse, M. B. "Structural and biological investigation of ferrocene-substituted 3-methylidene-1,3-di- hydro-2H-indol-2-ones" *Dalton Trans.* **2009** 6, 918–921

146: Kondapi, A.K.; Satyanarayana, N.; Saikrishna, A. D. "A study of the topoisomerase II activity in HIV-1 replication using the ferrocene derivatives as probes." *Arch. Biochem. Biophys.* **2006** 450, 123–132

147: Saikrishna, A. D.; Panda, G.; Kondapi, A.K. "Mechanism of action of ferrocene

derivatives on the catalytic activity of topoisomerase IIα and β—Distinct mode of action of two derivatives" *Arch. Biochem. Biophys.* **2005** 438, 206–216

148: Edwards, E. I.; Epton, R.; Marr, G. "Organometallic derivatives of penicillins and cephalosporins a new class of semi-synthetic antibiotics" *J. Organomet. Chem.* **1975** 85, C23-C25

149: Edwards, E. I.; Epton, R.; Marr, G. "1, 10-Ferrocenyldiacetic acid anhydride and its use in the preparation of heteroannularly substituted ferrocenyl-penicillins and -cephalosporins" *J. Organomet. Chem.* **1976** 107, 351-357

150: Biot, C.; Glorian, G.; Maciejewski, L.A.; Brocard, J.S. "Synthesis and antimalarial activity *in vitro* and *in vivo* of a new ferrocene-chloroquine analogue" *J. Med. Chem.* **1997** 40, 3715–3718

151: Delhaes, L.; Abessolo, H.; Biot, C.; Berry, L.; Delcourt, P.; Maciejewski, L.A.; Brocard, J. S.; Camus, D.; Dive, D. "*In vitro* and *in vivo* antimalarial activity of ferrochloroquine, a ferrocenyl analogue of chloroquine against chloroquine-resistant malaria parasites" *Parasitol. Res.* **2001** 87(3), 239-244

152: Wu, X.; Wilairat, P.; Go, M. L. "Antimalarial Activity of Ferrocenyl Chalcones" *Bioorg. Med. Chem. Lett.* **2002** 12, 2299–2302

153: Wu, X.; Tiekink, E. R.T.; Kostetski, I.; Kocherginsky, N.; Tan, A. L. C.; Khoo, S. B.; Wilairat, P.; Go, M. L. "Antiplasmodial activity of ferrocenyl chalcones: Investigations into the role of ferrocene" *Eur. J. Pharm. Sci.* **2006** 27, 175–187

154: Hauser C. R.; Lindsay, J. K. "Certain Acylations of Ferrocene and Some Condensations Involving the α-Hydrogen of Acetylferrocene" *J. Org. Chem.* **1957** 22(5), 482-485

155: Hauser C. R.; Lindsay, J. K. "Some Typical Aldehyde Addition and Condensation Reactions of Formylferrocene" *J. Org. Chem.* **1957** 22(8), 906–908

Chapter 2

Ferrocenyl chalcones and their adducts

Synthesis and biological properties

A. Background

Ferrocenyl chalcones were first described in 1957. These studies were made in a fundamental context, that is to say, to simply explore ferrocene reactivity. The first synthesis was achieved in five steps using ferrocene as a starting material.[1, 2] The first four steps resulted in the preparation of ferrocene carboxaldehyde, as shown in Figure 2.1.

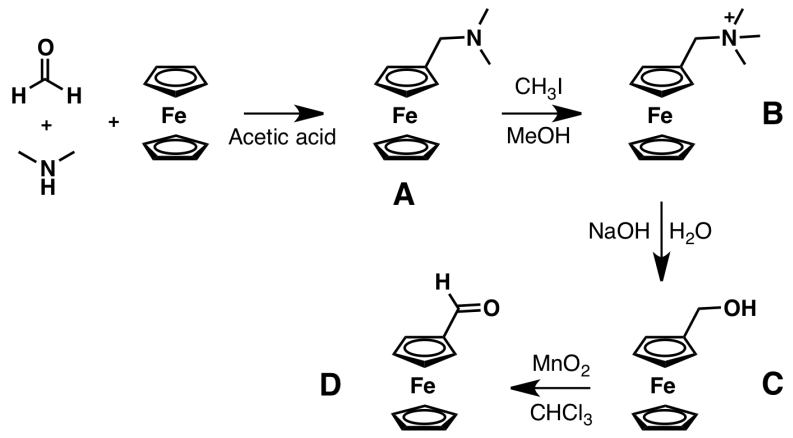

Figure 2.1. First synthesis of ferrocene carboxaldehyde

Ferrocene was first reacted with formadehyde and dimethyl amine in acetic acid to give *N*,*N*-dimethylaminomethylferrocene (A). The amine function of A was then methylated using methyl iodide in methanol, affording (B), which, in a basic aqueous solution becomes hydroxymethylferrocene (C). Finally, C was oxidized to ferrocene carboxaldehyde using manganese dioxide in chloroform.[2]

Nowadays, ferrocene carboxaldehyde is synthesized in one step from ferrocene, using a lithium reagent. The functionalization of ferrocene using its lithium salt as an intermediate was described in 1995 by Guillaneux and Kagan.[3] Once the ferrocene lithium salt is formed, a simple quenching by dry DMF affords ferrocene carboxaldehyde.

From the ferrocene carboxaldehyde, the ferrocenyl chalcone was made by aldol condensation with acetophenone in a mixture of water and ethanol, using sodium hydroxide. The synthetic scheme is presented in Figure 2.2.

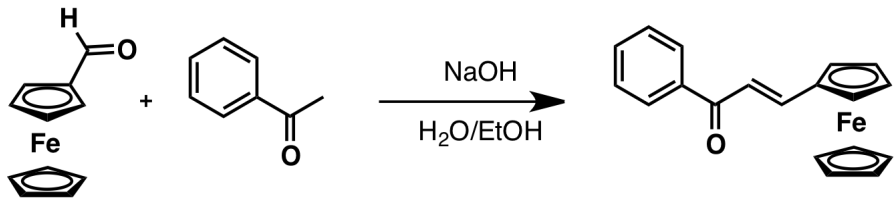

Figure 2.2. First synthesis of ferrocenyl chalcone

Later on, the ferrocenyl chalcones shown in Figure 2.3 were shown to be suitable for the development of chemosensors for Ca^{2+} and Ba^{2+}. When the chalcones interact with Ca^{2+} and Ba^{2+}, their UV/visible absorption bands shift in energy, together with their NMR signature. Moreover, the ferrocene oxidation potential is also modified in the case of chelation with Ca^{2+} and Ba^{2+}, allowing electrochemical detection.[4, 5]

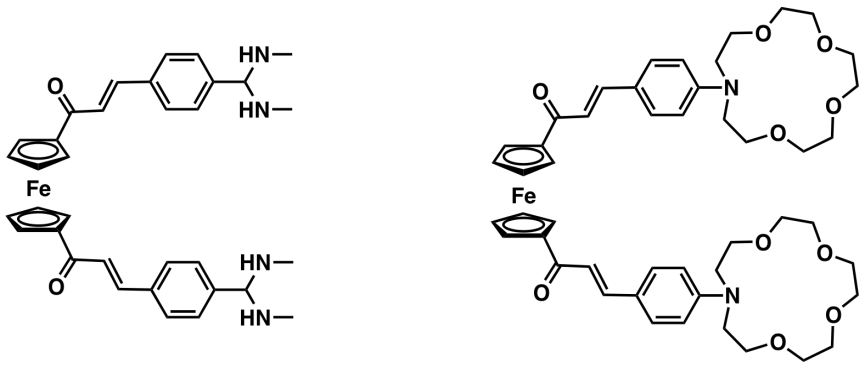

Figure 2.3. Ferrocenyl chalcones used as chemosensors

The biological properties of ferrocenyl chalcones have only been studied in the last ten years. In 2002, Go and coworkers became interested in the antiplasmodial activity of these compounds.[6] The authors suspected that these compounds could be active in this regard according to prior work on antiplasmodial ferrocene derivatives such as ferroquine (see chapter 1), and wished to investigate the role of ferrocene on antiplasmodial activity. This work resulted more recently in a more complete study of ferrocenyl chalcones, which was presented in chapter 1 section B.2.4.b.[7]

Another study by Sohár and coworkers examined the antitumor activity of ferrocenyl chalcones and their glycosides on HL60 leukemia cells.[8] The four compounds represented on Figure 2.4 possess IC_{50} values between 1 and 4 μM.

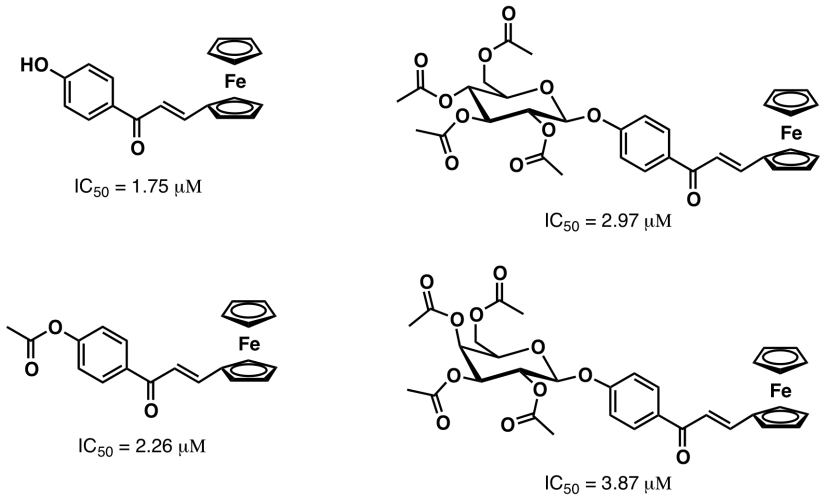

Figure 2.4. Structures and IC_{50} values on HL-60 cells of ferrocenyl chalcones and glycosides

Other chalcones shown in Figure 2.5, where the A ring has been replaced by a ferrocene moiety, have also shown interesting effects. They have been tested against tumoral and normal cells. On normal HEF human fibroblasts and L929 mouse fibroblasts, both compounds induced less than 50% growth inhibition at a concentration of 1 mM. On F10 mouse melanoma cells, the compounds demonstrated IC_{50} values of 90 μM for the compound **A** and 75 μM for compound **B**. On human carcinoma Hep2 cells, IC_{50} values of 4 μM for compound **A** and 2.5 μM for compound **B** were found.

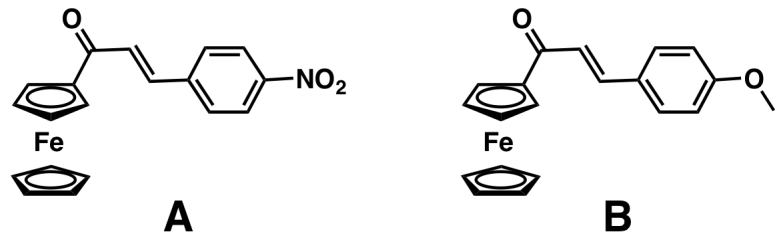

Figure 2.5. Ferrocenyl chalcones active on Hep2 carcinoma cells and F10 melanoma cells

The authors attribute the selectivity for cancer cells to the redox properties of ferrocene, and show the interest of these molecules as selective anti-cancer agents.[9]

Ferrocenyl chalcones have also shown a nematocidal effect on *Caenorhabditis elegans*.[10] Nematodes, or roundworms, are parasites which cause diseases such as elephantiasis. In this experiment, they were exposed to organic chalcones and their ferrocenyl analogues, and two parameters were studied using SAR techniques. First, the direct toxicity of the compounds was evaluated and it was found that the organic chalcones were more active than their ferrocenyl analogues. The authors attribute this behavior to the difference in lipophilicity of the two series of compounds. The organic derivatives being more lipophilic, they possess a better ability to penetrate the protective cuticle on the nematode embryos.

The second subject of study was the inhibition of nematode reproduction. In this regard, the ferrocenyl derivatives were more active than their organic analogues.

B. Aims of the study

We decided to synthesize a series of ferrocene chalcone derivatives for two major purposes. The first interest was the evaluation of their biological properties against diseases other than malaria, which had been previously well studied by Go and coworkers. We chose for our study an evaluation of the effects of ferrocenyl chalcones against cancer, bacteria and HIV. The second interest in synthesizing these molecules concerns obtaining access to other members of the flavonoid family. As discussed before, none of the ferrocene flavonoid subclasses other than chalcones have ever been synthesized, and, in principle, ferrocene chalcones can serve as starting materials for the other ferrocenyl flavonoids.

We designed a series of ferrocenyl chalcones whose general pattern is shown in Figure 2.6. In these molecules ferrocene has replaced the B ring and the A ring is diversely substituted. The 2-hydroxy substitution on the A ring is absolutely essential to access the other families of flavonoids, although there is only one report of a ferrocenyl chalcone possessing this function in the literature, corresponding to R = H.[7]

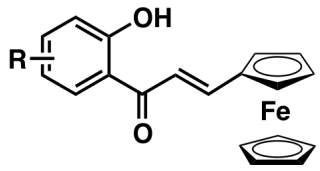

Figure 2.6. General pattern of our ferrocenyl chalcone derivatives

Our choice to screen these molecules against cancer cells was motivated by our hypothesis that the addition of an additional redox-active group to the flavonoid skeleton could improve, or at least modify, their antiproliferative effects. As discussed in chapter 1, redox-active compounds in the treatment of cancer is a growing field of interest, since cancer cells

generally produce more ROS than normal cells. Both ferrocene and flavonoids are known to be activated by oxidation; therefore their combination may provide interesting results. B16 murine melanoma cells are very robust and aggressive and constitute a good model for the determination of anti-cancer properties. The IC_{50} values of compounds **1a-j** and **2a-j** were determined using the standard MTT test, described in a further section.

The compounds' antiangiogenic properties were also evaluated. The design of antiangiogenic compounds is currently a subject of great interest in the discovery of new anti-cancer agents. As previously discussed, angiogenesis is the growth of new blood vessels from pre-existing vessels. Tumor cells induce angiogenesis for the tumor to receive nutrients and oxygen that are essential for the tumor growth. Moreover, the creation of new vessels allows the dissemination of cancer cells throughout the organism, creating metastases. Therefore, antiangiogenic agents both weaken the tumor and help prevent metastases formation. Two main types of antiangiogenic agents exist: angiogenesis inhibitors and vascular disrupting agents (VGA), which destroy vessels directly. This latter class of molecules is more active on tumor vessels than on normal vessels, since it takes advantage of differences existing between the two; tumor vessels exhibit increased permeability and reduced blood flow when compared to normal ones.

Flavonoids are an important class of VGAs[11] and one compound, flavone acetic acid (FAA), has undergone phase II clinical trials for this purpose. Its mechanism of action as a VGA seems to be due to apoptosis induction in tumor blood vessel endothelial cells.[12] FAA was abandoned in phase II due to its inactivity on humans.[13] One of its derivatives, (5,6-Dimethyl-9-oxo-9H-xanthen-4-yl)-acetic acid (ASA404), also based on a flavonoid skeleton, is presented in Figure 2.7. ASA404 is the first VGA entering in phase III clinical trials.[14]

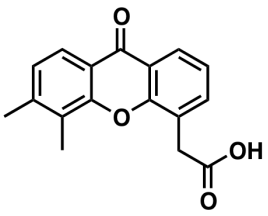

Figure 2.7. Structure of ASA404

Tests evaluating antiangiogenic abilities of all presented molecules have been performed, the technique and results will be presented in a further section.

The interest of using ferrocene in the design of anti-HIV agents was presented in section B.2.2 of chapter 1. Moreover, chalcones have been studied in this regard in studies conducted by Neamati and coworkers. This work showed the potential of chalcones as IN inhibitors,[15] which is currently an emerging target for HIV treatment. IN catalyzes the insertion of HIV proviral DNA into the host genome. This integration occurs via a multi-step process, in which the cleavage of two nucleotide bases from each 3'-end of the proviral DNA (3'- processing) and the subsequent insertion of the shortened strand into the host genome (strand transfer) are the key catalytic functions of the enzyme.[16] Compounds inhibiting IN block one or both of these steps.

It is important to mention that the major problem of IN inhibition concerns very fast acquired resistance. Thus molecules like Elvitegravir (GS-9137), shown in Figure 2.8, although still in advanced clinical trials, already face this problem.[17] Therefore, designing such inhibitors possessing a ferrocene moiety, known to help avoid drug-resistance problems, seemed promising.

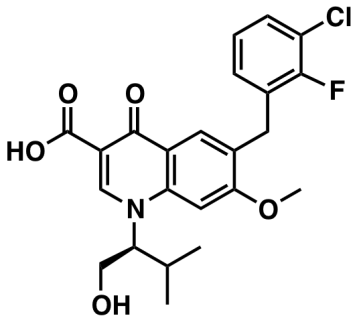

Figure 2.8. Structure of Elvigravir

The major disadvantage with chalcone derivatives as IN inhibitors is their rather poor activity. However, the addition of a BF_2 moiety on a molecule possessing a 1,3-ketol motif is known to result in an enhanced activity, Such as in the case of the pyr-R molecules shown in Figure 2.9. These molecules seem to have a better affinity for IN than analogous compounds

lacking the BF_2 group, as demonstrated for pyr-Br and pyr-F, were the inhibition abilities are 7 to 25 times higher than their free acid analogs.[18]

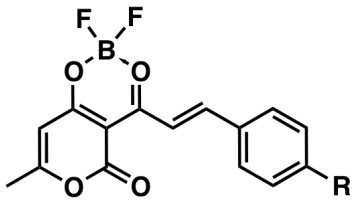

Figure 2.9. Structures of IN inhibitors, pyr-R R = Br, F

Thus, we synthesized a series of ferrocene chalcone adducts possessing the BF_2 motif; their general pattern in presented in Figure 2.10. Their ability to inhibit IN was then measured, using an IN-specific *in vitro* assay created by Nouri Neamati at the University of Southern California; this test will be described in a further section.

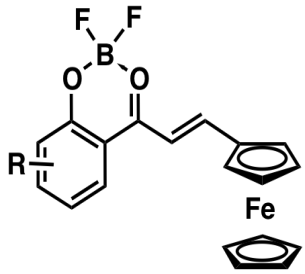

Figure 2.10. General pattern of BF_2 ferrocenyl chalcone adducts

C. Synthesis and chemical properties of ferrocenyl chalcone derivatives

1. Synthesis

1.1. Ferrocenyl chalcones

The synthesis of the ferrocenyl chalcones presented in Figure 2.11 was accomplished by a simple aldolic condensation as described in the literature. The protocol consists in refluxing a diversely substituted 2-hydroxyacetophenone and ferrocene carboxaldehyde in ethanol for 2 h in the presence of excess NaOH.[6] Compounds **1a-1j** were obtained in good yield after purification by silica gel column chromatography.

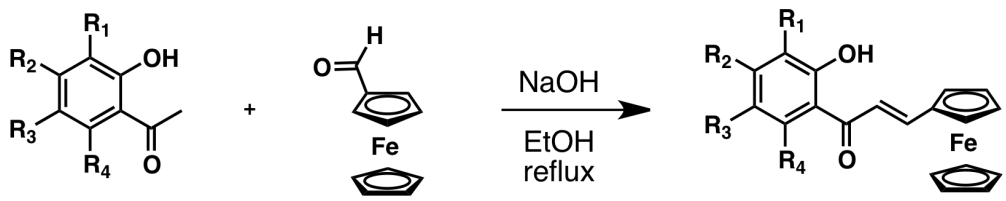

1a: R_1=R_2=R_3=R_4=H (81%)
1b: R_3=Cl (82%)
1c: R_3=Br (79%)
1d: R_1= R_3=Cl (82%)
1e: R_1=R_3=Br (76%)

1f: R_1=R_3=F (80%)
1g: R_2=OMe (80%)
1h: R_3=OMe (85%)
1i: R_4=OMe (81%)
1j: R_2=R_4=OMe (78%)

Figure 2.11. General synthesis of the ferrocenyl chalcones

Concerning the purification, silica gel column chromatography was performed using a mixture of DCM and petroleum ether. The acetophenones are pale yellow to colorless, ferrocene carboxaldehyde is orange-red and compounds **1a-j** are red-violet. Therefore, following the separation using TLC analysis was not required, since the separation of the different fractions was clearly visible. In order to obtain crystalline solids, **1a-j** were recrystallized from a mixture of DCM and pentane.

1.2. Ferrocenyl chalcone adducts

The further grafting of a BF_2 unit on compounds **1a-j** resulted in compounds **2a-j**. This step was achieved by simply deprotonating **1a-j** with NaH, and then adding an excess of $BF_3.OEt_2$ in DCM at room temperature, as shown in Figure 2.12.

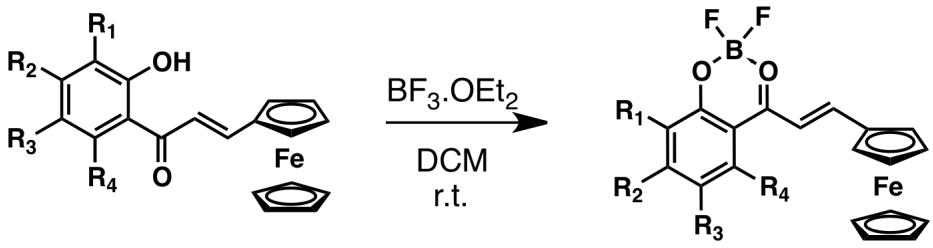

2a: R_1=R_2=R_3=R_4=H (80%)
2b: R_3=Cl (85%)
2c: R_3=Br (98%)
2d: R_1=R_3=Cl (84%)
2e: R_1=R_3=Br (67%)
2f: R_1=R_3=F (75%)
2g: R_2=OMe (84%)
2h: R_3=OMe (86%)
2i: R_4=OMe (82%)
2j: R_2=R_4=OMe (74%)

Figure 2.12. Synthesis of compounds **2a-j**

In this case, the purification was not always accomplished by column chromatography. Especially for **2a-f**, the stability of the compounds on silica gel was very limited, and a fast loss of BF_2 was observed. More precisely, when **2a-j** were left a couple of hours on silica, their characteristic green color turned to violet, and TLC analysis showed the new compounds to be the corresponding chalcones **1a-j**. Moreover, **2a-j** also exhibited poor stability in ethyl acetate, which we originally selected as a co-eluent for chromatographic separation. Therefore, compounds **2a-j** were purified by recrystallization only, using a mixture of DCM and pentane at +4 °C.

2. Characterization

All compounds were unambiguously characterized using routine techniques, that is to say NMR spectroscopy, mass spectrometry, elemental analysis and so on (c.f. experimental

section). The *E* configuration of the enone in all compounds was determined by ^{1}H NMR, where the coupling constants of the vinylic protons were between 14 and 15 Hz.

2.1. Crystal structure of 2a

A crystal structure was obtained by X-ray diffraction for compound **2a**; unfortunately its quality was not sufficient for publication in the peer-reviewed literature (R factor = 0.1116 and wR_2 factor = 0.2624). This structure and associated data are presented in Figure 2.13 and Table 2.1.

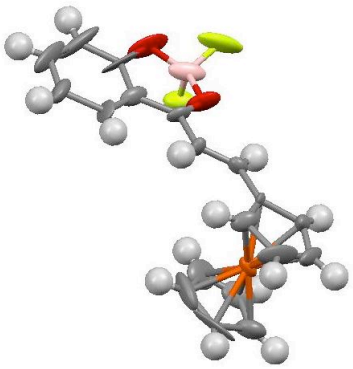

Figure 2.13. Structure of compound **2a** created by Hg software.

Table 2.1. Crystal data for molecule **2a**.

	2a	Z	4
	$C_{19}H_{15}BF_2FeO_2$	T	200
M	379.98	No. reflections	15527
Crystal system	monoclinic	No. independent reflections	4489
Space group	C1c1	R_{int}	0.045
a (Å)	13.634(3)	2θ	60.02°
b (Å)	13.6158(17)	R_1 (all data)	0.1116
c (Å)	10.3428(11)	wR_2 (all data)	0.2624
β (°)	118.901(11)	R_1 (with cutoff)	0.0941
V (Å^3)	1680.9(5)	wR_2 (with cutoff)	0.2513

2.2. UV/visible spectroscopy of 1a-j

One remarkable aspect of the ferrocenyl chalcones is their highly saturated color. Indeed, the color changes depending on the substitution pattern of the chalcones, going from violet for the most electron-withdrawing substituents (the dihalogenated compounds) to red-violet for the compounds with the most electron-donating substituents (the methoxylated compounds). These colors are a big advantage at the bench, facilitating column purification and reaction monitoring by TLC. Moreover, they are the sign of an altered electronic structure compared to the organic chalcones, which are pale yellow.

The color of the ferrocenyl chalcones suggests the presence of a strong absorption in the visible region. UV-visible absorption spectra of **1a-j** were therefore recorded, and the molar extinction coefficients (ε) at λ_{max} in the visible region were calculated for each molecule. The results are summarized in Table 2.2.

Table 2.2. Molar absorptivity values at λ_{max} (in the visible or near UV) for series **1**

Compound	λ_{max} (nm)	ε	Compound	λ_{max} (nm)	ε
1a	342	6715	**1f**	353	16923
	526	1741		544	5027
1b	365	12310	**1g**	353	15564
	538	3827		513	2734
1c	344	9685	**1h**	351	7685
	535	2567		526	1789
1d	354	14818	**1i**	344	12937
	550	4059		519	2646
1e	355	13779	**1j**	349	21835
	552	4013		512	3578

The UV/visible spectra of substituted organic chalcones have been calculated by a variety of theoretical methods, all semi-empirical. The first DFT study on chalcone spectral properties identified the lowest energy transition (around 300-400 nm) as having $\pi \rightarrow \pi^*$ character.[19] In the ferrocenyl chalcones, strong peaks are also observed in this region. The position of these peaks is not strongly influenced by substitution on the A ring, consistent with previous reports.[19] The lower energy peaks between 510 and 550 nm observed in the visible region of the ferrocene chalcones are not present in the organic series. They likely correspond to a metal to ligand charge transfer involving a Fe-based HOMO and a π^* LUMO.

In general, electron-withdrawing groups decrease the energy of the visible λ_{max}, while electron-donating groups increase it relative to the unsubstituted molecule. Moreover, we can see that in both cases, the effects on disubstituted molecules are stronger than the effects on monosubstituted ones. This is likely due to a destabilization of the π^* molecular orbital by electron-donating groups. This is consistent with the DFT calculations indicating that electron-donating groups cause increasing MO energy and electron withdrawing groups cause decreasing MO energy.

For ferrocene, the molar absorption coefficient (ε) at about 450 nm is very weak, around 100 $L.mol^{-1}.cm^{-1}$, because it corresponds to a forbidden iron d-d* transition.[20] In the case of compounds **1a**-**j**, the molar absorption coefficient of the lowest energy transition is much too high to be a purely ferrocene-centered transition.

2.3 IR spectroscopy

In order to study the effect of the BF_2 moiety on the C=O and the C=C double bonds, IR spectra of **1a-j** and **2a-j** were recorded. The results are summarized in Table 2.3. The first observation that can be made is that, with the exception of **2j**, the energy of the C=O stretch decreases (by 5-35 cm^{-1}) when the BF_2 moiety is present. Likewise, in the case of C=C stretching, *v* decreases when the BF_2 moiety is present in all cases, except for **2a**. The range of shifts is however larger, from 5 to 65 cm^{-1}. These bathochromic shifts in the presence of the BF_2 group suggests that this electron-withdrawing moiety is polarizing and thus weakening the C=O and C=C bonds. For series 2, another band, corresponding to the B-F

stretch, appears in the same region. In this case, the values are rather constant, the major substituent influence being in the case of **2f**, where the difluoro substitution induces a shift of 22cm^{-1} when compared to the unsubstituted **2a**.

Table 2.3. IR characteristic values (in cm^{-1}) for **1a-j** and **2a-j**

	Series **1** chalcones		Series **2** chalcone adducts		
	C=O	C=C	C=O	B-F	C=C
a	1627	1554	1623	1594	1580
b	1630	1555	1617	1591	1549
c	1628	1573	1612	1590	1544
d	1631	1550	1609	1584	1546
e	1629	1550	1595	1577	1540
f	1624	1566	1592	1572	1511
g	1630	1574	1620	1598	1553
h	1646	1618	1630	1590	1555
i	1616	1550	1613	1589	1562
j	1618	1551	1622	1586	1558

2.4 Electrochemistry

The oxidation chemistry of **1a-j** was analyzed by cyclic voltammetry. The results are presented in Table 2.4. As a general tendency, electron-withdrawing groups increase the oxidation potential of the ferrocene moiety, while electron-donating groups decrease it. For compound **3h**, the substitution doesn't seem to have any influence on the oxidation potential of the ferrocene moiety.

The shift in oxidation potentials is the direct consequence of the electronic effects on the ferrocenyl moiety. With the assumption that the visible transition is a MLCT transition, the stability of the ferrocene-based molecular orbital should also impact the energy of this transition.

Table 2.4. Shift of the ferrocene oxidation potential for compounds **1a-j**

Compound	$E_{1/2}$ (Fc+/Fc)
1a	0.181
1b	0.183
1c	0.191
1d	0.197
1e	0.200
1f	0.187
1g	0.145
1h	0.181
1i	0.135
1j	0.103

To understand the influence of the substituents on the relative energies of the frontier orbitals, we plotted the energy corresponding to this transition as a function of the ferrocene oxidation potential for each molecule. The graph is presented in Figure 2.14.

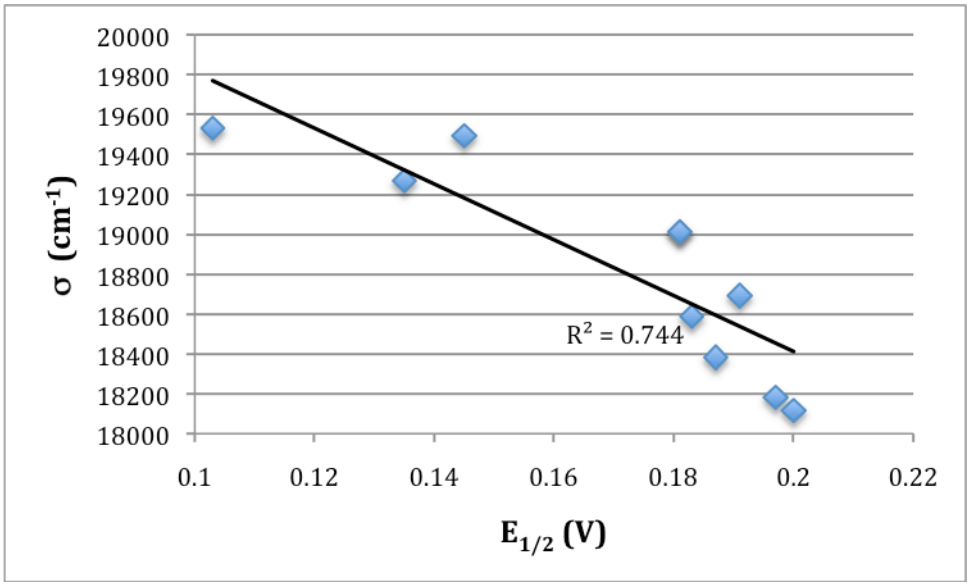

Figure 2.14. Plot of the wavenumber in function of the ferrocene moiety oxidation potential for each compound of series **1**

In general, the visible transition becomes less energetic with increasing redox potential. The increasingly positive redox potential is due to a stabilization of the ferrocene-based orbital towards ionization. However, increasing stabilization of this orbital appears to be

accompanied by a decrease in the transition energy. Therefore, as predicted by published calculations, it appears the electron-withdrawing substituents also stabilize the π^* orbital, and that substituents have a stronger effect on stabilization of the π^* orbital than they do towards the ferrocene-based HOMO. This is as expected when one considers the geometry of the molecule.

3. Stability of the chalcone adducts

In our attempts to analyze compound **2a-j** using ^{13}C NMR spectroscopy, we faced a solubility problem in deuterated chloroform. Therefore, we decided to use another deuterated solvent, DMSO, to make this analysis. When we dissolved the compounds of series **2** in DMSO, we noticed that the deep green solution slowly become brown, and then completely orange when exposed to light.

From this observation, we selected the compound for which the conversion seemed the slowest, **2j**, and we performed a photodecomposition study using simple solar irradiation, followed by UV-visible absorption spectroscopy. The result of this study is presented in Figure 2.15.

In Figure 2.15, the arrows represent the general evolution of each band. t = 0 corresponds to the sample without irradiation, i.e. when **2j** is intact. Large absorption bands around 630 nm and 410 nm were observed. These two absorptions provide to **2j** its characteristic deep green color. At t = 300s, **2j** has completely disappeared. At first glance, the observation of the point framed in red suggests a clean conversion in another species, characterized by an isosbestic point. However, the evolution framed in green shows a more complex pattern, particularly the shift of the peak at 420 to 440 nm suggesting the presence of a stable intermediate.

Our attempts to characterize the photodecomposition products were not very conclusive. ^{11}B NMR spectroscopy of **2j** in deuterated DMSO after irradiation by ambient light showed the presence of at least 3 species, one being the starting boron adduct.

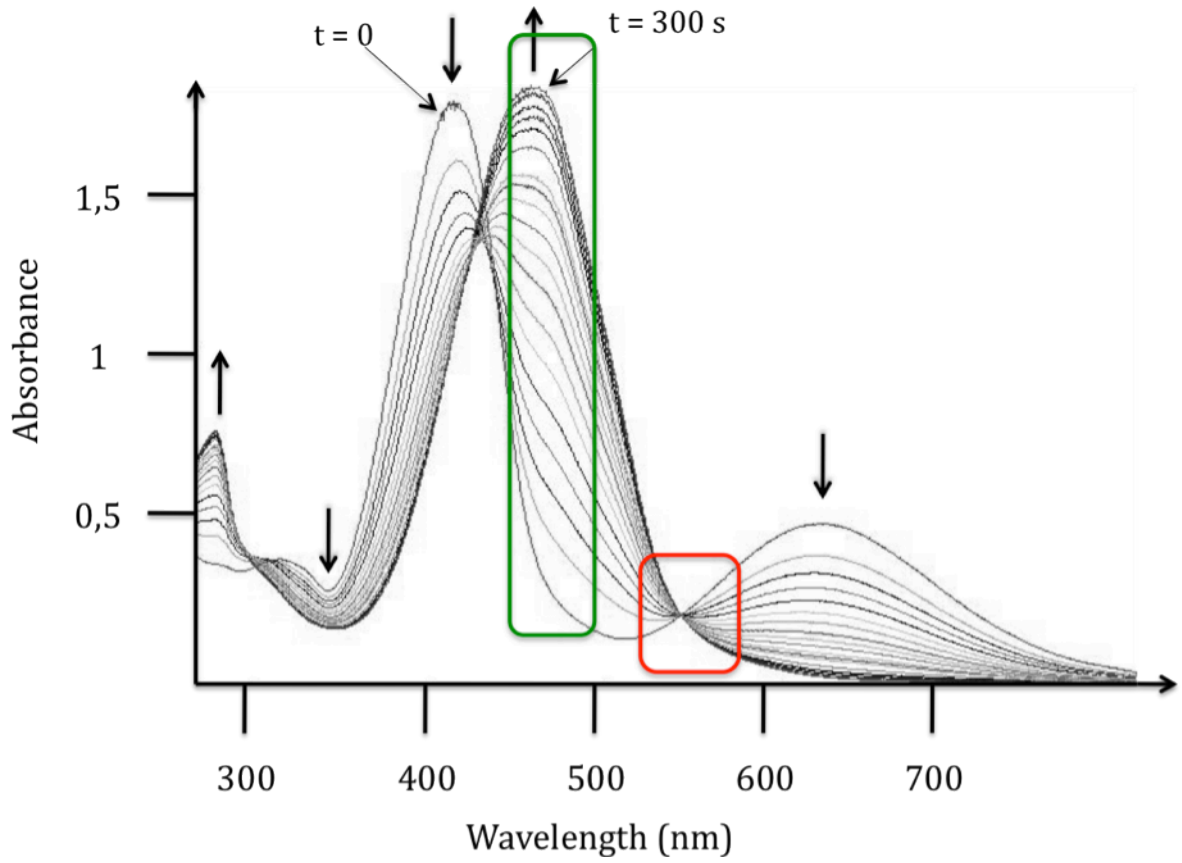

Figure 2.15. Photodecomposition study of **2j** performed in DMSO

Control experiments suggested that solvated BF_3 was not one of the decomposition products. Likewise, the ^{1}H NMR spectrum of **2j** in deuterated DMSO showed a very complex mixture, where the ferrocene signature was absent. Mass spectrometry also gave ambiguous results. For example, the analysis of the decomposition product of **2a** by electron impact (EI) at 20 eV gave a peak with m/z = **2a** + 18, suggesting a decoordination of the ketone from the boron atom, and its replacement by a molecule of water. However, the same sample in ESI shows no peak at higher than 300 m/z, while the original chalcone **1a** has a molecular weight of 332 g.mol^{-1}. ESI being a very mild technique, it is surprising to not see any species corresponding to the intact chalcone. This could be due to the use of an HPLC column in sample preparation.

Another experiment was performed to check the stability of the compounds in the dark, i.e. under the conditions of the IN inhibition assay. Compounds **2b**, **2f** and **2j** were dissolved in DMSO-d_6 and incubated in NMR tubes at 37°C for 2 h. ^{1}H NMR spectra after incubation

showed the almost total decomposition of **2b** and **2f**, while **2j** was stable over the incubation period. This demonstrates the strong influence of substituents on the coordinating power of the chalcone ligand.

D. Biological properties

1. Antiproliferative effects on B16 melanoma cells

In collaboration with Guy G. Chabot form Paris-Descartes University, the antiproliferative effects of **1a-j** and **2a-j** on murine B-16 melanoma cells were evaluated by the MTT test. The principle of this test is to use the dye 3-(4,5-dimethylthiazol-2-yl)-2,5-diphenyltetrazolium bromide (MTT), a yellow tetrazole that is reduced as a consequence of mitochondrial activity. Mitochondrial reductase enzymes have the ability to reduce MTT to formazan, which is purple.[21] The reduction process is presented in Figure 2.16.

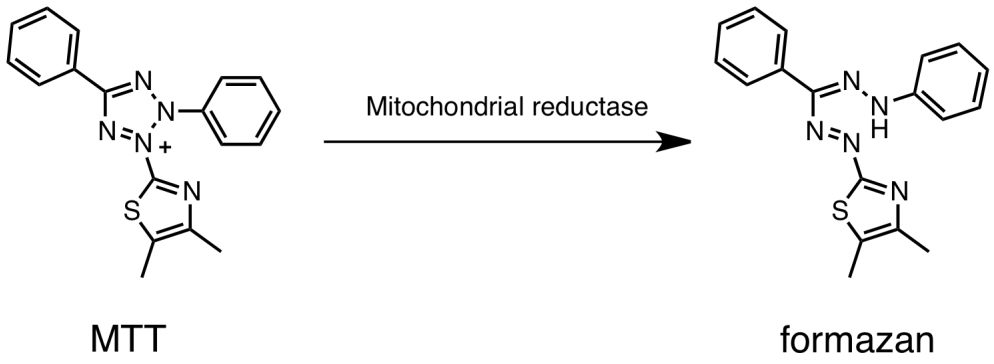

Figure 2.16. Reduction of MTT in formazan

This transformation only occurs in the presence of active mitochondria; therefore the production of formazan is proportional to the number of living cells and to mitochondrial activity. The measurement of the absorption density at the specific formazan wavelength (562 nm) thus indicates the relative quantity of living cells that are metabolically active. The use of a control permits the measurement and quantification of the impact of a drug on cell

proliferation. This test was performed at different concentrations of the compounds, and IC_{50} values were calculated from these results.

The results are presented in Figure 2.16. Except for compound **2b**, all the compounds' IC_{50} values are above 25 μM and thus they cannot be considered to be strongly cytotoxic compounds. On average, the activities of series **1** and **2** are on the same order of magnitude, although the boron adducts displayed slightly higher cytotoxicities.

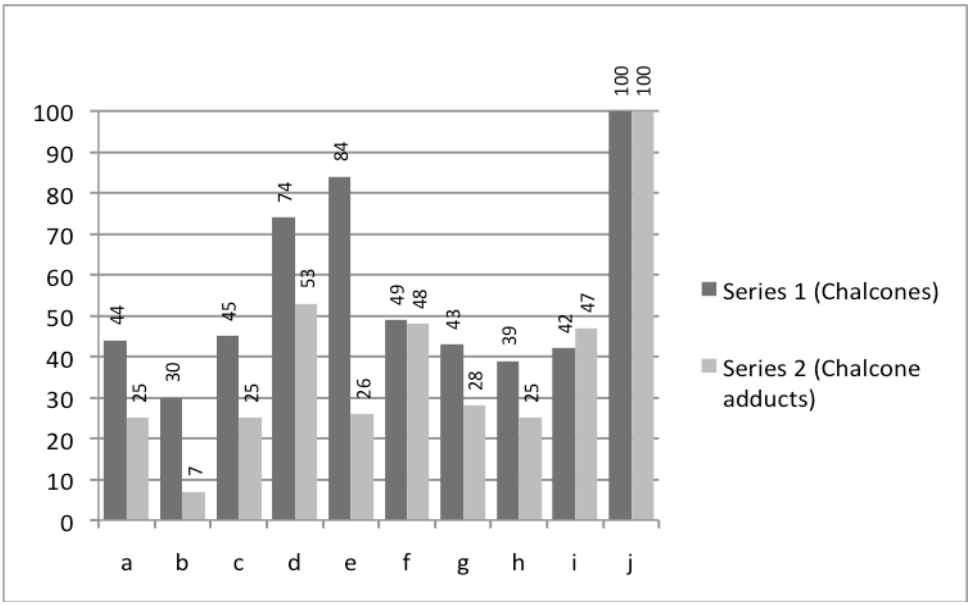

Figure 2.16. IC_{50} values of compounds **1a-j** and **2a-j** on B16 murine melanoma cells

2. Antiangiogenic effects EA·hy 926 endothelial cells

Angiogenesis is required in the formation process of metastases, the new vessels acting as carriers for cancer cells. Although not directly affecting the tumor cells, blocking angiogenesis indirectly blocks the tumors growth and dispersion. A high rate of endothelial cell proliferation is a characteristic of tumor vessels. Endothelial cells compose the innermost layer of blood vessels at the interface with the blood. Therefore, a morphological change of these cells upon treatment with a VDA should have important effects on blood vessels, such as their porosity.

The laboratory of G. Chabot also tested **1a-j** and **2a-j** against EA·hy 926 endothelial cells, and the minimal concentrations inducing "rounding-up" of EA·hy 926 endothelial cells were determined by direct observation through a light microscope. Chemically-induced morphological changes, specifically "rounding up" are indicative of tubulin polymerization inhibition. This parameter toward EA·hy 926 human umbilical vein cells are often used as a predictive model for antivascular antitumor activity.[22] The lower the inhibitory concentration, the better the activity of the molecule. The results are summarized in Figure 2.17.

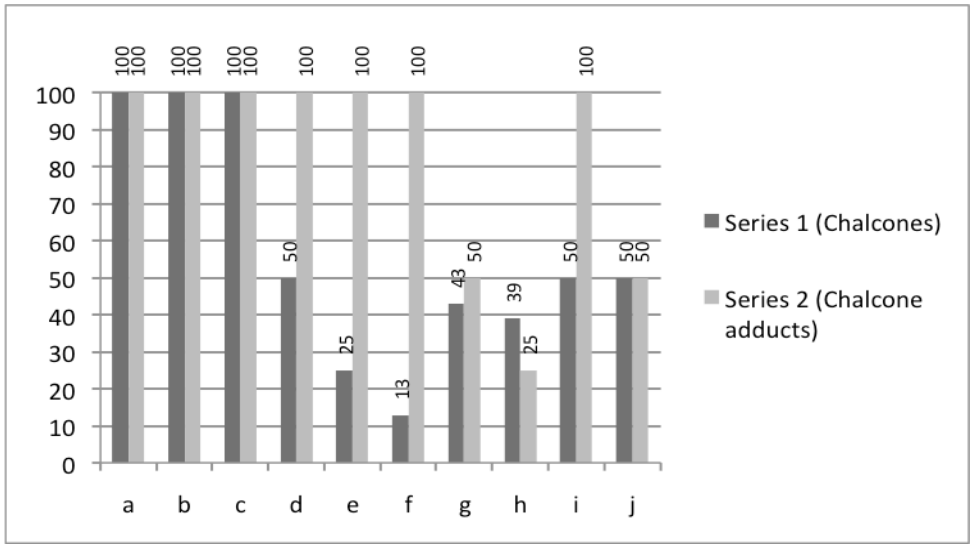

Figure 2.17. Minimal concentration of **1a-j** and **2a-j** for rounding up of EA·hy 926 cells

Similarly to their antiproliferative effects, we can see that these two series of compounds are not very promising as cytotoxics or VDAs. Therefore, we decided to investigate other biological properties, especially the inhibition of IN.

3. HIV-integrase inhibitors

Before assessing the activity of the compounds against IN, we performed a theoretical docking study in collaboration with Michel Huché using Titan and Odyssey software

(Wavefunction Society) on the crystal structure of IN co-crystalized with 5-CITEP.[23] Only the amino acids constituting the cavity wall were conserved and hydrogen atoms were added as necessary. The 5-CITEP molecule was digitally removed from the cavity and replaced by compound **2a** after geometry optimization. With all heavy atoms of the cavity being immobilized, the best position for the test molecule was obtained using the semi-empirical method PM3 energy minimization routine. The energy of the test molecule-protein complex was then determined and compared to the enthalpy of geometry-optimized test molecule alone after energy minimization, thereby allowing the calculation of the enthalpy of the docking reaction. This processes yielded a binding enthalpy of -12.2 kcal.mol^{-1} for **2a**, and -6.5 kcal.mol^{-1} for the standard molecule 5-CITEP, suggesting that **2a** binds more strongly to IN than 5-CITEP. Figure 2.18 shows the orientation of these representative compounds in the active site of IN. The stronger affinity of **2a** for the cavity seems to be due to the hydrogen bonding interaction of the fluoride of **2a** with ASP116 of the cavity, with a calculated distance of 2.072 Å and a bond energy of -8.8 kcal.mol^{-1}.

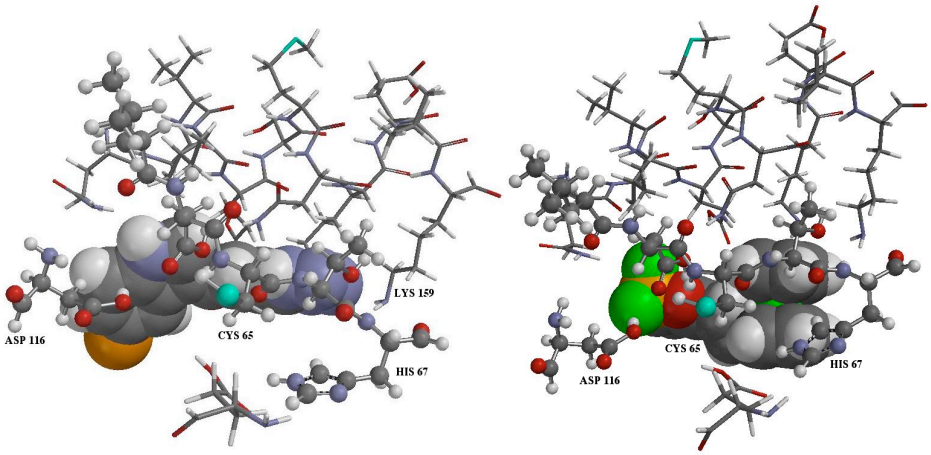

Figure 2.18. Representation of 5-CITEP (left) and **2a** (right) in the IN cavity

Comparatively, the hydrogen bond between the amine of the triazole group of 5-CITEP and LYS159 was calculated as 2.432 Å and -3.4 kcal.mol^{-1}. Although the cavity can accommodate the ferrocene, no particular non-covalent interactions between the cavity and the metallocene were observed.

Inhibition of the IN catalytic activities were measured using an IN-specific in vitro assay, using wild-type IN in the presence of different concentrations of test compounds. The inhibition of the catalytic functions of IN were measured using a ^{32}P-labeled IN substrate and the concentrations where these functions were inhibited by 50% (IC_{50}) were then calculated. Table 2.5 presents the IC_{50} values for 3' P and ST inhibition for compound series **1** and **2**.

Table 2.5. IC_{50} (μM) of **1a**-**j** and **2a**-**j** for IN inhibition

Compound	R	3' P	ST	SI*
1a	H	>20	>20	--
2a		10.7 ± 4.25	6.0 ± 2	0.6
1b	5-Cl	n.d.	n.d.	--
2b		5.6 ±4.13	6.0 ± 4.36	1.1
1c	5-Br	>20	>20	--
2c		4.6 ± 0.53	5.7 ± 4.73	1.2
1d	3,5-diCl	n.d.	n.d.	--
2d		7.8± 2.93	0.7 ± 0.14	0.1
1e	3,5-diBr	>20	>20	--
2e		4.3 ±2.52	3.6 ± 3.84	0.8
1f	3,5-diF	12	6.2	--
2f		5.0 ± 2.83	2.0 ±0.2	0.4
1g	4-OMe	>20	>20	--
2g		4.7 ± 1.53	2.6 ± 1.15	0.5
1h	5-OMe	14	10.3	--
2h		8.7 ± 1.53	7.3 ± 4.6	0.8
1i	6-OMe	>20	>20	--
2i		16.3 ± 7.52	9.3 ± 2.31	0.6
1j	4,6-diOMe	>33	11.6	--
2j		10.5 ± 5.6	7.6 ± 5.56	0.7

*Selectivity Index (SI) : ST/3'P

In all cases, the borates **2a-j** showed significantly better inhibitory activities compared to the free ferrocenyl chalcones **1a-j**. With IC_{50} values in the low micromolar range for both processes, it appears that the cavity of IN can tolerate diverse aromatic substituents. While only moderate variability in 3'P activities were observed for **2a-j** (IC_{50} values between 4 and 16 μM), ST activities varied over an order of magnitude, with IC_{50} values between 0.7 and 9 μM.

These activities are similar or higher than those previously reported for difluoridoborate 3-acetyl-4-hydroxy-2-pyranone derivatives,[18] and are significantly higher than those found for most organic chalcones.[15, 24] With similar activities for 3'P and ST, these compounds are not selective, except for **2d**, which shows excellent ST inhibition (IC_{50} = 0.7 μM). This is in contrast with previous observations that diketo acids typically act selectively against the ST process.

In order to assess the general influence of ferrocene on the inhibition of IN, a series of some 40 ferrocenyl derivatives based for the most part on the diphenylbutene skeleton, were evaluated. These compounds were randomly selected from our library of compounds studied for their antiproliferative effects against cancer. None of the compounds showed inhibitory activity at concentrations lower than 20 μM, suggesting that the presence of a ferrocene group alone is not sufficient for inhibitory activity.

In summary, **2a-j** showed moderate to good 3' processing and strand transfer inhibition, better than that of their parent chalcones and a randomly generated library of some 40 ferrocenyl compounds. Compounds **2a-j**, generally showed only mild antiproliferative effects against B16 cancer cells, with IC_{50} values greater than 25 μM for nine out of ten of the compounds and weak effects on the morphology of endothelial cells. The dichloro compound **2d** is a particularly promising lead for IN inhibition, with nanomolar ST inhibition and low toxicity towards human cells.

4. Antibacterial properties

Compounds of series **1** have also been evaluated as anti-bacterial agents, in collaboration with Claude Jolivalt from Chimie ParisTech. The compounds have been tested against 4

bacterial lines: *Escherichia coli* ATCC35922 (bacteria of reference), *Staphylococcus aureus* ATCC25923 (bacteria of reference), *Staphylococcus aureus* 1199B (bacteria line over-expressing the efflux pump NorA), *Staphylococcus aureus* MsrA (bacteria line over-expressing the efflux pump MsrA). The activities for **1a-j** at a concentration of 100 mg/mL are presented in Table 2.6.

Table 2.6. Screening of series **1** at 100 µg/mL

	E. coli ATCC25922	*S. aureus* ATCC25923	*S. aureus* 1199B	*S. aureus* MsrA
1a	-	-	-	n.d.
1b	-	++	-	-
1c	-	-	-	-
1d	-	+	-	++
1e	-	+	-	-
1f	-	+	-	n.d.
1g	-	-	-	-
1h	-	-	-	++
1i	-	-	-	-
1j	-	-	-	n.d.

The code ++ indicates a growth inferior to 5% when compared with the control, the code + a growth inferior to 10% when compared with the control. The code - means the growth was superior to 10% when compared with the control. From the table, we can see that at this concentration, only 3 compounds are very active, but two of them, **1d** and **1h**, are active against a resistant bacterial line.

A second screening was performed for **1a-j**, at a concentration of 20mg/mL. The results are presented in Table 2.7. At this concentration, only low activity was observed. From these results, it seems clear that these particular ferrocenyl chalcones are not adapted for anti-bacterial applications.

Table 2.7. Screening of series **1** at 20 μg/mL

	E. coli ATCC25922	*S. aureus* ATCC25923	*S. aureus* 1199B	*S. aureus* MsrA
1a	-	-	-	-
1b	-	-	-	-
1c	-	-	-	-
1d	-	-	-	+
1e	-	-	-	n.d.
1f	-	-	-	+
1g	-	-	-	-
1h	-	-	-	-
1i	-	-	-	-
1j	-	-	-	-

E. Experimental

General comments. All aldol condensation reactions were performed under argon atmosphere, using a standard Schlenk line. ^{1}H and ^{13}C NMR spectra were recorded with a 300 or 400 MHz Bruker Avance spectrometer, and δ are given in ppm and referenced to the residual solvent peaks (^{1}H, δ 7.26 and $^{13}C\{1H\}$, δ 77.1 for $CDCl_3$ and ^{1}H, δ 2.05 and $^{13}C\{^{1}H\}$, δ 29.7 for Acetone-d_6). High-resolution mass spectra were determined by ESI/ESCI-TOF using a Waters LCT Premier XE or a Thermo Fischer LTQ-Orbitrap XL. Melting points were determined using an Electrothermal 9100 apparatus.

Synthesis

General preparation of 1a-j.[6] Ferrocene carboxaldehyde (1 equiv, 50-200 mg) and the appropriate 2-hydroxyacetophenone (1 equiv) were dissolved in absolute EtOH in a round

bottom flask. After stirring the mixture 10 to 15 min at r.t., NaOH (3 equiv) was added, and the solution was stirred at reflux for 2 hours. The mixture was poured into water and HCl 12 M, extracted with DCM, and washed with water. The organic phase was dried over $MgSO_4$, filtered, and the solvent removed by evaporation. The product was purified by silica gel chromatography, using a mixture of petroleum ether/DCM 4:1 as an eluent, and again using HPLC in MeCN/water (90:10). After HPLC purification, the acetonitrile was removed under reduced pressure and the aqueous phase extracted with DCM. The NMR spectra of all purified compounds showed residual DCM, even after being dried under vacuum for several hours.

(E)-1-(2'-hydroxyphenyl)-3-ferrocenylprop-2-en-1-one 1a. Violet solid. δ_H (300 MHz; $CDCl_3$) 4.20 (s, 5H, C_5H_5), 4.55 (s, 2H, C_5H_4), 4.64 (s, 2H, C_5H_4), 6.93 (t, *J* = 7.7 Hz, 1H, Aromatic), 7.02 (d, *J* = 7.8 Hz, 1H, Aromatic), 7.25 (d, *J* = 15.1 Hz, 1H, Vinyl), 7.48 (t, *J* = 7.8 Hz, 1H, Aromatic), 7.86 (d, *J* = 7.7 Hz, 1H, Aromatic), 7.90 (d, *J* = 15.1 Hz, 1H, Vinyl). δ_C (75 MHz; $CDCl_3$) 69.3 (C_5H_4), 69.9 (C_5H_5), 71.8 (C_5H_4), 78.9 (C_5H_4 ipso), 116.7 (Aromatic), 118.6 (Aromatic), 118.7 (Aromatic), 120.0 (Vinyl), 129.3 (Aromatic), 135.9 (Aromatic), 147.9 (Vinyl), 162.6 (Aromatic), 192.7 (C=O). MS (APCI) m/z 332.07 $[M+H]^+$. Elemental analysis: Found: C 64.43, H 4.89. Calc. for $C_{19}H_{16}O_2Fe$·0.35 DCM: C 64.22, H 4.65.

(E)-1-(5'-chloro-2'-hydroxyphenyl)-3-ferrocenylprop-2-en-1-one 1b. Violet solid. δ_H (300 MHz; $CDCl_3$) 4.22 (s, 5H, C_5H_5), 4.51 (s, 2H, C_5H_4), 4.66 (s, 2H, C_5H_4), 6.96 (d, *J* = 9 Hz, 1H, Aromatic), 7.14 (d, *J* = 15 Hz, 1H, Vinyl), 7.42 (dd, *J* = 9 Hz, *J* = 2.4 Hz, 1H, Aromatic), 7.80 (d, *J* = 2.4 Hz, 1H, Aromatic), 7.94 (d, *J* = 15 Hz, 1H, Vinyl). δ_C (75 MHz; $CDCl_3$) 69.5 (C_5H_4), 70.0 (C_5H_5), 72.2 (C_5H_4), 78.6 (C_5H_4 ipso), 115.9 (Aromatic), 120.2 (Aromatic), 120.7 (Aromatic), 123.3 (Vinyl), 128.5 (Aromatic), 135.6 (Aromatic), 149.4 (Vinyl), 162.1 (Aromatic), 191.7 (C=O). MS (APCI) m/z 366.03 $[M+H]^+$. Elemental analysis: Found: C 61.75, H 4.02. Calc. for $C_{19}H_{15}O_2FeCl$·0.06 DCM: C 61.59, H 4.1.

(E)-1-(5'-bromo-2'-hydroxyphenyl)-3-ferrocenylprop-2-en-1-one 1c. Violet solid. δ_H (300 MHz; $CDCl_3$) 4.22 (s, 5H, C_5H_5) 4.58 (s, 2H, C_5H_4), 4.66 (s, 2H, C_5H_4), 6.92 (d, *J* = 8.1 Hz, 1H, Aromatic), 7.13 (d, *J* = 14.5 Hz, 1H, Vinyl), 7.55(d, *J* = 8.1 Hz, 1H, Aromatic), 7.92 (m, 1H, Aromatic), 7.94 (d, *J* = 14.4 Hz, 1H, Vinyl). δ_C (75 MHz; $CDCl_3$) 69.5 (C_5H_4) 70.1 (C_5H_5), 72.3

(C_5H_4), 78.6 (C_5H_4 ipso), 110.3 (Aromatic), 115.9 (Aromatic), 120.6 (Aromatic), 121.3 (Vinyl), 131.6 (Aromatic), 138.4 (Aromatic), 149.4 (Vinyl), 162.5 (Aromatic), 191.6 (C=O). MS (APCI) m/z410.05 $[M+H]^+$. Elemental analysis: Found: C 55.04, H 3.73. Calc. for $C_{19}H_{15}O_2FeBr$·0.05 DCM: C 55.09, H 3.66.

(E)-1-(3',5'-dichloro-2'-hydroxyphenyl)-3-ferrocenylprop-2-en-1-one 1d. Violet solid. δ_H (300 MHz; $CDCl_3$) 4.23 (s, 5H, C_5H_5), 4.62 (s, 2H, C_5H_4), 4.67 (s, 2H, C_5H_4), 7.01 (d, *J* = 15 Hz, 1H, Vinyl), 7.57 (s, 1H, Aromatic), 7.74 (s, 1H, Aromatic), 8.00 (d, *J* = 15 Hz, 1H, Vinyl). δ_C (75 MHz; $CDCl_3$) 68.7 (C_5H_4), 69.1 (C_5H_5), 71.6 (C_5H_4), 77.3 (C_5H_4 ipso), 114.2 (Vinyl), 120.2 (Aromatic), 122.0 (Aromatic), 122.9 (Aromatic), 126.1 (Aromatic), 134.1 (Aromatic), 149.8 (Vinyl), 157.0 (Aromatic), 190.2 (C=O). MS (APCI) m/z 400.08 [M+H]+. Elemental analysis: Found: C 55.72, H 3.49. Calc. for $C_{19}H_{14}O_2FeCl_2$·0.125 DCM: C 55.80, H 3.49.

(E)-1-(3',5'-dibromo-2'-hydroxyphenyl)-3-ferrocenylprop-2-en-1-one 1e. Violet solid. δ_H (400 MHz; $CDCl_3$) 4.23 (s, 5H, C_5H_5), 4.62 (s, 2H, C_5H_4), 4.67 (s, 2H, C_5H_4), 7.10 (d, *J* = 14.7 Hz, 1H, Vinyl), 7.86 (d, *J* = 1.8 Hz, 1H, Aromatic), 7.91 (d, *J* = 1.8 Hz, 1H, Aromatic), 7.99 (d, *J* = 14.7 Hz, 1H, Vinyl). δ_C (75 MHz; $CDCl_3$) 69.7 (C_5H_4), 70.1 (C_5H_5), 72.6 (C_5H_4), 78.37 (C_5H_4 ipso) 110.1 (Aromatic), 113.3 (Aromatic), 115.1 (Vinyl), 121.7 (Aromatic), 130.8 (Aromatic), 140.7 (Aromatic), 150.8 (Vinyl), 159.3 (Aromatic), 191.0 (C=O). MS (APCI) m/z 488.01 [M+H]+. Elemental analysis: Found: C 45.24, H 2.70. Calc. for $C_{19}H_{14}O_2FeBr_2$·0.25 DCM: C 45.23, H 2.86.

((E)-1-(3',5'-difluoro-2'-hydroxyphenyl)-3-ferrocenylprop-2-en-1-one 1f. Violet solid. δ_H (400 MHz; $CDCl_3$) 4.22 (s, 5H, C_5H_5), 4.61 (s, 2H, C_5H_4), 4.66 (s, 2H, C_5H_4), 7.06 (m, 1H, Vinyl, Aromatic), 7.34 (s, 1H, Aromatic), 7.98 (d, *J* = 15 Hz, 1H, Vinyl). δ_C (100 MHz; $CDCl_3$) 69.7 (C_5H_4), 70.2 (C_5H_5), 72.6 (C_5H_4), 78.4 (C_5H_4 ipso), 109.6 (d, ^2J = 23 Hz, Aromatic), 110.5 (dd, ^2J = 26 Hz, ^2J = 21 Hz, Aromatic), 115.7 (Vinyl), 120.9 (Aromatic), 148.8 (d, ^2J = 11.9 Hz, Aromatic), 150.5 (Vinyl), 151 (Aromatic overlap), 153.3 (dd, ^1J = 238.6 Hz, ^3J = 9 Hz, Aromatic), 191.6 (C=O). MS (APCI) m/z 368.07 [M+H]+. Elemental analysis: Found: C 60.25, H 4.04. Calc. for $C_{19}H_{14}O_2FeF_2$·0.2 DCM: C 59.88, H 3.77.

(*E*)-1-(4'-methoxy-2'-hydroxyphenyl)-3-ferrocenylprop-2-en-1-one, 1g. Violet solid, mp 142°C; δ_H (300 MHz; $CDCl_3$) 3.81 (s, 3H, OMe), 4.14 (s, 5H, C_5H_5), 4.46 (s, 2H, C_5H_4), 4.56 (s, 2H, C_5H_4), 6.39-6.43 (m, 2H, Aromatic), 7.11 (d, *J* = 15.0 Hz, 1H, Vinyl), 7.71 (d, *J* = 9.5 Hz, 1H, Aromatic), 7.78 (d, *J* = 15.0 Hz, 1H, Vinyl), 13.63 (s, 1H, phenol). δ_C (100 MHz; $CDCl_3$) 55.6 (OMe), 69.1 (C_5H_4), 69.9 (C_5H_5), 71.6 (C_5H_4), 79.1 (C_5H_4 ipso), 101.0 (Aromatic), 107.5 (Vinyl), 114.0 (Aromatic), 116.9 (Aromatic), 131.0 (Aromatic), 146.6 (Vinyl), 165.8 (Aromatic), 166.6 (Aromatic), 191.1 (C=O). HRMS (ESI) calcd. for $C_{20}H_{18}FeO_3^+$: 362,06054, found: 362,05999.

(*E*)-1-(5'-methoxy-2'-hydroxyphenyl)-3-ferrocenylprop-2-en-1-one, 1h. Violet solid, mp 173°C; δ_H (300 MHz; $CDCl_3$) 3.85 (s, 3H, OMe) 4.20 (s, 5H, C_5H_5), 4.55 (s, 2H, C_5H_4), 4.63 (s, 2H, C_5H_4), 6.96 (d, 1H, *J* = 8.9 Hz, Aromatic), 7.11-7.25 (m, 2H, Aromatic+Vinyl), 7.31 (s, 1H, Aromatic), 7.90 (d, 1H, *J* = 14.7 Hz, Vinyl), δ_C (75 MHz; $CDCl_3$) 56.2 (OMe), 69.3 (C_5H_4), 70.0 (C_5H_5), 71.9 (C_5H_4), 78.9 (C_5H_4-C_{ipso}), 113.1 (Aromatic), 116.7 (Vinyl), 119.2 (Aromatic), 119.7 (Aromatic), 123.0 (Aromatic), 148.1 (Vinyl), 151.6 (Aromatic), 157.9 (Aromatic), 192.4 (C=O). (CI NH_3) m/z 362.0 (MH^+). HRMS (ESI) calcd. for $C_{20}H_{18}FeO_3Na^+$: 362,06054, found: 362,04976.

(*E*)-1-(6'-methoxy-2'-hydroxyphenyl)-3-ferrocenylprop-2-en-1-one, 1i. Violet solid, mp 136°C; δH (300 MHz; $CDCl_3$) 3.86 (s, 3H, OMe), 4.11 (s, 5H, C_5H_5), 4.41 (s, 2H, C_5H_4), 4.50 (s, 2H, C_5H_4), 6.34-6.35 (m, 1H, Aromatic), 6.53 (d, *J* = 6.6 Hz, 1H, Aromatic), 7.24-7.27 (m, 1H, Aromatic), 7.40 (d, *J* = 15.3 Hz, 1H, Vinyl), 7.72 (d, *J* = 15.3 Hz, 1H, Vinyl), 13.27 (s, 1H, phenol). δ_C (100 MHz; $CDCl_3$) 55.9 (OMe), 69.2 (C_5H_4), 69.9 (C_5H_5), 71.4 (C_5H_4), 79.6 (C_5H_4 ipso), 101.6 (Aromatic), 110.9 (Vinyl), 112.0 (Aromatic), 124.6 (Aromatic), 135.4 (Aromatic), 145.5 (Vinyl), 160.9 (Aromatic), 164.8 (Aromatic), 193.4 (C=O). HRMS (ESI) calcd. for $C_{20}H_{18}FeO_3^+$: 362,06054, found: 362,05999.

(*E*)-1-(4,6'-dimethoxy-2'-hydroxyphenyl)-3-ferrocenylprop-2-en-1-one, 1j. Violet solid, mp 131°C; δ_H (400 MHz; $CDCl_3$) 3.78 (s, 3H, OMe), 3.83 (s, 3H, OMe), 4.13 (s, 5H, C_5H_5), 4.41 (s, 2H, C_5H_4-H_β), 4.52 (s, 2H, C_5H_4-H_α), 5.90 (s, 1H, Aromatic), 6.05 (s, 1H, Aromatic), 7.46 (d, *J* = 15.3 Hz, 1H, Vinyl), 7.70 (d, *J* = 15.3 Hz, 1H, Vinyl), 14.47 (s, 1H, phenol). δ_C (100 MHz; $CDCl_3$) 55.6 (OMe), 55.8 (OMe), 69.1 (C_5H_4), 69.9 (C_5H_5), 71.2 (C_5H_4), 80.0 (C_5H_4 ipso), 91.3 (Aromatic), 93.9 (Vinyl), 106.2 (Aromatic), 124.5 (Aromatic), 144.6 (Vinyl), 162.4 (Aromatic),

165.8 (Aromatic), 168.4 (Aromatic), 191.8 (C=O). HRMS (ESI) calcd. for $C_{20}H_{18}FeO_3^+$: 392,07110, found: 392,07055.

General Synthesis of 2a-j. To a solution of 10-50 mg **1a-j** in 50 mL of distilled CH_2Cl_2 were added 3 eq. of NaH. The reaction mixture was stirred for 10 min. Three eq. of $BF_3{\cdot}OEt_2$ were added dropwise to the reaction mixture, which immediately became green. The reaction mixture was extracted with a solution of hydrochloric acid (37% in water). Then the aqueous phase was extracted 3 times with 100 mL CH_2Cl_2. The organic phase was dried over $MgSO_4$, and distilled off using a rotary evaporator at 650 mbar. The crystals were purified by recrystallization: crystals were dissolved in a few drops of dichloromethane, and a large excess of petroleum spirit was added on the mixture. The mixture was then placed at 4°C during 10 minutes, filtered by means of a Büchner funnel and rinsed with petroleum spirit.

[1-(2-hydroxyphenyl)-3-(ferrocenyl)-2-propen-1-onato-O,O] difluoridoborate, 2a. Green solid, mp 220°C; δ_H (300 MHz; $CDCl_3$) 4.31 (s, 5H, C_5H_5), 4.81 (s, 2H, C_5H_4), 4.95 (s, 2H, C_5H_4), 6.9-7.1 (m, 2H, Aromatic+Vinyl), 7.11 (d, *J* = 8.7 Hz, 1H, Aromatic), 7.70 (t, *J* = 7.5 Hz, 1H, Aromatic), 7.8-7.9 (m, 1H, Aromatic), 8.61 (d, *J* = 14.4 Hz, 1H, Vinyl); m/z (EI 20 eV) 380,0 (M^+). HRMS (ESI) calcd. for $C_{19}H_{15}FeO_2BF_2$-NH_4^+: 398.0826, found: 398.0810.

[1-(5-chloro-2-hydroxyphenyl)-3-(ferrocenyl)-2-propen-1-onato-O,O] difluoridoborate, 2b. Green solid, mp 190°C; δ_H (300 MHz; $CDCl_3$): 4.36 (s, 5H, C_5H_5), 4.87 (s, 2H, C_5H_4), 5.06 (s, 2H, C_5H_4), 6.94 (d, *J* = 14.0 Hz, 1H, Vinyl), 7.06 (d, *J* = 8.4 Hz, 1H, Aromatic), 7.61 (d, *J* = 8.4 Hz, 1H, Aromatic), 7.76 (s, 1H, Aromatic), 8.66 (d, *J* = 14.0 Hz, 1H, Vinyl); (EI 20 eV) 414.17 (M^+). HRMS (ESI) calcd. for $C_{19}H_{14}ClFeO_2BF_2$-NH_4^+: 412.0140, found: 412.0143.

[1-(5-bromo-2-hydroxyphenyl)-3-(ferrocenyl)-2-propen-1-onato-O,O] difluoridoborate, 2c. Green solid, mp 222°C; δ_H (300 MHz; Acetone-d_6) 4.43 (s, 5H, C_5H_5), 5.18 (t, *J* = 1.7 Hz, 2H, C_5H_4), 5.25 (t, *J* = 1.7 Hz, 2H, C_5H_4), 7.01 (d, *J* = 8.9 Hz, 1H, Aromatic), 7.62 (d, *J* = 14.5 Hz, 1H, Vinyl), 7.88 (dd, *J* = 2.3 Hz, *J* = 8.9 Hz, 1H, Aromatic), 8,39 (d, *J* = 2.3 Hz, 1H, Aromatic), 8.75 (d, 1H, *J* = 14.5 Hz, Vinyl); (EI 20 eV) m/z 458.05-460.05 (M^+); HRMS (ESI) calcd. for $C_{19}H_{14}BrFeO_2BF_2$-Na^+: 479.9554, found: 479.9548.

[1-(3,5-dichloro-2-hydroxyphenyl)-3-(ferrocenyl)-2-propen-1-onato-O,O] difluoridoborate, 2d. Green solid, mp 172°C; δ_H (300 MHz; $CDCl_3$): 4.46 (s, 5H, C_5H_5), 5.30 (s, 4H, C_5H_4), 7.57 (d, *J* = 14.2 Hz, 1H, Vinyl), 7.94 (d, *J* = 2.5 Hz, 1H, Aromatic), 8.26 (d, *J* = 2.5 Hz, 1H, Aromatic), 8.85 (d, *J* = 14.2 Hz, 1H, Vinyl); (EI 20 eV) 448.14 (M^+). HRMS (ESI) calcd. for $C_{19}H_{13}BCl_2F_2FeO_2$-$NH_4^+$: 465.0083, found: 465.0070.

[1-(3,5-dibromo-2-hydroxyphenyl)-3-(ferrocenyl)-2-propen-1-onato-O,O] difluoridoborate, 2e. Green solid, mp 192°C; δ_H (300 MHz; Acetone-d_6): 3.88 (s, 5H, C_5H_5), 4.70 (s, 2H, C_5H_4), 4.71 (s, 2H, C_5H_4), 7.00 (d, *J* = 14.3 Hz, 1H, Vinyl), 7.60 (d, *J* = 2.3 Hz, 1H, Aromatic), 7.83 (d, *J* = 2.3 Hz, 1H, Aromatic), 8.26 (d, *J* = 14.3 Hz, 1H, Vinyl); (EI 20 eV) 538.06 (M^+). HRMS (ESI) calcd. for $C_{19}H_{13}BBr_2F_2FeO_2^+$: 535.8693, found: 535.8688.

[1-(3,5-difluoro-2-hydroxyphenyl)-3-(ferrocenyl)-2-propen-1-onato-O,O] difluoridoborate, 2f. Green solid, mp 183°C; δ_H (300 MHz; $CDCl_3$): 4.38 (s, 5H, C_5H_5), 4.87 (s, 2H, C_5H_4), 5.13 (s, 2H, C_5H_4), 6.85 (d, *J* = 12.0 Hz, 1H, Vinyl), 7.1-7.4 (m, 2H, Aromatic, 8.76 (d, *J* = 12.0 Hz, 1H, Vinyl); (EI 20 eV) m/z 416.17 (M^+). HRMS (ESI) calcd. for $C_{19}H_{13}BF_4FeO_2$-NH_4^+: 433.0674, found: 433.0690.

[1-(4-methoxy-2-hydroxyphenyl)-3-(ferrocenyl)-2-propen-1-onato-O,O] difluoridoborate, 2g. Green solid, mp 220°C; δ_H (300 MHz; Acetone-d_6): 3.98 (s, 3H, OCH_3), 4.40 (s, 5H, C_5H_5), 4.97 (s, 2H, C_5H_4), 5.16 (s, 2H, C_5H_4), 6.52 (d, *J* = 2.4 Hz, 1H, Aromatic), 6.64 (dd, *J* = 2.4 Hz, *J* = 9.2 Hz, 1H, Aromatic), 7.49 (d, *J* = 14.5 Hz, 1H, Vinyl), 8.15 (d, *J* = 9.2 Hz, 1H, Aromatic), 8.40 (d, *J* = 14.5 Hz, 1H, Vinyl); (EI 20 eV) 410.22 (M^+). HRMS (ESI) calcd. for $C_{20}H_{17}BF_2FeO_3$-NH_4^+: 428.0932, found: 428.0939.

[1-(5-methoxy-2-hydroxyphenyl)-3-(ferrocenyl)-2-propen-1-onato-O,O] difluoridoborate, 2h. Green solid, mp 190°C; δ_H (300 MHz; $CDCl_3$) 4.85 (s, 3H, OCH_3), 4.34 (s, 5H, C_5H_5), 4.84 (s, 2H, C_5H_4), 4.96 (s, 2H, C_5H_4), 6.94 (d, *J* = 14.4 Hz, 1H, Vinyl), 7.0-7.1 (m, 2H, Aromatic), 7.35 (d, *J* = 8.1 Hz, 1H, Aromatic), 8.55 (d, *J* = 14.4 Hz, 1H, Vinyl); (EI 20 eV) 410.21 (M^+). HRMS (ESI) calcd. for $C_{20}H_{17}BF_2FeO_3$-NH_4^+: 428.0932, found: 428.0919.

[1-(6-methoxy-2-hydroxyphenyl)-3-(ferrocenyl)-2-propen-1-onato-O,O] difluoridoborate, 2i. Green solid, mp 220°C; δ_H (300 MHz; $CDCl_3$): 3.98 (s, 3H, OCH_3), 4.30 (s, 5H, C_5H_5), 4.73 (s, 2H, C_5H_4), 4.85 (s, 2H, C_5H_4), 6.41(d, *J* = 7.8 Hz, 1H, Aromatic), 6.66 (d, *J* = 8.4 Hz, 1H,

Aromatic), 7.58 (m, 2H, Vinyl+Aromatic), 8.53 (d, *J* = 14.4 Hz, 1H, Vinyl); (EI 20 eV) m/z 410.20 (M^+). HRMS (ESI) calcd. for $C_{20}H_{17}BF_2FeO_3$-NH_4^+: 428.0932, found: 428.0939.

[1-(4,6-dimethoxy-2-hydroxyphenyl)-3-(ferrocenyl)-2-propen-1-onato-O,O] difluoridoborate, **2j**. Green solid, mp 220°C; δ_H (300 MHz; $CDCl_3$): 3.89 (m, 6H, OCH_3), 4.26 (s, 5H, C_5H_5), 4.68 (s, 2H, C_5H_4), 4.73 (s, 2H, C_5H_4), 5.95 (d, *J* = 9.0 Hz, 1H, Aromatic), 6.14 (m, 1H, Aromatic), 7.55 (d, *J* = 14.8 Hz, 1H, Vinyl), 8.37 (d, *J* = 14.8 Hz, 1H, Vinyl); (EI 20 eV) m/z 440.19 (M^+). HRMS (ESI) calcd. for $C_{21}H_{19}BF_2FeO_4$-NH_4^+: 458.1038, found: 458.1038.

Biological Assays

IN inhibition. All compounds were dissolved in DMSO, and stock solutions were stored at -20°C. γ-[^{32}P]-ATP was purchased either from Amersham Biosciences or ICN. The expression system for wild-type IN was a generous gift of Dr. Robert Craigie, Laboratory of Molecular Biology, NIDDK, NIH (Bethesda, MD).

21-mer oligonucleotides [top strand (5'-GTGTGGAAAATCTCTAGCAGT-3') and bottom strand (5'-ACTGCTAGAGATTTTCCACAC-3')] were purchased from Norris Comprehensive Cancer Center Microsequencing Core Facility (University of Southern California) and purified by UV shadowing on a polyacrylamide gel. To analyze the extent of 3'-processing and strand transfer with 5'-end labeled substrates, the 21-mer top strand was 5'-end labeled using T4 polynucleotide kinase (Epicentre, Madison, WI) and γ-[^{32}P]-ATP (Amersham Biosciences or ICN). The kinase was heat-inactivated and the bottom strand was added in 1.5 M excess. The mixture was then heated to 95°C, allowed to slowly cool to room temperature, and purified through a spin 25 minicolumn (USA Scientific, Ocala, FL) to separate annealed double-stranded oligonucleotide from unincorporated material.

To determine the extent of 3'-processing and strand transfer, wild-type IN was preincubated at a final concentration of 200 nM with the inhibitor in a reaction buffer [50 mM NaCl, 1 mM HEPES (pH 7.5), 50 μM EDTA, 50 μM dithiothreitol, 10% glycerol (w/v), 7.5 mM $MnCl_2$, 0.1 mg mL^{-1} bovine serum albumin, 10 mM 2-mercaptoethanol, 10% dimethyl sulfoxide, and 25 mM MOPS (pH 7.2)] at 30°C for 30 min. Next, 20 nM of the 5'-end ^{32}P-labeled linear oligonucleotide substrate was added, and the incubation was resumed for an additional 1 h.

Reactions were quenched by the addition of 50x of loading dye (98% deionized formamide, 10 mM EDTA, 0.025% xylene cyanol, and 0.025% bromophenol blue). An aliquot (5 μL) was subjected to electrophoresis on a denaturing polyacrylamide gel (0.09 M Tris–borate, pH 8.3, 2 mM EDTA, 20% acrylamide, 8 M urea). The gels were dried under vacuum, exposed in a PhosphorImager cassette, and visualized with a Typhoon 8610 Variable Mode Imager (Amersham Biosciences). Quantification was done with Image Quant 5.2 software. Percent inhibition (%*I*) was calculated using the following equation:

$$\%I = 100 \times [1 - (D - C) / (N - C)]$$

where *C*, *N*, and *D* are the fractions of 21-mer substrate converted into 19-mer (product of 3'-processing) or strand-transfer products for DNA alone, DNA plus IN, INwith drug, respectively.

IC_{50} values were determined by plotting the logarithm of drug concentration as a function of %I to obtain the concentration that produced 50% inhibition.

Cytotoxicity. Murine B16 melanoma was grown in Dulbecco's modified essential medium (DMEM) containing 2 mM l-glutamine, 10% fetal bovine serum, 100 U/mL penicillin, and 100 μg/mL streptomycin 37°C, 5% CO_2). Exponentially growing cancer cells were plated onto 96-well plates at 5,000 cells per well in 200 μL DMEM; and 24 h later, the cells were exposed for 48 h to the solvent alone or to the test compound at the indicated concentrations. Viability was assessed using the MTT (1-(4,5-dimethylthiazol-2-yl)-3,5-diphenyltetrazolium) test, and absorbance was read at 562 nm in a microplate reader (BioKinetics Reader, EL340, Fisher Bioblock Scientific, Illkirch, France). Control cells were exposed to 1% DMSO. Experiments were run in triplicate and repeated 3 times. Results are presented as the inhibitory concentrations for 50% (IC_{50}) of cells for a 48 h exposure time.

Morphologic Effects on EA·hy 926 Endothelial Cells. To assess the effect of **3a**-**j** on the morphology of endothelial cells EA·hy 926 endothelial cells were used. Cells were grown in DMEM containing 2 mM l-glutamine, 10% fetal bovine serum, 100 U/mL penicillin, and 100

μg/mL streptomycin (37°C, 5% CO_2). Exponentially growing cells were plated onto 96-well plates at 5,000 cells/200 μL/well. Twenty-four h after plating, the medium was aspirated, and 100 μL of medium containing the test compound was added to the well (triplicate) at the indicated final concentrations (37°C, 5% CO_2), and 2 h later digital photographs were recorded of representative center areas of each well at a magnification of ×320. Results are presented as the efficacious concentration for the change in cell shape for 50% of cells for a 2 h exposure time (EC_{50}) relative to controls.

Antibacterial activity

The inhibitory potential of the flavonoid derivatives was tested on four bacteria strains:

- *E. coli* ATCC 25922 (Gram negative strain)
- *Staphylococcus aureus* (ATCC 25923, sensitive Gram positive strain),
- *Staphylococcus aureus* 1199B: resistant to fluoroquinolones due notably to the overexpression of the NorA efflux pump (G. W. Kaatz, S. M. Seo, *Antimicrob. Agents Chemother*. 1995, *39*, 2650-2655)
- *Staphylococcus aureus* RN4220/pUL5054: resistant to erythrocycin by overexpressing the efflux pump MsrA from the high-copy pUL5054 plasmid (JI Ross, EA Eady, JH Cove, S Baumberg, Gene 1996, 183, 143-148).

The compounds were firstly solubilized in DMSO at 10 mg/mL and screened for their antibacterial activity in 96 wells at 100 and 20 mg/L. However, the high absorbance of some of the tested compounds interfered with the measurement of bacterial growth that was assayed at 620 nm.

Flavonoid derivatives were dispensed in a 96-wells microplate by dilutions in Muller-Hinton medium (MH, Bio Rad) using a Biomek 2000 (Beckman) handling robot. 100 μL of the bacterial inoculum (an overnight culture at 37 °C in 5 mL MH diluted 100-fold) was then added in each well. The total volume was 200 μL in each well and the final bacteria concentration 10^6 CFU/mL (CFU: colony forming unit). Growth was assayed with a microplate reader by monitoring absorption at 620 nm after 1, 2, 5, 7 and 24 h incubation at 37°C. In addition, the plates were read visually after 24 hours incubation. The activity of the

compounds was determined after 24 h incubation at 37°C. Control wells were MH broth containing 5µL of DMSO. In addition, two controls containing a sub-inhibitory or a inhibitory antibiotic concentration for the tested strain were performed. The antibiotics used were ampicillin (0.5 and 32 µg/mL) for *E. coli*, kanamycin (0.5 and 16 µg/mL) for *S. aureus* ATCC 25923, ciprofloxacin (4 and 64 mg/L) for *S. aureus* 1199B and erythromycin (16 and 256 mg/L) for *S. aureus* RN4220/pUL5054.

References

1: Hauser C. R.; Lindsay, J. K. "Certain Acylations of Ferrocene and Some Condensations Involving the α-Hydrogen of Acetylferrocene" *J. Org. Chem.* **1957** 22(5), 482-485

2: Hauser C. R.; Lindsay, J. K. "Aminomethylationof Ferroceneto Form *N,N* Dimethylaminomethylferrocene and Its Conversion to the Corresponding Alcohol and Aldehyde" *J. Org. Chem.* **1957** 22(4), 355-358

3: Guillaneux, D.; Kagan, H. B. "High Yield Synthesis of Monosubstituted Ferrocenes" *J.Org. Chem.* **1995** 60, 2502-2505

4: Delavaux-Nicot, B.; Maynadie, J.; Lavabre, D.; Fery-Forgues, S. "Ca^{2+} vs. Ba^{2+} electrochemical detection by two disubstituted ferrocenyl chalcone chemosensors. Study of the ligand–metal interactions in CH_3CN" *J. Organomet. Chem.* **2007** 692(4), 874-886

5: Delavaux-Nicot, B.; Maynadie, J.; Lavabre, D.; Fery-Forgues, S. "Two electroactive ferrocenyl chalcones as original optical chemosensors for Ca^{2+} and Ba^{2+} cations in CH_3CN" *J. Organomet. Chem.* **2007** 692(16), 3351-3362

6: Wu, X.; Wilairat, P.; Go, M. L. "Antimalarial Activity of Ferrocenyl Chalcones" *Bioorg. Med. Chem. Lett.* **2002** 12, 2299–2302

7: Wu, X.; Tiekink, E. R. T.; Kostetski, I.; Kocherginsky, N.; Tan, A. L. C.; Khoo, S. B.; Wilairat, P.; Go, M. L. "Antiplasmodial activity of ferrocenyl chalcones: Investigations into the role of ferrocene" *Eur. J. Pharm. Sci.* **2006** 27, 175–187

8: Zsoldos-Mády, V.; Csámpai, A.; Szabó, R.; Mészáros-Alapi, E.; Pásztor, J.; Hudecz, F.; Sohár P. "Synthesis, Structure, and in vitro Antitumor Activity of Some Glycoside Derivatives of Ferrocenyl-Chalcones and Ferrocenyl-Pyrazolines" *ChemMedChem* **2006** 1(10), 1119–1125

9: Ferle-Vidovic, A.; Poljak-Blazi, M.; Rapic, V.; Skare, D. "Ferrocenes (F168, F169) and Fero-Sorbitol-Citrate (FSC): Potential Anticancer Drugs" *Cancer Biother. Radiopharm.* **2000** 15(6), 617-625

10: Attar, S.; O'Briena, Z.; Alhaddadb, H.; Goldena, M. L.; Calderón-Urrea, A. "Ferrocenyl chalcones versus organic chalcones: A comparative study of their nematocidal activity" *Bioorg. Med. Chem.* **2011** 19(6), 2055-2073

11: Hinnen, P.; Eskens, F. A. L. M. "Vascular disrupting agents in clinical development" *Br. J. Cancer* **2007** 96, 1159–1165

12: Siemann, D. W. "The unique characteristics of tumor vasculature and preclinical evidence for its selective disruption by Tumor-Vasculature Disrupting Agents" *Cancer Treat Rev.* **2011** 37, 63-74

13: Kerr, D.J.; Kaye S.B. "Flavone Acetic Acid-Preclinical and Clinical Activity" *Eur. J. Cancer Clin. Oncol.* **1989** 25(9), 1271-1272

14: Rehman, F.; Rustin, G. "ASA404: update on drug development" Expert Opin. Investig. Drugs 2008 17(10), 1547-1551

15: Deng, J.; Sanchez, T.; Al-Mawsawi, L. Q.; Dayam, R.; Yunes, R. A.; Garofalo, A.; Bolger, M. B.; Neamati, N. "Discovery of structurally diverse HIV-1 integrase inhibitors based on a chalcone pharmacophore" *Bioorg. Med. Chem.* **2007** 15, 4985-5002

16: Marchand, C.; Zhang, X.; Pais, G. C. G.; Cowansage, K.; Neamati, N.; Burke, T. R.; Pommier, Y. "Structural Determinants for HIV-1 Integrase Inhibition by β-Diketo Acids" *J. Biol. Chem.* **2002** 277(115), 12596–12603

17: Pendri, A.; Meanwell, N.; Peese, K.; Walker, M. "New first and second generation inhibitors of human immunodeficiency virus-1 integrase" *Expert Opin. Ther. Pat.* **2011**, in press.

18: Ramkumar, K.; Tambov, K. V.; Gundla, R.; Manaev, A. V.; Yarovenko, V.; Traven, V. F.; Neamati, N. "Discovery of 3-acetyl-4-hydroxy-2-pyranone derivatives and their difluoridoborate complexes as a novel class of HIV-1 integrase Inhibitors" *Bioorg. Med. Chem.* **2008** 16, 8988-8998

19: Xue, Y.; Mou, J.; Liu, Y.; Gong, X.; Yanga, Y.; An, L. "An ab initio simulation of the UV/Visible spectra of substituted chalcones" *Cent. Eur. J. Chem.* **2010** 8(4) 928–936

20: Sohn, Y. S.; Hendrickson, D. N.; Gray H. B. "Electronic Structure of Metallocenes" *J. Am. Chem. Soc.* **1971** 93(15), 3603-3612

21: Mosmann, T. "Rapid colorimetric assay for cellular growth and survival: application to proliferation and cytotoxicity assays" *J. Immunol. Meth.* **1983** 65(1–2), 55-63

22: Touil, Y. S.; Fellous, A.; Scherman, D.; Chabot, G. G. “Flavonoid-induced morphological modifications of endothelial cells through microtubule stabilization” *Nutr. Cancer* **2009**, 61, 310-321

23: Goldur, Y.; Craigie, R.; Cohe, G. H.; Fujiwara, T.; Yoshinaga, T.; Fujashita, T.; Sugimoto, H.; Endo, T.; Murai, H.; Davies, D. R. “Structure of the HIV-1 integrase catalytic domain complexed with an inhibitor: A platform for antiviral drug design” *Proc. Natl. Acad. USA* **1999** 96, 13040-13043

24: Sharma, H.; Patil, S.; Sanchez, T. W.; Neamati, N.; Schinazi, R. F.; Buolamwini, J. K. “Synthesis, biological evaluation and 3D-QSAR studies of 3-keto salicylic acid chalcones and related amides as novel HIV-1 integrase inhibitors” *Bioorg. Med. Chem.* **2011**, 19, 2030-2045

Chapter 3

Ferrocenyl Aurones

Synthesis and biological properties

A. Aurones in the literature

Aurones are without any doubt the smallest subclass of the known natural flavonoids. They are flavone isomers, but their skeleton, presented in Figure 3.1, possesses a benzofuranone motif, unlike the other flavonoids.

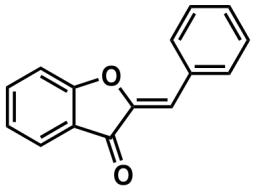

Figure 3.1. General pattern of aurone derivatives

Their name comes from their bright yellow color, “aurum” meaning gold in Latin, and they are plant pigments that are, for example, responsible for the color of *Coreopsis* flowers (also

called tickseed), shown in Figure 3.2. The most well-known aurone may be the pigment aureusidin, presented in Figure 3.2, found in a variety of plants, such as in *Cyperaceous*, a large family of flowering plants that include cottongrass for example.[1]

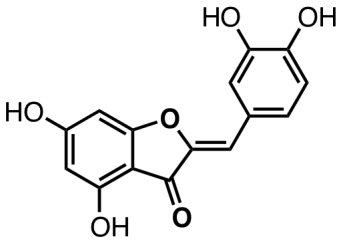

Figure 3.2. *Coreopsis* flower, and structure of aureusidin

In addition to their role in pigmentation, aurones have other functions in the plant kingdom, such as combating infections. For example, when treated with elicitor, a substance inducing a plant immune response, the cells of the cactus *Cephalocereus senilis* produce an aurone called cephalocerone, shown in Figure 3.3. Cephalocerone exhibits toxic properties on a variety of bacteria, such as *Pseudomonas aeruginosa* and *Escherichia coli*.[2]

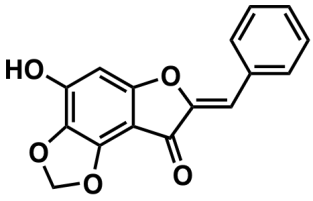

Figure 3.3. Structure of cephalocerone

The biological properties of aurones are not limited to the plant kingdom, and we will be more specifically interested in their role in animals.

1. Roles of aurones in animals

Compared to the extensive studies on the biological properties of flavones and flavonols, the application of aurones in medicine is still in its infancy. However, some very important activities have been discovered.

1.1. Aurones in cancer therapy

One of the most remarkable properties of aurones is their ability to bind with proteins. This characteristic is shared with all classes of flavonoids, but has been of particular interest for the aurone subclass. As we will see further, the five-membered ring included in the aurone skeleton endows a structural similarity to other biomolecules known for their protein interactions, such as ATP. Thus, their use as enzyme inhibitors and their action on cancer related proteins has been studied.

1.1.1. Aurones as Pgp inhibitors

As mentioned in chapter 1, one of the biggest challenges in cancer therapy is to avoid the onset of drug resistance. Efflux proteins, among which P-glycoprotein (Pgp) is the most well-known, are responsible for resistance phenomena by preventing therapeutics from accumulating inside cells. Therefore, molecules that can prevent Pgp action are very promising in combination with cytotoxic agents. A series of aurones were designed in this regard, and their affinities with the nucleotide-binding domain of Pgp (crucial for Pgp activity) were evaluated. The compound exhibiting the best activity, presented in Figure 3.4., was found to exhibit a higher affinity (K_D = 0.15) than the most active flavonols or chalcones tested.[3]

Further studies focused on the impact of this molecule on Pgp inhibition. K562 leukemia cells were incubated with the fluorescent probe rhodamine-123, in the presence and absence of the aurone shown in figure 3.4. The aurone dramatically increased intracellular rhodamine-123 accumulation, showing the inhibitory effect of these molecules on Pgp activity.[4]

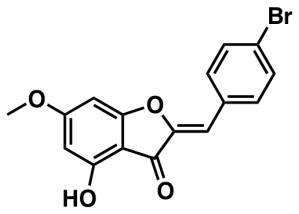

Figure 3.4. Structure of the aurone binding on Pgp

1.1.2. Aurones as CDK inhibitiors

Cyclin-dependent kinases (CDK) are enzymes involved in the regulation of the cell cycle, and are therefore implicated in the replication of cancer cells. Therefore, designing CDK inhibitors is of interest in the search for antiproliferative agents. Flavopiridol, shown in Figure 3.5, is a well-known CDK inhibitor, and is currently in clinical trials for the treatment of several different types of cancer, such as leukemia, lymphoma, lung, and esophageal, and pleural cancer.

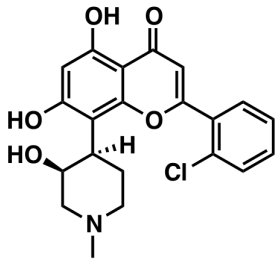

Figure 3.5. Structure of flavopiridol

The affinity of flavopiridol for CDK is due to its structural similarities with ATP; the benzopyranone moiety of flavopiridol resembles adenine. Aurone derivatives, of the general pattern presented in Figure 3.6, have been designed for CDK inhibition, and some have been found to be even more potent and selective than flavopiridol.[6] The best results were obtained for the molecule where R = *p*-SO_2NH_2. Affinity for this molecule with CDK2 was

calculated by docking experiments, which gave a binding energy of -20.6 kcal.mol^{-1}, slightly better than that of flavopiridol (-19.3 kcal.mol^{-1}). Moreover, flavopiridol exhibited IC_{50} values for CDK inhibition of 0.10, 0.22 and 0.40 μM for CDK1, CDK2 and CDK4, respectively, while the same aurone sulfamine derivative yielded values of 0.009, 0.03 and 1.87 μM. The observed selectivity for CDK2 over CDK4 is particularly interesting. Although structurally very similar, these kinases possess a specific role in the cell life cycle, therefore finding selective inhibitors can provide a broader palette of treatment options.

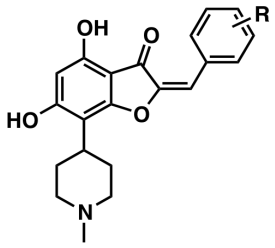

Figure 3.6. General pattern of flavopiridol mimics based on the aurone skeleton

1.1.3. Aurones as chemopreventive agents

As mentioned in chapter 1, flavonoids are generally considered to be beneficial to health, especially due to their radical scavenging behavior. Aurones also possess such antioxidant properties. For example, when polyphenols were isolated from the tree *Cotinus coggygria*, most of them were found to be aurone derivatives. The most potent isolated antioxidant is the dimer of 3',4,4'-trihydroxyaurone depicted in Figure 3.7.[7]

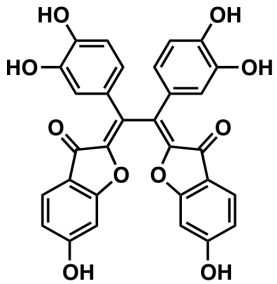

Figure 3.7. Structure of the most potent antioxidant isolated from *Cotinus coggygria*

Enzyme-based mechanisms can also be involved in chemoprevention processes. For example, the enzyme NADPH quinone oxidoreductase 1 (NQO1) is involved in the detoxification of xenobiotics, therefore its induction protects cells against exterior attack. Moreover, NQO1 stabilizes the tumor suppressor p53 in response to DNA-damaging stimuli. Aurones were shown to induce NQO1 in Hepa1c1c7 murine hepatoma cells *in vitro*. For example, the 3'-chloro-5-hydroxyaurone presented in Figure 3.8 tripled the NQO1 activity at a concentration of 10 μM.[8]

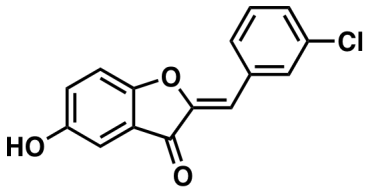

Figure 3.8. Structure of an aurone inducing NQO1 activity.

1.2. Other uses of aurones as bioactive agents

Similarly to other flavonoids, the impact of aurones on animal biology is very broad and thus they have been investigated in the treatment of a variety of diseases. Some of these studies will be detailed below.

1.2.1. Aurones as anti-parasitic agents

Aurones, like other flavonoid subclasses such as chalcones, are known to act as anti-parasitic agents. For example, a series of aurones and auronols were investigated against the parasitic protist* *Cryptospordium parvum. C. parvum* is an opportunistic protozoan, which attacks the intestinal epithelial cells of AIDS-infected patients, and for which there is no current

* Protists are eukaryotic microorganisms that don't belong to animal, plant or fungus kingdom. For example, foraminifera are protists.

treatment. The tested compounds were all active at concentrations between 25 to 100 µM. They inhibited the intracellular growth by more than 90% at concentrations that posed an acceptable toxicity for host cells. The most active compound, 3',4',6-trihydroxyaurone, is presented in Figure 3.9.[9]

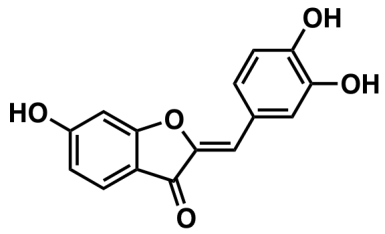

Figure 3.9. Structure of 3',4',6-trihydroxyaurone

The same authors also investigated the activity of aurones on *Plasmodium falciparum*, using both chloroquine-resistant and chloroquine-sensitive strains. Some aurones were very active, with IC_{50} values in the nanomolar range. Remarkably, the chloroquine resistant strain was more sensitive to the aurones than the chloroquine sensitive strain. A structure activity relationship study was performed, and aurones possessing several hydroxy, methoxy and/or acetyl groups showed the best activity. For example, 4,6,4'-triacetyl-3',5'-dimethoxyaurone shown in Figure 3.10 exhibited an IC_{50} of 7 nM.[10]

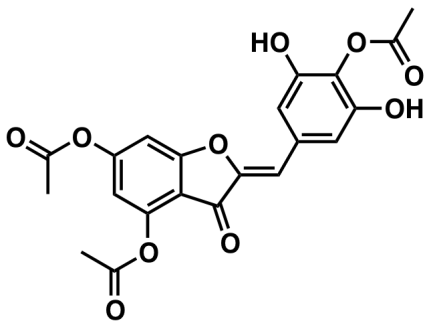

Figure 3.10. Structure of 4,6,4'-triacetyl-3',5'-dimethoxyaurone

1.2.2. Aurones as anti-diabetes agents

Diabetes mellitus is a group of metabolic diseases where glucose levels are dysregulated due to a low production of or a resistance to the hormone insulin. Type 1 diabetes is an autoimmune disease, which causes the destruction of insulin-producing pancreatic β-cells. A key step in this harmful process implicates the activation of the nuclear factor-kappa B (NF-κB), a transcription factor linked to immune response. Sulfuretin, shown in Figure 3.11, is known to suppress the NF-κB pathway and its ability to protect β-cells in case of type 1 diabetes mellitus have been evaluated.[11] RINm5F cells (a rat pancreatic β-cell line) were exposed to cytokines in order to simulate an immune response and were evaluated in the presence and absence of sulfuretin. Sulfuretin clearly showed a protective effect on these cells: sulfuretin pretreated cells exhibited normal insulin secretion in response to glucose at the end of the experiment by suppressing the NF-κB pathway. Moreover, *in vivo* experiments were performed on mice, for which streptozotocin was used as a model of Type 1 diabetes mellitus induction. When pretreated with sulfuretin, mice were not affected by streptozotocin.

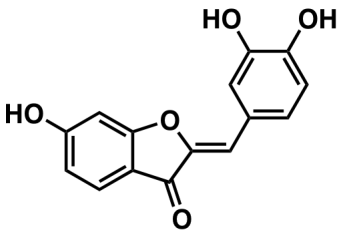

Figure 3.11. Structure of sulfuretin

1.2.3. Aurones as anti-microbial agents

Aurones have also been evaluated as anti-microbial agents, and some of them enjoy patent protection. Compounds whose general formula is presented in Figure 3.12 have been tested *in vivo* on mice infected with a pathogenic strain of *Candida albicans*, an infection-causing fungus.[12] Mice sensitive and resistant to the antifungal fluconazole were used. All untreated

control animals died after 16 days. Fluconazole sensitive mice treated with fluconazole, had a survival rate of about 30%, while the survival in the group treated with the aurone was about 60% to 70% depending on the mode of administration (40 mg/kg body weight by oral administration or 20 mg/kg body weight by intra peritoneal injection). The survival for fluconazole-resistant mice treated with the aurone (40 mg/kg body weight by oral administration) was 80% after 20 days, whereas untreated animals or those treated with fluconazole all died in the same period of time.

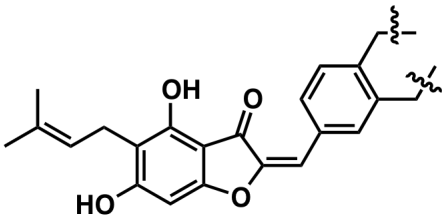

Figure 3.12. Structure of aurones used as anti-microbial agents

2. Synthesis of aurones

As a consequence of the low aurone abundance in nature, most of the aurone derivatives that have been evaluated as bioactive agents are from synthetic origin. Three main methods exist to build this skeleton.

2.1. Functionalization of the benzofuranone core

The first approach, shown in Figure 3.13, requires a key intermediate, benzofuran-3(2H)-one (also called 3-coumaranone), obtained from a substituted phenol. Subsequent condensation with a benzaldehyde yielded the desired aurones in 60 % to quantitative yields.[13]

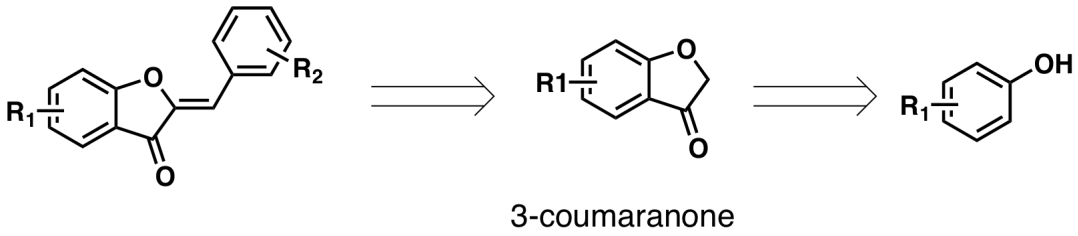

Figure 3.13. Synthesis of the aurone core from a phenol core

The formation of the coumaranone is achieved in two steps from the phenol, detailed in Figure 3.14 The first step is a Friedel-Craft acylation, using a halogeno-acetonitrile and zinc chloride, followed by the hydrolysis of the of the newly created imine, molecule **A**, to generate the ketone, molecule **B**. The second step consists of the intramolecular cyclization of **B** in basic medium, affording the coumaranone **C**.

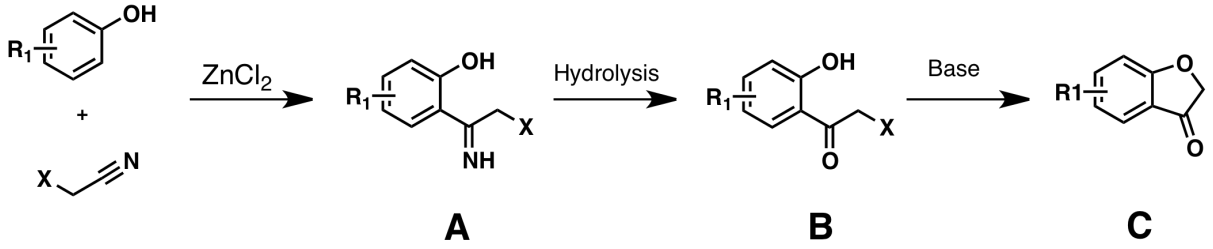

Figure 3.14. Obtention of the coumaranone core

Once the coumaranone is obtained, a simple condensation addition of a benzaldehyde yields the desired aurone. This condensation can be catalyzed either by acid or base. Microwave assistance and solvent-free conditions have also been described.[14] In fact, the original condensation was carried out on the surface of alumina particles.[15]

This approach presents several disadvantages. The synthesis is multi-step, and the first step is done in harsh conditions, thus limiting yields and the choice of the substitution pattern on the phenol.

2.2. Oxidative cyclization of chalcones

The second, and most common, way of synthesizing aurones uses chalcones as a key intermediate, similarly to the biosynthetic process. This approach can be classified in two categories: with or without metal assistance.

2.2.1. Metal-free oxidative cyclization of chalcones

This approach consists in the cyclization of an oxidized form of the chalcone. The first example of this synthetic pathway was described by Donelly and coworkers in 1977.[16] The dibrominated chalcone core, compound A, was first synthesized, and after elimination of HBr, the bromochalcone B was obtained. A cycloaddition can then result in the aurone derivative, as shown in Figure 3.15.

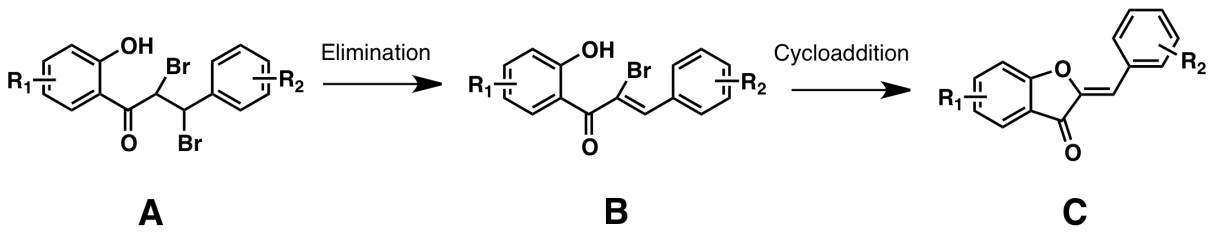

Figure 3.15. Synthesis of aurones from chalcones using Donelly's protocol

This method has serious drawbacks, particularly due to the fact that the elimination reaction is not selective. Compound A can lose one or the other Br atoms, depending on the nature of the phenyl substituents. Therefore, a mixture of flavones and aurones is generally obtained. To obtain regioselectivity, a similar protocol was proposed by Khan and coworkers in 2001.[17] By adding non-identical substituents over the double bond, as shown in Figure 3.16, the yield of the aurone was enhanced, although the formation of flavone was still observed.

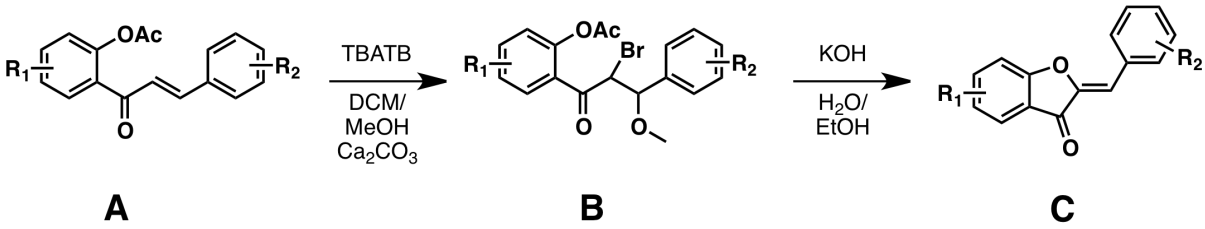

Figure 3.16. Synthesis of aurones from chalcones using Bose's protocol

2.2.2. Oxidative cyclization of chalcones with metal assistance

Various methods of direct oxidative cyclization of chalcones are described in the literature. For example, the use of thallium(III) led to a mixture of aurones and isoflavones.[18] Lead(IV) tetraacetate or manganese(II) acetate gave predominantly the aurones, but generally in low yield.[19,20] The most well-known synthesis using a metal reagent was achieved using mercury(II) acetate in acetic acid[21] as described in Figure 3.17, although flavanone is also formed during this reaction. A protocol using other solvents, such as pyridine, was later described.[22] The mechanism of this reaction still remains elusive and will be discussed in a further section.

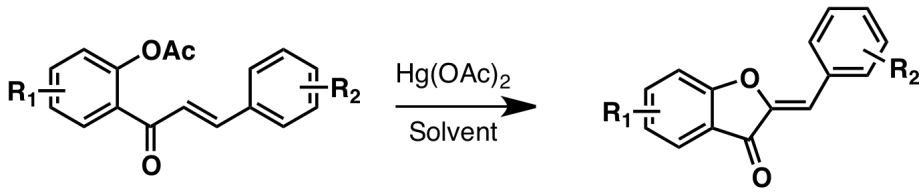

Figure 3.17. Synthesis of aurones using mercury(II) acetate

Other metals have been used in a similar fashion, and as we will see in the next chapter, the ratio between aurone and flavone obtained depends on the nature of the metal. Some metal systems produce the flavones as the major product.

2.3. Aurones from alkynes

The last main synthetic strategy to form aurones is the use of a key intermediate possessing a triple bond. Miranda and coworkers first explored this strategy in 1986.[23] The authors prepared compound **C** in Figure 3.18 in two steps. This first step is a condensation of phenylpropynoic acid with a substituted phenol, giving the ester **A**. A simple irradiation of **A** afforded **B** as major photoproduct. The cyclization of **B** yielded the aurone **C**. The base-dependence of the cyclization of the ynone **B** to the aurone **C** was the subject of study and it was found that NaOEt in EtOH gave the highest yield of aurones.

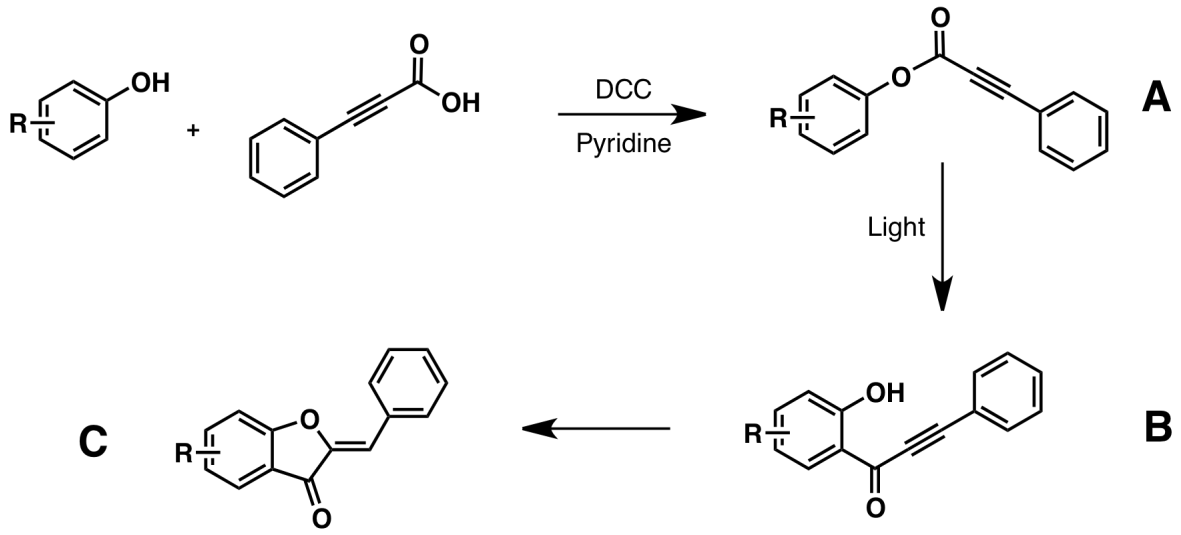

Figure 3.18. Synthesis of aurone using Miranda and coworkers method

Another study exploiting the properties of triple bonds was performed in 2007.[24] As shown in the Figure 3.19, the first step formed the ynol derivative A. The key step of this synthesis is the cyclization of **A** to **B**, catalyzed by gold(I), with yields of up to 86%. The oxidation of **B** generated the aurone **C**. The main advantage of this synthesis is the regioselectivity of the cyclization step.

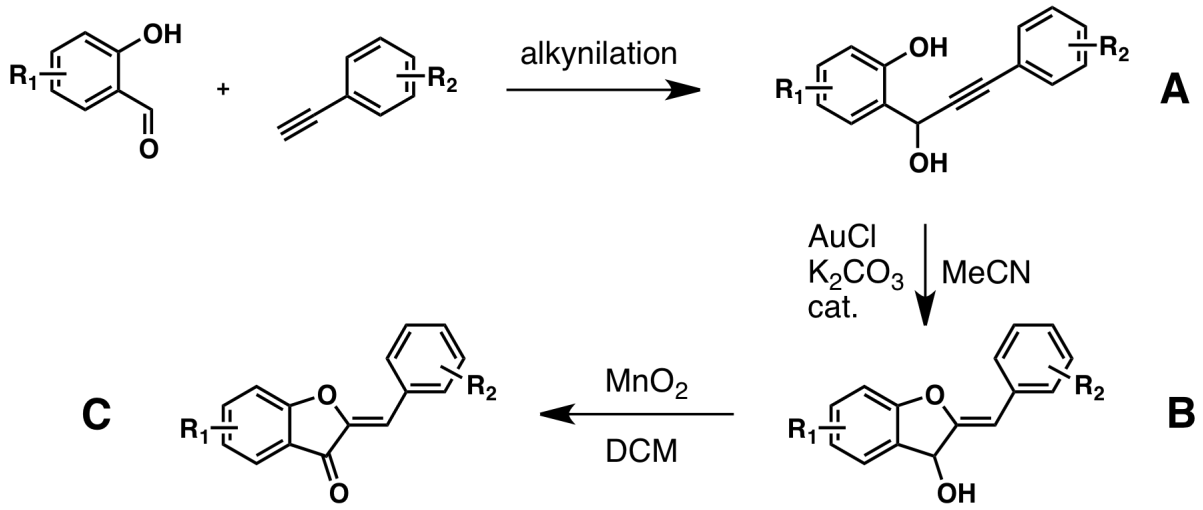

Figure 3.19. Synthesis of aurone using gold catalysis

B. Synthesis, chemical reactivity and analytical properties of ferrocenyl aurones

With a series of ten substituted ferrocenyl chalcones in hand, we first tried to obtain flavanone derivatives using different literatures' protocols. Protocols in basic media, using piperidine and NaOH in water,[25] acetate in ethanol[26] or pyridine[27] in methanol and water gave only decomposition products and starting material. Protocols in acidic media, either by refluxing a chalcone in acetic acid[28] or by addition of HCl[29] were also carried out, but only led to decomposition products. Finally, protocols using amino acids such as alanine[25] or proline[30] only gave starting material. The reactivity of the vinylic carbon adjacent to the ferrocene seems to be greatly modified by its presence. The multiple failures to obtain this series made us investigate oxidative cyclisations of chalcones rather than standard cyclisations. This approach was a success and the ferrocenyl aurones possessing the general structure shown in Figure 3.20 were obtained.

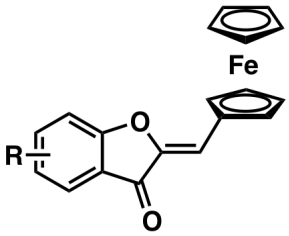

Figure 3.20. General pattern of ferrocenyl aurones

1. Synthesis

The literature procedure[22] using mercury(II) acetate in pyridine for a couple of hours was successfully used in order to obtain compound **3a-j** shown in Figure 3.21. This series of ten compounds represents the first examples of ferrocenyl aurones, obtained in excellent yields.

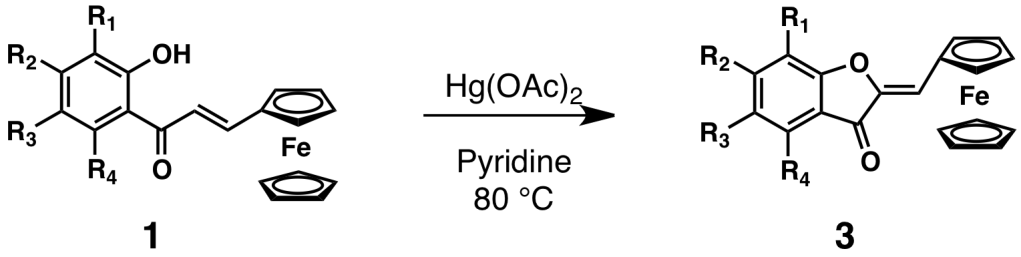

1 **3**

5a: R_1=R_2=R_3=R_4=H (75%)
5b: R_3=Cl (65%)
5c: R_3=Br (71%)
5d: R_1=R_3=Cl (64%)
5e: R_1=R_3=Br (60%)
5f: R_1=R_3=F (66%)
5g: R_2=OMe (75%)
5h: R_3=OMe (85%)
5i: R_4=OMe (66%)
5j: R_2=R_4=OMe (68%)

3.21. First examples of ferrocenyl aurones

Although efficient, this protocol presents the major disadvantage of using a toxic oxidizing agent and solvent. Another protocol, using silver triflate and sodium hydride in THF at the room temperature gave compounds **3a-f** in excellent yields in only ten minutes. Unfortunately, this protocol was not applicable to molecules possessing methoxy

substitution. This seems to be due to the high reactivity of this oxidant, which degrades the parent chalcone.

Apart from some minor degradation, aurones are the only species obtained using both sets of conditions, in excellent yields. The use of Ag salts in this type of reaction is unprecedented, probably because it is not effective in the cyclization of organic chalcones. This suggests the reactions with $Hg(OAc)_2$/pyridine and AgOTf/NaH/THF may follow two different mechanisms of action, and that the presence of a ferrocene group is necessary for the formation of aurones with AgOTf/NaH/THF.

In order to follow the reaction of the chalcone with $Hg(OAc)_2$, ^1H proton NMR spectra were collected at r.t. over 16 hours of a solution containing **1c** and an excess of $Hg(OAc)_2$ in pyridine-d^5. As shown in figure 3.22, at t = 1 h, signals corresponding to chalcone **1c** and the aurone **3c** (in a 3:2 ratio) were observed. Over time, those signals corresponding to the chalcone diminished and those corresponding to the aurone intensified. No signals of any intermediate structure or any other product were observed. This suggests that the rate-limiting step is the formation of an intermediate that is too reactive to be observed or that the cyclization follows a concerted mechanism.

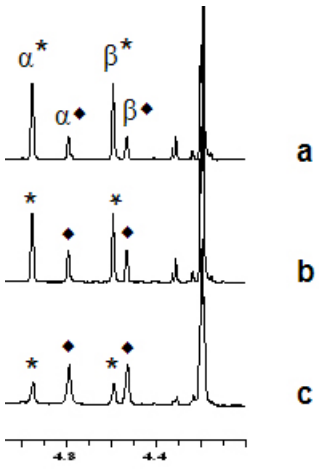

Figure 3.22. ^1H NMR spectrum of the ferrocene region of **1c** in pyridine-d_6 and $Hg(OAc)_2$. Diamonds = **3c** and stars = **1c**; a) after 1 h; b) after 12 h; c) after 18 h

In another effort to characterize a possible intermediate, we attempted to halt the cyclization by methylation of the phenol group of the chalcone. Methylation of **1c** was effected with MeI/NaH in THF at room temperature after 6 h. The new compound, *(E)*-1-(5'-methoxy-2'-hydroxyphenyl)-3-ferrocenylprop-2-en-1-one, was dissolved in pyridine-d^5 and an excess of $Hg(OAc)_2$ was added. The solution was monitored at room temperature by ^1H NMR over 13 h. No change in the spectrum was observed, suggesting Hg does not interact with the double bond of the enone, and more generally, with the compound. Finally, the interaction of **1c** and $Hg(OAc)_2$ was examined in the absence of base. Likewise, no reaction was observed via ^1H NMR in MeOD over 12 h. These results suggest that the mechanism of cyclization involves coordination of Hg to the oxygen atom of the phenolate, as previously proposed.

We further investigated the reaction of the chalcone in pyridine by replacing $Hg(OAc)_2$ with randomly selected metal salts. We screened five metal salts using TLC: $CuCl_2$, $AuCl_3$, $CuSO_4$, $ZnSO_4$ and $PdCl_2$ and except for $CuCl_2$, these conditions yielded only starting material and/or decomposition products (Table 3.1, experiments 1-5). Using $CuCl_2$, we observed traces of aurone among primarily decomposition products, as determined by TLC.

As previously mentioned, the AgOTf/NaH system in THF is very efficacious in the transformation of ferrocenyl chalcones to aurones. Looking at other solvent/base combinations, we found that DMF does not support the formation of aurones in any case. NaOH, piperidine and ^{t}BuOK are effective in EtOH, MeOH, CH_2Cl_2 and MeCN, while sodium carbonate was only effective in CH_2Cl_2 (Table 3.1, experiments 6-25).

All of these reactions were very fast; the reaction was complete after about 5 min., although conversion did not reach 100%, such as observed with the AgOTf/NaH/THF system. The only exception was the use of ^{t}BuOK in EtOH, which was furthermore effective in the synthesis of methoxy-substituted **3h**. Modifying the metal (or oxidant) system, but using the standard THF/NaH solution did not lead to the formation of aurone (Table 3.1, experiments 26-36).

Table 3.1. Reaction of **1a** with different metal, solvent and base systems.

Exp. No.	Metal or oxidant	Solvent	Base	Aurone	Exp. No.	Metal or oxidant	Solvent	Base	Aurone
1	$CuCl_2$	pyridine	pyridine	Traces	21	AgOTf	EtOH	^tBuOK	+
2	$AuCl_3$	pyridine	pyridine	-	22	AgOTf	MeOH	^tBuOK	+
3	$CuSO_4$	pyridine	pyridine	-	23	AgOTf	DMF	^tBuOK	-
4	$ZnSO_4$	pyridine	pyridine	-	24	AgOTf	CH_2Cl_2	^tBuOK	+
5	$PdCl_2$	pyridine	pyridine	-	25	AgOTf	MeCN	^tBuOK	+
6	AgOTf	EtOH	NaOH	+	26	$KMnO_4$	EtOH	^tBuOK	+
7	AgOTf	MeOH	NaOH	+	27	$AgPF_6$	THF	NaH	-
8	AgOTf	DMF	NaOH	-	28	$AgNO_3$	THF	NaH	-
9	AgOTf	CH_2Cl_2	NaOH	+	29	Ag_2O	THF	NaH	-
10	AgOTf	MeCN	NaOH	+	30	$AuCl_3$	THF	NaH	-
11	AgOTf	EtOH	piperidine	+	31	$NiCl_2$	THF	NaH	-
12	AgOTf	MeOH	piperidine	+	32	CuI	THF	NaH	-
13	AgOTf	DMF	piperidine	-	33	$SnCl_2$	THF	NaH	-
14	AgOTf	CH_2Cl_2	piperidine	+	34	DDQ	THF	NaH	-
15	AgOTf	MeCN	piperidine	+	35	$Tl(NO_3)_3$	THF	NaH	-
16	AgOTf	EtOH	$NaCO_3$	+	36	$NOBF_4$	THF	NaH	-
17	AgOTf	MeOH	$NaCO_3$	-	37	AgOTf	THF	---	-
18	AgOTf	DMF	$NaCO_3$	-	38	AgOTf	pyridine	pyridine	-
19	AgOTf	CH_2Cl_2	$NaCO_3$	+					
20	AgOTf	MeCN	$NaCO_3$	-					

The use of AgOTf in the oxidative cyclization of chalcones is unprecedented and, surprisingly, it is not effective in the cyclization of organic chalcones, suggesting that the presence of a ferrocene group is necessary for the formation of aurones with AgOTf/NaH/THF. Therefore, we hypothesized that oxidation of the ferrocene group could be the first step in the reaction. However, reaction with the chalcone **1c** with AgOTf in THF gave only a brown, diamagnetic product that could not be eluted on a TLC plate.

We subsequently investigated if an inductive effect by the ferrocene group modified the electronic structure of the α,β unsaturated ketone enough to favor aurone formation. The ^{1}H and ^{13}C NMR of **1a**, **c** and **h** together with their organic analogues is shown in Table 3.2.

Table 3.2. Chemical shifts (δ) for ferrocenyl and organic chalcones

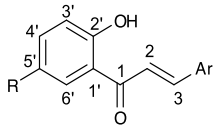

Compound	δ (H_2)	δ (H_3)	δ (C_1)	δ (C_2)	δ (C_3)	δ ($C_{1'}$)
1a	7.67	7.93	193.8	120.2	145.6	120.1
Organic a	7.25	7.90	192.8	116.7	148.0	120.1
1c	7.56	7.94	192.8	119.4	146.7	121.3
Organic c	7.13	7.93	191.6	115.9	149.5	121.4
1h	7.59	7.92	193.4	120.2	145.7	119.7
Organic h	7.20	7.90	192.4	116.7	148.1	119.7

On this table, we observe that C_3 (adjacent to the ferrocenyl group) is shielded (Δδ = -2.4-2.8 ppm), and C_2 is deshielded (Δδ = +3.5 ppm) relative to the organic compound. This suggests that the mesomeric effect of the enone conjugation is decreased in the case of the ferrocenyl compounds, and that the double bond is indeed less polarized than that found in the organic compounds. However, while it appears that the presence of ferrocene lessens the partial negative charge on C_2 compared to the phenyl group, C_3 remains by far the more electrophilic atom of the two, with Δδ between C_3 and C_2 of +26 ppm.

We also attempted to perform the chalcone cyclization with AgOTf in pyridine, which led only to decomposition (Table 3.1, exp. 37-38).

Mechanistic investigations on the formation of organic aurones have been previously conducted. In 1975, Grundon and coworkers identified the intermediate presented in Figure 3.23, resulting from an anti-Markovnikov addition of the mercury phenolate on the double bond.[31]

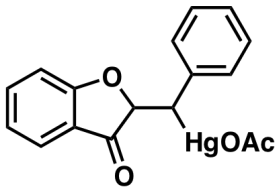

Figure 3.23. Structure of the isolated ntermediate to the aurone formation

Thus, a coordination of the mercury with the double bond as presented in Figure 3.24 might occur, even if it hasn't been observed experimentally.

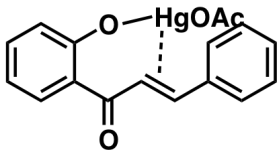

Figure 3.24. Probable transition state for the formation of aurone.

Unfortunately, the similarity between organic and ferrocenyl aurone can only be postulated, since no intermediate state can be identified in the ferrocenyl case. Moreover, it should also be mentioned that metallic mercury was observed at the end of the reaction, instead of the $Hg^{I}OAc$ reportedly isolated in the organic reaction.

In case of monoelectronic oxidants, like silver salts, another study was found in the literature using manganese acetate, as shown in Figure 3.25. The manganese phenolate transition

state (**1**) has been suspected, followed by a homolysis of the Mn-O bond that leads to a phenoxy radical (**2**). The radical would then attack the C-H bond, resulting in aurone formation.[23]

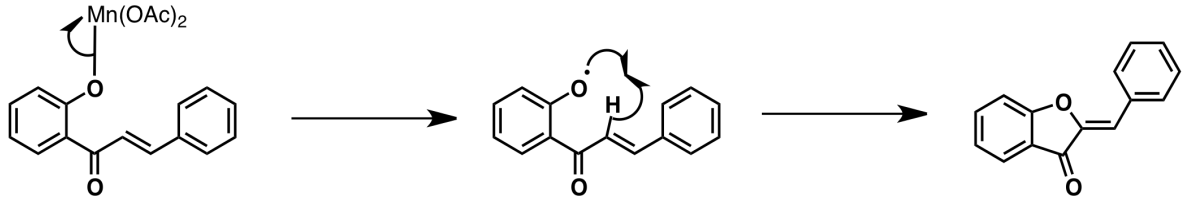

Figure 3.25. Suspected mechanism for the formation of aurone with manganese acetate

2. Chemical reactivity

Treatment of the ferrocenyl aurones **3a**, **3c** and **3h** with lithium diisopropylamide (LDA) in THF yielded, after workup, deep red solids which were identified as 1-(2-hydroxyphenyl)-3-ferrocenylprop-2-yn-1-one derivatives as shown in Figure 3.36. Presumably, deprotonation of the vinyl proton leads to a rearrangement and ring-opening, and ynones **4a**, **4c** and **4h** were the sole products obtained in about 70% purified yield. Conversely, it has been previously observed that organic aurones do not react readily with LDA, although some minor ynone product has been detected.[32]

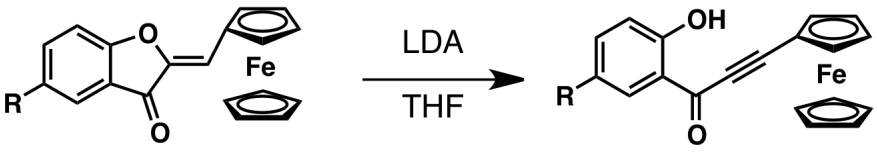

4a: R=H (78%)
4c: R=Br (65%)
4h: R=OMe (73%)

Figure 3.26. Synthesis of ferrocene ynones

Ferrocenyl ynones have also been synthesized by Pd catalyzed coupling of ethynyl ferrocene and acyl chlorides,[33] and although the protocol described herein requires more steps than the coupling reaction, it is very economical from the point of view of the ferrocenyl starting material (ferrocene carboxyaldehyde).

A crystal structure by X-ray diffraction was obtained for compound **4a**. This structure and associated data are presented in Figure 3.27 and Table 3.3.

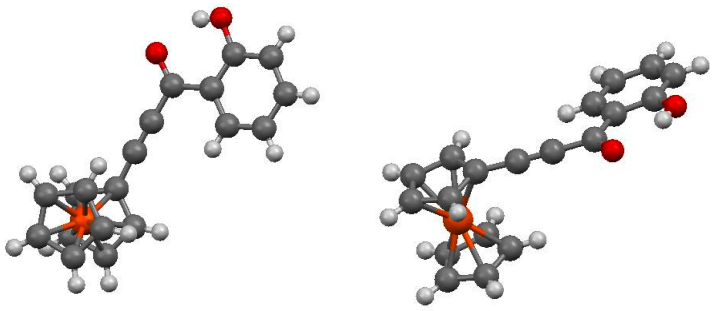

Figure 3.27. Two views of the structure of compound **4a** created by Hg software. Cif data has been deposited with the Cambrige Structure Database number 823195

Table 3.3. Crystal data for molecule **4a**

Compound	**4a**	Z	4
Formula	$C_{19}H_{14}FeO_2$	T	200 K
M	330.17	No. reflections	13536
Crystal system	monoclinic	No. independent reflections	4177
Space group	P21/c	R_{int}	0.000
a (Å)	9.8786(6)	2θ	54.6°
b (Å)	13.7386(7)	R_1 (all data)	0.0526
c (Å)	10.6891(6)	wR_2 (all data)	0.0610
β (°)	95.745(5)	R_1 (with cutoff)	0.0322
V ($Å^3$)	1443.42(14)	wR_2 (with cutoff)	0.0502

3. Characterization

All compounds were unambiguously characterized using routine techniques, that is to say NMR spectroscopy, mass spectrometry, elemental analysis and so on.

The structural similarity between aurones and flavones made the structural attribution non-trivial. A comparative 2D NMR study between ferrocenyl aurones and ferrocenyl flavones addresses this point, and will be presented in the next chapter.

3.1. Crystal structure of 3c

A crystal structure by X-ray diffraction was obtained for compound **3c**. This structure and associated data are presented in Figure 3.28 and Table 3.4.

Table 3.4. Crystal data for **3c**

Compound	**3c**	Z	4
Formula	$C_{19}H_{13}BrFeO_2$	T	200 K
M	409.06	No. reflections	21523
Crystal system	monoclinic	No. independent reflections	3471
Space group	P21/a	R_{int}	0.059
a (Å)	7.5434(7)	2θ	52.8°
b (Å)	14.7364(17)	R_1 (all data)	0.0644
c (Å)	13.8726(8)	wR_2 (all data)	0.0622
β (°)	99.146(8)	R_1 (with cutoff)	0.0365
V ($Å^3$)	1522.5(2)	wR_2 (with cutoff)	0.0506

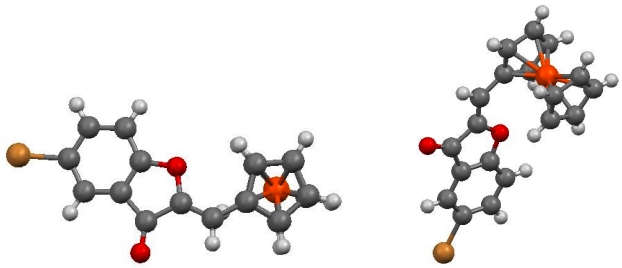

Figure 3.28. Two views of the structure of compound **3c** created by Hg software. Cif data has been deposited with the Cambrige Structure Database number 787469

3.2. UV/visible spectroscopy of 3a-j

Similarly to ferrocenyl chalcones, the spectral properties of ferrocenyl aurones are quite different from those of their organic analogs. UV-visible absorption spectra of **3a-j** were therefore recorded, and the molar extinction coefficients (ε) at λ_{max} in the visible region were calculated for each molecule. The results are summarized in Table 3.5.

Table 3.5. Values of ε at λ_{max} of each member of the series **3**

Compound	λ_{max} (nm)	ε	Compound	λ_{max} (nm)	ε
3a	386	7595	**3f**	395	16944
	545	2144		575	5625
3b	394	16624	**3g**	365	16563
	565	5485		534	3813
3c	392	10043	**3h**	400	4719
	559	2713		545	2019
3d	397	15698	**3i**	390	17347
	581	12384		536	4554
3e	394	14400	**3j**	368	17301
	570	4400		522	3599

The color of ferrocenyl aurones is even more saturated than that of ferrocenyl chalcones, ranging from violet for the most electron-donating substituents, to blue for the most electron-withdrawing substituents. Similar to the chalcones, ferrocenyl aurones present a supplementary absorption band whose wavelength is superior to 500 nm, induced by the presence of ferrocene. The molar extinction coefficients for the least energetic absorption band are somewhat larger as those found for the ferrocenyl chalcones. For the same absorption band, the evolution in wavelength similarly follows the nature of the substituents: the more electron-withdrawing, the less energetic the transition.

3.3. IR spectroscopy

IR spectra of **3a-j** were recorded, and the characteristic stretching values are presented in Table 3.6.

Table 3.6. IR characteristic values (in cm^{-1}) for **3a-j**

	C=O	C=C
3a	1698	1642
3b	1700	1639
3c	1701	1639
3d	1697	1635
3e	1697	1639
3f	1701	1654
3g	1685	1639
3h	1689	1632
3i	1700	1643
3j	1693	1643

The first observation that can be made is that the different substitutions don't seem to have a strong effect on the strength of the two studied bonds. The strongest shift observed for

the ketone bond is the case of compound **3g**, with a shift of 13 cm^{-1} compared to the unsubstituted compound. For the alkene bond, the strongest shift is observed for **3f**, with a 12 cm^{-1} difference when compared to the unsubstituted compound. A more interesting comparison to make is the one between series **3** and series **1**. Indeed, the average of frequencies for the stretching of the ketone function in series **1** is around 1630 cm^{-1}, while around 1700 cm^{-1} for series **3**. The same effect is even stronger on the alkene bond, with average values of 1560 cm^{-1} for series **1** versus 1640 cm^{-1} for series **3**. This effect can be explained by the newly created C-O bond between the phenol moiety and the position α of the ketone. The oxygen of the phenol acts as an electron-withdrawing group on the carbon in α of the ketone, therefore decreasing the polarization of each double bond around, increasing their strength, as well as their stretching frequencies.

3.4. Electrochemistry

The oxidation chemistry of **3a-j** was analyzed by cyclic voltammetry. The results are presented in Table 3.7.

Table 3.7. Shift of the ferrocene oxidation potential for series **3**

Compound	$E_{1/2}$ (Fc+/Fc)
3a	0.156
3b	0.174
3c	0.161
3d	0.197
3e	0.191
3f	0.187
3g	0.118
3h	0.153
3i	0.125
3j	0.103

As previously seen for the ferrocenyl chalcones, electron-withdrawing groups increase the oxidation potential of the ferrocene moiety, while electron-donating groups decrease it. The only exceptions to this rule are the case of **3h**, where R_3 = OMe: the substitution does not seem to have any effect when compared to the unsubstituted derivative **3a**, and the case of **3b** and **3d**, where R_3 = Cl and R_1 = R_3 = Cl respectively: the impact of chloro substitutions seems more important than any other substitution by halogens.

As for ferrocenyl chalcones, we plotted the energy of the visible electronic transition as a function of the ferrocene moiety potential for each molecule. The graph is presented in Figure 3.29. From the graph, we can see that the correlation is clear; once again, the more electron-withdrawing the substituents, the higher the oxidation potential, and the less energetic the transition. The electron-withdrawing substituents have a greater role in stabilizing the π* LUMO, than they do towards the ferrocene-based HOMO.

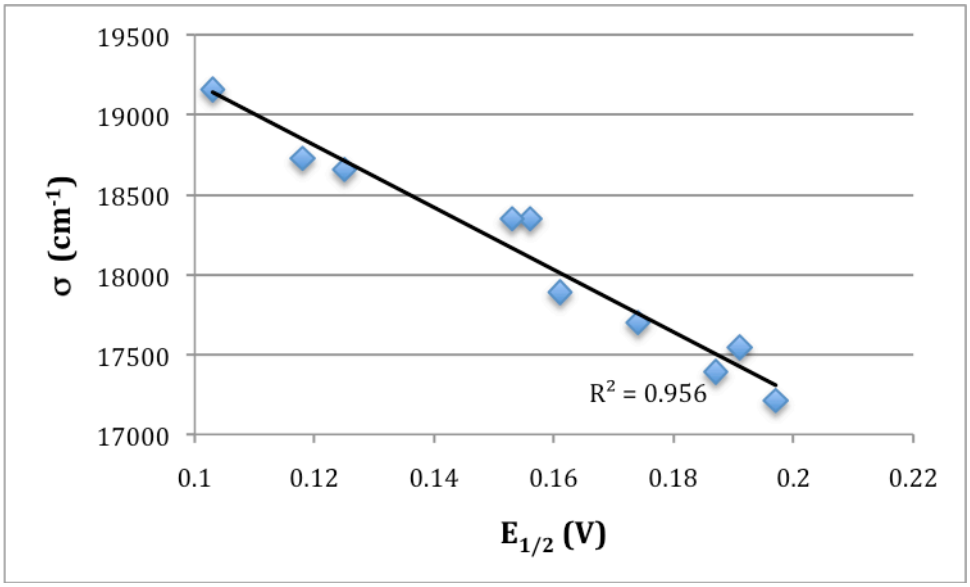

Figure 3.29. Plot of the wavenumber in function of the ferrocene moiety oxidation potential for each compound of series **3**,

C. Biological properties of ferrocenyl aurones

1. Antiproliferative effects on B16 melanoma cells

Similarly to series **1** and **2**, the antiproliferative effects of compounds **3a-j** were evaluated by the MTT test on murine B-16 melanoma cells in collaboration with Guy G. Chabot. The results are presented in Figure 3.30, together with the chalcone results already presented in the previous chapter, for comparison.

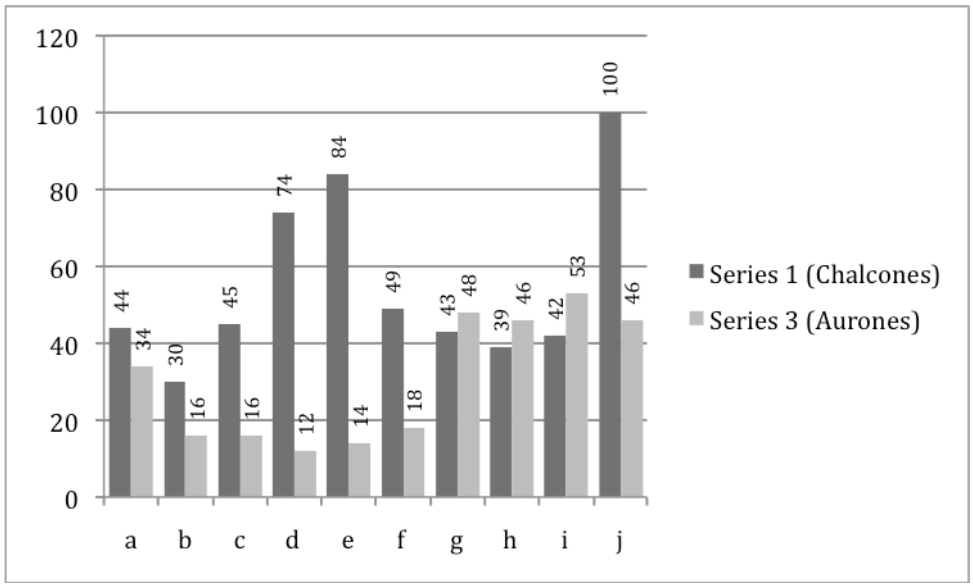

Figure 3.30. IC_{50} values (μM) of compounds **3a-j** on B16 murine melanoma cells

Methoxy substituents induced rather poor antiproliferative effects, while halogen substitution give rise to better activity, with IC_{50} values in the low micromolar range. What is particularly remarkable is the differences in activity between series **1** and series **3** for the dihalogenated compounds. For example, in the case of **1d**/**2d** or **1e**/**2e**, the aurone is more than 6 times more active than the corresponding chalcone.

2. Antiangiogenic effects EA·hy 926 endothelial cells

Antiangiogenic properties have also been measured for series **3.** The minimal rounding up concentrations against EA·hy 926 endothelial cells are presented, together with the results for series **1**, in Figure 3.31.

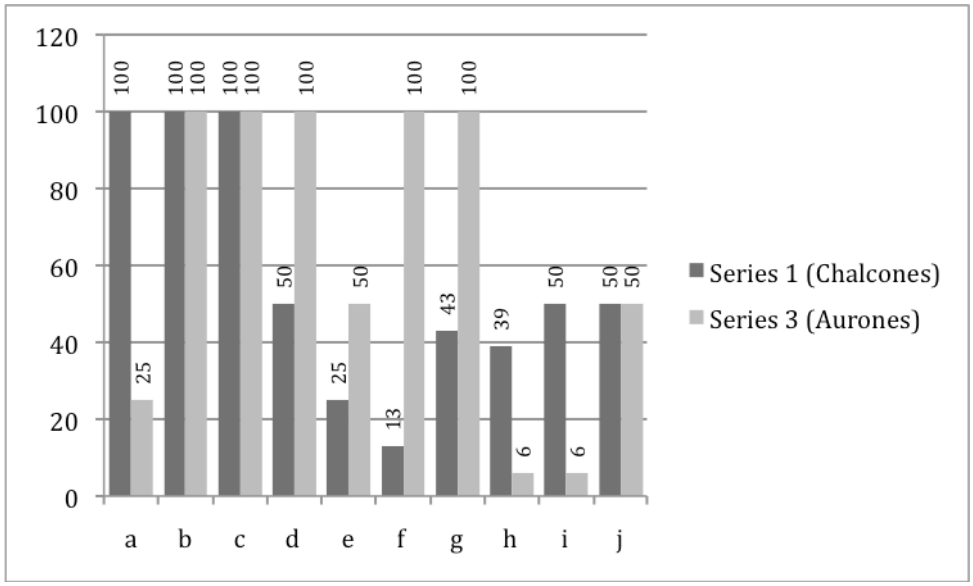

Figure 3.31. Minimal concentration (μM) of **1a-j** and **3a-j** for rounding up of EA·hy 926 cells

From this graph, it is clear that compounds **3h** and **3i** are more potent than the parent chalcones. The minimal rounding up concentrations are less than 10 μM, rendering these compounds as good candidates for antiangiogenic applications. Moreover, their antiproliferative abilities being quite poor (IC_{50} values around 50 μM), these molecules can be considered as pure antiangiogenic agents.

From these biological results, it is clear that aurones are more potent candidates for anti-cancer applications than the chalcones.

3. Antibacterial properties

Similarly to series **1**, compounds of series **3** have been evaluated as anti-bacterial agents, in collaboration with Claude Jolivalt from Chimie ParisTech. The results of the test at 100 mg/mL are presented in Table 3.8.

Table 3.8. Screening of series **3** at 100 µg/mL

	E. coli ATCC25922	*S. aureus* ATCC25923	*S. aureus* 1199B	*S. aureus* MsrA
3a	++	++	++	++
3b	-	-	-	++
3c	-	++	-	++
3d	-	++	-	++
3e	-	-	-	n.d.
3f	-	++	++	++
3g	++	++	++	++
3h	++	++	++	++
3i	++	++	++	++
3j	-	++	++	++

From this table, it is clear that the series **3** is generally very active against all 4 bacterial lines. For the drug-sensitive line of *S.aureus*, only two compounds were not active, and the drug-resistant lines of *S. aureus* are also susceptible to the tested aurones. For 1199B, six compounds of the 10 tested were active, and on MsrA, all the nine compounds tested were active. It is remarkable that in the case of series **3** like in the case of series **1**, the *S.aureus* MsrA line is more strongly affected by the compounds than the sensitive strain.

The same experiment was also conducted at a concentration of 20 mg/mL, and the results are presented in Table 3.9. At this lower concentration, the activities of **3a**-**j** are still very interesting. The effects of four compounds, **3a**, **3g**, **3h** and **3I** on the three different lines of *S.*

aureus is particularly interesting, since the mutations of the bacteria don't seem to play a role in the compounds' activity. Moreover, we can see that the most active compounds are the non-substituted and the methoxy-substituted compounds; none of the halogen-substituted derivatives present interesting activity.

Table 3.9. Screening of series **3** at 20 µg/mL

	E. coli ATCC25922	*S. aureus* ATCC25923	*S. aureus* 1199B	*S. aureus* MsrA
3a	-	++	++	++
3b	-	-	-	-
3c	-	-	-	-
3d	-	-	-	++
3e	-	-	-	+
3f	-	-	-	-
3g	-	++	++	++
3h	-	++	++	++
3i	-	++	++	++
3j	-	-	-	++

The non-halogenated molecules presenting an exceptional behavior, the minimal inhibition concentrations (MIC) of **3a** and **3g-j** were determined by successive dilutions. The results are presented in Table 3.10. The compounds are all active on *S. aureus* MsrA, and their MIC is in the low micromolar range. The best results are obtained for **3g** and **3j**, with respective MIC of 5.5 and 5 µM, respectively. For the two other lines of *S. aureus*, the activity of the compounds is also high, generally in the low micromolar range. The compounds are however less active on *E. coli*. In all, these results show the potential of methoxy-substituted ferrocenyl aurones as antibacterial agents.

Table 3.10. Determination of the MIC of lead compounds in series **3** (μM)

	E. coli ATCC25922	*S. aureus* ATCC25923	*S. aureus* 1199B	*S. aureus* MsrA
3a	100	100/25	25	12.5
3g	44/22	11	11	5.5
3h	88	22	44	22
3i	44	11	11	11
3j	40/20	10	10	5

D. Experimental

General preparation of ferrocenyl aurones (Method A)

Ferrocene chalcone, **1a-j**, (10 mg) was dissolved in 15 mL of THF in a 50 mL two-necked round bottom flask. NaH (3 equiv) was added and the solution went from deep violet to a light red. After stirring for 5 min at room temperature, AgOTf (2.5 eq.) was added, and the mixture was stirred for another 5 min, before being poured into H_2O (100 mL) and HCl 12 M (15 mL). The mixture was extracted with DCM (3x50 mL), and washed with water. The organic phase was dried over $MgSO_4$, filtered and evaporated. The product was purified by silica gel column chromatography with a mixture of petroleum ether/DCM 1/1 to afford **3a-j**.

General preparation of ferrocenyl aurones (Method B)

Ferrocene chalcone, **1a-j**, (10 mg) was dissolved in pyridine (15 mL) in a 50 mL two-necked round bottom flask. After stirring for 5 min at room temperature, $Hg(OAc)_2$ (2.5 equiv) was added, and the mixture was stirred at reflux until the starting chalcone was consumed (2-3h). The reaction mixture was then poured into a H_2O (100 mL) and HCl 12 M (15 mL). The mixture was extracted with CH_2Cl_2 (3x50 mL), and washed with water. The organic phase was dried over $MgSO_4$, filtered and evaporated. The product was purified using a silica gel column, using a mixture of petroleum ether/ethyl acetate 4/1 as an eluent.

(*Z*)-2-(ferrocenylidene)benzofuran-3-one 3a. Yield with AgOTf/NaH in THF: 8.0 mg, 80%. Violet solid. δ_H (300 MHz; $CDCl_3$) 4.22 (s, 5H, C_5H_5), 4.60 (s, 2H, C_5H_4), 4.92 (s, 2H, C_5H_4), 6.89 (s, 1H, vinyl), 7.19 (t, *J* = 7.5 Hz, 1H, Aromatic), 7.29 (d, *J* = 7.2 Hz, 1H, Aromatic), 7.64 (t, *J* = 7.2 Hz, 1H, Aromatic), 7.80 (d, *J* = 7.5 Hz, 1H, Aromatic). δ_C (75 MHz; $CDCl_3$) 70.0 (C_5H_5), 71.5 (C_5H_4), 71.8 (C_5H_4), 75.1 (C_5H_4 ipso), 112.9 (Aromatic), 116.4 (vinyl), 122.6 (Aromatic), 123.1 (Aromatic), 124.5 (Aromatic), 136.1 (Aromatic), 146.0 (vinyl), 165.4 (Aromatic), 182.9 (C=O). MS (APCI) m/z 331.07 [M+H]+ Found: C 67.60, H 4.66. Calc. for $C_{19}H_{14}O_2Fe{\cdot}0.5\ H_2O$: C 67.28, H 4.46.

(*Z*)-5-chloro-2-(ferrocenylidene)benzofuran-3-one 3b. Yield with AgOTf/NaH in THF: 7.8 mg, 78%. Violet solid. δ_H (300 MHz; $CDCl_3$) 4.24 (s, 5H, C_5H_5), 4.63 (s, 2H, C_5H_4), 4.91 (s, 2H, C_5H_4), 6.92 (s, 1H, vinyl), 7.24 (m, 1H, Aromatic), 7.57 (dd, ^4J = 2.1 Hz, ^3J = 8.7 Hz, 1H, Aromatic), 7.77 (d, *J* = 2.1 Hz, 1H, Aromatic). δ_C (75 MHz; $CDCl_3$) 70.0 (C_5H_5), 71.6 (C_5H_4), 72.2 (C_5H_4), 74.7 (C_5H_4 ipso), 114.2 (Aromatic), 117.9 (vinyl), 123.8 (Aromatic), 124.0 (Aromatic), 128.8 (Aromatic), 135.8 (Aromatic), 146.1 (vinyl), 163.5 (Aromatic), 181.4 (C=O). MS (APCI) m/z 364.02 [M+H]+ Found: C 61.65, H 3.67. Calc. for $C_{19}H_{13}O_2FeCl{\cdot}0.25\ H_2O$: C 61.66, H 3.69.

(*Z*)-5-bromo-2-(ferrocenylidene)benzofuran-3-one 3c. Yield with AgOTf/NaH in THF: 6.4 mg, 64%. Violet solid. δ_H (300 MHz; $CDCl_3$) 4.19 (s, 5H, C_5H_5), 4.60 (m, 2H, C_5H_4), 4.86 (m, 2H, C_5H_4), 6.94 (s, 1H, vinyl), 7.20 (d, *J* = 8.7 Hz, 1H, Aromatic), 7.72 (dd, ^4J = 2.1 Hz, ^3J = 8.7 Hz, 1H, Aromatic), 7.93 (d, *J* = 2.1 Hz, 1H, Aromatic). δ_C (75 MHz; $CDCl_3$) 70.1 (C_5H_5), 71.7 (C_5H_4), 72.2 (C_5H_4), 74.7 (C_5H_4 ipso), 114.7 (Aromatic), 115.9 (Aromatic), 118.0 (vinyl), 124.4 (Aromatic), 127.1 (Aromatic), 138.5 (Aromatic), 145.9 (vinyl), 163.9 (Aromatic), 181.2 (C=O). MS (APCI) m/z 408.08 [M+H]+ Found: C 55.77, H 3.65. Calc. for $C_{19}H_{13}O_2FeBr{\cdot}0.165\ H_2O$: C 55.39, H 3.26.

(*Z*)-5,7-dichloro-2-(ferrocenylidene)benzofuran-3-one 3d. Yield with AgOTf/NaH in THF: 6.2 mg, 62%. Blue solid. δ_H (300 MHz; $CDCl_3$) 4.22 (s, 5H, C_5H_5), 4.66 (s, 2H, C_5H_4), 4.93 (s, 2H, C_5H_4), 7.06 (s, 1H, Vinyl), 7.64 (d, *J* = 2.1 Hz, 1H, Aromatic), 7.69 (d, *J* = 2.1 Hz, 1H, Aromatic). δ_C (75 MHz; $CDCl_3$) 69.2 (C_5H_5), 71.0 (C_5H_4), 71.7 (C_5H_4), 73.3 (C_5H_4 ipso), 118.4 (Aromatic), 118.9 (Vinyl), 121.4 (Aromatic), 124.1 (Aromatic), 127.9 (Aromatic), 134.0 (Aromatic), 144.8 (Vinyl), 158.2 (Aromatic), 179.3 (C=O). MS (APCI) m/z 398.00 [M+H]+ Found: C 56.05, H 3.31. Calc. for $C_{19}H_{12}O_2FeCl_2{\cdot}0.5\ H_2O$: C 55.93, H 3.21.

(*Z*)-5,7-dibromo-2-(ferrocenylidene)benzofuran-3-one 3e. Yield with AgOTf/NaH in THF: 8.0 mg, 80%. Blue solid. δ_H (300 MHz; $CDCl_3$) 4.22 (s, 5H, C_5H_5), 4.67 (s, 2H, C_5H_4), 4.93 (s, 2H, C_5H_4), 7.03 (s, 1H, Vinyl), 7.86 (d, J = 1.5 Hz, 1H, Aromatic), 7.92 (d, J = 1.5 Hz, 1H, Aromatic). δ_C (75 MHz; $CDCl_3$) 69.2 (C_5H_5) 71.0 (C_5H_4), 71.7 (C_5H_4), 73.3 (C_5H_4 ipso), 115.0 (Aromatic), 119.0 (Vinyl), 124.5 (Aromatic), 125.0 (Aromatic), 129.8 (Aromatic), 139.2 (Aromatic), 144.4 (Vinyl), 159.9 (Aromatic), 179.3 (C=O). MS (APCI) m/z 485.99 [M+H]+ Found: C 46.47, H 2.60. Calc. for $C_{19}H_{12}O_2FeBr_2 \cdot 0.25\ H_2O$: C 46.34, H 2.56.

(*Z*)-5,7-difluoro-2-(ferrocenylidene)benzofuran-3-one 3f. Yield with AgOTf/NaH in THF: 8.6 mg, 86%. Violet-blue solid. δ_H (400 MHz; $CDCl_3$) 4.22 (s, 5H, C_5H_5), 4.65 (s, 2H, C_5H_4), 4.91 (s, 2H, C_5H_4), 7.02 (s, 1H, Vinyl), 7.22 -7.15 (m, 1H, Aromatic), 7.31-7.29 (m, 1H, Aromatic). δ_C (100 MHz; $CDCl_3$) 70.2 (C_5H_5), 71.9 (C_5H_4), 72.6 (C_5H_4), 74.3 (C_5H_4 ipso), 105.5 (dd, ^2J = 23.8 Hz, ^4J = 4.1 Hz, Aromatic), 110.9 (dd, ^2J = 19.7 Hz, ^2J = 24.3 Hz, Aromatic), 119.8 (Vinyl), 125.6 (d, ^3J = 7.7 Hz, Aromatic), 145.9 (Vinyl), 148.1 (dd, ^1J = 254.7 Hz, ^3J = 11.2 Hz, Aromatic), 148.8 (d, ^2J = 11.3 Hz, Aromatic), 157.9 (dd, ^1J = 246.5 Hz, ^3J = 7.3 Hz, Aromatic), 180.7 (C=O). MS (APCI) m/z 366.04 [M+H]+ Found: C 61.04, H 3.22. Calc. for $C_{19}H_{12}O_2FeF_2 \cdot 0.5\ H_2O$: C 60.83, H 3.49.

(**Z)-6-methoxy-2-(ferrocenylidene)benzofuran-3-one 3g:** mp 142°C, violet solid. δ_H (300 MHz; $CDCl_3$) 3.93 (s, 3H, OMe), 4.19 (s, 5H, C_5H_5), 4.53 (s, 2H, C_5H_4), 4.85 (s, 2H, C_5H_4), 6.74 (s, 1H, vinyl), 6.72-6.79 (m, 2H, Aromatic), 7.71 (d, *J* = 8.1 Hz, 1H, Aromatic). δ_C (100 MHz; $CDCl_3$) 55.7 (OMe), 69.5 (C_5H_5), 70.9 (C_5H_4), 71.2 (C_5H_4), 74.8 (C_5H_4 ipso), 96.3 (Aromatic), 111.8 (Aromatic), 114.4 (Vinyl), 115.4 (Aromatic), 125.2 (Aromatic), 146.5 (Vinyl), 166.6 (Aromatic), 167.5 (Aromatic), 181.1 (C=O). HRMS (ESI) calcd. for $C_{20}H_{16}FeO_3^+$: 360,04489, found: 360,04434.

(*Z*)-5-methoxy-2-(ferrocenylidene)benzofuran-3-one 3h. mp 140°C, violet solid. δ_H (300 MHz; $CDCl_3$) 3.91 (s, 3H, OMe), 4.17 (s, 5H, C_5H_5), 4.52 (t, ^3J = 1.7 Hz, 2H, C_5H_4), 4.87 (t, ^3J = 1.7 Hz, 2H, C_5H_4), 6.47 (s, 1H, H_3), 7.26 (dd, ^3J = 9.1 Hz, ^4J = 3.0 Hz, 1H, H_7), 7.44 (d, ^3J = 9.1 Hz, 1H, H_8), 7.59 (d, ^4J = 3.0 Hz, 1H, H_5). δ_C (75 MHz; $CDCl_3$), 55.9 (OMe), 67.4 (C_5H_4), 70.2 (C_5H_5), 71.3 (C_5H_4), 75.0 (C_5H_4-C_{ipso}), 104.9 (C_5), 105.1 (C_3), 119.1 (C_8), 123.1 (C_7), 124.7 (C_{10}), 151.0 (C_9), 156.8 (C_6), 167.9 (C_2), 177.3 (C_4), (CI NH_3) *m/z* 361.0 (MH^+), HRMS (ESI) calcd. for $C_{20}H_{16}FeO_3^+$: 383.03466, found: 383.03411.

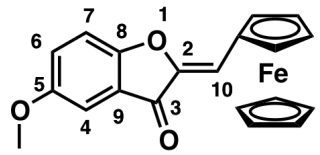

(Z)-4-methoxy-2-(ferrocenylidene)benzofuran-3-one 3i: mp 174°C, violet solid. δ_H (300 MHz; Acetone d_6) 4,00 (s, 3H, OMe), 4.24 (s, 5H, C_5H_5), 4.59 (t, *J* = 1.8 Hz, 2H, C_5H_4), 4.95 (t, *J* = 1.8 Hz, 2H, C_5H_4), 6.68 (s, 1H, Vinyl) 6.78 (d, J = 8.4 Hz, 1H, Aromatic) 6.98 (d, *J* = 8.4 Hz, 1H, Aromatic) 7.66 (t, *J* = 8.4 Hz, 1H, Aromatic). δ_C (100 MHz; $CDCl_3$) 55.8 (OMe), 69.5 (C_5H_5), 70.9 (C_5H_4), 71.2 (C_5H_4), 74.8 (C_5H_4 ipso), 104.2 (Aromatic), 104.4 (Aromatic), 110.8 (Aromatic), 114.4 (Vinyl), 137.3 (Aromatic), 145.4 (Vinyl), 157.9 (Aromatic), 165.9 (Aromatic), 180.3 (C=O). HRMS (ESI) calcd. for $C_{20}H_{16}FeO_3Na^+$: 383,03411, found: 383,03411.

(Z)-4,6-dimethoxy-2-(ferrocenylidene)benzofuran-3-one 3j: mp 166°C, violet solid. δ_H (300 MHz; $CDCl_3$) 3.90 (s, 3H, OMe), 3.93 (s, 3H, OMe), 4.15 (s, 5H, C_5H_5), 4.47 (s, 2H, C_5H_4), 4.78 (s, 2H, C_5H_4), 6.11 (s, 1H, Aromatic), 6.35 (s, 1H, Aromatic), 6.72 (s, 1H, Vinyl). δ_C (75 MHz; $CDCl_3$) 56.0 (OMe), 56.1 (OMe), 69.7 (C_5H_5), 70.9 (C_5H_4), 71.1 (C_5H_4), 75.3 (C_5H_4 ipso), 89.0 (Aromatic), 93.7 (Aromatic), 105.9 (Aromatic), 113.2 (Vinyl), 117.1 (Aromatic), 146.8 (Vinyl), 159.2 (Aromatic), 168.3 (Aromatic), 179.3 (C=O). HRMS (ESI) calcd. for $C_{20}H_{16}FeO_3Na^+$: 413,04467, found: 413,04467.

Synthesis and characterization of ferrocenyl ynones 4a, c and h. Ferrocene aurone **3** (100 mg) was dissolved in THF and cooled in an acetone/liquid nitrogen bath. Lithium diisopropylamide (1.1 eq, 2M in THF) was added and the solution color changed from deep violet to pale red. The solution was allowed to return to rt, poured into H_2O and HCl 12 M, extracted with EtOAc and washed with water. The organic phase was dried over $MgSO_4$, filtered and evaporated. The product was purified using a silica gel column, using petroleum ether/dichloromethane 1/1 as an eluent.

1-(2'-hydroxyphenyl)-3-ferrocenylprop-2-yn-1-one, 4a. Red solid, mp 130°C. δ_H (400 MHz; $CDCl_3$) 4.30 (s, 5H, C_5H_5), 4.47 (t, ^3J = 1.7 Hz, 2H, C_5H_4), 4.71 (t, ^3J = 1.7 Hz, 2H, C_5H_4), 6.96-7.02 (m, 2H, $H_{3'}$, $H_{5'}$), 7.52 (td, ^3J = 8.2 Hz, ^4J = 1.3 Hz, 1H, $H_{4'}$), 8.05 (dd, ^3J = 8.2 Hz, ^4J = 1.3 Hz, 1H, $H_{6'}$). δ_C (100 MHz; $CDCl_3$) 59.8 (C_5H_4-C_{ipso}), 70.7 (C_5H_5), 71.3 (C_5H_4), 73.4 (C_5H_4), 84.5 (C_2), 100.2 (C_3), 118.2 ($C_{3'}$), 119.4 ($C_{5'}$), 121.0 ($C_{1'}$), 132.9 ($C_{6'}$), 136.7 ($C_{4'}$), 162.8 ($C_{2'}$), 181.9 (C_1), (CI NH_3) *m/z* 330 (MH^+), HRMS (ESI) calcd. for $C_{19}H_{14}FeO_2^+$: 330.03432, found: 330.03377.

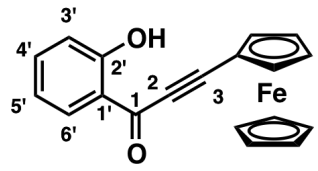

1-(5'-bromo-2'-hydroxyphenyl)-3-ferrocenylprop-2-yn-1-one, 4c. Red solid, mp 132°C. δ_H (400 MHz; $CDCl_3$) 4.32 (s, 5H, C_5H_5), 4.50 (t, ^3J = 1.8 Hz, 2H, C_5H_4), 4.74 (t, ^3J = 1.8 Hz, 2H, C_5H_4), 6.90 (d, ^3J = 8.9 Hz, 1H, $H_{3'}$), 7.58 (dd, ^3J = 8.9 Hz, ^4J = 2.5 Hz, 1H, $H_{4'}$), 8.13 (d, 1H, ^4J = 2.5 Hz, $H_{6'}$). δ_C (100 MHz; $CDCl_3$) 59.3, (C_5H_4-C_{ipso}), 70.7 (C_5H_5), 71.5 (C_5H_4), 73.5 (C_5H_4), 84.2 (C_2), 101.8 (C_3), 110.8 ($C_{5'}$), 120.3 ($C_{3'}$), 122.2 ($C_{1'}$), 134.9 ($C_{6'}$), 139.3 ($C_{4'}$), 161.7 ($C_{2'}$), 180.6 (C_1), (CI NH_3) *m/z* 409.04 (MH^+), HRMS (ESI) calcd. for $C_{19}H_{13}BrFeO_2^+$: 407.9448 and 409.9428, found : 407.9482 and 409.9530.

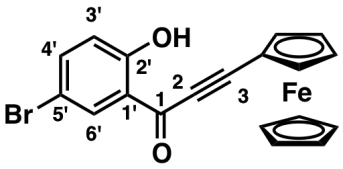

1-(5'-methoxy-2'-hydroxyphenyl)-3-ferrocenylprop-2-yn-1-one, 4h. Red solid, mp 120°c. δ_H (400 MHz; Acetone-d_6) 3.91 (s, 3H, OMe), 4.37 (s, 5H, C_5H_5), 4.59 (t, ^3J = 1.9 Hz, 2H, C_5H_4), 4.84 (t, ^3J = 1.9 Hz, 2H, C_5H_4), 6.94 (d, ^3J = 9.1 Hz, 1H, $H_{3'}$), 7.26 (dd, ^3J = 9.1 Hz, ^4J = 3.1 Hz, 1H, $H_{4'}$), 7.58 (d, ^4J = 3.1 Hz, 1H, $H_{6'}$). δ_C (100 MHz; acetone-d_6) 56.0 (OMe), 60.1 (C_5H_4-C_{ipso}), 71.3

(C_5H_5), 72.2 (C_5H_4), 74.0 (C_5H_4), 84.6 (C_2), 100.9 (C_3), 114.8 ($C_{6'}$), 119.7 ($C_{3'}$), 121.0 ($C_{1'}$), 125.9 ($C_{4'}$), 153.1 ($C_{5'}$), 157.8 ($C_{2'}$), 181.8 (C_1), (CI NH_3) *m/z* 361.11 (MH^+), HRMS (ESI) calcd. for $C_{20}H_{16}FeO_3^+$: 360.04489, found: 360.04422.

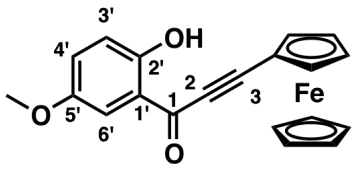

Cytotoxicity. Murine B16 melanoma was grown in Dulbecco's modified essential medium (DMEM) containing 2 mM l-glutamine, 10% fetal bovine serum, 100 U/mL penicillin, and 100 μg/mL streptomycin 37°C, 5% CO_2). Exponentially growing cancer cells were plated onto 96-well plates at 5,000 cells per well in 200 μL DMEM; and 24 h later, the cells were exposed for 48 h to the solvent alone or to the test compound at the indicated concentrations. Viability was assessed using the MTT (1-(4,5-dimethylthiazol-2-yl)-3,5-diphenyltetrazolium) test, and absorbance was read at 562 nm in a microplate reader (BioKinetics Reader, EL340, Fisher Bioblock Scientific, Illkirch, France). Control cells were exposed to 1% DMSO. Experiments were run in triplicate and repeated 3 times. Results are presented as the inhibitory concentrations for 50% (IC_{50}) of cells for a 48 h exposure time.

Morphologic Effects on EA·hy 926 Endothelial Cells. To assess the effect of **3a**-**j** on the morphology of endothelial cells EA·hy 926 endothelial cells were used. Cells were grown in DMEM containing 2 mM l-glutamine, 10% fetal bovine serum, 100 U/mL penicillin, and 100 μg/mL streptomycin (37°C, 5% CO_2). Exponentially growing cells were plated onto 96-well plates at 5,000 cells/200 μL/well. Twenty-four h after plating, the medium was aspirated, and 100 μL of medium containing the test compound was added to the well (triplicate) at the indicated final concentrations (37°C, 5% CO_2), and 2 h later digital photographs were recorded of representative center areas of each well at a magnification of ×320. Results are presented as the efficacious concentration for the change in cell shape for 50% of cells for a 2 h exposure time (EC_{50}) relative to controls.

Antibacterial activity

The inhibitory potential of the flavonoid derivatives was tested on four bacteria strains:

- *E. coli* ATCC 25922 (Gram negative strain)
- *Staphylococcus aureus* (ATCC 25923, sensitive Gram positive strain),
- *Staphylococcus aureus* 1199B: resistant to fluoroquinolones due notably to the overexpression of the NorA efflux pump (G. W. Kaatz, S. M. Seo, *Antimicrob. Agents Chemother*. 1995, *39*, 2650-2655)
- *Staphylococcus aureus* RN4220/pUL5054: resistant to erythrocycin by overexpressing the efflux pump MsrA from the high-copy pUL5054 plasmid (JI Ross, EA Eady, JH Cove, S Baumberg, Gene 1996, 183, 143-148).

The compounds were firstly solubilized in DMSO at 10 mg/mL and screened for their antibacterial activity in 96 wells at 100 and 20 mg/L. However, the high absorbance of some of the tested compounds interfered with the measurement of bacterial growth that was assayed at 620 nm.

Flavonoid derivatives were dispensed in a 96-wells microplate by dilutions in Muller-Hinton medium (MH, Bio Rad) using a Biomek 2000 (Beckman) handling robot. 100 µL of the bacterial inoculum (an overnight culture at 37 °C in 5 mL MH diluted 100-fold) was then added in each well. The total volume was 200 µL in each well and the final bacteria concentration 10^6 CFU/mL (CFU: colony forming unit). Growth was assayed with a microplate reader by monitoring absorption at 620 nm after 1, 2, 5, 7 and 24 h incubation at 37°C. In addition, the plates were read visually after 24 hours incubation. The activity of the compounds was determined after 24 h incubation at 37°C. Control wells were MH broth containing 5µL of DMSO. In addition, two controls containing a sub-inhibitory or a inhibitory antibiotic concentration for the tested strain were performed. The antibiotics used were ampicillin (0.5 and 32 µg/mL) for *E. coli*, kanamycin (0.5 and 16 µg/mL) for *S. aureus* ATCC 25923, ciprofloxacin (4 and 64 mg/L) for *S. aureus* 1199B and erythromycin (16 and 256 mg/L) for *S. aureus* RN4220/pUL5054.

MIC values were determined in the same conditions, with highest final flavonoid derivative concentration was 128 mg/L decreasing by two fold serial dilutions. The MIC was defined as

the minimal concentration of the flavonoid compound that completely inhibited cell growth during 24 h incubation at 37°C.

The accepted variance on MIC value can be estimated to a 2-fold difference due to the microdilution method used. All experiments were performed in duplicate.

References

1: Harborne, J. B.; Williams, C. A.; Wilson, K. L. "Flavonoids in leaves and inflorescences of Australian *Cyperaceae*" *Phytochemistry* **1985** 24(4), 151-166

2: Pare, P. W.; Dmitrieva, N.; Mabry, T. J. "Phytoalexin aurone induced in Cephalocereus senilis liquid suspension culture" *Phytochemistry* **1991** 30(4), 1133-1135

3: Boumendjel, A.; Beney, C.; Deka, N.; Mariotte, A.M.; Lawson, M.A.; Trompier, D.; Baubichon-Cortay, H.; Di Pietro, A. "4-Hydroxy-6-methoxyaurones with High-Affinity Binding to Cytosolic Domain of P-Glycoprotein" *Chem. Pharm. Bull.* **2002** 50(6), 854-856

4: Hadjeri, M.; Barbier, M.; Ronot, X.; Mariotte, A.-M.; Boumendjel, A.; Boutonnat, J. "Modulation of P-Glycoprotein-Mediated Multidrug Resistance by Flavonoid Derivatives and Analogues" *J. Med. Chem.* **2003** 46(11), 2125–2131

5: Kim, K. S.; Sack, J. S.; Tokarski, J. S.; Qian, L.; Chao, S. T.; Leith, L.; Kelly, Y. F.; Misra, R. N.; Hunt, J. T.; Kimball, S. D.; Humphreys, W. G.; Wautlet, B. S.; Mulheron, J. G.; Webster, K. R. "Thio- and Oxoflavopiridols, Cyclin-Dependent Kinase 1-Selective Inhibitors: Synthesis and Biological Effects" *J. Med. Chem*. **2000** *43*, 4126-4134

6: Schoepfer, J.; Fretz, H.; Chaudhuri, B.; Muller, L.; Seeber, E.; Meijer, L.; Lozach, O.; Vangrevelinghe, E.; Furet, P. "Structure-Based Design and Synthesis of 2-Benzylidene-benzofuran-3-ones as Flavopiridol Mimics" *J. Med. Chem.* **2002** *45*(9), 1741–1747

7: Westenburg, H. E.; Lee, K.-J.; Lee, S.K.; Fong, H. H. S.; Van Breemen, R. B.; Pezzuto, J. M.; Kinghorn, A. D. "Activity-Guided Isolation of Antioxidative Constituents of *Cotinus coggygria*" *J. Nat. Prod*., **2000**, *63*, 1696-1698

8: Lee, C.-Y.; Chew, E.-H.; Go, M.-L. "Functionalized aurones as inducers of NAD(P)H:quinone oxidoreductase 1 that activate AhR/XRE and Nrf2/ARE signaling pathways: Synthesis, evaluation and SAR" *Eur. J. Med. Chem.* **2010** 45, 2957-2971

9: Kayser, O.; Waters, W.R.; Woods, K.M.; Upton, S.J.; Keithly, J.S.; Kiderlen, A.F. "Evaluation of *In Vitro* Activity of Aurones and Related Compounds against *Cryptosporidium parvum*" *Planta Medica* **2001** 67, 722-725

10: Kayser, O.; Kiderlen, A.F.; Brun, R. "*In vitro* activity of aurones against *Plasmodium falciparum* strains NF1 and K54" *Planta Medica*, **2001**, 718-721

11: Song, M.-Y.; Jeong, G.-S.; Kwon, K.-B.; Ka, S.-O.; Jang, H.-Y.; Park, J.-W.; Kim, Y.-C.; Park, B.-H. "Sulfuretin protects against cytokine-induced β-cell damage and prevents streptozotocin-induced diabetes" *Exp. Mol. Med.* **2010** 42(9), 628-638

12: Chu, W. L. A.; Jensen, F. R.; Jensen, T. B.; McAlpine, J. B.; Sokilde, B.; Santana-Sorensen, A. M.; Ratnayake, S.; Jiang, J. B.; Noble, C.; Stafford, A. M. "Methods of treating fungal infections" US patent US 2002086895(A1) **2002**

13: Beney, C.; Mariotte, A. M.; Boumendjel, A. "An Efficient Synthesis of 4,6-Dimethoxyaurones" *Heterocycles* **2001** 55, 967-972

14: Villemin, D.; Martin, B.; Bar, N. ": Application of Microwave in Organic Synthesis. Dry Synthesis of 2-Arylmethylene-3(2)-naphthofuranones" *Molecules* **1998** *3*, 88-93

15: Varma, R. S.; Varma, M. "Alumina-mediated condensation. A simple synthesis of aurones" *Tet. Lett.* **1992** 33, 5937-5940

16: Donnelly, D. J.; Donnelly, J. A.; Keegan, J.R. "The modes of cyclization of 4-nitrochalcone dibromides and α-bromo-4-nitrochalcones" *Tetrahedron* **1977** *33*, 3285-3294

17: Bose, G.; Mondal, E.; Khan, A. T.; Bordoloi, M. J. "An environmentally benign synthesis of aurones and flavones from 2′-acetoxychalcones using n-tetrabutylammonium tribromide" *Tet. Lett.* **2001** 42(50), 8907-8909

18: Lévai, A.; Tõkés, A. "Synthesis of Aurones by the Oxidative Rearrangement of 2′-Hydroxychalcones with Thallium (III) Nitrate" Synthetic Commun. **1982** 12(9), 701-707

19: Kurosawa, K. "manganic acetate oxidation of 2'-hydroxy chalcones" *Bull. Chem. Soc. Jap.* **1969** 42, 1556-1558

20: Kurosawa, K.; Higuchi, J. "Study on Oxidation of Chalcones with Lead Tetraacetate and Manganic Acetate" *Bull. Chem. Soc. Jpn*. **1972** 45(4), 1132-1136

21: Seikizaki, H. “Synthesis of 2-Benzylidene-3(2*H*)-benzofuran-3-ones (Aurones) by Oxidation of 2’-Hydroxychalcones with Mercury(II) acetate” *Bull. Chem. Soc. Jpn.* **1988** 61, 1407-1409.

22: Agrawal, N. N.; Soni, P. A. “A new process for the synthesis of aurones by using mercury (II) acetate in pyridine and cupric bromide in dimethyl sulfoxide” *Indian journal of chemistry* **2006** 45B, 1301-1303

23: Garcia, H.; Iborra, S.; Primo, J.; Miranda, M. A. “6-Endo-Dig vs. 5-Exo-Dig Ring Closure in *o*-Hydroxyaryl Phenylethynyl Ketones. A New Approach to the Synthesis of Flavones and Aurones” *J. Org. Chem.* **1986** 51, 4432-4436

24: Harkat, H.; Blanc, A.; Weibel, J.-M.; Pale, P. “Versatile and Expeditious Synthesis of Aurones *via* Au(I)-Catalyzed Cyclization” *J. Org. Chem.* **2008** 73, 1620-1623

25: Tanaka, K.: Sugino, T. “Efficient conversion of 2'-hydroxychalcones into flavanones and flavanols in a water suspension medium” *Green Chem.* **2001** 3(3), 133-134

26: Akcok, I.; Cagir, A. “Synthesis of stilbene-fused 2'-hydroxychalcones and flavanones” *Bioorg. Chem.* **2010** 38(4), 139-143

27: Singh, O. V. Muthukrishnan M. and Sunderavadivellu, M. “Synthesis of Isoflavones Containing Naturally Occurring Substitution Pattern by Oxidative Rearrangement of Respective Flavanones Using Thallium(III) p-Tosylate” *Indian J. Chem., Sect. B: Org. Chem. Incl. Med. Chem*. **2005** 44, 2575-2581

28: Cabrera, M.; Simoens, M.; Falchi, G.; Lavaggi, M. L.; Piro, O. E.; Castellano, E. E.; Vidal, A.; Azqueta, A.; Monge, A.; López de Ceráin, A.; Sagrera, G.; Seoane, G.; Cerecetto, H.; González, M. “Synthetic chalcones, flavanones, and flavones as antitumoral agents: Biological evaluation and structure–activity relationships” *Bioorg. Med. Chem.* **2007** 15(10), 3356-3367

29: Mandar, D.; Blacka,D. S.; Naresh Kumar, N. “Acid catalyzed stereoselective rearrangement and dimerization of flavenes: synthesis of dependensin” *Tetrahedron* **2007** 63(24), 5227-5235

30: Chandrasekhar, S.; Vijender, K.; Reddy, K.; Venkatram “New synthesis of flavanones catalyzed by L-proline” *Tet. Lett*. **2005** 46, 6991-6993

31: Grundon, M. F.; Stewart, D.; Watts, W. E. “Oxidative cyclisation of 2′-hydroxychalcones to aurones using mercury(II) acetate in dimethyl sulphoxide” *J. Chem. Soc. Chem. Commun.* **1975**, 772-773

32: Costa, A. M. B. S. R. C. S; Dean, F. M.; Jones, M. A.; Varma, R. S. “Lithiation in Flavones, Chromones, Coumarins, and Benzofuran Derivatives” *J. Chem. Soc. Perkin Trans. I* **1985** 799-808

33: Lv, Q.-R.; Meng, X.; Wu, J.-S.; Gao, Y.-J.; Li, C.-L.; Zhu, Q.-Q.; Chen, B.-H. “Palladium-, copper- and water solvent facile preparation of ferrocenylethynyl ketones by coupling” *Catalysis Communications* **2008** 9(11-12), 2127-2130

Chapter 4

Ferrocenyl Flavones and Flavonols

Synthesis and biological properties

Flavones and flavonols are the most well-represented flavonoids in the literature, both from a biological and a chemical point of view. Chapter 1 reviewed some of the biological properties of flavonoids, and most of the cited molecules are flavones or flavonols. The present chapter presents the chemical pathways to these molecules.

A. Synthesis of flavones in the literature

1. From chalcones

Although there are many different pathways to obtain the flavones, the major strategy remains the 1,6-oxidative cyclization of chalcones, similar to the 1,5-oxidative cyclization resulting in the aurones. The central reagent used to realize such reactions is the oxidant; and those that are most commonly used are reviewed in this section.

1.1. Selenium

Selenium oxide was, to our knowledge, the first oxidant used to cyclize a chalcone into a flavone in 1935.[1] The reaction was achieved at the reflux temperature of pentan-1-ol, *i.e.* around 140 °C for 12 h, resulting in yields below 50%. The synthesis is presented in Figure 4.1.

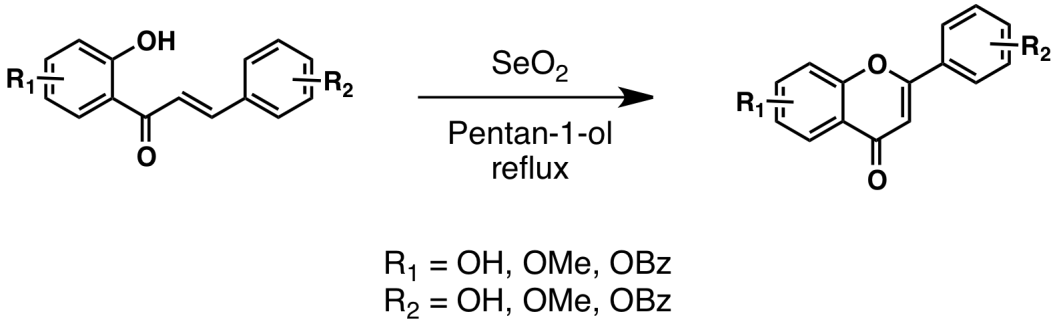

Figure 4.1. Cyclization of chalcone using selenium oxide in pentan-1-ol

Other solvent systems were later used, such as DMSO,[2] 3-methyl butan-1-ol[3] and dioxane.[4] The latter method allows yields up to 80%, and decreases the number of side reactions. However, due to the toxicity of SeO_2, and its use in stoichiometric amounts, other methods are nowadays preferred.

1.2. DDQ

The use of 2,3-dichloro-5,6-dicyano-1,4-benzoquinone (DDQ), shown in Figure 4.2, as an oxidant to convert chalcones into flavones was first mentioned by Tanaka and coworkers in 1984.[5] DDQ was also extensively used by Iinuma and coworkers for the synthesis of diversely substituted flavones.[6, 7] The studied substituents were either hydroxy, methoxy or benzoate, and are present in various positions.

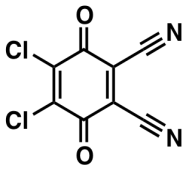

Figure 4.2 Structure of DDQ

The general procedure is presented in Figure 4.3. The yields vary from 30% to more than 70%. Aurone formation is often observed for this protocol, up to 26% of the flavonoid product. This protocol is still used nowadays. For example, Shen, Lu and coworkers synthesized luteolin analogues via this protocol in 2008, in order to investigate their biological properties.[8]

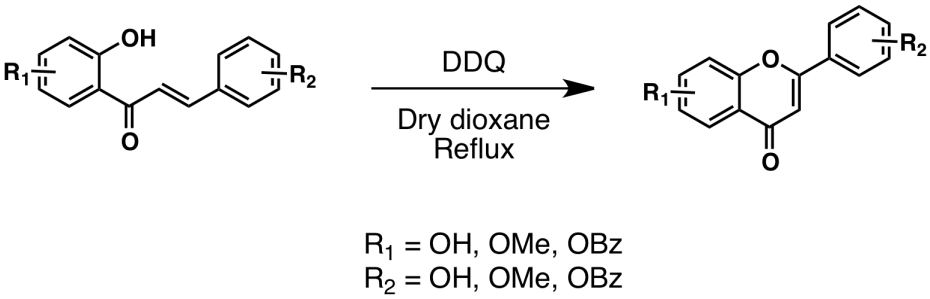

Figure 4.3. Synthesis of flavones from chalcones using DDQ

1.3. Bromine

The most common synthesis of flavones from chalcones involves a prior dihalogenation of the chalcone double bond, followed by a cyclization. The dihalogenation can be achieved with bromine,[9] and the treatment of the resulting dibromide derivative with KOH provides the flavone, as a result of an Emilewicz-von Kostanecki cyclization.[10, 11] The synthetic pathway is shown in Figure 4.4.

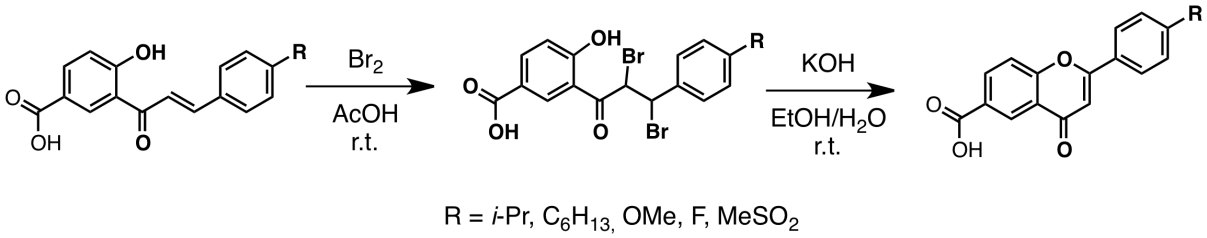

R = *i*-Pr, $C_6H_{13,}$ OMe, F, $MeSO_2$

Figure 4.4. Synthesis of flavone using Br_2 as an oxidant

This procedure gives yields between 45 and 85 %. Bromine-mediated synthesis of flavones is still used, for example, in a patent published in 2005.[12] Generally, however, the use of bromine is avoided, since it is a toxic liquid that evaporates easily. The use of iodine on the other hand has been extensively studied.

1.4. Iodine

Iodine-mediated cyclization of chalcone is the most common pathway to the flavones. The original protocol was proposed in 1986 by Doshi and coworkers,[13] using iodine in hot DMSO. Although harsh, these conditions allow different substitutions on both rings. The reaction, presented in Figure 4.5, was conducted with alkyl, halogens and methoxy substituents.

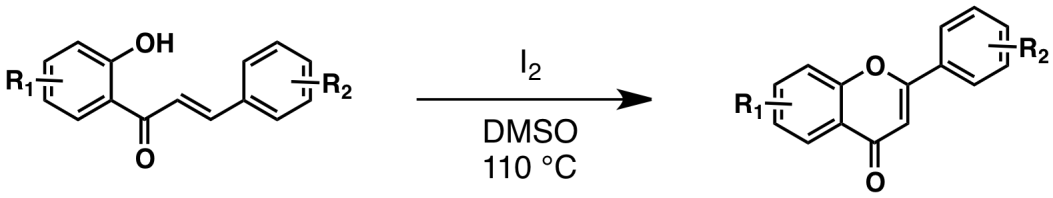

Figure 4.5. Conversion of chalcones into flavone using iodine in hot DMSO

Very similar protocols are still used nowadays, especially in medicinal chemistry.[14, 15] Other solvents have been used instead of DMSO, mainly because of toxicity issues. For example,

triethylene glycol is used to replace DMSO, but it is less efficient and requires a higher temperature.[16]

Iodine can also be adsorbed on alumina, producing a heterogeneous reagent, and used with the assistance of microwave radiation. In these conditions, all kinds of substituted flavones are obtained in excellent yields, sometimes superior to 90 %, for a reaction time between 1 and 5 min. Not only does this represent a real improvement in the protocol, but, more importantly, no side products have been identified using this method.[17]

1.5. Indium

Other supported catalysts have been used for the conversion of chalcones into flavones. For example, indium salts are adsorbed on SiO_2, following a similar procedure to the one used for I_2 on alumina.[18] The synthetic procedure using this reagent is presented in Figure 4.6. The main advantage of this protocol is the fast and clean conversion of chalcones into flavones. In 30 min to 2 hours, most of the substitution patterns allow a quantitative conversion, and the absence of solvent renders this procedure environmentally friendly. Because of its short reaction time avoiding decomposition, this protocol is compatible with a variety of substituents, such as hydroxy, methoxy, halogens and amines.

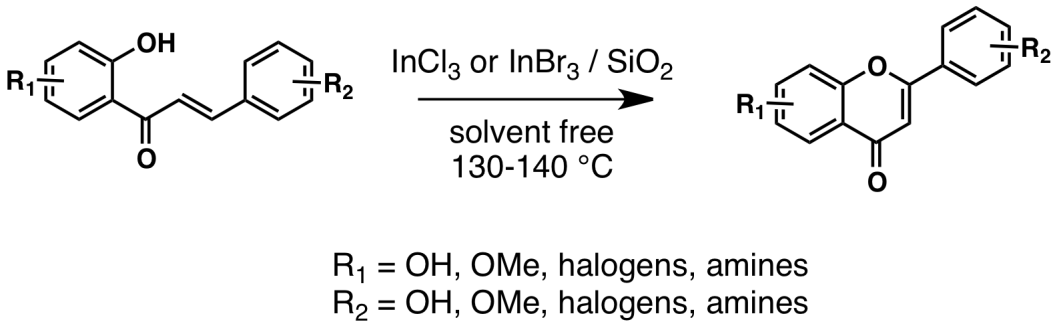

Figure 4.6. Synthesis of flavones from chalcones using supported indium catalysts

2. From ynones

The particularity of the synthesis of flavones from chalcones is the dual character of this reaction, involving an oxidation step coupled with a cyclization. Starting with an ynone instead of a chalcone greatly simplifies the problem, by limiting the chemical transformation to the cyclization. A study of the cyclization of ynones into flavones was performed by Miranda and coworkers in 1986.[19] The synthetic sequence is presented in Figure 4.7. The major disadvantage of this method is the systematic production of a mixture of aurone and flavone. Different conditions (A, B, C) have been studied. The use of a protic solvent (conditions B and C) favors the 1,5-exo dig addition, resulting in the majority formation of aurone, while the use of an aprotic solvent (condition A) favors a 1,6-endo dig cyclization, resulting a majority formation of flavone.

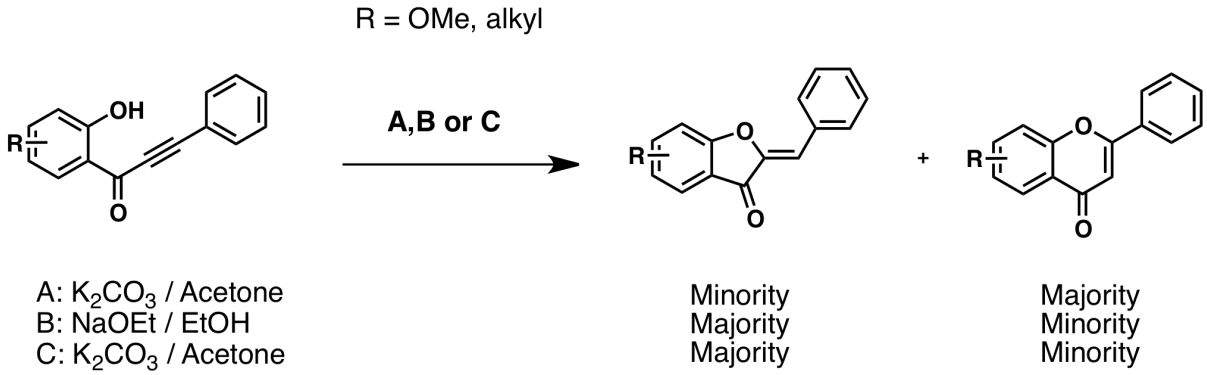

Figure 4.7. Cyclisation of ynones into flavones and aurones

Although this method has been used with only a very limited variety of substituents, the mildness of the conditions suggests a compatibility with a wide range of chemical functions. A gold catalyzed version of this reaction has been developed, giving only the aurone derivative in good yields.[20]

3. From aurones

Another approach to the flavones consists in the isomerization of an aurone. Indeed, these molecules are structural isomers, and a method of direct isomerization of aurone into flavone, that is a ring expansion method, exists.[21] The principle of this reaction, presented in Figure 4.8, is to use a nucleophile catalyst, in this case a cyanide ion. The cyanide performs a nucleophilic attack on the most electrophilic site of the aurone.

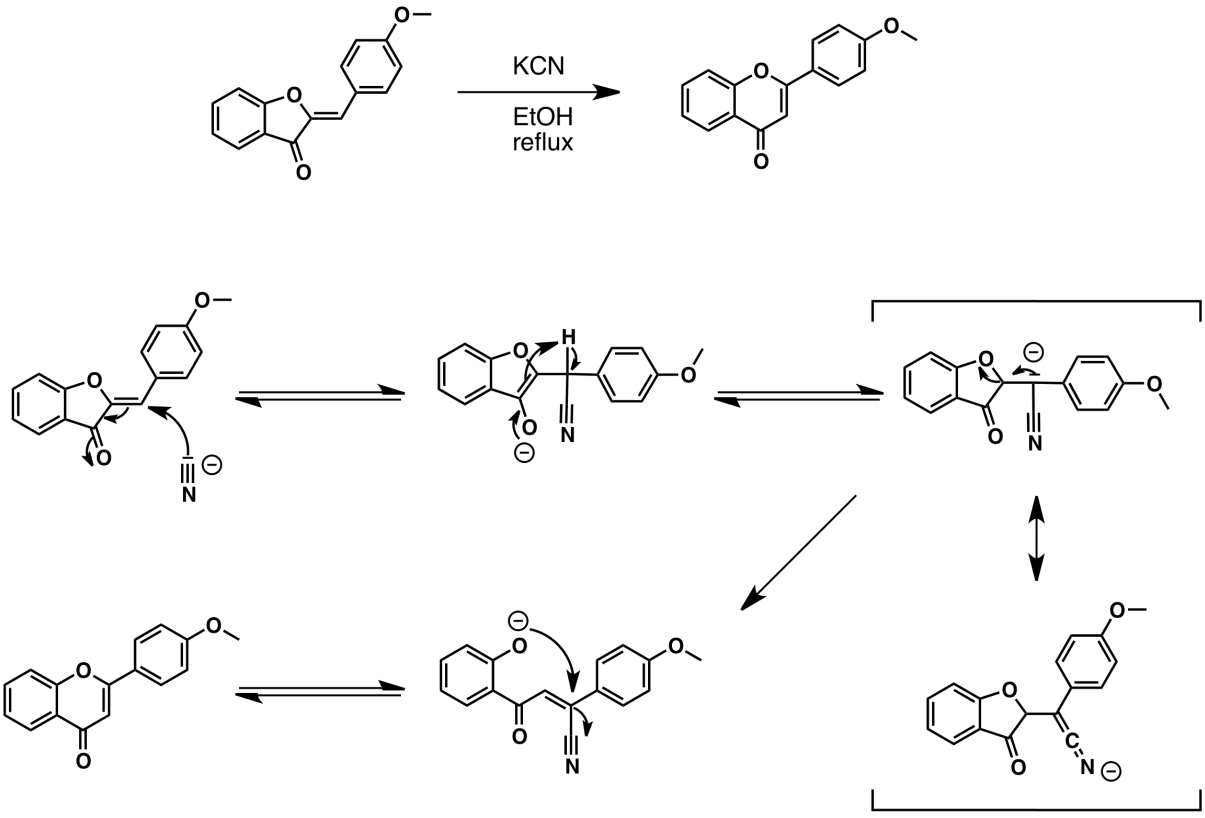

Figure 4.8. Cyanide-catalyzed aurone-chalcone isomerization

The enolate thus generated can deprotonate the carbon bound to the cyano group, which strongly stabilizes the negative charge by delocalization. By rearranging, the carbanion opens the 5-membered ring, leaving a chalcone possessing a cyano leaving group. A 1,6 nucleophilic addition regenerating the cyanide ion then occurs, and results in the creation of the flavone.

Another study has been conducted using this reaction to form flavones. The desired compounds are usually obtained in yields ranging from 50 to 70%.[22]

B. Synthesis of flavonols in the literature

1. From chalcones

Flavonols can directly be prepared from chalcones, in one step, via the Algar-Flynn-Oyamada (AFO) reaction, which was described in 1934 by two independent teams.[23, 24] The AFO reaction, for which the general pattern is presented in Figure 4.9, is an oxidative cyclization assisted by hydrogen peroxide in basic media.

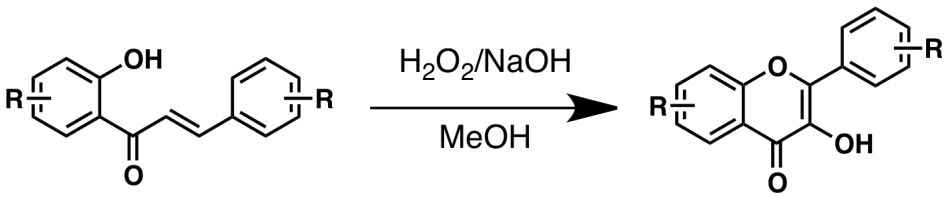

Figure 4.9. General procedure of AFO reaction

The mechanism of this reaction still remains elusive; the different propositions of pathways are presented in Figure 4.10. In any case, all of the proposed mechanisms agree on a flavanonol intermediate being further oxidized into a flavonol. Originally, the formation of an epoxide derivative from the chalcone was postulated,[25] followed by an intramolecular addition, in blue in Figure 4.10, resulting in a flavanonol derivative. This approach has been challenged, through two arguments. The first one proposes a direct addition of the chalcone phenolate over the double bond, resulting in a flavanone enolate, which further reacts with hydrogen peroxide, thus resulting in the flavanonol derivative. This approach corresponds to the red pathway. The other one proposes a concerted reaction between the deprotonated chalcone and the hydrogen peroxide to create the flavanonol derivative.[26] This approach is presented in green.

All the schools of thought agree on the mechanism of formation of the side product aurone from the epoxyde derivative, symbolized in purple on the Figure 4.10, even if they offer different explanations for the formation of flavone.

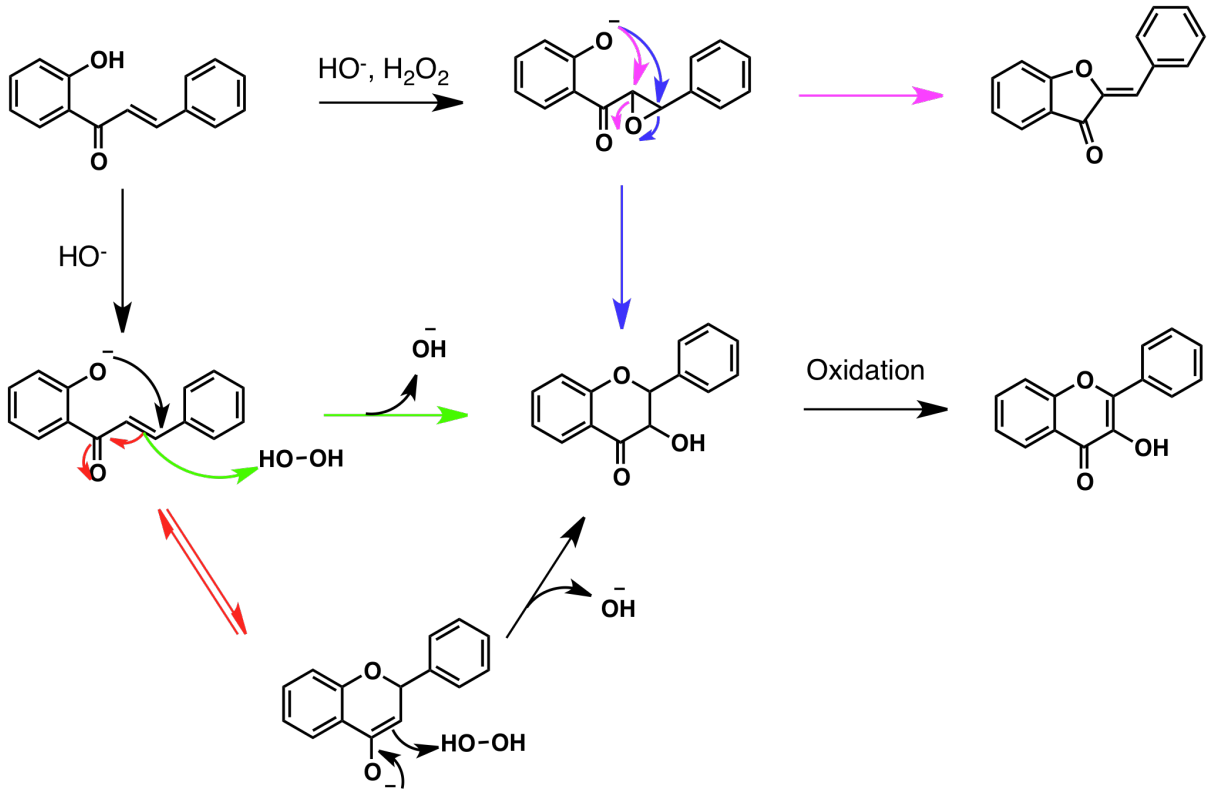

Figure 4.10. Propositions of mechanism for the Algar-Flynn-Oyamada reaction

The AFO reaction has some drawbacks, such as a high variability of yields, (30-90%), a long reaction time (16 h) and harsh oxidative conditions. The difference in the yields is generally due to the substituents on the B ring. However, although variable, average yields are around 60-70%.[9]

2. From flavones

The simple grafting of a hydroxy group on a flavone skeleton is without any doubt the easiest way to make flavonols. Several hydroxylating techniques are presented below.

2.1. PIDA

Phenyliodine diacetate (PIDA), together with hypervalent iodine compounds, are known to perform all kind of oxidations and hydroxylations.[27,28]

PIDA is used to generate flavonol from flavone, as shown in Figure 4.11. This process is achieved in two steps. The first consists in the treatment of flavone **A** with PIDA in alkaline methanol, which results in the creation of compound **B** in 67% yield. Acidic treatment of **B** in acetone induces the elimination of the methoxy group, leading to the flavonol **C** in 85% yield.

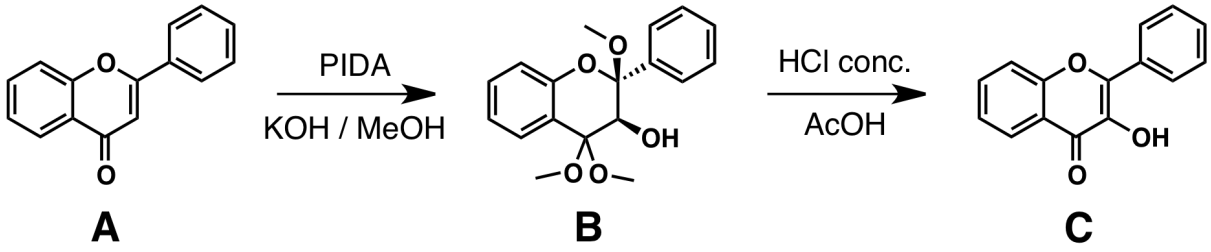

Figure 4.11. Pathway from flavone to flavonol using PIDA

The mechanism of PIDA-mediated hydroxylation is presented in Figure 4.12. The first step consists in the addition of a methoxylate to the flavone **A** skeleton, generating the enolate **B**, which coordinates the iodine atom of PIDA, regenerating the ketone function in **C**. A second methoxylate then undergoes a nucleophilic addition on this ketone function, creating a hemi-acetal **D**, whose free oxygen eliminates the PIDA molecule by forming the epoxyde **E**. The epoxyde function is then opened by a third methoxylate addition, generating a stable acetate **F**, bearing the hydroxy function of the flavonol.

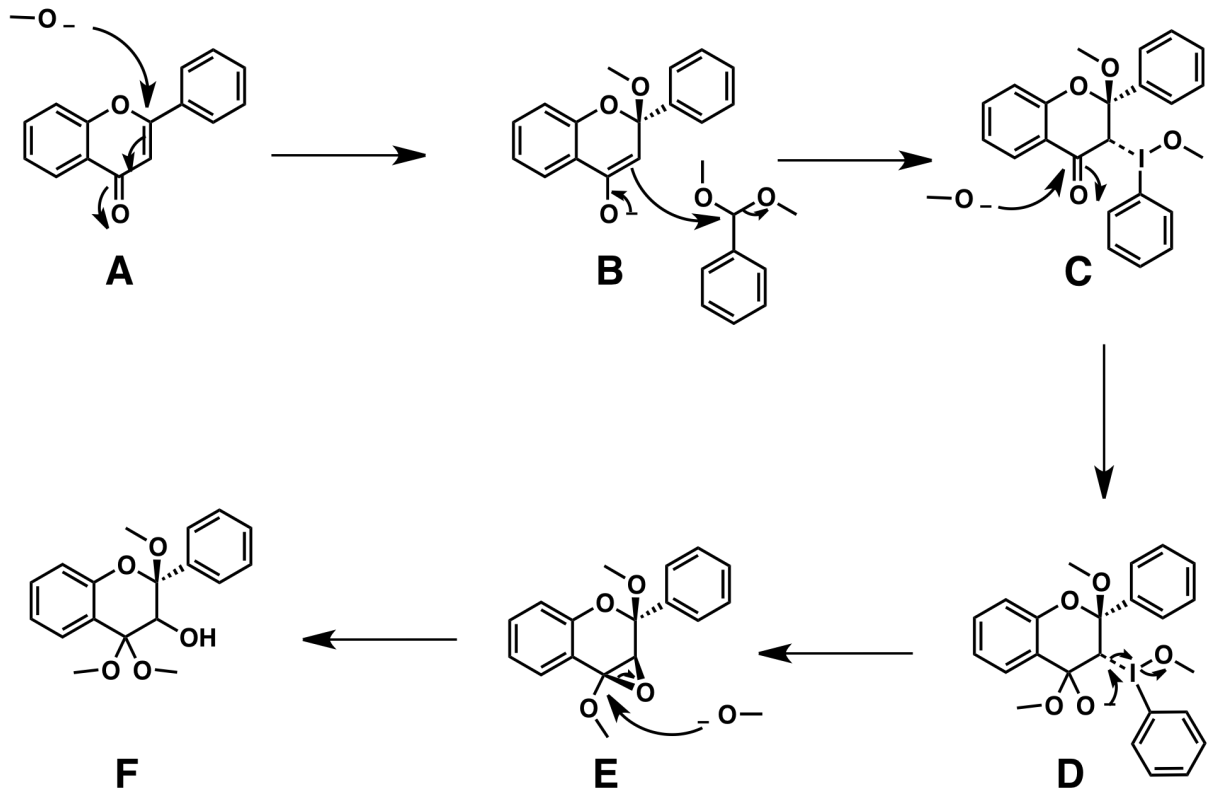

Figure 4.12. Mechanism of PIDA-mediated hydroxylation of flavone

2.2. LDA / Hydrogen peroxide

Another technique, developed in 1985,[29] consists in the synthesis of a 3-lithio flavone derivative by deprotonation of a flavone as a key intermediate. The synthesis is presented in Figure 4.13.

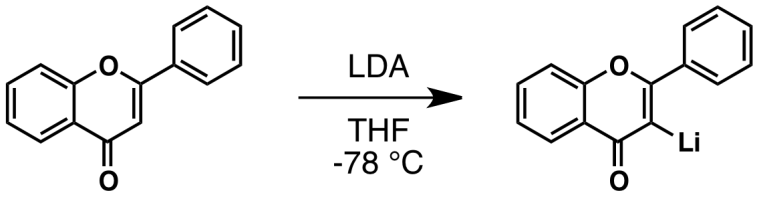

Figure 4.13. Synthesis of 3-lithio flavone

The 3-lithio flavone derivative then reacts with trimethyl borate, and is finally treated with hydrogen peroxide, which allows the creation of the flavonol derivative in quantitative yield, exploiting the known properties of borane derivatives. The synthetic sequence is presented in Figure 4.14.

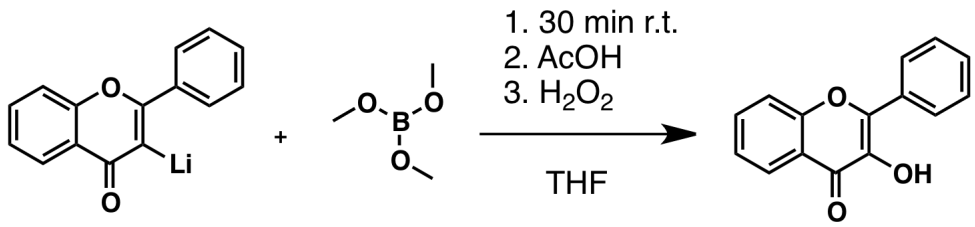

Figure 4.14. Hydroxylation of a 3-lithio flavone using trimethyl borate

Developments of this protocol have recently been published, showing a compatibility with hydroxy, methoxy and benzylidene substitutions, with excellent yields.[30, 31]

2.3. DMDO

An approach of the synthesis of flavonol from flavone by direct oxidation of the double bond can also be achieved. Indeed, as presented in Figure 4.15, the use of dimethyldioxirane (DMDO) on a flavone **A** in dichloromethane at an initial low temperature, followed by slowly returning to room temperature, results in the creation of the epoxyde **B** in quantitative yields. **B** is thermally labile, and stirring at room temperature for some hours in chloroform results in the flavonol derivative **C**. The use of a catalytic amount of *p*-toluenesulfonic acid (PTSA) creates the same flavonol derivative only in a few minutes. The yields are quantitative.[32]

Although this protocol was first studied with a limited variety of substituents, later studies showed the general character of these mild conditions, allowing for example benzoate and acetate substituents.[33]

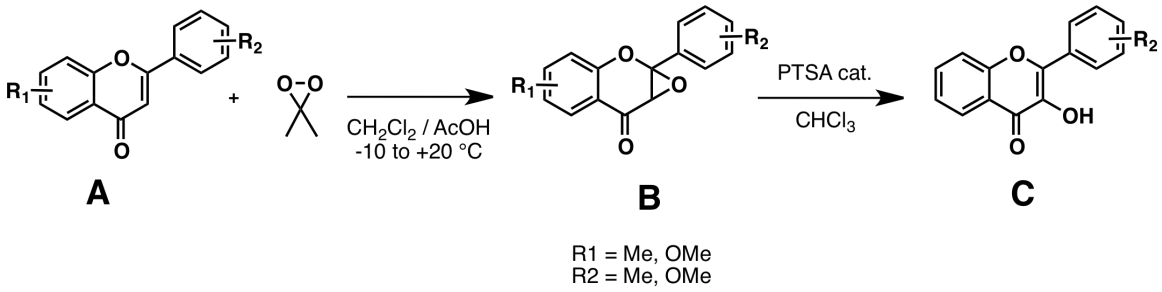

Figure 4.15. Synthesis of flavonol from flavone using DMDO

2.4. Oxone

DMDO is known to be generated from acetone using potassium peroxymonosulfate salt, the active component of the reagent commonly known as Oxone*. Recently, a protocol in biphasic conditions generating DMDO *in situ* has shown to be more efficient than the use of isolated DMDO, with 53% yield. This protocol is presented in Figure 4.16.[31]

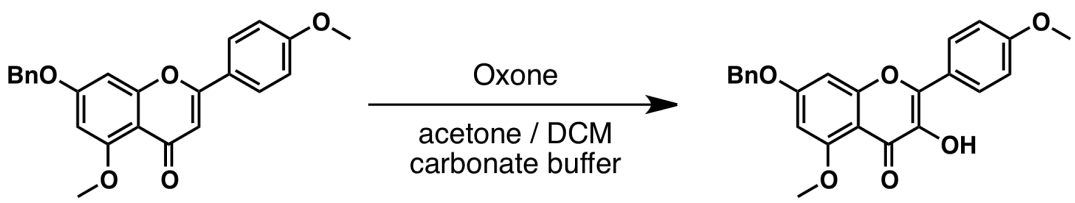

Figure 4.16. Conversion of flavone into flavonol using oxone

* Oxone is in fact a commercial combination of three salts with the formula $2KHSO_5 \cdot KHSO_4 \cdot K_2SO_4$.

C. Synthesis, analytical and biological properties of ferrocenyl flavones

As part of our strategy of synthesizing ferrocenyl flavonoids, we designed ferrocenyl flavone derivatives, whose general pattern is presented in Figure 4.17, in order to investigate their chemical and biological properties.

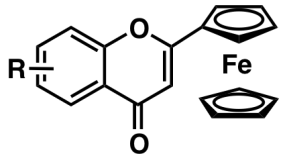

Figure 4.17. General pattern of ferrocenyl flavones

1. Synthesis

1.1. From ynones

The standard protocols described in section A.1. of this chapter were applied on the previously-synthesized ferrocenyl chalcones, without success. Indeed, each of these methods that we tried resulted in either decomposition of the starting material or no reaction. Therefore, with the ferrocenyl ynones (series **4**) in hand, we investigated their base-catalyzed cyclization. As previously seen, such reactions of organic ynones usually give a mixture of flavones and aurones. The proportion of aurones to flavones was reported to increase when using a protic solvent. In our hands, treatment of **4a**, **c** and **h** with NaOEt in EtOH at room temperature gave a single orange product that was identified as having the flavone structure with 65-70% purified yield, as shown in Figure 4.18. Although the reaction is slow, taking 24 h, it is very clean. Ferrocenyl flavones constitute series **5**.

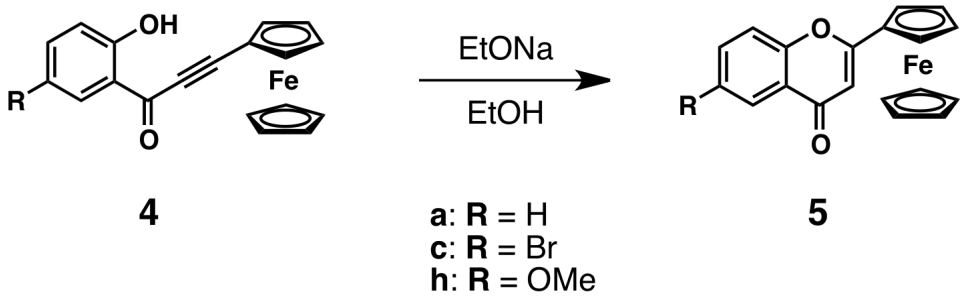

4 **5**

a: **R** = H
c: **R** = Br
h: **R** = OMe

Figure 4.18. Synthesis of ferrocenyl flavones from aurones

In this case, the presence of the ferrocene group completely changes the selectivity of this addition, allowing the addition of the phenolate only in one position. Although this result is remarkable, this synthesis of ferrocenyl flavones is not very practical, involving three steps from the ferrocenyl chalcones. Synthesis of ferrocenyl flavones directly from aurones could save one step, and was therefore studied as well.

1.2. From aurones

As presented in section A.3 of this chapter, organic flavones can readily be obtained from aurones by base-assisted or cyanide-assisted isomerization. Isomerization of **3** to **5** was not observed during the formation of **3** in the presence of NaH or pyridine. However, treatment of isolated **3a** with KOtBu in EtOH slowly yielded the flavone **5a** along with decomposition products. Treatment of aurones **3a-j** with KCN in refluxing EtOH allowed a more effective isomerization to flavones **5a-j**, complete after 2h with yields of 55-80%. These procedures are presented in Figure 4.19.

This procedure being more efficient both in terms of yield and having fewer steps than the use of the ynone intermediate, we synthesized the complete series **5** using cyanide-mediated isomerization of aurones.

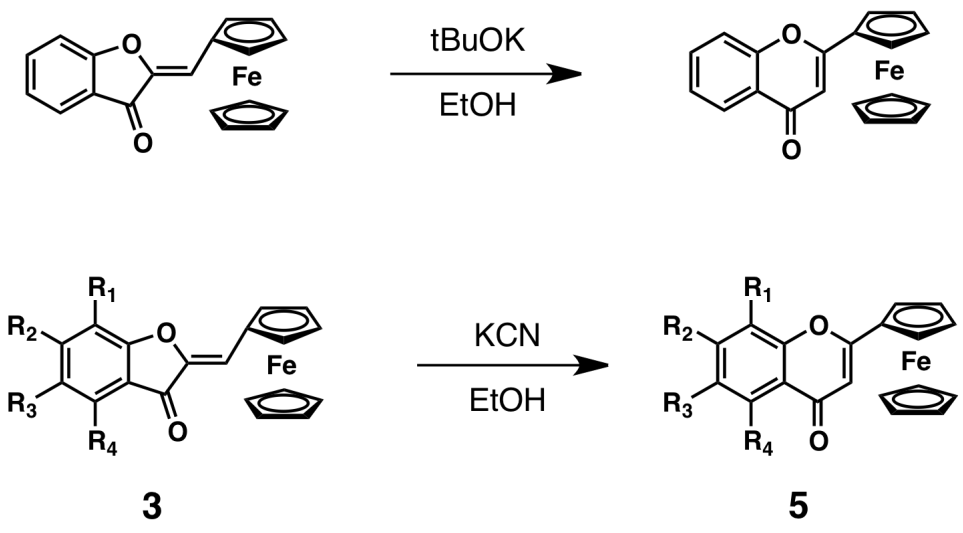

3 **5**

5a: R_1=R_2=R_3=R_4=H (88%)
5b: R_3=Cl (72%)
5c: R_3=Br (75%)
5d: R_1=R_3=Cl (60%)
5e: R_1=R_3=Br (55%)
5f: R_1=R_3=F (60%)
5g: R_2=OMe (70%)
5h: R_3=OMe (78%)
5i: R_4=OMe (68%)
5j: R_2=R_4=OMe (67%)

Figure 4.19. Isomerisation of ferrocenyl aurones in ferrocenyl flavones

2. Characterization

All compounds were unambiguously characterized using routine techniques, that is to say NMR spectroscopy, mass spectrometry, elemental analysis and so on.

2.1. Crystal structure of 5c

A crystal structure by X-ray diffraction was obtained for compound **5c**. This structure and associated data are presented in Figure 4.20 and table 4.1. Whereas the structures of the ferrocenyl aurone and ferrocenyl ynone show a planar arrangement of the Cp ring of the ferrocene with the organic pi system, here the Cp ring is twisted out of plane by 18.71 °.

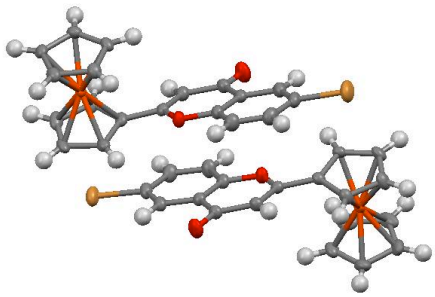

Figure 4.20. Structure of compound **5c** created by Hg software. Cif data has been deposited with the Cambridge database number 823196

Table 4.1. crystal data for molecule **5c**

	5c	Z	8
	$C_{19}H_{13}BrFeO_2$	T	200
M	409.06	No. reflections	36796
Crystal system	monoclinic	No. independent reflections	9784
Space group	P21/c	R_{int}	0.037
a (Å)	7.3599(2)	2θ	61.1°
b (Å)	15.1457(5)	R_1 (all data)	0.0624
c (Å)	27.5266(8)	wR_2 (all data)	0.0655
β (°)	90.2090(10)	R_1 (with cutoff)	0.0388
V ($Å^3$)	3068.39(16)	wR_2 (with cutoff)	0.0556

2.2. UV/visible spectroscopy of 5a-j

Similarly to the other classes of ferrocenyl flavonoids, the spectral properties of ferrocenyl flavones are quite different from those of their organic analogs. Their color, usually orange-red, is more saturated than their organic counterparts, which are pale yellow to colorless. Ferrocenyl flavones also present a supplementary absorption band, whose wavelength is between 450 and 500 nm, induced by the presence of ferrocene. However, compared to

ferrocenyl chalcones and aurones, their color is much less saturated, and the molar extinction coefficients are smaller. This is likely due to the deviation from planarity observed in the X-ray crystal structure.

UV-visible absorption spectra of **5a-j** were recorded, and the molar extinction coefficients (ε) at λ_{max} in the visible region were calculated for each molecule. The results are summarized in Table 4.2. In the case of series **5**, the usual tendency of the transitions to be less energetic with electron-withdrawing substituents is still valid, although less clear than for series **3**. The methoxy substituents seem to have no effect when compared to the unsubstituted molecule, while halogens decrease the energy of the least energetic transition, and the effect is stronger when 2 halogens are grafted to the molecule.

Table 4.2. Values of ε at λ_{max} of each member of the series **5**

Compound	λ_{max} (nm)	ε	Compound	λ_{max} (nm)	ε
5a	362	1330	**5f**	376	2953
	466	622		477	1900
5b	371	3016	**5g**	361	3384
	473	1738		467	1448
5c	369	1804	**5h**	364	3362
	475	935		463	979
5d	367	2947	**5i**	366	3397
	487	1592		463	1397
5e	368	3194	**5j**	366	2891
	492	1754		464	1128

2.3. IR spectroscopy

IR spectra of **5a-j** were recorded and the values of the characteristic peaks are listed in Table 4.3. Similarly to series **3**, the electronic effects of the substituents are not characteristic in the stretching frequencies of the C=C and C=O bonds. However, comparisons between series

3 and series **5** are interesting and illustrative, particularly because characteristic absorption frequencies in the IR allow the differentiation between the aurone and flavone isomers. Contributions of mesomeric canonical structures in the flavone result in C=O and C=C bond orders of less than two. Therefore, in the flavone geometry, the C=O and C=C stretching frequencies are expected at lower energy than those found in the aurones, which is exactly what is observed.

Table 4.3. IR characteristic values (in cm^{-1}) for **5a-j**

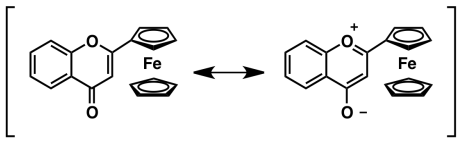

	C=O	C=C
5a	1631	1605
5b	1639	1608
5c	1643	1612
5d	1646	1612
5e	1643	1612
5f	1639	n.d.
5g	1631	1604
5h	1627	1612
5i	1635	1608
5j	1643	1608

2.4. Electrochemistry

The oxidation chemistry of **5a-j** was analyzed by cyclic voltammetry. The results are presented in Table 4.4. Like for ferrocenyl chalcones, electron-withdrawing groups increase the oxidation potential of the ferrocene moiety, while electron-donating groups decrease it. The only exceptions to this rule are the case of **5e**, where $R_1 = R_3 =$ Br: the second bromine

atom does not seem to have any effect when compared to the mono-bromo derivative **5c**, and the case of **5h**, where R_3 = OMe, for which the substituent seems to have a weak reverse effect: the potential is increased when compared to the unsubstituted derivative **5a**. However, this effect is very weak, **5a** and **5h** have nearly the same oxidation potential

Table 4.4. Shift of the ferrocene oxidation potential for compounds **5a-j**

Compound	$E_{1/2}$ (Fc+/Fc)
5a	0.240
5b	0.251
5c	0.257
5d	0.275
5e	0.260
5f	0.277
5g	0.222
5h	0.247
5i	0.228
5j	0.211

As for ferrocenyl chalcones and aurones, we plotted the wavenumber corresponding to the visible electronic transition as a function of the ferrocene moiety potential for each molecule. The graph is presented in Figure 4.21. In case of series **5**, the correlation is very approximate, but shows a tendency for the visible transition to increase in energy with electron-donating groups, due to a predominant destabilization of the π* acceptor orbital.

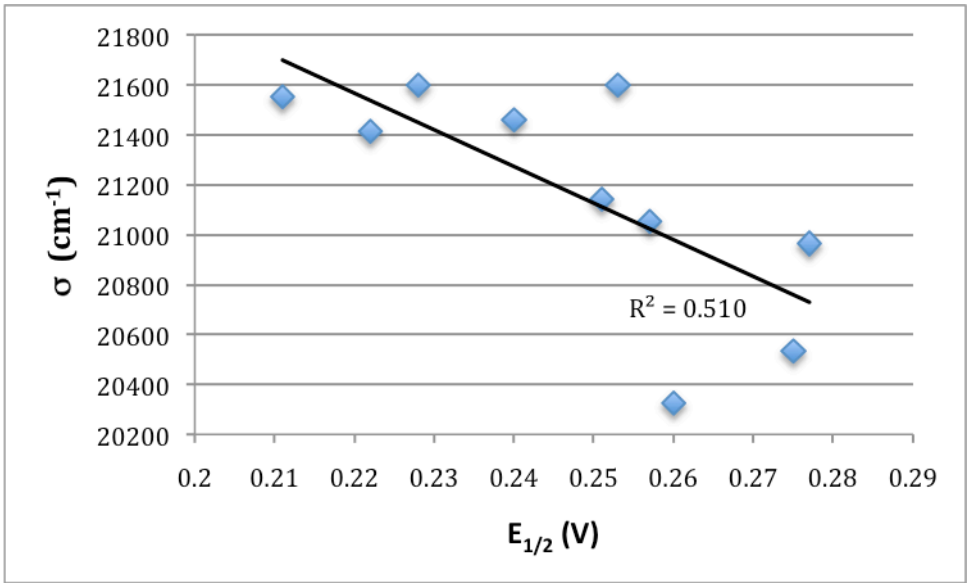

Figure 4.21. Plot of the wavenumber in function of the ferrocene moiety oxidation potential for each compound of series **5**

2.5. Structural comparisons between flavones and aurones

The bulk solids of representative aurones and flavones were structurally characterized by 2D HMQC and HMBC, as presented in Figure 4.22 To facilitate the discussion, the numbering of the atoms of **3c** and **5c** is also presented in Figure 4.22. For **3c**, the HMBC experiment showed vinylic proton (H_{10}) correlations with the ketone carbon (C_3) and C_α of C_5H_4, indicating an aurone structure. For **5c**, we observed correlations involving the vinylic H_3 with C_5H_4-C_{ipso} and aromatic C_{10} and weaker correlations with the aromatic C_5, consistent with a flavone structure.

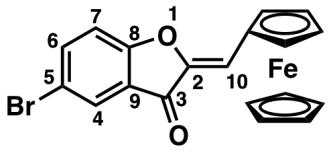
7
8
1
O
6
5
Br
4
9
2
10
Fe
3
O

3c

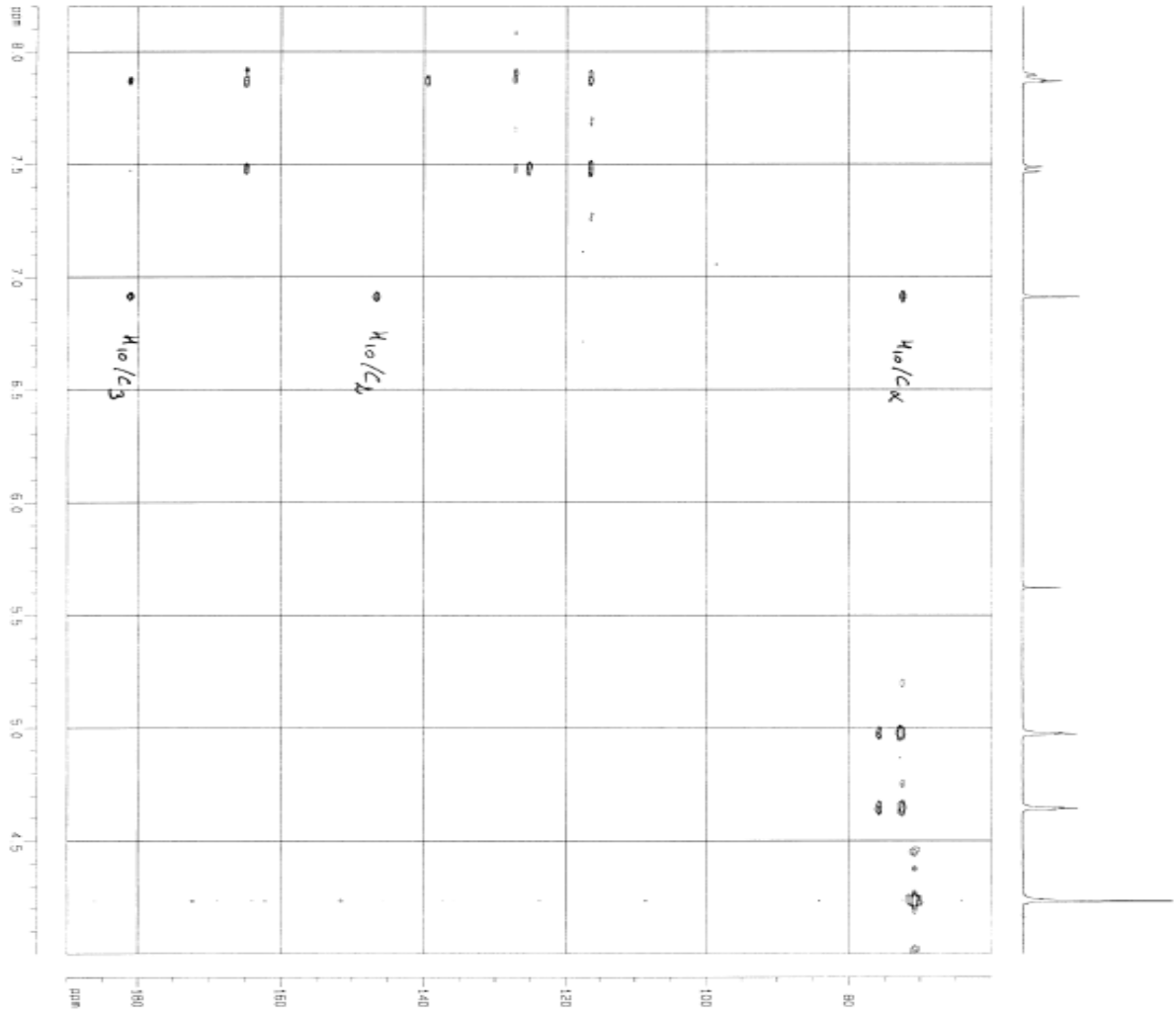
H10/C3
H10/C9
H10/C1'
ppm
180
160
140
120
100
80

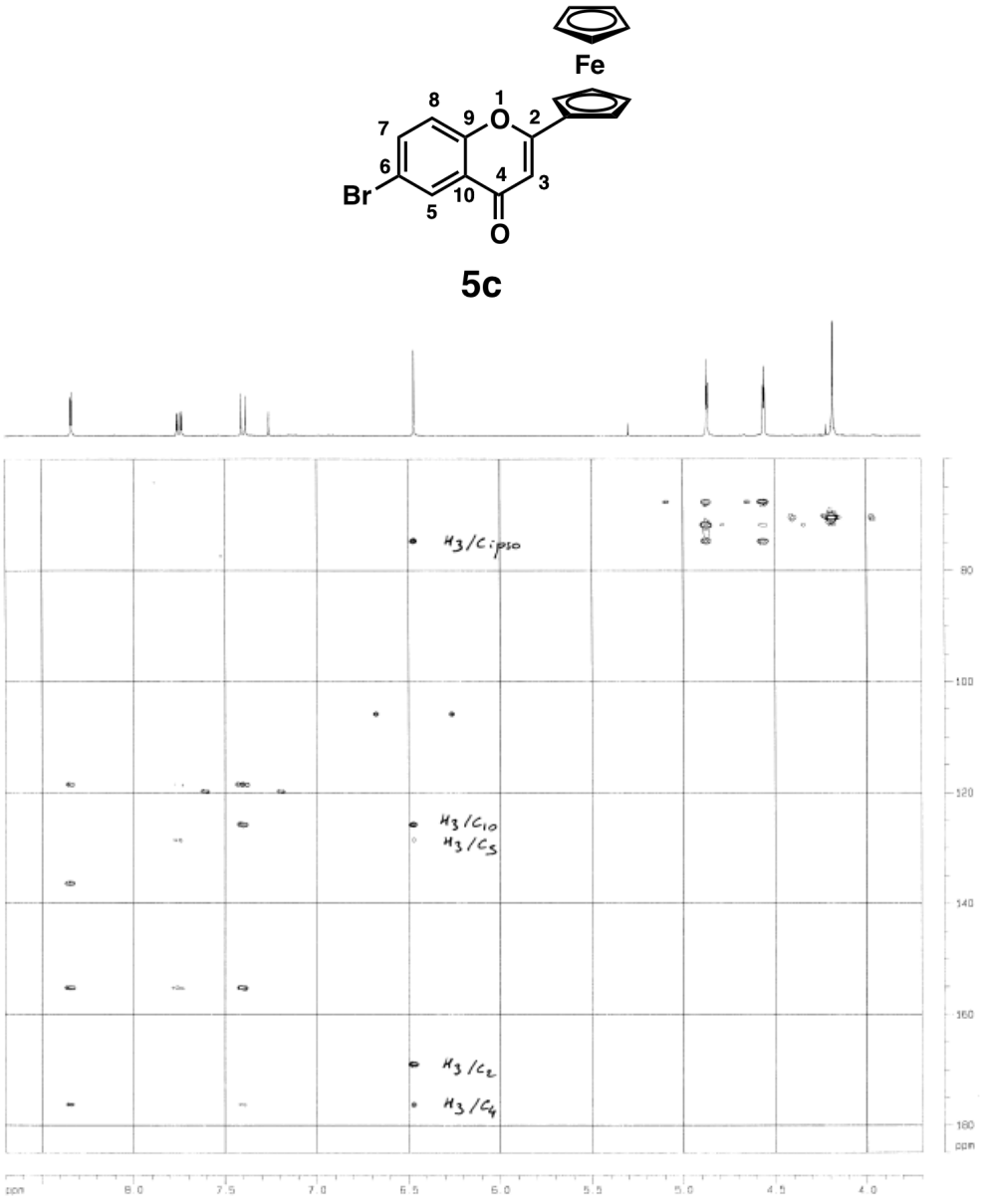

Figure 4.22. 2D HMBC spectra for **3c** and **5c** and numbering of the atoms of **3c** and **5c**.

The 2D NMR experiments furthermore allowed us to fully attribute the ^{1}H and ^{13}C spectra of **3a**, **c** and **h** and **5a**, **c** and **h**. Characteristic peaks, presented in Table 4.5, are the vinyl proton and carbon as well as the tertiary carbon adjacent to the oxo group. In the aurone, the vinyl proton and carbon are in the 4-position of the ketone, and thus are deshielded compared to the flavone structure, where these atoms are in the 3-position of the ketone. Similarly, the quaternary carbon is in the shielded 3-position in the aurone and the deshielded 4-position in the flavone. While substitution on the phenyl ring of the benzofurone or benzopyrone

groups only slightly influence the chemical shifts of characteristic peaks, a given structural isomer can be easily identified by the large difference chemical shifts.

Table 4.5. Selected ^{1}H and ^{13}C NMR for **3a**, **c**, **h** and **5a**, **c**, **h**

	δ (H_{vinyl})/ppm	δ (CH_{vinyl})/ppm	δ (C_q)/ppm
3a	6.90 (H_{10})	116.6 (C_{10})	146.1 (C_2)
3c	6.91 (H_{10})	117.6 (C_{10})	146.5 (C_2)
3h	6.88 (H_{10})	116.4 (C_{10})	146.6 (C_2)
5a	6.45 (H_3)	105.7 (C_3)	168.3 (C_2)
5c	6.47 (H_3)	105.8 (C_3)	168.8 (C_2)
5h	6.43 (H_3)	105.1 (C_3)	167.9 (C_2)

3. Biological properties

3.1. Antiproliferative effects on B16 melanoma cells

Similarly to series **1**, **2** and **3**, the antiproliferative effects of compounds **5a-j** were evaluated by the MTT test on murine B-16 melanoma cells in collaboration with Guy G. Chabot. The results are presented in Figure 4.23, together with the corresponding organic flavone, series **6**. From the figure, we can easily see that although more active than their organic analogues, ferrocenyl flavones have generally low antiproliferative effects, with IC_{50} values superior to 35 μM. The least active compound is the dibromo-substituted **5e**, with an IC_{50} value of 91 μM.

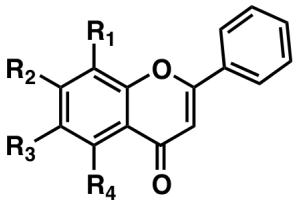

6a: R_1=R_2=R_3=R_4=H
6b: R_3=Cl
6c: R_3=Br
6d: R_1=R_3=Cl
6e: R_1=R_3=Br
6f: R_1=R_3=F,
6g: R_2=OMe
6h: R_3=OMe
6i: R_4=OMe
6j: R_2=R_4=OMe

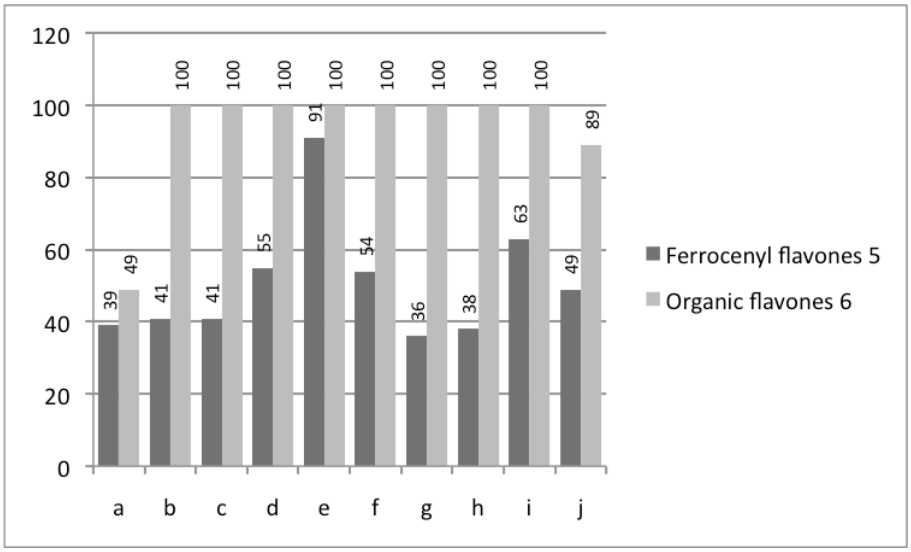

Figure 4.23. Structure of series 6 and IC_{50} values (μM) of compounds **5a-j** and **6a-j** on B16 murine melanoma cells

3.2. Antiangiogenic effects EA·hy 926 endothelial cells

Antiangiogenic properties were also measured for series **5** and **6**. The minimal rounding up concentrations against EA·hy 926 endothelial cells are presented in Figure 4.24.

From this figure, we can see that both series **5** and **6** present excellent activity, with minimal concentration values of 1 μM, rendering them good candidates as antiangiogenic agents. We can also observe that although possessing the same substitution pattern, no parallel can be made between the members of series **5** and **6**.

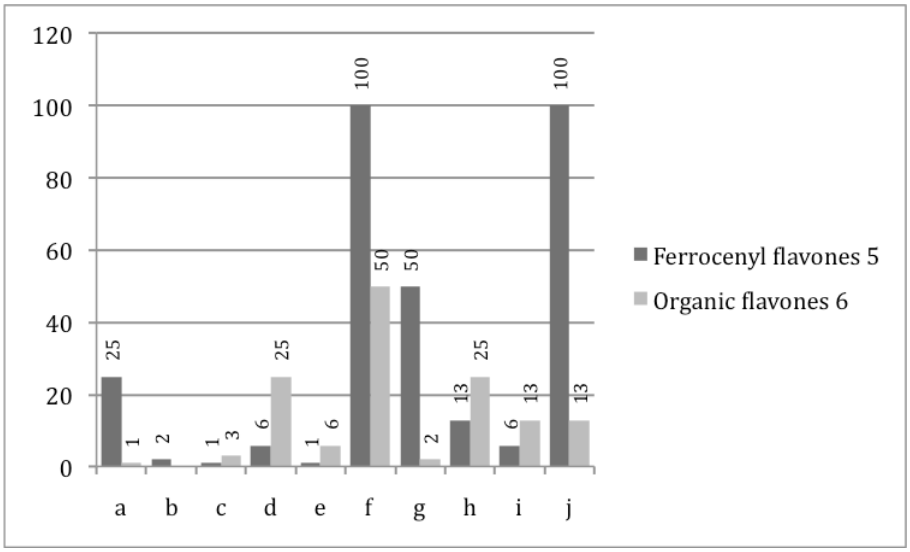

Figure 4.24. Minimal concentration (μM) of **5a-j** and **6a-j** for rounding up of EA·hy 926 cells

The ferrocenyl flavone **5e** is of particular interest, with a minimal concentration for rounding up of EA·hy 926 cells of 1 μM, and an IC_{50} value of 91 μM on B16 murine melanoma cells, as a pure antivascular agent.

3.3. Antibacterial properties

Similarly to series **1** and **3**, compounds of series **5** have been evaluated as anti-bacterial agents, in collaboration with Claude Jolivalt from Chimie ParisTech. The results of the test at 100 mg/mL are presented in Table 4.6.

From this table, it is clear that the series **5** is less active than series **3**, although generally more active than series **1**. The methoxy-substituted derivatives seem once again to be more potent than the halogen-substituted derivatives.

Table 4.6. Screening of series **5** at 100 µg/mL

	E. coli ATCC25922	*S. aureus* ATCC25923	*S. aureus* 1199B	*S. aureus* MsrA
5a	-	-	-	-
5b	-	-	-	-
5c	-	-	-	++
5d	-	-	-	-
5e	-	-	-	-
5f	-	-	-	-
5g	-	++	++	++
5h	-	-	-	n.d.
5i	-	++	++	++
5j	-	++	++	++

A second screening was performed for **5a-j**, at a concentration of 20mg/mL. The results are presented in Table 4.7. At this concentration, all activity has disappeared. Thus we can conclude that series **5** is not very interesting for its antibacterial properties.

Table 4.7. Screening of series **5** at 20 µg/mL

	E. coli ATCC25922	*S. aureus* ATCC25923	*S. aureus* 1199B	*S. aureus* MsrA
5a	-	-	-	-
5b	-	-	-	-
5c	-	-	-	-
5d	-	-	-	-
5e	-	-	-	-
5f	-	-	-	-
5g	-	-	-	+
5h	-	-	-	-
5i	-	-	-	-
5j	-	-	-	-

D. Synthesis and analytical properties of ferrocenyl flavonols

1. Synthesis

For the synthesis of ferrocenyl flavonols, the AFO reaction was attempted from the chalcones, but without success; treatment of ferrocenyl chalcones with hydrogen peroxide only resulted in decomposition products. The result was the same in case of ferrocenyl flavones as starting materials. Other procedures such as the reaction of ferrocenyl flavones with PIDA or DMDO only decomposed the starting material as well. We subsequently tried the less often used Oxone protocol described in section B.2.4 of this chapter, that is in a carbonate buffer-acetone/DMC biphasic solvent system.

This protocol was a success for several substitutions, and the synthesis of the first examples of ferrocenyl flavonols, series **7**, is presented in Figure 4.25.

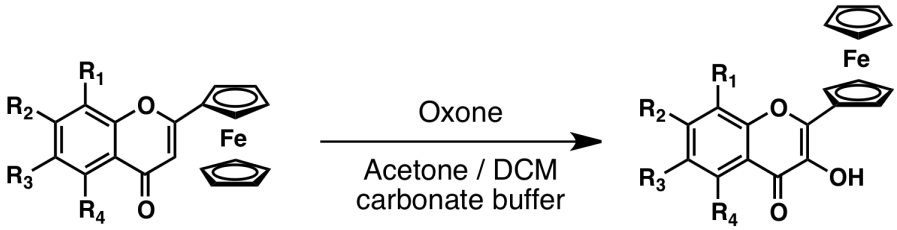

7a: R_1=R_2=R_3=R_4=H (80%)
7c: R_3=Br (76%)
7g: R_2=OMe (78%)

Figure 4.25. Synthesis of ferrocenyl flavonols using oxone

2. Characterization

2.1. UV/visible spectroscopy of 7a, c and g

UV/visible spectra of the three ferrocenyl flavonols were recorded, and the characteristic peaks are presented in Table 4.6.

Table 4.6. Values of ε at λ_{max} of three members of the series **7**

Compound	λ_{max} (nm)	ε
7a	348	12410
	483	2150
7c	352	14190
	494	3190
7g	342	10598
	461	2021

2.2. IR spectroscopy

IR spectra of the three ferrocenyl flavonols were also recorded, and the characteristic stretching bands are presented in Table 4.7. From the results, we can observe that the C=O stretching is stronger than in the case of flavone, and resembles that observed in the aurone series This effect can be attributed to the hydroxy group in position 3, which depolarizes the C=O bond by its electron withdrawing effects. The characteristics of the C=C bond however, remains unchanged when compared with flavones.

Table 4.7. IR characteristic values (in cm^{-1}) for **7a-j**

	OH	C=O	C=C
7a	3247	1731	1608
7c	3309	1739	1604
7g	3251	1716	1608

3. Biological properties

Compounds **7a**, **7c** and **7g** have so far only been evaluated on B16 and EA·hy 926 cells. These three compounds seem completely inoffensive to both cell lines. Their IC_{50} values for B16 cells are greater than 100 µM, and their minimum concentration for rounding-up of EA·hy 926 cells is also superior to 100 µM.

Compounds **7a**, **7c** and **7g** do not seem suitable for anti-angiogenic applications. They are currently being tested against other biological targets, such as bacteria.

E. Experimental

Synthesis and characterization of ferrocenyl flavones 5a-j.

From ynone: Ferrocene ynone **4** (40 mg) was dissolved in EtOH. NaOEt (excess) was added and the solution was stirred at rt for 24 h, changing from red to orange. The reaction mixture was poured into H_2O and HCl 12 M, extracted with CH_2Cl_2 and washed with water. The organic phase was dried over $MgSO_4$, filtered and evaporated. The product was purified using a silica gel column, using petroleum ether/dichloromethane 1/1 as an eluent and was isolated as an orange solid. Yields after purification: 68% (**5a**), 65% (**5b**) and 63% (**5c**).

From aurone: Alternatively, ferrocenyl aurone **3** (30 mg) and potassium cyanide (1.5 equiv.) were dissolved in ethanol (25 mL), and stirred at reflux for 2 h; the solution went from deep violet to deep red. The solution was then allowed to return to rt before being poured into an aqueous solution of NaOH 1M (100 mL). The mixture was extracted with EtOAc (3x50 mL), and washed with water. The organic phase was dried over $MgSO_4$, filtered and evaporated, and the crude product was purified using a silica gel column, using petroleum ether/ethyl acetate 60:40 as an eluent and was isolated as an orange solid.

2-ferrocenyl-chromen-4-one, 5a. Orange solid, mp 110°C. δ_H (400 MHz; $CDCl_3$) 4.18 (s, 5H, C_5H_5), 4.54 (t, ^3J = 1.8 Hz, 2H, C_5H_4), 4.88 (t, ^3J = 1.8 Hz, 2H, C_5H_4), 6.48 (s, 1H, H_3), 7.39 (td, ^3J = 7.9 Hz, ^4J = 1.1 Hz, 1H, H_6), 7.51 (dd, ^3J = 7.2 Hz, ^4J = 1.1 Hz, 1H, H_8), 7.63-7.69 (m, 1H, H_7), 8.21 (dd, ^3J = 7.9 Hz, ^4J = 1.6 Hz, 1H, H_5). δ_C (100 MHz; $CDCl_3$) 67.6 (C_5H_4), 70.3 (C_5H_5), 71.5 (C_5H_4), 75.1 (C_5H_4-C_{ipso}), 105.9 (C_3), 117.8 (C_8), 124.3 (C_{10}), 125.1(C_6), 125.8 (C_5), 133.4 (C_7), 156.3 (C_9), 168.3 (C_2), 177.6 (C_4), HRMS (ESI) calcd. for $C_{19}H_{14}FeO_2Na^+$: 353.02409, found: 353.02354.

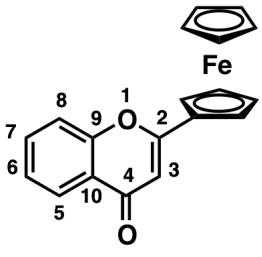

6-chloro-2-ferrocenyl-chromen-4-one, 5b. Orange solid, mp 202°C. δ_H (300 MHz; $CDCl_3$) 4.17 (s, 5H, C_5H_5), 4.54 (s, 2H, C_5H_4), 4.85 (s, 2H, C_5H_4), 6.45 (s, 1H, Vinyl), 7.45 (d, *J* = 8.5 Hz, 1H, Aromatic), 7.59 (d, *J* = 8.5 Hz, 1H, Aromatic), 8.16 (s, 1H, Aromatic). δ_C (75 MHz; $CDCl_3$) 67.5 (C_5H_4), 70.3 (C_5H_5), 71.6 (C_5H_4), 74.5 (C_5H_4 ipso), 105.6 (Vinyl), 111.6 (Aromatic), 119.4 (Aromatic), 125.1 (Aromatic), 130.9 (Aromatic), 133.4 (Aromatic), 154.5 (Aromatic), 168.7 (vinyl), 176.2 (C=O). HRMS (ESI) calcd. for $C_{19}H_{14}ClFeO_2^+$: 365.0032, found: 365.0027.

6-bromo-2-ferrocenyl-chromen-4-one, 5c. Orange solid, mp 177°C. δ_H (400 MHz; $CDCl_3$) 4.18 (s, 5H, C_5H_5), 4.56 (t, ^3J = 1.9 Hz, 2H, C_5H_4), 4.87 (t, ^3J = 1.9 Hz, 2H, C_5H_4), 6.47 (s, 1H, H_3), 7.40 (d, ^3J = 8.8 Hz, 1H, H_8), 7.75 (dd, ^3J = 8.8 Hz, ^4J = 2.4 Hz, 1H, H_7), 8.34 (d, ^4J = 2.4 Hz, 1H, H_5). δ_C (100 MHz; $CDCl_3$), 67.6 (C_5H_4), 70.4 (C_5H_5), 71.8 (C_5H_4), 74.6 (C_5H_4-C_{ipso}), 105.8 (C_3), 118.5 (C_6), 119.8 (C_8), 125.7 (C_{10}), 128.5 (C_5), 136.3 (C_7), 155.1 (C_9), 168.8 (C_2), 176.0 (C_4), HRMS (ESI) calcd. for $C_{19}H_{13}BrFeO_2^+$: 430.93460 and 432.93256 found : 430.93406 and 432.93201.

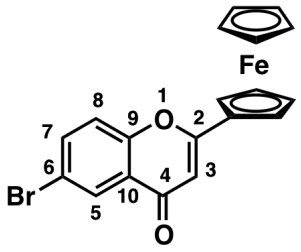

6,8-dichloro-2-ferrocenyl-chromen-4-one, 5d. Orange solid, mp 193°C. δ_H (300 MHz; $CDCl_3$) 4.18 (s, 5H, C_5H_5), 4.58 (t, *J* = 1.9 Hz, 2H, C_5H_4), 4.88 (t, *J* = 1.9 Hz, 2H, C_5H_4), 6.44 (s, 1H, Vinyl), 7.71 (d, *J* = 1.8 Hz, 1H, Aromatic), 8.07 (d, *J* = 1.8, 1H, Aromatic). δ_C (75 MHz; $CDCl_3$) 67.7 (C_5H_4), 70.4 (C_5H_5), 71.9 (C_5H_4), 74.1 (C_5H_4 ipso), 105.3 (Vinyl), 123.5 (Aromatic), 123.9 (Aromatic), 125.9 (Aromatic), 130.5 (Aromatic), 133.3 (Aromatic), 150.4 (Aromatic), 168.9 (Vinyl), 175.4 (C=O), HRMS (ESI) calcd. for $C_{19}H_{13}Cl_2FeO_2^+$: 398.9642, found: 398.9642. (CI NH_3) m/z 408.9-410.9 (MH^+).

6,8-dibromo-2-ferrocenyl-chromen-4-one, 5e. Orange solid, mp 194°C. δ_H (300 MHz; $CDCl_3$) 4.22 (s, 5H, C_5H_5), 4.59 (t, *J* = 1.9 Hz, 2H, C_5H_4), 4.93 (t, *J* = 1.9 Hz, 2H, C_5H_4), 6.44 (s, 1H, Vinyl), 8.01 (d, *J* = 2.4 Hz, 1H, Aromatic), 8.27 (d, *J* = 2.4 Hz, 1H, Aromatic). δ_C (75 MHz;

$CDCl_3$), 67.8 (C_5H_4), 70.4 (C_5H_5), 71.8 (C_5H_4), 74.1 (C_5H_4 ipso), 105.2 (Vinyl), 112.5 (Aromatic), 118.1 (Aromatic), 127.8 (Aromatic), 136.6 (Aromatic), 138.8 (Aromatic), 151.7 (Aromatic), 169.0 (Vinyl), 175.3 (C=O), HRMS (ESI) calcd. for $C_{19}H_{13}{}^{79}Br_2FeO_2^+$: 486.8632, found: 486.8629.

6,8-difluoro-2-ferrocenyl-chromen-4-one, 5f. Orange solid, mp 155°C. δ_H (400 MHz; $CDCl_3$) 4.15 (s, 5H, C_5H_5), 4.52 (s, 2H, C_5H_4), 4.85 (s, 2H, C_5H_4), 6.40 (s, 1H, Vinyl), 7.16 (dd, *J* = 8.8 Hz, *J* = 2.4 Hz, 1H, Aromatic), 7.59 (d, *J* = 8.8 Hz, 1H, Aromatic), δ_C (100 MHz; $CDCl_3$), 67.7 (C_5H_4), 70.5 (C_5H_5), 71.9 (C_5H_4), 74.2 (C_5H_4 ipso), 105.4 (Vinyl), 106.0 (dd, ^2J = 23.7 Hz ^4J = 4.0 Hz Aromatic), 108.7 (dd, ^3J = 20.1 Hz, ^3J = 28,5 Hz, Aromatic), 126.8 (bs, Aromatic), 141,9 (d, ^2J = 9.4 Hz, Aromatic), 151.3 (dd, ^1J = 256 Hz, ^3J = 11.6 Hz, Aromatic), 158.3 (dd, ^1J = 249 Hz, ^3J = 9.7 Hz, Aromatic), 168.7 (Vinyl), 175.5 (C=O), HRMS (ESI) calcd. for $C_{19}H_{13}F_2FeO_2^+$: 367.0233, found: 367.0244.

7-methoxy-2-ferrocenyl-chromen-4-one, 5g. Orange solid, mp 174°C. δ_H (300 MHz; $CDCl_3$) 3.93 (s, 3H, OMe) 4.17 (s, 5H, C_5H_5), 4.50 (t, *J* = 1.8 Hz, 2H, C_5H_4), 4.83 (t, *J* = 1.8 Hz, 2H, C_5H_4), 6.40 (s, 1H, Vinyl), 6.89 (d, *J* = 2.3 Hz, 1H, Aromatic), 6.95 (dd, *J* = 2.3 Hz, *J* = 8.9 Hz, 1H, Aromatic), 8.10 (d, *J* = 8.9 Hz, 1H, Aromatic). δ_C (75 MHz; $CDCl_3$) 55.6 (OMe), 67.1 (C_5H_4), 70.0 (C_5H_5), 71.0 (C_5H_4), 75.1 (C_5H_4 ipso), 100.1 (Aromatic), 105.4 (Vinyl), 113.7 (Aromatic), 117.7 (Aromatic), 126.7 (Aromatic), 157.7 (Aromatic), 163.6 (Aromatic), 167.4 (Vinyl), 176.8 (C=O), HRMS (ESI) calcd. for $C_{20}H_{17}FeO_3^+$: 361.0520, found: 361.0527.

6-methoxy-2-ferrocenyl-chromen-4-one, 5h. Orange solid, mp 140°C. δ_H (300 MHz; $CDCl_3$) 3.91 (s, 3H, OMe), 4.17 (s, 5H, C_5H_5), 4.52 (t, ^3J = 1.7 Hz, 2H, C_5H_4), 4.87 (t, ^3J = 1.7 Hz, 2H, C_5H_4), 6.47 (s, 1H, H_3), 7.26 (dd, ^3J = 9.1 Hz, ^4J = 3.0 Hz, 1H, H_7), 7.44 (d, ^3J = 9.1 Hz, 1H, H_8), 7.59 (d, ^4J = 3.0 Hz, 1H, H_5). δ_C (75 MHz; $CDCl_3$), 55.9 (OMe), 67.4 (C_5H_4), 70.2 (C_5H_5), 71.3 (C_5H_4), 75.0 (C_5H_4-C_{ipso}), 104.9 (C_5), 105.1 (C_3), 119.1 (C_8), 123.1 (C_7), 124.7 (C_{10}), 151.0 (C_9), 156.8 (C_6), 167.9 (C_2), 177.3 (C_4), HRMS (ESI) calcd. for $C_{20}H_{16}FeO_3Na^+$: 383.03466, found: 383.03411.

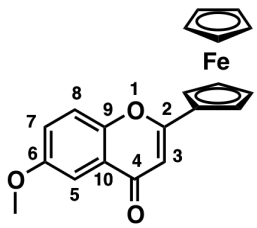

5-methoxy-2-ferrocenyl-chromen-4-one, 5i. Orange solid, mp 165°C. δ_H (300 MHz; $CDCl_3$) 3.99 (s, 3H, OMe), 4.16 (s, 5H, C_5H_5), 4.49 (t, *J* = 1.8 Hz, 2H, C_5H_4), 4.82 (t, *J* = 1.8 Hz, 2H, C_5H_4), 6.38 (s, 1H, Vinyl), 6.80 (d, *J* = 8.2 Hz, 1H, Aromatic), 7.06 (d, *J* = 8.4 Hz, 1H, Aromatic), 7.54 (t, *J* = 8.4 Hz, 1H, Aromatic). δ_C (75 MHz; $CDCl_3$) 55.3 (OMe), 67.0 (C_5H_4), 69.9 (C_5H_5), 70.9 (C_5H_4), 74.8 (C_5H_4 ipso), 106.1 (Aromatic), 107.7 (Aromatic), 109.7 (Aromatic), 114.4 (Vinyl), 133.0 (Aromatic), 158.1 (Aromatic), 159.5 (Aromatic), 165.4 (Vinyl), 177.4 (C=O), HRMS (ESI) calcd. for $C_{20}H_{17}FeO_3^+$: 361.0527, found: 361.0527.

5,7-dimethoxy-2-ferrocenyl-chromen-4-one, 5j. Orange solid, mp 179°C. δ_H (300 MHz; $CDCl_3$) 3.90 (s, 3H, OMe), 3.93 (s, 3H, OMe), 4.14 (s, 5H, C_5H_5), 4.45 (t, *J* = 1.8 Hz, 2H, C_5H_4), 4.77 (t, *J* = 1.8 Hz, 2H, C_5H_4), 6.30 (s, 1H, Vinyl), 6.34 (d, *J* = 2.3 Hz, 1H, Aromatic), 6.48 (d, *J* = 2.3 Hz, 1H, Aromatic). δ_C (75 MHz; $CDCl_3$) 55.4 (OMe), 56.1 (OMe), 66.8 (C_5H_4), 69.8 (C_5H_5), 70.6 (C_5H_4), 74.6 (C_5H_4-ipso), 92.4 (Aromatic), 95.6 (Aromatic), 106.9 (Aromatic), 109.0 (Vinyl), 159.5 (Aromatic), 160.5 (Aromatic), 163.4 (Aromatic), 164.5 (Vinyl), 176.6 (C=O). HRMS (ESI) calcd. for $C_{21}H_{19}FeO_4^+$: 391.0622, found: 391.0633.

Synthesis and characterization of ferrocenyl flavanols 7a-7b. Carbonate buffer (15 mL) was added to a solution of ferrocenyl flavone **5** (40 mg) in DCM/acetone (2:1, 10 mL) and stirred vigrorously at rt. A 5 mL aqueous solution of oxone (0.6 g) was added in four portions every 10 min. and the pH of the solution was checked to ensure that it remained alkaline (pH 9). The consumption of starting material was followed by TLC. After the reaction was complete, the two phases were separated and the aqueous phase was extracted with DCM (3x50 mL). The combined organic layer was washed with sodium thiosulfate solution, dried with $MgSO_4$, filtered and evaporated; The crude product was purified using a silica gel column with petroleum ether/ethyl acetate 80:20 as eluent.

3-hydroxy-2-ferrocenyl-chromen-4-one, 7a. Orange solid, mp 160°C. δ_H (400 MHz; $CDCl_3$) 4.17 (s, 5H, C_5H_5), 4.54 (t, ^3J = 1.8 Hz, 2H, C_5H_4), 5.19 (t, ^3J = 1.8 Hz, 2H, C_5H_4), 7.40 (td, ^3J = 8.0 Hz, ^4J = 1.1 Hz, 1H, H_6), 7.54 (d, ^3J = 7.2 Hz, 1H, H_8), 7.65-7.70 (m, 1H, H_7), 8.24 (dd, ^3J = 7.9 Hz, ^4J = 1.6 Hz, 1H, H_5). δ_C (100 MHz; $CDCl_3$), 68.7 (C_5H_4), 70.0 (C_5H_5), 71.0 (C_5H_4), 74.2 (C_5H_4-

C_{ipso}), 118.1 (C_8), 121.3 (C_{10}), 124.5 (C_5 or C_6), 125.4 (C_5 or C_6), 132.9 (C_7), 136.9 (C_3), 150.5 (C_2), 155.4 (C_9), 171.5 (C_4), HRMS (ESI) calcd. for $C_{19}H_{14}FeO_3^+$: 346.0292, found: 346.0286.

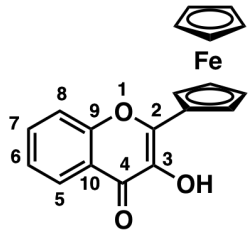

6-bromo-3-hydroxy-2-ferrocenyl-chromen-4-one 7c. Orange solid, mp 178°C. δ_H (400 MHz; $CDCl_3$) 4.16 (s, 5H, C_5H_5), 4.55 (t, ^3J = 1.8 Hz, 2H, C_5H_4), 5.17 (t, ^3J = 1.8 Hz, 2H, C_5H_4), 7.43 (d, ^3J = 8.8 Hz, 1H, H_8), 7.74 (dd, ^3J = 8.8 Hz, ^4J = 2.3 Hz, 1H, H_7), 8.36 (d, ^4J = 2.3 Hz, 1H, H_5). δ_C (100 MHz; $CDCl_3$), 68.8 (C_5H_4), 70.1 (C_5H_5), 71.2 (C_5H_4), 73.7 (C_5H_4-C_{ipso}), 117.8 (C_6), 120.0 (C_8), 122.7 (C_{10}), 127.9 (C_5), 135.8 (C_7), 137.0 (C_3), 151.2 (C_2), 154.1 (C_9), 170.2 (C_4), (HRMS (ESI) calcd. for $C_{19}H_{13}BrFeO_3^+$: 423.9397 and 425.9377, found: 423.9392 and 425.9371.

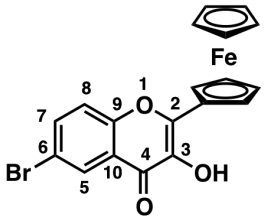

7-methoxy-3-hydroxy-2-ferrocenyl-chromen-4-one 7g. Orange solid, δ_H (400 MHz; $CDCl_3$) 3.90 (s, 3H, OMe), 4.11 (s, 5H, C_5H_5), 4.46 (t, ^3J = 1.9 Hz, 2H, C_5H_4), 5.10 (t, ^3J = 1.9 Hz, 2H, C_5H_4), 6.85 (d, ^4J = 2.3 Hz, 1H, H_8), 6.95 (dd, ^3J = 8.9 Hz, 1H, H_6), 8.08 (d, ^3J = 8.9 Hz, 1H, H_5). δ_C (100 MHz; $CDCl_3$), 55,9 (OMe) 68.4 (C_5H_4), 70.0 (C_5H_5), 70.7 (C_5H_4), 74.5 (C_5H_4-C_{ipso}), 100.0 (C_8), 114.5 (C_6), 115.2 (C_{10}), 126.7 (C_5), 136.5 (C_3), 149,4 (C_2), 157.3 (C_9), 163.8 (C_7), 171.2 (C_4), (HRMS (ESI) calcd. for $C_{20}H_{16}FeO_4^+$: 376.03980, found: 376.03939.

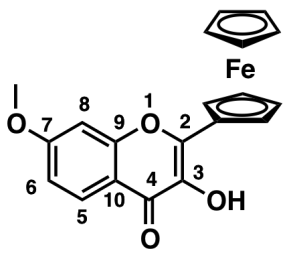

Cytotoxicity. Murine B16 melanoma was grown in Dulbecco's modified essential medium (DMEM) containing 2 mM l-glutamine, 10% fetal bovine serum, 100 U/mL penicillin, and 100 μg/mL streptomycin 37°C, 5% CO_2). Exponentially growing cancer cells were plated onto 96-well plates at 5,000 cells per well in 200 μL DMEM; and 24 h later, the cells were exposed for 48 h to the solvent alone or to the test compound at the indicated concentrations. Viability was assessed using the MTT (1-(4,5-dimethylthiazol-2-yl)-3,5-diphenyltetrazolium) test, and absorbance was read at 562 nm in a microplate reader (BioKinetics Reader, EL340, Fisher Bioblock Scientific, Illkirch, France). Control cells were exposed to 1% DMSO. Experiments were run in triplicate and repeated 3 times. Results are presented as the inhibitory concentrations for 50% (IC_{50}) of cells for a 48 h exposure time.

Morphologic Effects on EA·hy 926 Endothelial Cells. To assess the effect of **3a**-**j** on the morphology of endothelial cells EA·hy 926 endothelial cells were used. Cells were grown in DMEM containing 2 mM l-glutamine, 10% fetal bovine serum, 100 U/mL penicillin, and 100 μg/mL streptomycin (37°C, 5% CO_2). Exponentially growing cells were plated onto 96-well plates at 5,000 cells/200 μL/well. Twenty-four h after plating, the medium was aspirated, and 100 μL of medium containing the test compound was added to the well (triplicate) at the indicated final concentrations (37°C, 5% CO_2), and 2 h later digital photographs were recorded of representative center areas of each well at a magnification of ×320. Results are presented as the efficacious concentration for the change in cell shape for 50% of cells for a 2 h exposure time (EC_{50}) relative to controls.

Antibacterial activity

The inhibitory potential of the flavonoid derivatives was tested on four bacteria strains:

- *E. coli* ATCC 25922 (Gram negative strain)
- *Staphylococcus aureus* (ATCC 25923, sensitive Gram positive strain),

- *Staphylococcus aureus* 1199B: resistant to fluoroquinolones due notably to the overexpression of the NorA efflux pump (G. W. Kaatz, S. M. Seo, *Antimicrob. Agents Chemother*. 1995, *39*, 2650-2655)
- *Staphylococcus aureus* RN4220/pUL5054: resistant to erythrocycin by overexpressing the efflux pump MsrA from the high-copy pUL5054 plasmid (JI Ross, EA Eady, JH Cove, S Baumberg, Gene 1996, 183, 143-148).

The compounds were firstly solubilized in DMSO at 10 mg/mL and screened for their antibacterial activity in 96 wells at 100 and 20 mg/L. However, the high absorbance of some of the tested compounds interfered with the measurement of bacterial growth that was assayed at 620 nm.

Flavonoid derivatives were dispensed in a 96-wells microplate by dilutions in Muller-Hinton medium (MH, Bio Rad) using a Biomek 2000 (Beckman) handling robot. 100 µL of the bacterial inoculum (an overnight culture at 37 °C in 5 mL MH diluted 100-fold) was then added in each well. The total volume was 200 µL in each well and the final bacteria concentration 10^6 CFU/mL (CFU: colony forming unit). Growth was assayed with a microplate reader by monitoring absorption at 620 nm after 1, 2, 5, 7 and 24 h incubation at 37°C. In addition, the plates were read visually after 24 hours incubation. The activity of the compounds was determined after 24 h incubation at 37°C. Control wells were MH broth containing 5µL of DMSO. In addition, two controls containing a sub-inhibitory or a inhibitory antibiotic concentration for the tested strain were performed. The antibiotics used were ampicillin (0.5 and 32 µg/mL) for *E. coli*, kanamycin (0.5 and 16 µg/mL) for *S. aureus* ATCC 25923, ciprofloxacin (4 and 64 mg/L) for *S. aureus* 1199B and erythromycin (16 and 256 mg/L) for *S. aureus* RN4220/pUL5054.

References

1: Mahal, H. S.; Rai, H. S.; Venkataram, K. "Synthetical Experiments in the Chromone Group. Part XVI. Chalkones and Flavanones and their Oxidation to Flavones by Means of Selenium Dioxide." *J. Chem. Soc.* **1935**, 866-868

2: Makrandi, J. K.; Seema, P. "An efficient procedure for cyclization of 2'-hydroxychalcones into flavones." *Chem. Ind.* **1989**, 607- 608

3: Akama, T.; Shida, Y.; Sugaya, T.; Ishida, H.; Gomi, K.; Kasai, M. "Novel 5-Aminoflavone Derivatives as Specific Antitumor Agents in Breast Cancer" *J. Med. Chem.* **1996** 39, 3461–3469

4: Zwaagstra, M. E.; Timmerman, H.; van de Stolpe, A. C.; de Kanter, F. J. J.; Tamura, M.; Wada, Y.; Zhang, M.-Q. "Synthesis and Structure−Activity Relationships of Carboxyflavones as Structurally Rigid *CysLT*$_1$ (LTD_4) Receptor Antagonists " *J. Med. Chem.* **1998** 41, 1428–1438

5: Tanaka, T.; Iwashima, K.; Matsuura, S. "Synthetic Studies of the Flavone Derivatives. X. The Use of 2,3-Dichloro-5,6-dicyano-1,4-benzoquinone in the Dehydrogenation of 2'-Hydroxychalcones" *Yakugaku Zasshi* **1984** 104, 1306-1308

6: Iinuma, M.; Matoba, Y.; Tanaka, T.; Mizuno, M. "Flavonoids Synthesis. I. Synthesis and Spectroscopic Properties of Flavones with Two Hydroxy and Five Methoxy Groups at C-2',3',4',5,6,6',7 and C-2',3,4',5,5',6,7 " *Chem. Pharm. Bull.* **1987** 35(2), 660-667

7: Iinuma, M.; Tanaka, T.; Ito, K.; Mizuno, M. "Flavonoids Synthesis. V. Hydroxy and Four Synthesis Methoxy of Flavonoids with Groups and Their Three Spectral Properties" *Chem. Pharm. Bull.* **1986** 34(4), 1656-1662

8: Cheng, L.; Tan, H.; Wu, X.; Hu, R.; Aw, C.; Zhao, M.; Shen, H.-M.; Lu, Y. "Novel synthetic luteolin analogue-caused sensitization of tumor necrosis factor-α-induced apoptosis in human tumor cells" *Org. Biomol. Chem.* **2008** 6, 4102–4104

9: Pfister, J. R.; Wymann, W. E.; Schuler, M. E.; Roszkowski, A. P. "Inhibition of Histamine-Induced Gastric Secretion by Flavone-6-carboxylic Acids" *J. Med. Chem.* **1980** 23(3), 335-338

10: Emilewicz, T.; von Kostanecki, S. “Synthesis of the 3-Oxyflavones” Chem. Ber. 1**898** 31, 696-705

11: Donelly, J. A.; Doran, H. J.; “Synthesis and cyclisation of the stereoisomers of 2’,6’-disubstituted α-bromochalcones” *Tetrahedron* **1975** 31(15), 1791-1794.

12: Schmitz, F. U.; Roberts, C. D.; Griffith, R. C.; Botyanszki, J.; Gezginci, M. H.; Gralapp, J. M.; Shi, D. F.; Liehr, S. J. R. “A preparation of bicyclic imidazole derivatives, useful for the treatment of viral infections mediated by Flaviviridae family of viruses” PCT Int. Appl. **2005**, 2005012288

13: Doshi, A. G.; Soni, P. A.; Ghiya, B. J. “Oxidation of 2'-hydroxychalcones” *Indian J. Chem.* **1986** 25B(7), 759

14: Larsen, L.; D. H. Yoon, D. H.; Weavers, R. T. “Synthesis of a Range of Polyhydroxy 8-Aryl Flavones” *Synth. Commun.* **2009** 39, 2935–2948

15: Chan, K.-F.; Zhao, Y.; Chow, T. W. S.; Yan, C. S. W.; Ma, D. L.; Burkett, B. A.; Wong, I. L. K.; Chow, L. M. C.; Chan, T. H. “Flavonoid Dimers as Bivalent Modulators for P-Glycoprotein-Based Multidrug Resistance: Structure–Activity Relationships” *ChemMedChem* **2009** 4, 594-614

16: Miyake, H.; Takizawa, E.; Sasaki, M. “Syntheses of Flavones via the Iodine-Mediated Oxidative Cyclization of 1,3-Diphenylprop-2-en-1-ones. — An alternative, inexpensive method is used for the preparation of flavones” *Bull. Chem. Soc. Jpn.* **2003** 76, 835–836

17: Sarda, S. R.; Jadhav, W. N.; Pawar, R. P. “I_2-Al_2O_3: A suitable heterogeneous catalyst for the synthesis of flavones under microwave irradiation” *Int. J. ChemTech Res.* **2009** 1(3), 539-543

18: Ahmed, N.; Ali, H.; van Lier, J. E. “Silica gel supported $InBr_3$ and $InCl_3$: new catalysts for the facile and rapid oxidation of 2’-hydroxychalcones and flavanones to their corresponding flavones under solvent free conditions” *Tet. Lett.* **2005** 46, 253–256

19: Garcia, H.; Iborra, S.; Primo, J.; Miranda, M. A. "6-Endo-Dig vs. 5-Exo-Dig ring closure in o-hydroxyaryl phenylethynyl ketones. A new approach to the synthesis of flavones and aurones." *J. Org. Chem.* **1986** 51(23), 4432-4436

20: Harkat, H.; Blanc, A.; Weibel, J.-M.; Pale, P. "Versatile and Expeditious Synthesis of Aurones via Au(I)-Catalyzed Cyclization." *J. Org. Chem.* **2008** 73(4), 1620-1623

21: Fitzgerald, D. M.; O'Sullivan, J. F.; Philbin, E. M.; Wheeler, T. S. "Ring Expansion of 2-Benzylidenecouma.ran-3-ones-A Synthesis of Flavones." *J. Chem. Soc.* **1955** 860-862

22: Kumar, P. E.; Prasad, K. J. R. "Synthesis of 3,4-dihydro-2,2-dimethyl-2H-pyranoflavones" *Ind. J. Chem B Org.* **1998** 37B(2), 158-160

23: Algar, J.; Flynn, J. P. "New synthesis of flavonols" *Proc. R. Ir. Acad., Sect. B* **1934** B42, 1-8

24: Oyamada, B. "A new general method for the synthesis of flavonol derivatives" *J. Chem. Soc. Japan* **1934** *55*, 1256-1261

25: Geissman, T.A.; Fukushima, D. K. "Flavonones and Related Compounds. V. The Oxidation of 2'-Hydroxychalcones with Alkaline Hydrogen Peroxide" *J. Am. Chem. Soc.* **1948** 70, 1686-1689

26: Dean F. M.; Podimuang, V. "The Course of the Algar-Flynn-Oyamada (A.F.O.) Reaction" *J. Chem. Soc.* **1965**, 3978-3987

27: Moriarty, R. M.; Prakash, O. *Organic reactions vol. 54* **1999** chap.2; John Wiley & sons, inc.

28: Moriarty, R. M.; Prakash, O.; Musallam, H. A. "Use of hypervalent iodine oxidation for the C(3)-hydroxylation of chromone, flavone and α-naphthoflavone" *J. Heterocycl. Chem.* **1985** 22, 583-584

29: Costa, A. M. B. S. R. C. S; Dean, F. M.; Jones, M. A.; Varma, R. S. "Lithiation in Flavones, Chromones, Coumarins, and Benzofuran Derivatives" *J. Chem. Soc. Perkin Trans. I* **1985** 799-808

30: Kim, J.; Lee, H. S.; Park, K.-S.; Chong, Y. "Unexpected Desilylative-alkylation of 3-O-tert-Butyl-dimethylsilyl Galangin" *Bull. Korean Chem. Soc.* **2008** 29(9), 1667-1668

31: Adams, T. E.; El Sous, M.; Hawkins, B. C.; Hirner, S.; Holloway, G.; Khoo, M. L.; Owen, D. J.; Savage, G. P.; Scammells, P. J.; Rizzacasa, M. A. "Total Synthesis of the Potent Anticancer *Aglaia* Metabolites (-)-Silvestrol and (-)-Episilvestrol and the Active Analogue (-)-4′-Desmethoxyepisilvestrol" *J. Am. Chem. Soc.* **2009** 131, 1607–1616

32: Adam, W.; Golsch, D.; Hadjiarapoglou, L. "Epoxidation of Flavones by Dimethyldioxirane" *J.Org. Chem.* **1991** 56, 7292-7297

33: Compton, B. J.; Larsen, L.; Weavers, R. T. "Use of acyl substituents to favour 2,3-epoxidation of 5,7-dioxygenated flavones with dimethyldioxirane" *Tetrahedron* **2011** 67, 718-726

Conclusions and perspectives

Flavonoids constitute one of the largest classes of antioxidants from natural sources, specifically, plants. Due to their presence from the first stages of life on earth, animal and plants have evolved in the presence of flavonoids. They exhibit an incredible broadness of biological effects in plants, as well as in animals, where they can interact with all kinds of biological targets. Thanks to their most famous characteristic, that is their antioxidant behavior, they protect mammals against all manners of aggressions, and can help prevent diseases such as cancer.

The combination of a bioactive molecule with a ferrocene moiety is known in medicinal chemistry to increase the activity and therapeutic spectrum of the parent compound. In our case, this combination results in the discovery of the first ferrocenyl flavones, aurones, and flavonols from their precursor chalcones. This work, undertaken with a medicinal chemistry perspective, concerns the design, synthesis, chemical characterization and preliminary biological evaluation of such molecules, hopefully with the result of identifying promising hits.

A series of ferrocenyl chalcones has been synthesized *via* an aldolic condensation between the ferrocene carboxaldehyde and diversely substituted acetophenones. The main role of ferrocenyl chalcones was synthetic. From these chalcones, boron adducts have been made using boron trifluoride. Ferrocenyl aurones have also been made from chalcones, via a mercury-mediated oxidative cyclisation. An original silver-mediated protocol has also been developed. These ferrocenyl aurones were then isomerized using cyanide to result in the ferrocenyl flavone series. Finally, the grafting of a hydroxy group on ferrocenyl flavones gave the ferrocenyl flavonone series.

Similarly to their organic analogues, the biological impact of ferrocenyl flavonoids is very broad, and hits have been identified for each tested disease. A chalcone derivative, presented as molecule **2d**, shows potent IN inhibition. Series **2** in general presents attractive properties as IN inhibitors, although possessing a weakness concerning stability. Further

developments will therefore be focused on the investigation of a substitution pattern increasing this stability, in order to obtain compounds suitable for tests on the virus itself.

Methoxy-substituted compounds of the series **3** in general are promising antibacterial agents. They exhibit the very interesting property of being more active on bacteria lines that are known to present resistance to other drugs. Because the aurones were most active on the strain that overexpresses an efflux pump (MsrA), these compounds will also be tested in combination with standard anti-bacterial agents. Among them, molecule **3j**, is the most promising candidate. Further developments include a full structure-activity relationship study, where the effects of substitutions in all positions of the ring A by methoxy groups can be investigated.

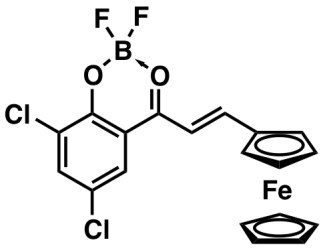

2d

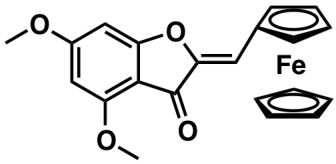

3j

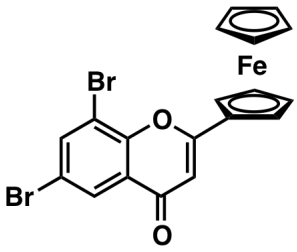

5e

Finally, series **5** presents interesting antivascular properties, the hit of this series being **5e**; molecules possessing pure antivascular properties on tumors are of great interest. Antiangiogenic properties are difficult to quantify *in vitro*, so the next step concerning the biological evaluation of this series is *in vivo* testing on mice, alone or in combination with cytotoxins.

From this work, it is clear that combining ferrocene with a flavonoid core results in interesting biological agents. Moreover, the chemistry giving access to ferrocenyl flavonoids implicates new types of reactivity, and especially new selectivities. Original methods giving access to the first ferrocenyl derivatives of three subclasses of flavonoids are presented.